Mechanism of myostatin action during satellite cell activation and muscle wasting.

A thesis

submitted in partial fulfilment

of the requirements for the degree

of

Doctor of Philosophy in Biological Sciences

at

The University of Waikato

by

CRAIG DESMOND MCFARLANE

The University of Waikato

Te Whare Wānanga o Waikato

The University of Waikato

2007

Abstract

Myostatin, a Transforming Growth Factor-beta (TGF-β) superfamily member, has been well characterised as a negative regulator of muscle growth and development. In support, inactivation or mutation of the *myostatin* gene results in a dramatic increase in skeletal muscle mass, however excess myostatin inhibits myogenesis. Recently, myostatin has also been shown to have a role in post-natal muscle growth. Myostatin regulates activation, proliferation and self-renewal of the muscle satellite cell pool. Moreover, loss of *myostatin* results in enhanced skeletal muscle regeneration in response to injury, whereas increased post-natal myostatin expression is associated with many skeletal muscle wasting conditions. Furthermore, myostatin has been shown to directly induce cachexia following subcutaneous injection of Myostatin over-expressing cells into mice. Despite studies implicating myostatin in the regulation of post-natal skeletal muscle growth, little is known about the processes through which myostatin activity is regulated or the mechanisms through which myostatin functions. Thus this thesis examines regulation of myostatin activity through proteolytic processing, and signaling mechanisms through which myostatin acts to regulate the satellite cell pool and to promote skeletal muscle proteolysis.

In this thesis it is demonstrated that processing and secretion of Myostatin is relatively reduced in differentiated myotubes as compared to proliferating myoblasts. Furthermore, processing of Myostatin is developmentally regulated, with decreased Myostatin processing occurring during foetal muscle development when compared to post-natal adult muscle. It is also demonstrated that mature Myostatin negatively regulates *furin* promoter activity. Furin protease is critical for the processing of several members of the TGF-β superfamily, thus a mechanism is proposed whereby myostatin negatively auto-regulates its proteolytic processing during development to facilitate the process of myoblast differentiation.

It was further demonstrated that over-expression of Pax7 in C3H10T1/2 multipotent cells enhances myogenic conversion in these cells. However, over-expression of Pax7 in C2C12 myoblasts delays the onset of differentiation, concomitant with an increase in the population of quiescent, satellite cell-like

reserve cells. Furthermore, treatment with Myostatin down-regulates Pax7 expression, while Pax7 expression was higher in *myostatin*-null myoblasts as compared to wild-type myoblast cultures. Furthermore, absence of *myostatin* alters cell heterogeneity, whereby an increase in $Pax7^{+}/MyoD^{-}$ reserve cell populations is observed. Pax7 expression persists longer through differentiation in cultured primary myoblasts from *myostatin*-null animals when compared to wild-type counterparts. Reserve cell populations were also measured, and consistent with increased expression of Pax7, there is an increased pool of quiescent "self-renewed" reserve cells in differentiated cultures from *myostatin*-null mice as compared with wild-type cultures. Taken together, these results suggest that increased expression of Pax7 regulates the self-renewal process of satellite cells, and furthermore, growth factors such as myostatin signal through Pax7 to regulate the self-renewed pool of satellite cells.

In this thesis it is shown that myostatin induces cachexia through a mechanism independent of NF-κB. Myostatin treatment results in a cachexia phenotype with a reduction in myotube number and size *in vitro*, as well as a loss of body mass *in vivo*. Furthermore, the expression of the myogenic genes *myoD* and *pax3* are reduced, while NF-κB localisation and expression remains unchanged. Expression of the ubiquitin-associated genes Atrogin-1, MuRF-1 and $E2_{14k}$ are shown to be up-regulated following Myostatin treatment. The mechanism behind myostatin-mediated cachexia was further investigated. It is shown that myostatin antagonises the IGF-1/PI3-K/AKT hypertrophy pathway by inhibiting AKT phosphorylation, thereby increasing the levels of active FoxO1, allowing for increased expression of atrophy-related genes.

In addition, microarray analysis resulted in the identification of a potentially interesting downstream target gene of myostatin during the induction of cachexia. Initial characterisation of CXXC5, or MM1 as it was renamed, was also performed. Over-expression of MM1 *in vitro* results in the up-regulation of components of the ubiquitin-proteasome pathway including Atrogin-1, $E2_{14k}$, $E2_{20k}$ and RC2. It was further demonstrated that increased expression of MM1 enhances the level of protein ubiquitin-conjugation. Furthermore, over-expression of MM1 results in myotube collapse and the formation of multinucleated myosacs. It was also demonstrated that the MM1-induced myotube collapse

results in disruption of the typical myotube microtubule structure. Therefore, these data suggest that MM1 is a muscle wasting-inducing gene which functions in the regulation of myostatin-mediated cachexia.

Therefore data presented in this thesis highlights a mechanism through which myostatin is regulated, and further delineates the role of myostatin in controlling several key processes during post-natal myogenesis, namely satellite cell replenishment and skeletal muscle wasting.

Acknowledgements

First and foremost, I would like to extend my deepest appreciation to Dr Ravi Kambadur and Dr Mridula Sharma, thank you for giving me the opportunity to undertake this PhD project; it has been an invaluable learning experience. Ravi, you have been my mentor and friend, your knowledge has guided me through this chapter of my career and you have given me something to aspire to in my future. Mridula, thank you for your constant guidance and support during the course of my thesis.

Thanks to my university supervisor Dr Nick Ling for taking time out of your busy schedule to review my thesis and for the valuable suggestions.

Thanks to Mark Thomas and Trevor Watson, our friendly local tissue culture managers. You are the backbone of the work undertaken in our lab. Thanks Mark for your invaluable assistance with my cell culture projects and for helping with the clonal cell line generation. Thanks also for proofreading the manuscripts presented in this thesis.

Thanks to Alex Hennebry for help with the overwhelming number of clonal cell lines made during the course of this thesis and thanks for putting up with me during the last stages of my thesis writing. Thanks also for taking time out of your fatherly duties to proofread my thesis. I guess I should also thank Miranda and Cody for that too!

Thanks to Erin Plummer for help with the almost endless stream of Western Blots and for your brilliant proofreading skills.

Thanks also to my MM1 partner-in-crime Bridgette Wilson (B-Unit) for making the "Boy's Lab" a crazy but enjoyable place to work. Thanks to Yasuhiro Kishioka for help during the course of my project. Yasu, you have made us all look bad with your dedication and commitment to work, thanks for raising the bar.

Thanks to Victoria Siriett for help with the stubborn Pax7 and MyoD ICCs. Thanks also to Dr Mônica Senna Salerno for guiding me through my first international conference, further thanks to Varun Arora for help with the difficult,

and sometimes impossible cloning of the promoter elements. Thanks to Dr Brett Langley, Dr Seumas McCroskery, Carole Berry, Dr Gina Nicholas, Leanne Platt, Todd Davies and Kelly Dyer for your help during the course of my studies. I would also like to extend my thanks to the Functional Muscle Genomics team both past and present. The Functional Muscle Genomics group has been a fantastic team to work with and it will continue to be so in the future, you all make it a pleasure to come into work each day.

Thanks also to Dr Barry O'brien for guidance with the confocal microscope and timelapse experiments.

To Mum and Dad, thank you for your unconditional love and support over the last 29 years. You will always be a source of inspiration for me and I can't thank you enough.

To Deanne, words cannot express the happiness I have with you in my life. You have supported me in every way throughout the course of this endeavour. I could not have done it without your love and support, thank you! Finally, I would like to thank the two little people that remind me what is really important in life, Natalie and Jack. I can't wait to see you both grow up; you have made this dad very proud.

Table of Contents

List of Figures

List of Tables

List of Abbreviations

The following abbreviations have been used in this thesis:

3’	3 prime
5’	5 prime
15-HETE	15-Hydroxyeicosatetraenoic acid
α	Alpha
A	Adenine
aa	Amino acid
A_{260}	Absorbance at 260 nm
ActRIIB	Activin receptor type IIB
ADP	Adenosine diphosphate
AH130	Yoshida ascites hepatoma-130
AIDS	Acquired immune deficiency syndrome
AKT	Serine/threonine protein kinase
ALK4/5	Activin receptor like kinase 4/5
Amp	Ampicillin
ATCC	American type culture collection
ATP	Adenosine triphosphate
β	Beta
β-gal	Beta-galactosidase
βMe	Beta-mercaptoethanol
bGH p(A)	Bovine growth hormone polyadenylation system
bHLH	Basic helix-loop-helix
BMD	Beckers muscular dystrophy
BME	Eagle’s basal medium
BMP	Bone morphogenetic protein
bp	Base pair
BrdU	Bromo-deoxyuridine
BSA	Bovine serum albumin
C2C12	Murine myoblast cell line
˚C	Degrees Celsius

C	Cytosine
Cλ	Carrageenen Lambda
C57Bl/6J	C57 black mice from Jackson laboratories
Ca^{2+}	Calcium ion
CBP	CREB binding protein
cdk	Cyclin-dependent kinase
cDNA	Complementary DNA
CEE	Chicken embryo extract
CHO	Chinese hamster ovary
Ci	Curie
CKI	Cyclin-dependent kinase inhibitor
cm	Centimetre
c-Met	Tyrosine kinase receptor
Cmpt	Compact mouse mutant
CMV	Cytomegalovirus
CO_2	Carbon dioxide
CoCl	Cobalt Chloride
Co-Smad	Common smad; Smad 4
C-terminal	Carboxy-terminal; COOH
DAB	3,3-Diaminobenzidine tetrahydrochloride
DAPI	4',6-Diamidino-2-phenylindole
dCTP	2'-deoxycytidine 5'-triphosphate
DEPC	Diethylpyrocarbonate
Dex	Dexamethasone
Diff	Differentiating
DMD	Dystrophin gene
DMD	Duchenne muscular dystrophy
DMEM	Dulbecco's Modified Eagle Medium
DML	Dorsal medial lip
DMSO	Dimethyl sulfoxide
dn	Dominant negative
DNA	Deoxyribonucleic acid
dNTP	Deoxyribonucleotide triphosphate
DTT	Dithiothreitol
dy	Laminin-II associated dystrophy

E1	Ubiquitin-activating enzyme
E2	Ubiquitin-conjugating enzyme
E3	Ubiquitin-ligating enzyme
EBSS	Earle's balanced salt solution
E. coli	*Escherichia coli*
ECM	Extracellular matrix
EDL	*M. Extensor digitorum longus*
EDTA	Ethylenediaminetetraacetic acid
EGF	Endothelial growth factor
ER	Endoplasmic reticulum
ERBA	20S, 21-epoxy-resibufogenin-3-acetate
ERK	Extracellular signal-regulated kinase
FBS	Foetal bovine serum
FGF	Fibroblast growth factor
FGFR	Fibroblast growth factor receptor
FITC	Fluorescein isothiocynate complex
FLRG	Follistatin-related gene
FoxO	Forkhead box O
Fwd	Forward
G	Guanidine
g	Gram
γ	Gamma
×g	Gravity
G_0	Gap 0 phase of the cell cycle / quiescent phase of the cell cycle
G_1	Gap 1 phase of the cell cycle
G_2	Gap 2 phase of the cell cycle
GAPDH	Glyceraldehyde-3-phosphate dehydrogenase
GASP	Growth and differentiation factor-associated serum protein
GDF	Growth and differentiation factor
GFP	Green fluorescent protein
GLDG	Glycine-leucine-aspartate-glycine
GRE	Glucocorticoid response elements
GSK3	glycogen synthase kinase-3
H_2O	Water
HAT	Histone acetylase

HDAC	Histone deacetylase
HGF	Hepatocyte growth factor/scatter factor
His	Histidine
HIV	Human immunodeficiency virus
HLH	Helix-loop-helix
hr	Hour
HRP	Horse radish peroxidase
HS	Horse serum
hSGT	human small glutamine-rich tetratricopeptide repeat-containing protein
IκB	Inhibitor of kappa B
ICC	Immunocytochemistry
IGF	Insulin like growth factor
IGFBP	IGF binding protein
IgG	Immunoglobulin G
IL	Interleukin
INF	Interferon
IPTG	Isopropyl thio-β-galactoside
I-Smad	Inhibitory Smad
k	Kilo ($\times 10^3$)
κ	Kappa
kb	Kilo base
kDa	Kilo Dalton
λ	Lambda
L	Litres
LacZ	Betagalactosidase reporter gene
LAP	Latency ssociated peptide
LB	Lennox L broth
LDH	Lactate dehydrogenase
LF2000	Lipofectamine 2000
LLC	Lewis lung carcinoma
LMP	Low melting point
LTBP	Latent TGF-β binding proteins
M	Molar, moles per litre
m	Milli ($\times 10^{-3}$)

m.	Musculus
M phase	Mitosis phase of the cell cycle
µ	Micro ($\times 10^{-6}$)
µg	Microgram
µJ	Microjoules
µL	Microlitre
µM	Micromolar
mA	Milli amp(s)
MAPK	Mitogen activated protein kinase
mdx	Mouse model of DMD
MEM	Minimum essential medium
mh	Muscular hypertrophy
MHC	Myosin heavy chain
min	Minute
MLC	Myosin light chain
MM1	Menos músculo-1
MNF	Myocyte nuclear factor
MOPS	3-(N-Morpholino)propanesulfonic acid
MQ	Milli Q
MRF	Myogenic regulatory factor
mRNA	Messenger RNA
Mstn	Recombinant myostatin protein
mTOR	Mammalian target of rapamycin
MuRF-1	Muscle specific ring finger-1
n	Nano ($\times 10^{-9}$)
n	Number
nm	Nanometre
Neo	Neomycin
NF-κB	Nuclear factor-kappa B
NGS	Normal goat serum
NOS	Nitric oxide synthase
NP-40	Nonidet P-40
NSS	Normal sheep serum
N-terminal	Amino-terminal; NH2
OD	Optical density

ORF	Open reading frame
P	Phosphorous
P	Probability
p	Pico ($\times 10^{-12}$)
PAGE	Polyacrylamide gel electrophoresis
PCAF	p300/CBP-associated factor
PCR	Polymerase chain reaction
PDGF	Platelet Derived Growth Factor
PDK-1	3-phosphoinositide-dependent protein kinase-1
PEG	Polyethylene glycol
pH	Hydrogen ion concentration
PI3-K	Phosphatidylinositol 3-kinase
Prolif	Proliferating
PVP	Poly vinyl perrolidone
Q-RT-PCR	Semi-quantitative RT-PCR
Rb	Retinoblastoma susceptibility gene product
RD	Rhabdomyosarcoma cell line
Rev	Reverse
RNA	Ribonucleic acid
rpm	Revolutions per minute
R-Smad	Receptor Smad
RSRR	Arginine-serine-arginine-arginine
RT	Reverse transcriptase
RT-PCR	Reverse transcription polymerase chain reaction
S	Synthesis phase of the cell cycle
s	seconds
SDF	Stromal-derived factor
SDS	Sodium dodecyl sulphate
SE	Standard error
SEM	Standard error of the mean
SF/HGF	Scatter Factor or hepatocyte growth factor
siRNA	Small interfering RNA
shRNA	Short hairpin interfering RNA
SP	Side population
SV40	Simian vacuolating virus 40

T	Thymidine
TA	*M. tibialis anterior*
TAE	Tris acetate EDTA
Taq	DNA polymerase from *Thermus aquaticus*
TBS	Tris buffered saline
TBST	Tris buffered saline tween 20
TE	Tris EDTA
TEMED	N,N,N',N'-tetramethylethylenediamine
TGF-β	Transforming growth factor-β
TLD	tolloid
TNF-α	Tumour necrosis factor-α
TNF-R2	Subtype 2 TNF-α receptor
Tris	2-amino-2-(hydroxymethyl)-1,3-propanediol
TWEAK	Tumor necrosis factor-like weak inducer of apoptosis
U	Units
UTR	Untranslated region
UV	Ultraviolet
V	Volts
v/v	Volume per volume
VLL	Ventral lateral lip
w/v	Weight per volume
x	multiply
XAR	X-ray autoradiography
Zn^{2+}	Zinc ion

This Thesis is dedicated to
My Beautiful Wife, Deanne
and My Two Wonderful Children,
Natalie and Jack.

Chapter 1 Literature review

1.1 Muscle and embryonic myogenesis

Three distinct classes of muscle exist in vertebrates: smooth, cardiac and skeletal. Skeletal muscle, is primarily involved with the production of active force, resulting in voluntary movement of the skeletal system. The following section reviews literature on the structure of skeletal muscle and the process of embryonic myogenesis.

1.1.1 Skeletal muscle structure

Skeletal muscle is a highly structured tissue consisting of several distinct compartments. Skeletal muscle is enclosed by a connective tissue sheath termed the epimysium. A layer of connective tissue, termed the perimysium, further divides the muscle into a number of compartments called fascicles. Each fascicle contains a bundle of skeletal muscle fibres, which are themselves enclosed within a third layer of connective tissue, the endomysium (Figure 1.1A) (Martini 2001). Skeletal muscle fibres, or myofibres, are composed of myofibrils (Figure 1.1B); myofibrils contain bundles of myofilaments, which comprise both thick and thin filaments, consisting of myosin and actin respectively. The myofilaments are organised into parallel, longitudinally repeated units called sarcomeres. The sarcomeres are the basic functional unit for force production and fibre contraction in the muscle (Figure 1.1C) (Fung 1981; Bagshaw 1993; Martini 2001). The sarcomere can be separated into two distinct regions (Figure 1.1C): the A-band, which corresponds to the central region where thick filaments overlap with thin filaments, and the I-band, which is comprised of thin filaments only and is the region between the A-bands of adjacent sarcomeres. In the middle of the A-band is an area termed the H-zone, composed only of thick myosin filaments (Martini 2001)

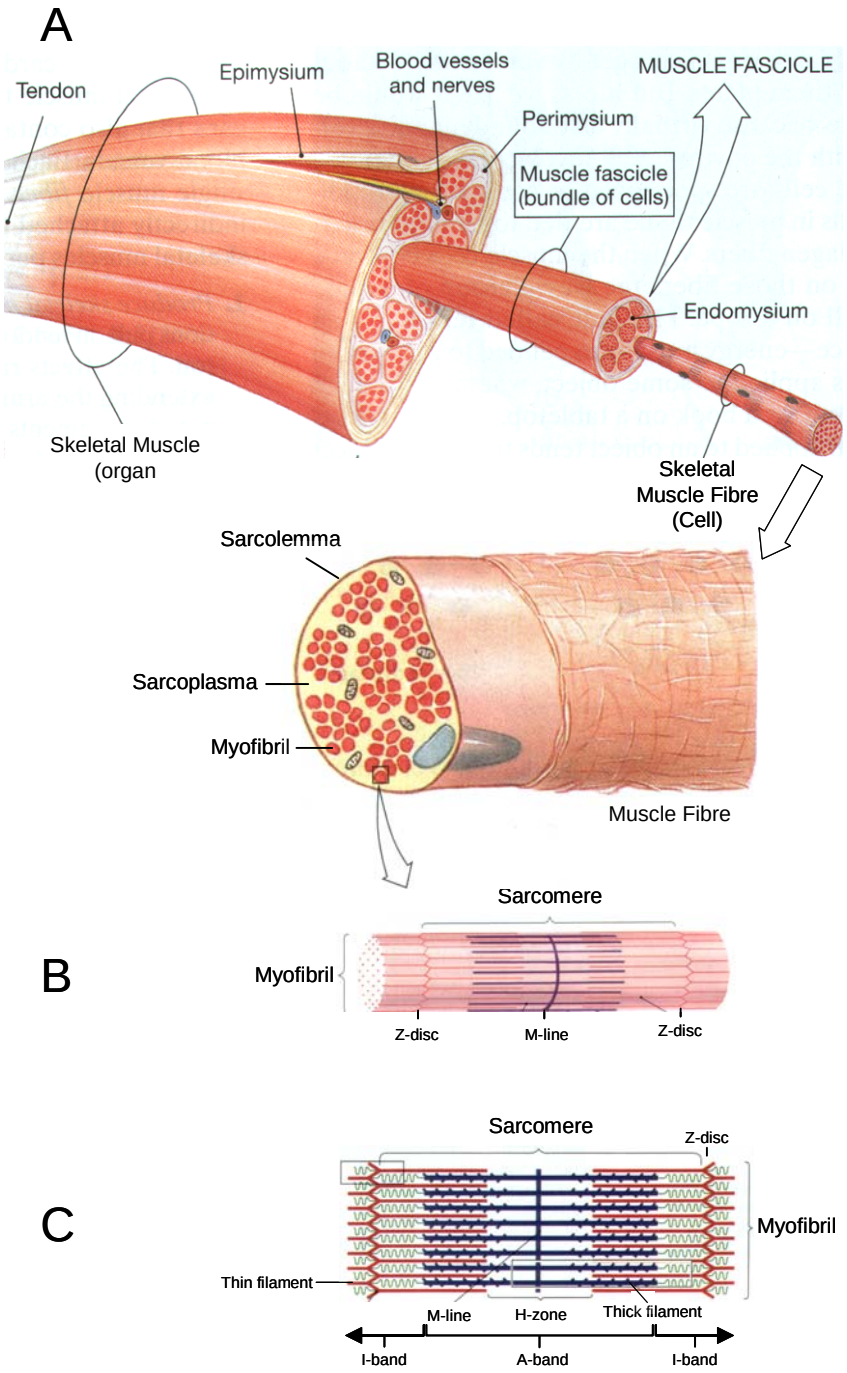

Figure 1.1 *Skeletal muscle structure*

A) The epimysium, a connective tissue sheath, encloses the entire muscle. The perimysium, a further connective tissue, separates the muscle into compartments called fascicles. Fascicles enclose the myofibres, which are surrounded by a fine layer of connective tissue termed the endomysium. B) The myofibre is further divided into myofibrils**.** C) Myofibrils are composed of sarcomeres, the basic unit of contraction in the muscle. Sarcomeres are themselves comprised of an ordered alignment of thick and thin filaments. Modified from Martini (Martini 2001).

The M-line, a network of proteins located at the centre of the H-zone, is responsible for connecting thick filaments together and maintaining their orientation. Finally, the Z-line defines the boundaries of the sarcomere and is responsible for binding thin filaments of adjacent sarcomeres (Fung 1981; Martini 2001). The "sliding filament theory" describes the mode of action during skeletal muscle contraction. During contraction, actin filaments are actively pulled between the thick myosin filaments. The sliding of the actin filaments results in shortening of the muscle towards the centre of the sarcomere. With regard to the sarcomere, contraction results in a change in length of the I-band and H-zone, whereas the length of the A-band remains constant (Fung 1981; Martini 2001).

1.1.2 *Embryonic myogenesis*

The majority of vertebrate skeletal muscles, with the exception of craniofacial muscles, are derived from somites (Figure 1.2) (Buckingham 1992; Cossu *et al.* 1996). Somites are transient structures consisting of mesenchymal cells which arise from segmentation of the paraxial mesoderm on either side of the neural tube and notochord (Christ and Ordahl 1995). Somites quickly become compartmentalised, whereby the ventral region forms the sclerotome, giving rise to vertebrae and ribs (Cossu *et al.* 1996; Buckingham *et al.* 2003; Hollway and Currie 2005); while the dorsal somite region forms the dermomyotome, and is responsible for the formation of the dermis and the body and limb musculature (Buckingham *et al.* 2003; Hollway and Currie 2005). Myogenic precursor cells delaminate from the dermomytome to form the myotome (Hollway and Currie 2005). The dorsal myotome gives rise to the deep back and intercostal muscles, or what is termed epaxial muscle (Christ and Ordahl 1995; Brand-Saberi *et al.* 1996). In contrast cells derived from the lateral myotome and the lateral region of the dermomyotome give rise to myogenic precursor cells which migrate to limb buds to form hypaxial muscles, such as those of the body wall and the limb (Cossu *et al.* 1996; Brand-Saberi and Christ 1999). Skeletal muscle precursor cells give rise to skeletal muscle cells, termed myoblasts, which subsequently differentiate into multinucleated primary myotubes (Harris *et al.* 1989). Following this period of primary myogenesis, secondary myogenesis ensues whereby primary myotubes act as a template for a wave of secondary myoblasts.

Here the secondary myoblasts line up on the primary myotubes, fuse and form secondary myotubes. The resulting differentiated myotubes further fuse, forming myofibres which then align to produce the functional muscle (Gullberg *et al.* 1998).

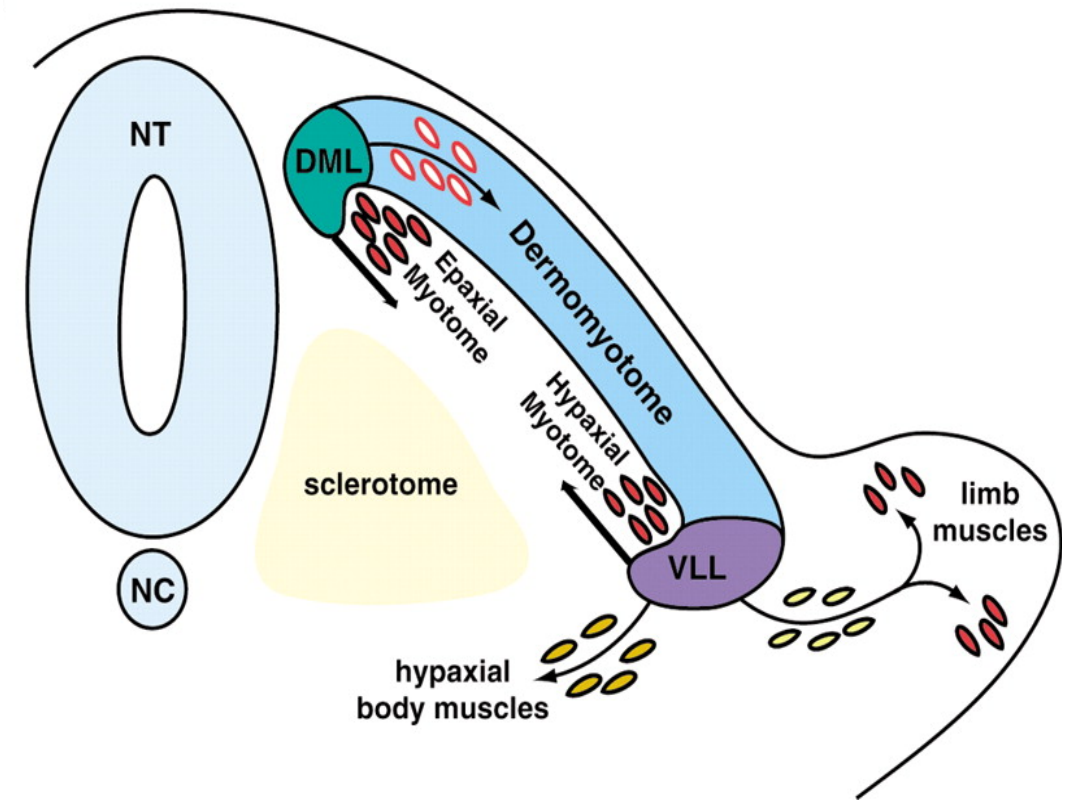

Figure 1.2 *Somitogenesis*

Somites specify dorsally into the dermomyotome and ventrally into the sclerotome. The dermomyotome gives rise to a second layer of cells termed the myotome. Myogenic precursor cells from the dorsal medial lip (DML) contribute to the medial (epaxial) region of the myotome and will give rise to back musculature; while myogenic precursor cells produced from the ventral lateral lip (VLL) will contribute to the lateral (hypaxial) region of the myotome, forming limb and body wall musculature. Modified from (Pownall *et al.* 2002).

Members of the Myogenic Regulatory Factor (MRF) family are critical for the timely progression of skeletal muscle myogenesis. The MRFs, consisting of Myf-5 (Braun *et al.* 1989), MyoD (Davis *et al.* 1987), myogenin (Edmondson and Olson 1989) and MRF4 (Rhodes and Konieczny 1989), are a family of basic helix-loop-helix (bHLH) transcription factors. Myf-5 expression is initially detected at day 8 in the developing somite (Ott *et al.* 1991), and has recently been shown to function together with MRF4 to specify commitment of progenitor cells to the myogenic lineage (Kassar-Duchossoy *et al.* 2004). MyoD expression is also detected early in the somite at about day 10.5 (Sassoon *et al.* 1989). MyoD may also specify progenitor cells to the myogenic lineage in the absence of *myf-5*. In agreement with this, mice lacking either *myoD* (Rudnicki *et al.* 1992) or *myf-5* (Braun *et al.* 1992) are still able to generate skeletal muscle, while mice lacking both *myoD* and *myf-5* are not (Rudnicki *et al.* 1993), thus suggesting a compensatory role for MyoD and Myf-5 during myogenic specification. Once specified, progenitor cells form myoblasts which differentiate into multinucleated myotubes. Myogenin and MRF4 are important for myogenic differentiation; indeed mice containing a mutated form of myogenin die peri-natally due to a severe deficiency in differentiated myofibres, however, myoblast cell number remains unaffected (Hasty *et al.* 1993; Nabeshima *et al.* 1993). Furthermore, *MRF4*-null embryos have been shown to be devoid of any differentiated skeletal muscle (Olson *et al.* 1996).

The paired-box transcription factors Pax3 and Pax7 also have an important role in regulation of skeletal muscle myogenesis. Pax3 expression is detected throughout the somite, with progressive restriction to the dermomyotome and further concentration at the epaxial and hypaxial edges of the dermomyotome (Goulding *et al.* 1991; Tajbakhsh and Buckingham 2000). Pax3 is critical in cell delamination and migration of myogenic precursor cells to the limb buds. In support, progenitor cells do not delaminate from the hypaxial dermomyotome in *pax3*-null "Splotch" mice, and furthermore *pax3*-null mice are deficient in limb musculature (Franz *et al.* 1993; Tajbakhsh *et al.* 1997; Tremblay *et al.* 1998). In contrast to *pax3*-null, *pax7*-null mice have no discernable skeletal muscle defects during embryonic myogenesis (Mansouri *et al.* 1996). However, recently identified populations of myogenic progenitor cells, which express both Pax3 and Pax7, have been detected in the myotome region of the somite (Kassar-Duchossoy

et al. 2005; Relaix *et al.* 2005). These populations of $Pax3^{+}/Pax7^{+}$ cells have been shown to activate both Myf-5 and MyoD and give rise to myoblasts, which subsequently contribute to skeletal muscle formation (Relaix *et al.* 2005). The populations of $Pax3^{+}/Pax7^{+}$ cells appear to persist through to late foetal stages of growth and are further suggested to contribute to the skeletal muscle stem cell or satellite cell pool in adult muscle (Kassar-Duchossoy *et al.* 2005; Relaix *et al.* 2005).

1.2 Post-natal myogenesis

Adult skeletal muscle has the intrinsic ability to repair itself in response to injury. This repair process has been attributed to the satellite cell population present within skeletal muscle, making this population of cells especially important for post-natal myogenesis. Thus several aspects of satellite cell biology will be reviewed in the following section.

1.2.1 Satellite cells

Satellite cells, which are also referred to as muscle stem cells, were initially discovered in 1961 (Katz 1961; Mauro 1961). The term satellite cell was coined based on their peripheral location on skeletal muscle fibres (Katz 1961; Mauro 1961); specifically, satellite cells reside between the basal lamina and sarcolemma of muscle fibres (Grounds and Yablonka-Reuveni 1993; Bischoff and Heintz 1994). Satellite cells are located throughout skeletal muscle tissue, however, heterogeneity exists in the distribution of satellite cells with oxidative muscle fibres containing a greater population of satellite cells as compared to glycolytic fibres (Gibson and Schultz 1982; Holterman and Rudnicki 2005). At birth satellite cells account for 30% of the sub-laminar muscle nuclei in mice, however, in adult mice the number rapidly declines to only about 5% (Bischoff 1994a), presumably due to the contribution of satellite cells to post-natal muscle development (Gibson and Schultz 1983; Seale and Rudnicki 2000). Post-natal skeletal muscle growth, repair and maintenance are attributed to the myogenic precursor satellite cell population (Seale and Rudnicki 2000). Satellite cells are typically maintained in a quiescent state until induced to activate in response to such stimuli as stretching, exercise and injury (Rosenblatt *et al.* 1994; Grounds 1998; Hawke *et al.* 2003; Yan *et al.* 2003). The signals responsible for satellite cell activation are yet to be fully elucidated. However, studies have highlighted a role for Hepatocyte Growth Factor (HGF) in mediating satellite cell activation. Exogenous addition of HGF has been shown to induce activation; while antibody-mediated neutralisation of HGF inhibits satellite cell activation (Tatsumi *et al.* 1998). Moreover, Nitric Oxide Synthase (NOS) has been implicated in HGF-

mediated satellite cell activation. Inhibition of NOS reduces satellite cell activation and reduces the levels of HGF released following muscle stretching (Anderson 2000; Tatsumi *et al.* 2002); furthermore, it has been recently shown that HGF is released in a NOS-dependent manner during passive skeletal muscle stretch (Tatsumi *et al.* 2006). In addition, Fibroblast Growth Factor 2 (FGF2) has been demonstrated to promote recruitment of quiescent satellite cells towards proliferation (Yablonka-Reuveni *et al.* 1999). However, growth factors such as Insulin-like Growth Factor-1 (IGF-1), Endothelial Growth Factor (EGF), and Platelet-Derived Growth Factor (PDGF) appear to enhance satellite cell proliferation rather than promoting activation (Bischoff 1986; Johnson and Allen 1995). Once activated, satellite cells re-enter the cell cycle, proliferate and differentiate and then fuse to repair or replace damaged muscle fibres (Grounds and Yablonka-Reuveni 1993; Bischoff 1994b; Seale and Rudnicki 2000).

1.2.1.1 *Satellite cell origin*

There have been many articles published debating the specific origin of skeletal muscle satellite cells. However, it is commonly accepted that satellite cells are originally derived from the somites, as evidenced by several recent articles. Populations of cells that express both Pax3 and Pax7 but lack expression of muscle specific-markers have been detected within the mouse somite (Kassar-Duchossoy *et al.* 2005; Relaix *et al.* 2005). These cells form a pool of muscle progenitor cells which are able to become myogenic and give rise to skeletal muscle during development. These progenitor cells are further shown to adopt a satellite cell position later in foetal development (Kassar-Duchossoy *et al.* 2005; Relaix *et al.* 2005). Similar populations of muscle progenitor cells, initially detected in the dermomyotome compartment of chicken somites, are also suggested to be the origin of satellite cells (Gros *et al.* 2005). More recently, a study has traced the origins of satellite cells back to the hypaxial domain of the somite. It was further shown that these somitically-derived progenitor cells contribute to the satellite cell pool in post-natal musculature (Schienda *et al.* 2006).

In contrast, multipotent cells of non-somitic origin may also contribute to the satellite cell pool. For example, myogenic cells have been isolated from the

embryonic dorsal aorta which display a similar morphology and have comparable gene expression to that of adult satellite cells (De Angelis *et al.* 1999). Moreover, the aorta-derived myogenic cells were able to contribute to skeletal muscle growth and regeneration following transplantation. Therefore, it is possible that endothelial cells may in part give rise to satellite cells (De Angelis *et al.* 1999), or alternatively, endothelial cells and satellite cells may have a common origin; indeed it has been shown that endothelial and myogenic cells share a common somitic precursor (Kardon *et al.* 2002).

1.2.1.2 *Molecular markers of satellite cells*

Several studies have highlighted a number of molecular markers that identify the satellite cell lineage (Figure 1.3). Quiescent satellite cells have been shown to express a range of proteins, including a truncated form of the endothelial marker CD34 (Beauchamp *et al.* 2000), the hepatocyte growth factor receptor c-Met (Cornelison and Wold 1997), M-cadherin (Irintchev *et al.* 1994), myocyte nuclear factor (MNF) (Garry *et al.* 1997), syndecan-3/syndecan-4 (Cornelison *et al.* 2001) and Pax7 (Seale *et al.* 2000). M-cadherin, a cell adhesion molecule, is thought to play a role in the adhesion of satellite cells to the basal lamina of the muscle fibre (Hawke and Garry 2001). In addition, it may also play a role in the migratory response of these cells in response to stimuli (Hawke and Garry 2001). Syndecan-3 and syndecan-4 are cell surface proteoglycans which are reportedly expressed by satellite cells; indeed, expression of syndecan-3/syndecan-4 is detected under the basal lamina within the satellite cell compartment (Cornelison *et al.* 2001). The paired-box transcription factor Pax7 is a commonly used marker for satellite cells and is present in both quiescent and proliferating satellite cells (Seale *et al.* 2000; Zammit *et al.* 2004). Moreover, it has been recently demonstrated that Pax7 is transcriptionally active within quiescent satellite cells (Zammit *et al.* 2006b). Using *Myf5*$^{nlacZ/+}$ mice it has been established that the *Myf5* locus is active in quiescent satellite cells (Beauchamp *et al.* 2000; Shefer *et al.* 2006).

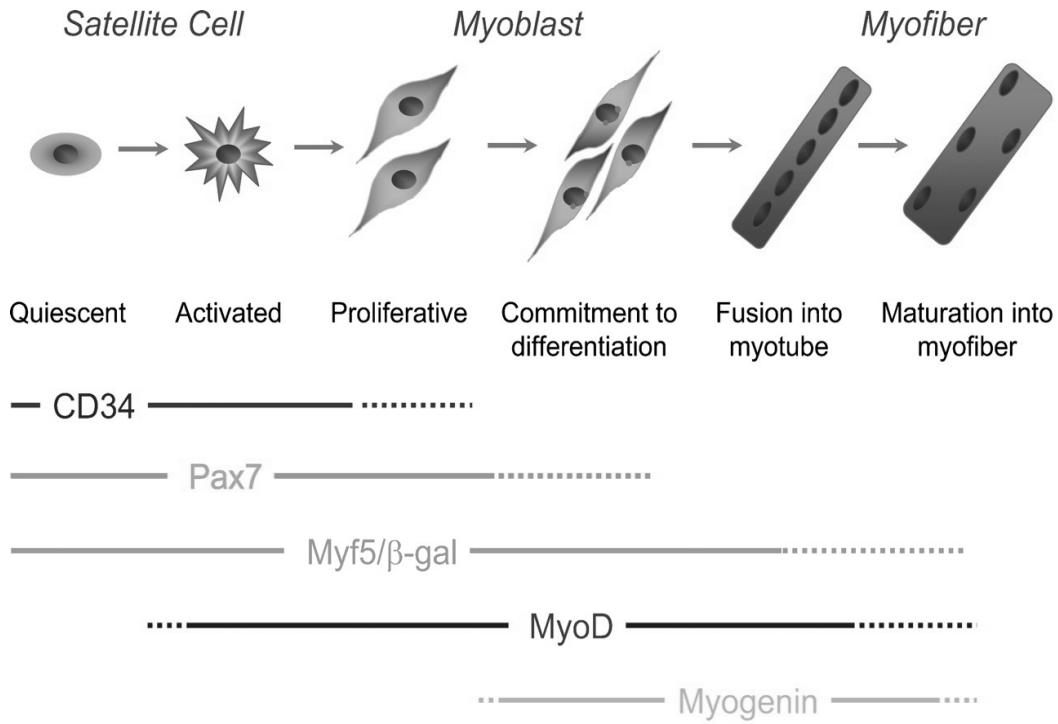

Figure 1.3 *Molecular markers of satellite cell growth*

Satellite cells normally exist in a quiescent state, but in response to several stimuli, including muscle injury, they activate and proliferate prior to differentiation and eventual fusing to form myotubes. Quiescent satellite cells express CD34, Pax7 and Myf-5/β-gal. Following activation, satellite cells express MyoD and maintain expression of Pax7, while myogenin expression is detected during the onset of differentiation. Modified from Zammit *et al*. (Zammit *et al.* 2006a).

Although the *Myf-5* locus is active, no published accounts have demonstrated Myf-5 mRNA or protein expression in quiescent satellite cells. Recent markers include the monoclonal antibody SM/C-2.6, which reacts with an epitope expressed on quiescent satellite cells (Fukada *et al.* 2004). Furthermore, caveolin-1 (Volonte *et al.* 2005) and lysenin (Nagata *et al.* 2006) have been recently identified as markers of quiescent satellite cells. To mediate skeletal muscle regeneration, satellite cells must activate, proliferate and terminally differentiate. Upon activation satellite cells begin expressing MyoD and desmin, along with continuing expression of Pax7, Myf-5, and M-cadherin (Yablonka-Reuveni and Rivera 1994; Cornelison and Wold 1997; Yablonka-Reuveni *et al.* 1999; Olguin and Olwin 2004; Zammit *et al.* 2004). Interestingly, activated satellite cells, unlike quiescent satellite cells, no longer express the truncated form of CD34; instead, expression of the full length isoform is detected (Beauchamp *et al.* 2000). During the progression of terminal differentiation, myogenin expression is up-regulated, while the expression of Pax7 is rapidly down-regulated during the induction of differentiation .(Cornelison and Wold 1997; Yablonka-Reuveni *et al.* 1999; Zammit *et al.* 2004).

1.2.1.3 *Satellite cell self-renewal*

The hallmark features of stem cells include the capacity to form differentiated tissue and the ability to self-renew their population (Weissman *et al.* 2001). Satellite cells, also referred to as skeletal muscle stem cells, have been shown to differentiate to form myotubes (Yablonka-Reuveni and Rivera 1994; Rosenblatt *et al.* 1995; Beauchamp *et al.* 2000). Furthermore, evidence is mounting to support the ability of satellite cells to self-renew their population, thus supporting their purported role as muscle stem cells. Satellite cell number remains constant through repeated cycles of skeletal muscle injury and regeneration, thus supporting the presence of mechanisms that replenish the satellite cell pool (Schultz and McCormick 1994). Evidence for satellite cell self-renewal has been obtained through several studies that analyse the function of transplanted myoblast populations *in vivo*. Skeletal muscle myoblasts have been shown to differentiate and contribute to muscle following injection into nude (immune-deficient) *mdx* mice (Morgan *et al.* 1994; Gross and Morgan 1999). Moreover,

injected muscle precursor cells were able to contribute to muscle formation following successive rounds of muscle injury due to notexin injection (Gross and Morgan 1999), thus providing evidence for the formation of a quiescent pool of cells capable of contributing to muscle repair. Furthermore, Montarras *et al.* demonstrated that injected $Pax3^{GFP/+}$ satellite cells contributed to muscle repair and were also located within the satellite cell compartment in nude *mdx* mice. The $Pax3^{GFP/+}$ cells were further shown to express the myogenic markers MyoD and Pax7 upon isolation from injected muscle (Montarras *et al.* 2005). A further study utilising the $Myf5^{nlacZ/+}$ mouse, whereby β-galactosidase (β-gal) activity was used to mark quiescent satellite cells, has yielded evidence to support satellite cell self-renewal (Heslop *et al.* 2001). Specifically, β-gal positive myoblasts were incorporated into muscles of recipient mice following injection. Heslop *et al.* further demonstrated that the β-gal positive cells occupied the satellite cell niche beneath the basal lamina and when isolated and cultured *in vitro* gave rise to myogenic cells. An elegant study by Collins *et al*. has provided direct evidence of satellite cell self-renewal *in vivo*. In that study they injected intact $Myf5^{nlacZ/+}$ muscle fibres into irradiated immune compromised *mdx* mice. Injection of muscle fibres, containing as few as seven satellite cells, produced more than one hundred new fibres. Furthermore, the transplanted satellite cells self-renewed to expand the population of new satellite cells, as determined by their location beneath the basal lamina and by expression of the satellite cell marker Pax7. In addition, following further injury these transplanted satellite cells were able to contribute to skeletal muscle regeneration (Collins *et al.* 2005).

Several cell culture models have provided further evidence for the ability of satellite cells to self-renew their population. C2C12 myoblast cultures proliferate until a decision is made to exit the cell cycle and differentiate to form multinucleated myotubes. During the induction of differentiation, through serum withdrawal, it has been shown that a subset of cells exit the cell cycle but fail to up-regulate the differentiation marker myogenin, and as a consequence do not commit to differentiation (Kitzmann *et al.* 1998; Yoshida *et al.* 1998). These "reserve cells" remain in a quiescent state until stimulated to activate, proliferate and contribute to further differentiation in culture (Kitzmann *et al.* 1998; Yoshida *et al.* 1998). Studies of satellite cell cultures have yielded more evidence for self-renewal. Heterogeneity in the expression of several key satellite cell markers is

observed in cultured single fibres (Olguin and Olwin 2004; Zammit *et al.* 2004). It has been shown that once activated, satellite cells express Pax7 and MyoD, proliferate, then down-regulate Pax7 prior to differentiation. However, sub-populations of satellite cells maintain expression of Pax7 but lose MyoD; these cells exit the cell cycle, fail to differentiate, and adopt a quiescent phenotype (Olguin and Olwin 2004; Zammit *et al.* 2004). Similarly, satellite cell populations from chickens, which are positive for Pax7 but lack MyoD, are phenotypically similar to quiescent reserve cells (Halevy *et al.* 2004). Further evidence for the role of Pax7 in self-renewal is obtained from studies of *pax7*-null mice. *Pax7*-null mice appear normal at birth but die between 2-3 weeks of age (Mansouri *et al.* 1996). Although *pax7*-null mice are born with satellite cells, the number quickly decreases with age, resulting in impaired regeneration (Oustanina *et al.* 2004; Relaix *et al.* 2006). While evidence points towards Pax7 as a key regulator of self-renewal, the unequivocal involvement and moreover the mode of action of Pax7 during self-renewal, remain matters of contention; indeed, loss of *pax7* has recently been shown to result in aberrant apoptosis (Relaix *et al.* 2006). Furthermore, Zammit *et al*. have recently demonstrated that constitutive expression of Pax7 is unable to induce quiescence or block myogenic differentiation in satellite cell cultures (Zammit *et al.* 2006b), thus Pax7 may mediate satellite cell survival, rather than self-renewal, to maintain the satellite cell pool.

The exact mechanism of satellite cell self-renewal is currently unknown, however, two alternative models have been proposed. The stochastic model, whereby satellite cells activate and proliferate until, by a yet undefined signal, one or more cells returns to quiescence (Dhawan and Rando 2005). Secondly, the asymmetric model has also been proposed. In this model, asymmetric division occurs immediately after satellite cell activation, at which point one daughter cell returns to quiescence, while the other daughter continues proliferating to contribute to the pool of myoblasts (Dhawan and Rando 2005). These myoblasts may also divide asymmetrically, thus further replenishing the satellite cell pool (Dhawan and Rando 2005). Support for the asymmetric hypothesis in seen in populations of actively growing satellite cells; sub-populations of satellite cells have been shown to undergo asymmetric division during mitosis resulting in selective sorting of DNA strands (Shinin *et al.* 2006). It is suggested that this selective DNA sorting

may provide a mechanism through which template DNA is protected from replication-induced errors (Shinin *et al.* 2006). Furthermore, the notch inhibitor numb is asymmetrically distributed in dividing satellite cells (Conboy and Rando 2002). It is suggested that segregation of numb may be critical in cell fate determination and in the decision to continue proliferating or to exit the cell cycle and differentiate (Conboy and Rando 2002).

1.2.2 *Muscle stem cells*

Self-renewal may not be the only method of satellite cell replenishment. Recent evidence has highlighted the possible contribution of other cell types in maintaining satellite cell number, including bone-marrow derived cells and multi-potent progenitor cells. The blood vessel-associated mesoangioblast stem cells have been detected at the periphery of muscle fibres following injection into mice, where they expressed the satellite cell markers M-cadherin and c-Met (Sampaolesi *et al.* 2003). In addition, transplantation of mesoangioblasts into the *alpha-sarcoglycan*-null mouse (α-SG$^{-/-}$), a model of limb girdle muscular dystrophy, results in the formation of new alpha-sarcoglycan expressing muscle fibres (Guttinger *et al.* 2006). Furthermore, Galvez *et al.* demonstrated that pre-treatment of mesoangioblasts with Stromal Derived Factor-1 (SDF-1) and Tumor Necrosis Factor-alpha (TNF-α), with increased expression α4-integrin enhanced the regenerative capacity of the mesoangioblasts, resulting in complete repair of skeletal muscle in the α-SG$^{-/-}$ mouse (Galvez *et al.* 2006). Populations of interstitial cells have been identified in skeletal muscle tissue and may contribute to post-natal skeletal muscle myogenesis. Tamaki *et al*. identified populations of CD45^{-}/CD34^{+}/Sca-1^{+} cells which are able to differentiate into adipocytes, endothelial and myogenic cells (Tamaki *et al.* 2002). More recently, a rare population of Pax3^{+} cells have been identified in the interstitial space of adult muscle. These cells were shown to have myogenic potential and co-express MyoD during regeneration (Kuang *et al.* 2006). Side population (SP) cells were initially identified by fluorescence-activated cell sorting (FACS) through their ability to efflux the vital dye Hoechst 33342.(Goodell *et al.* 1996; Gussoni *et al.* 1999; Seale *et al.* 2000). The majority of muscle SP cells express the early

haematopoietic stem cell marker Sca-1 but not CD45 (Buckingham 2001; Montanaro *et al.* 2004). Transplanted muscle-derived SP cells participate in muscle regeneration in *mdx* mice and appear capable of contributing to the satellite cell compartment (Gussoni *et al.* 1999). Recently it has been identified that, like satellite cells, a large proportion of limb muscle SP cells are derived from the hypaxial somite (Schienda *et al.* 2006). Further resident populations of $CD45^+$ and $Sca\text{-}1^+$ stem cells exist in skeletal muscle. However, these cells only commit to a myogenic fate after muscle injury, a process which seems to be controlled by Wnt signalling and the transcription factor Pax7 (Polesskaya *et al.* 2003; Seale *et al.* 2004). Bone marrow may also play an important role in satellite cell replenishment. Indeed, injected bone marrow-derived cells are able to contribute to skeletal muscle fibres and are able locate within the satellite cell compartment (LaBarge and Blau 2002; Dreyfus *et al.* 2004). However, a recent report demonstrates that a high proportion of bone marrow-derived cells injected into *mdx* mice fail to adopt a myogenic program (Wernig *et al.* 2005). Furthermore, Sherwood *et al.* have shown that, although bone marrow-derived cells are able to occupy the satellite cell niche and express several satellite cell markers, they are unable to contribute to the myogenic program (Sherwood *et al.* 2004). Therefore, the contribution of bone marrow-derived cells to replenishing the satellite cell population remains a matter of contention.

1.3 Skeletal muscle wasting

Muscle wasting, or atrophy, is an important process which afflicts post-natal musculature and is almost certainly responsible for the high morbidity and mortality associated with many diseases. Therefore, skeletal muscle wasting will be reviewed in the subsequent sections with emphasis on cachexia, proteolytic systems and molecular mechanisms responsible for the progression of skeletal muscle wasting.

1.3.1 Muscle atrophy

Skeletal muscle atrophy is the progressive change that occurs in post-natal musculature in response to circumstances of disuse (immobilisation, denervation and muscle unloading), starvation, ageing (sarcopenia) and disease states (cachexia; see Section 1.3.2). A number of characteristic changes define the progression of skeletal muscle atrophy, including an increase in protein degradation, a reduction in protein synthesis, a decrease in muscle fibre cross sectional area and a loss of muscle nuclei content (Mitchell and Pavlath 2001; Edgerton *et al.* 2002; Hudson and Franklin 2003; Jackman and Kandarian 2004; Sandri *et al.* 2004). These pathological changes most certainly contribute to the reduction in muscle force production and decreased resistance to fatigue that is associated with skeletal muscle atrophy.

1.3.2 Cachexia

The term cachexia is derived from the Greek words kakos (bad) and hexis (condition) and defines a condition of severe skeletal muscle loss as a result of chronic disease. Several common symptoms are associated with the progression of cachexia, including anorexia, anaemia, muscle loss and atrophy with associated asthenia (loss of muscle strength), loss of body fat and changes in lipid, carbohydrate and protein metabolism (Argiles *et al.* 1997; Argiles *et al.* 2005). Cachexia is associated with many diseases including cancer, acquired

immunodeficiency syndrome (AIDS), sepsis, congestive heart failure, diabetes and renal failure (Mitch and Goldberg 1996; Jackman and Kandarian 2004; Lecker *et al.* 2004; Boonyarom and Inui 2006). Cancer-associated cachexia often leads to a poor prognosis, with greater than half of all cancer patients experiencing some degree of cachexia (Argiles *et al.* 2003). Moreover, one third of cancer-related deaths can be attributed to the development of the cachexia syndrome rather than the disease itself (Acharyya *et al.* 2004). Early cachectic events include the release of amino acids from skeletal muscle tissue, which provides the liver with a source of amino acids for acute-phase protein synthesis and gluconeogenesis (Rosenblatt *et al.* 1983; Hasselgren and Fischer 2001; Argiles *et al.* 2006a). Both humoral (immune system released) and tumoral (tumour released) factors promote the severe muscle and fat loss observed during cachexia. Cytokines are the major humoral factors which regulate cancer-associated cachexia. Cytokines including Tumor Necrosis Factor-α (TNF-α), interleukin-1 (IL-1), interleukin-6 (IL-6) and interferon-γ (IFN-γ) have been shown to play a role in the cachectic response (Argiles *et al.* 2005; Argiles *et al.* 2006b) (reviewed in Section 1.3.4.1). In addition, the tumoral factors toxohormone-L, anaemia-inducing substance, lipid-mobilising factor and proteolysis-inducing factor (PIF) (reviewed in Section 1.3.4.2) are released by the tumour during the progression of cachexia (Argiles *et al.* 2005).

1.3.3 *Skeletal muscle proteolytic systems*

Skeletal muscle is a dynamic tissue undergoing constant cycles of degradation and subsequent regeneration. The degradation of skeletal muscle proteins is controlled by three major proteolytic systems, the ATP-dependent ubiquitin-proteasome pathway, the calcium-dependent calpain pathway and the lysosomal protease system. These three major proteolytic pathways are discussed in the subsequent sections.

1.3.3.1 Lysosomal protease system

Lysosomes play an important role in skeletal muscle proteolysis with a primary role in the degradation of membrane lipids and membrane proteins including receptors and ion channels (Bechet *et al.* 2005; Tisdale 2005). Lysosomes are membrane-bound vesicles which contain various acid hydrolases including proteases, glycosidases, lipases, nucleases and phosphatases (Bechet *et al.* 2005). The ubiquitously expressed cathepsins, L, B, D and H form the major component of lysosomal proteases (Bechet *et al.* 2005), and indeed have been shown to be associated with several forms of muscle wasting. In particular, *cathepsin B* mRNA expression is shown to increase in muscle tissue from patients with lung cancer (Jagoe *et al.* 2002). Increased mRNA expression of both *cathepsin B* and *cathepsin D* has also been reported during glucocorticoid-induced muscle wasting and disuse atrophy (Dardevet *et al.* 1995; Taillandier *et al.* 1996). Furthermore, Deval *et al*. have demonstrated that cathepsin L mRNA and protein levels were elevated in a rat model of sepsis, and that *cathepsin L* mRNA expression was increased following glucocorticoid (dexamethasone; Dex) treatment and in rats bearing the AH-130 tumour (Deval *et al.* 2001). In addition, microarray analysis has identified enhanced expression of *cathepsin L* in rat models of muscle wasting induced by fasting, uraemia (chronic renal failure), diabetes mellitus and tumour growth (Lecker *et al.* 2004). Conversely, IGF-1 mediated inhibition of burn-induced skeletal muscle wasting is associated with a decrease in Cathepsin B and Cathepsin L activity (Fang *et al.* 2002).

1.3.3.2 Calcium-dependent pathway

Calcium-dependent proteolysis is mediated through the action of calcium-activated cysteine proteases termed calpains (Costelli *et al.* 2005). Calpain-1 (μ-calpain), calpain-2 (m-calpain) and calpain-3 are all highly expressed in skeletal muscle tissue, however, in contrast to the ubiquitously expressed calpains 1 and 2, calpain-3 is reported to be expressed specifically in muscle tissue (Bartoli and Richard 2005; Kramerova *et al.* 2005). Calpains normally exist in a dormant state in the cytosol however, in response to increasing levels of intracellular calcium, calpains translocate to the plasma membrane to become activated by Ca^{2+} and

phospholipids (Goll *et al.* 2003; Costelli *et al.* 2005). Calpains appear to be critical for initiating the degradation of myofibrillar proteins, including the Z-disc associated proteins filamin, nebulin, titin, troponin-T and desmin (Solomon and Goldberg 1996; Huang and Forsberg 1998; Williams *et al.* 1999b; Bartoli and Richard 2005). In contrast, calpains are unable to degrade actin and myosin; instead calpains facilitate the release of these proteins from the sarcomere allowing for their subsequent degradation through the ubiquitin-proteasome pathway (Solomon and Goldberg 1996; Huang and Forsberg 1998; Williams *et al.* 1999b; Bartoli and Richard 2005). The calcium-dependent calpain pathway has been associated with several forms of muscle wasting. Calpains may have a role in the severe pathology associated with muscular dystrophy. Duchenne muscular dystrophy (DMD) is characterised by mutations in the *dystrophin* gene which results in the complete absence of Dystrophin. Dystrophin, a large cytoskeletal protein, associates with several sarcolemmal proteins and glycoproteins to form the dystrophin-glycoprotein complex, which is critical for interactions between the cytoskeleton and the extracellular matrix (Porter *et al.* 2002). Absence of dystrophin weakens the sarcolemma allowing influx of extracellular calcium into the myofibril (Costelli *et al.* 2005). Indeed, elevated levels of intracellular calcium are observed in *mdx* mice, a model of DMD, with an associated increase in calpain expression (Spencer *et al.* 1995; Hopf *et al.* 1996). Furthermore, it has been demonstrated that treatment of *mdx* mice with the calpain inhibitor Calpastatin alleviates the muscle wasting associated with this disease (Spencer and Mellgren 2002). Calpains may also play an important role in muscle wasting associated with sepsis. In fact, it has been recently shown that treatment with the calpain inhibitors calpeptin and BN82270 blocks sepsis-induced protein degradation in the rat (Fareed *et al.* 2006). In addition, transgenic mice over-expressing calpastatin demonstrate greatly reduced skeletal muscle atrophy following hindlimb unloading (Tidball and Spencer 2002). Calpains may also regulate protein degradation during cancer cachexia. Increased m-calpain has been observed in skeletal muscle tissue from rats containing the Yoshida AH-130 tumour (Temparis *et al.* 1994; Costelli *et al.* 2005); furthermore, increased calpain-dependent proteolytic activity is observed in AH-130 tumour-bearing rats (Costelli *et al.* 2002).

1.3.3.3 *Ubiquitin-proteasome pathway*

Ubiquitin-mediated degradation is an ordered process which results in the eventual poly-ubiquitination of substrate proteins and degradation by the 26S proteasome (Figure 1.4A and Figure 1.4B). Firstly, ubiquitin must be activated by an ubiquitin-activating enzyme (E1), an ATP-dependent 2-step process which results in the formation of an ubiquitin-E1 thiol ester product (Tisdale 2005; Wing 2005; Nandi *et al.* 2006) (Figure 1.4A). The activated ubiquitin is then transferred to an ubiquitin-conjugating enzyme (E2), also termed the ubiquitin carrier protein. These E2 enzymes associate with a third class of enzyme, E3 ubiquitin protein ligases (Figure 1.4A). The E3 enzymes are responsible for the transfer of the ubiquitin from the E2 to a specific target substrate or protein, with subsequent rounds of E3-mediated ubiquitin ligation resulting in poly-ubiquitination of target proteins (Figure 1.4A and Figure 1.4B). In some circumstances a fourth enzyme (E4) functions to lengthen the ubiquitin chains on target proteins (Tisdale 2005; Nandi *et al.* 2006). Ubiquitin-tagged proteins are marked for degradation by the 26S proteasome. The 26S proteasome complex is formed when two 19S cap particles associate, in an ATP-dependent manner, with each end of the 20S proteasome (Nandi *et al.* 2006) (Figure 1.4B). The 19S cap is responsible for unfolding proteins and facilitating their entry into the 20S proteasome. The 20S proteasome, comprised of two outer α rings and two inner β rings (Figure 1.4B), contains the proteolytic core and is responsible for degrading target proteins in an ATP-independent manner (Tisdale 2005; Nandi *et al.* 2006). The ubiquitin-proteasome pathway typically functions to degrade damaged or defective proteins within the cell. However, ubiquitin-mediated proteolysis is also involved in degradation of tumour-suppressor proteins, oncoproteins and cell cycle regulators including cyclins and cyclin-dependent kinases. In addition to degrading aberrant proteins, the ubiquitin-proteasome pathway is further implicated in transcriptional activation (Yu *et al.* 1998; Lipford and Deshaies 2003; Tisdale 2005; Wang *et al.* 2005). The ubiquitin-proteasome pathway plays a major role in protein degradation during muscle wasting with the majority of myofibrillar proteins targeted for degradation through this ATP-dependent mechanism (Solomon and Goldberg 1996). It has been shown that myosin, actin, troponin and tropomyosin are targeted for degradation by the ubiquitin-proteasome pathway (Solomon and Goldberg 1996).

However, it is noteworthy to mention that the ubiquitin-proteasome pathway is unable to degrade these proteins while the myofibrils remain intact (Solomon and Goldberg 1996), suggesting the involvement of more than one proteolytic pathway in the process of skeletal muscle degradation (see Section 1.3.3.2). Enhanced expression of ubiquitin-proteasome pathway components is linked with several forms of skeletal muscle wasting. Increased mRNA expression of both *polyubiquitin* and proteasome subunits (*C-1*, *C-3*, *C-5*, *C-8* and *C-9*) has been observed in models of starvation and denervation-induced muscle atrophy (Medina *et al.* 1995). In addition, enhanced levels of ubiquitin-conjugated proteins were observed during hindlimb unloading experiments in the rat (Vermaelen *et al.* 2005). Furthermore, higher mRNA expression of proteasome subunits, *ubiquitin* and the ubiquitin-conjugating enzyme $E2_{14k}$ were detected in rat models of diabetes and glucocorticoid-induced muscle proteolysis (Auclair *et al.* 1997; Mitch *et al.* 1999). Muscle degradation during cancer is also associated with enhanced ubiquitin-proteasome activity. Indeed, rats bearing the Yoshida ascites hepatoma-130 (AH-130) have enhanced expression of ubiquitin (Costelli *et al.* 2006) and ubiquitin-proteasome subunits, with an associated increase in the levels of ubiquitin-conjugated proteins (Baracos *et al.* 1995). Furthermore, several studies on cancer patients have identified an associated increase in the expression of ubiquitin-proteasome pathway genes, including ubiquitin, several proteasome subunits and the conjugating enzyme $E2_{14k}$ (Williams *et al.* 1999a; Bossola *et al.* 2001; Khal *et al.* 2005). Therefore, ubiquitin-mediated degradation may play a major role in the severe muscle loss associated with cancer.

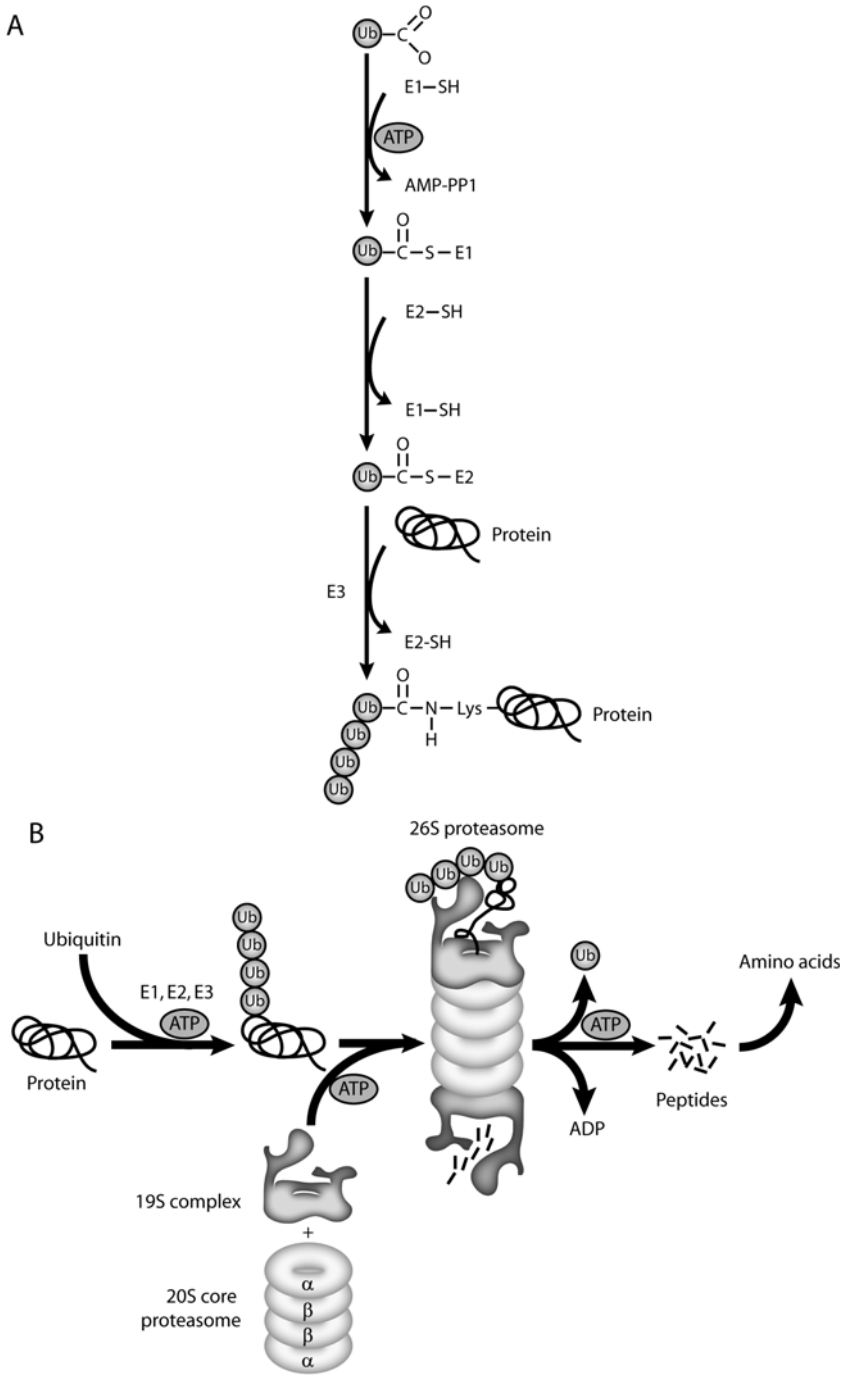

Figure 1.4 *The ubiquitin-proteasome pathway*

A) An ordered series of events results in the poly-ubiquitination of target proteins for their eventual degradation through the 26S proteasome. Firstly, ubiquitin is activated by an E1 enzyme and subsequently transferred to a conjugating enzyme (E2). The E3 enzymes transfer ubiquitin from the E2 enzyme to a target protein. Multiple rounds of E3-mediated ubiquitin ligation results in a poly-ubiquitinated protein ready for degradation. B) Poly-ubiquitinated proteins are targeted by the 26S proteasome for degradation in an ATP-dependent manner resulting in the breakdown of target proteins and the release of amino acids. Modified from Mitch and Goldberg (Mitch and Goldberg 1996).

The muscle-specific ubiquitin E3 ligases Atrogin-1 (MAFbx) and MuRF-1 (Bodine *et al.* 2001; Gomes *et al.* 2001) are gaining recognition as two important markers of muscle atrophy. The expression of both Atrogin-1 and MuRF-1 are consistently up-regulated in several forms of skeletal muscle wasting. Expression of *atrogin-1* and *MuRF-1* is shown to be dramatically increased in muscle atrophy associated with immobilisation, denervation, hindlimb suspension, glucocorticoid (Dex) treatment and addition of the cachectic cytokine, interleukin-1 (Bodine *et al.* 2001; Krawiec *et al.* 2005). Bodine *et al*. also demonstrated that mice deficient in *atrogin-1* or *MuRF-1* were more resistant to the effects of denervation-induced muscle atrophy (Bodine *et al.* 2001). Additional studies have identified increased expression of *atrogin-1* and *MuRF-1* in muscle wasting associated with fasting, diabetes, renal failure and cancer conditions (Gomes *et al.* 2001; Lecker *et al.* 2004; Costelli *et al.* 2006). Furthermore, in a recent study addressing age-associated muscle loss (sarcopenia), the levels of both *atrogin-1* and *MuRF-1* were significantly increased in an aged rat model (Clavel *et al.* 2006). However, in contrast, no differences were observed in the expression of both *atrogin-1* and *MuRF-1* in young versus old human patients, a phenomenon attributed to the physical inactivity of both groups (Whitman *et al.* 2005). Recently, Lang *et al.* have shown that burn-induced injury in rats results in an increase in the mRNA expression of both *atrogin-1* and *MuRF-1,* concomitant with a reduction in *M. gastrocnemius* muscle weight. Thus Atrogin-1 and MuRF-1 appear to be useful molecular markers for measuring the incidence of skeletal muscle atrophy associated with various causes (Lang *et al.* 2006).

Recently, Atrogin-1 has been shown to degrade the myogenic regulatory factor MyoD, and in fact over-expression of Atrogin-1 is demonstrated to antagonise MyoD-mediated myogenic differentiation with a subsequent loss in myotube formation (Tintignac *et al.* 2005). Thus Atrogin-1 may be important in timely regulation of skeletal muscle differentiation through regulation of MyoD expression (Tintignac *et al.* 2005). The Nuclear Factor-kappa B (NF-κB) pathway has been implicated in skeletal muscle wasting. Indeed, transgenic mice which have enhanced NF-κB activity show a dramatic muscle wasting phenotype. Furthermore, the profound muscle wasting in these mice was associated with an increase in the expression of MuRF-1 (Cai *et al.* 2004). Interestingly, activation of the NF-κB pathway requires ubiquitin-mediated degradation of Inhibitor of

kappa B (IκB) protein, which binds to, and represses NF-κB nuclear import and thus transcriptional activity. Furthermore, the NF-κB sub-units p50 and p52 are generated through proteasome-mediated degradation of p105 and p100 respectively (Chen 2005), highlighting a role for the ubiquitin-proteasome pathway in regulation of NF-κB activity.

1.3.4 Factors associated with muscle wasting

1.3.4.1 Cytokines - Tumor Necrosis Factor and Interleukins

Tumor necrosis factor-α (TNF-α), formerly cachectin, is a pro-inflammatory cytokine which is involved in many aspects of cachexia. TNF-α is associated with many forms of muscle wasting including that associated with disease. Elevated levels of TNF-α are seen in patients with cachexia associated with prostate cancer, chronic obstructive pulmonary disease and chronic heart failure (Di Francia *et al.* 1994; Zhao and Zeng 1997; Nakashima *et al.* 1998). Furthermore, the levels of TNF-α as well as the pro-inflammatory cytokines interleukin-1β (IL-1β), and interleukin-6 (IL-6), are elevated during the progression of human immunodeficiency virus (HIV) in women (Belec *et al.* 1995). In addition, TNF-α is also detected in serum samples of patients with pancreatic cancer (Karayiannakis *et al.* 2001). Karayiannakis *et al.* also reported that elevated levels of TNF-α were associated with reduced body weight and body mass index and a greatly reduced serum protein level (Karayiannakis *et al.* 2001). Over-expression of TNF-α has also been shown to promote skeletal muscle wasting. Two studies have analysed the effect of injecting TNF-α-secreting Chinese hamster ovary (CHO) cells into nude mice. Results indicated that continual release of TNF-α into the nude mice promoted the development of severe cachexia (Oliff *et al.* 1987; Tracey *et al.* 1990).

Several *in vitro* studies have provided insights into the possible mechanism through which cytokines function. Over-expression of TNF-α in the C2C12 system enhanced cell proliferation, however the increased levels of TNF-α reduced the expression of MyoD and myogenin and prevented the appearance of

myogenic differentiation markers such as myosin heavy chain (MHC) (Szalay *et al.* 1997). Guttridge *et al.* have further studied the role of TNF-α in regulation of MyoD and skeletal muscle differentiation. TNF-α-mediated NF-κB activation resulted in inhibition of MyoD, with subsequent inhibition of differentiation. Furthermore, it was reported that TNF-α, in conjunction with interferon-γ (IFN-γ), was required for down-regulation of MyoD in differentiated myotubes (Guttridge *et al.* 2000). TNF-α is a potent activator of NF-κB. Indeed, TNF-α has been shown to promote ubiquitin-mediated degradation of the NF-κB inhibitor IκBα, resulting in enhanced NF-κB binding to its target sequence (Li *et al.* 1998). Furthermore, Li and Reid generated C2C12 stable cell lines transfected with constructs expressing a mutated form of IκBα, which is resistant to ubiquitin-mediated degradation and thus functions to selectively inhibit NF-κB signalling. In control cells, treatment with TNF-α resulted in a reduction in protein content and myosin expression, while in mutant cell lines no effect on protein or myosin levels were detected. Thus it was suggested that NF-κB is required for TNF-α-mediated proteolysis (Li and Reid 2000). TNF-α has been demonstrated to result in enhancement of the ubiquitin-proteasome pathway. Indeed, administration of TNF-α was shown to increase the levels of ubiquitin-conjugated proteins (Garcia-Martinez *et al.* 1993). Conversely, inhibition of TNF-α, through injection of anti-TNF antibodies, inhibited TNF-α-mediated up-regulation of ubiquitin and the proteasome subunit C-8 in AH-130 tumour-bearing rats (Llovera *et al.* 1996). More recently it has been demonstrated that *in vitro* and *in vivo* addition of TNF-α, resulted in an up-regulation of *atrogin-1* mRNA expression (Li *et al.* 2005a). Li *et al*. further demonstrated that the TNF-α-induced up-regulation of *atrogin-1* is mediated through the p38 mitogen-activated protein kinase (MAPK) signalling pathway. Treatment of C2C12 myoblasts with TNF-α has been shown to induce apoptosis (Stewart *et al.* 2004). Furthermore, Tolosa *et al.* have demonstrated that treatment with IFN-γ prevented TNF-α-mediated apoptosis in C2C12 cells, through targeted down-regulation of the subtype 2 TNF-α receptor (TNF-R2) (Tolosa *et al.* 2005).

Recently, tumour necrosis factor-like weak inducer of apoptosis (TWEAK) has been shown to regulate myoblast differentiation (Dogra *et al.* 2006). Treatment with TWEAK resulted in activation of the NF-κB signalling cascade and inhibition of differentiation in C2C12 and primary myoblasts. Furthermore,

TWEAK inhibited the expression of MyoD and myogenin and also promoted MyoD degradation. Therefore, Dogra *et al* suggested that TWEAK negatively regulates myogenesis through preceding activation of NF-κB and degradation of MyoD.

In addition to TNF-α, the interleukin family of cytokines play important roles in the progression of skeletal muscle wasting. The anorectic cytokine interleukin-1 (IL-1) has been associated with diminished food intake and subsequent induction of anorexia (Hellerstein *et al.* 1989; Laviano *et al.* 1999). However, the role of IL-1 in cachexia is a matter of contention. Indeed, injection of an IL-1 receptor antagonist failed to ameliorate the symptoms of cancer-induced cachexia (Argiles *et al.* 2005). Interleukin-1β (IL-1β) has been shown to impair IGF-1-dependent C2C12 myoblast differentiation, resulting in the inhibition of protein synthesis and a reduction in the expression of myogenin and myosin (Broussard *et al.* 2004). Interleukin-6 (IL-6) has been implicated in the progression of cachexia. Increased serum levels of IL-6 are detected in patients with Hodgkin's lymphoma (Kurzrock *et al.* 1993). Furthermore, increased circulating levels of IL-6 were detected in non-small-cell lung cancer patients with associated weight loss (Scott *et al.* 1996). Conversely, treatment of colon-26 tumour-bearing mice with the IL-6 specific antagonist, 20S, 21-epoxy-resibufogenin-3-acetate (ERBA), greatly reduced the body weight loss associated with this model of cancer cachexia (Enomoto *et al.* 2004). In addition, antibody-mediated inhibition of IL-6, inhibits the severe cachexia associated with injection of human melanoma and prostate cells into nude mice (Zaki *et al.* 2004). Subcutaneous injection of IL-6 has also been shown to induce myocardial dysfunction with associated skeletal muscle atrophy (Janssen *et al.* 2005). Furthermore, Haddad *et al.* demonstrated that administration of IL-6 to rats resulted in skeletal muscle atrophy concomitant with a reduction of myofibrillar protein (Haddad *et al.* 2005).

Another cytokine of particular interest with respect to cachexia is interferon-γ (IFN-γ). IFN-γ is produced by activated T and natural killer cells and shares common functions to those of TNF-α (Argiles *et al.* 2005). Matthys *et al*. demonstrated that injection of IFN-γ-specific monoclonal antibodies into a tumour-bearing (Lewis lung carcinoma; LLC) mouse model alleviated the muscle loss associated with the presence of this tumour (Matthys *et al.* 1991). In addition, severe cachexia develops in nude mice following injection of CHO cells

constitutively expressing IFN-γ (Matthys *et al.* 1991). More recently, a study by Acharyya *et al*. has demonstrated a dual requirement for TNF-α and IFN-γ in suppression of the myofibrillar protein myosin (Acharyya *et al.* 2004).

1.3.4.2 *Proteolysis-inducing factor (PIF)*

The sulfated glycoprotein proteolysis-inducing factor (PIF) was initially purified from the cachexia-inducing MAC16 colon adenocarcinoma (McDevitt *et al.* 1995). PIF is detected in urine samples of cancer patients who have experienced weight loss, while in contrast, PIF is absent in urine from cancer patients with no associated weight loss, suggesting a role for PIF in the cachectic state associated with cancer (Cariuk *et al.* 1997). Injection of PIF into mice has been shown to result in 10% body weight loss, which was accounted for in equal amounts by increased protein degradation and decreased protein synthesis (Lorite *et al.* 1997). Furthermore, Smith *et al.* have demonstrated that treatment of C2C12 myoblasts with PIF resulted in a dose-dependent decrease in protein synthesis, concomitant with an increased rate of protein degradation through a mechanism involving increased production of 15-hydroxyeicosatetraenoic acid (15-HETE) (Smith *et al.* 1999). The ATP-dependent ubiquitin-proteasome pathway appears to be the major mechanism through which PIF induces skeletal muscle proteolysis. Indeed exposure of MAC16 tumour-bearing mice to PIF results in enhanced levels of ubiquitin-conjugated proteins and increased mRNA expression of $E2_{14k}$ and the *C-9* proteasome subunit (Lorite *et al.* 1998). Similarly, injection of PIF into normal mice resulted in an increase in mRNA expression of *ubiquitin*, $E2_{14k}$, and the *C-9* proteasome sub-unit. Furthermore, enhanced protein expression of the 20S and 19S proteasome components was observed following injection of PIF (Lorite *et al.* 2001). More recently, addition of PIF to C2C12 myotubes has been shown to result in enhanced protein degradation with an associated increase in the mRNA expression of proteasome *C-2* and *C-5* subunits (Wyke *et al.* 2005). PIF has also been shown to interact with the NF-κB signalling pathway. Whitehouse and Tisdale demonstrated that addition of PIF to C2C12 myotubes reduced the levels of the NF-κB inhibitor IκBα and also enhanced the nuclear entry of NF-κB (Whitehouse and Tisdale 2003). More recently, Wyke and Tisdale have studied the involvement of the NF-κB in PIF-mediated proteolysis. In this study C2C12

cells were transfected with a construct harboring a mutant form of the NF-κB inhibitor IκBα, which is resistant to ubiquitin-proteasome degradation, and thus acts as a potent inhibitor of NF-κB mediated transcription. In the presence of mutant IκBα, administration of PIF was unable to induce protein degradation and loss of myosin in the C2C12 cell line. Furthermore, PIF-mediated up-regulation of the 20S and 19S proteasome sub-units and the $E2_{14k}$ conjugating enzyme was abolished in the presence of mutated IκBα (Wyke and Tisdale 2005). Therefore, it is suggested that functional NF-κB signalling is critical for the ability of PIF to induce protein degradation and the expression of members of the ubiquitin-proteasome pathway (Wyke and Tisdale 2005).

1.3.4.3 *Insulin-like growth factor-1 (IGF-1)*

Insulin-like growth factor-1 (IGF-1) is a positive regulator of skeletal muscle mass and has critical functions in regulating growth, repair and maintenance of skeletal muscle (Heszele and Price 2004; Glass 2005). Furthermore, IGF-1 appears to play a major role in regulating increases in skeletal muscle mass or hypertrophy. Indeed, skeletal muscle hypertrophy is accompanied by an increase in the expression of IGF-1 (DeVol *et al.* 1990). Furthermore, muscle-specific over-expression of IGF-1 in mice results in a dramatic increase in skeletal muscle hypertrophy, while mice over-expressing a muscle-specific dominant-negative form of the IGF-1 receptor exhibit reduced skeletal muscle mass and hypoplasia (Musaro *et al.* 2001; Fernandez *et al.* 2002). In contrast, treatment of C2C12 myotubes with IGF-1 results in myotube hypertrophy (Rommel *et al.* 2001). Rommel *et al*. have further highlighted a potential mechanism through which IGF-1 regulates skeletal muscle hypertrophy, specifically, IGF-1 was shown to induce hypertrophy through the phosphatidylinositol 3-kinase (PI3-K)-AKT pathway. Briefly, IGF-1 receptor binding initiates activation of PI3-K; once activated, PI3-K facilitates binding of AKT to the cell membrane, where it is subsequently phosphorylated and activated by the 3-phosphoinositide-dependent protein kinase PDK-1. AKT is the downstream mediator of IGF-1 signalling and affects several downstream targets, including mTOR and GSK3 which are both implicated in IGF-1-mediated skeletal muscle hypertrophy (Rommel *et al.* 2001; Vivanco and Sawyers 2002).

Several studies have highlighted a critical role for IGF-1 in the prevention of skeletal muscle atrophy. Muscle-specific over-expression of IGF-1 in the *mdx* mouse model of DMD alleviates the dramatic muscle loss associated with this disease (Barton *et al.* 2002). Specifically, increased IGF-1 expression resulted in a 40% increase in *M. extensor digitorum longus* (EDL) muscle mass with an associated improvement in muscle force production (Barton *et al.* 2002). Furthermore, Sacheck *et al.* have demonstrated that treatment of C2C12 myotube cultures with IGF-1 prevents Dex-mediated proteolysis, concomitant with a rapid down-regulation of *atrogin-1* mRNA expression (Sacheck *et al.* 2004). In addition, transgenic mice over-expressing skeletal muscle specific IGF-1 were shown to be resistant to angiotensin-II-mediated skeletal muscle loss (Song *et al.* 2005). Song *et al* further demonstrated that over-expression of IGF-1 blocked angiotensin-II-induced expression of the ubiquitin E3 ligases Atrogin-1 and MuRF-1. Thus IGF-1-mediated inhibition of skeletal muscle proteolysis may be due to regulation of the ubiquitin-proteasome pathway.

The Forkhead box O (FoxO) class of transcription factors, consisting of FoxO1 (FKHR), FoxO3 (FKHRL1) and FoxO4 (AFX) (Barthel *et al.* 2005), are reported targets of the IGF-1/PI3-K/AKT pathway. Indeed, activation of the PI3-K/AKT pathway results in the phosphorylation of FoxO proteins. The phosphorylated FoxO proteins are subsequently excluded from the nucleus, resulting in an inhibition of FoxO-mediated transcription (Brunet *et al.* 1999). In support, AKT has been shown to block FoxO1-mediated transcription through specific phosphorylation of FoxO1 at three different phospho-acceptor sites (Tang *et al.* 1999). Interestingly, deactivation of the IGF-1/PI3-K/AKT pathway highlights a connection between FoxO activation and the transcriptional regulation of ubiquitin components during atrophy. Indeed, angiotensin-II-induced muscle wasting is associated with dephosphorylation of AKT, FoxO1, and FoxO3 with a subsequent increase in the mRNA expression of *atrogin-1* and *MuRF-1* (Song *et al.* 2005). A similar pattern of gene regulation is observed in starvation and dexamethasone-induced myotube atrophy *in vitro* (Sandri *et al.* 2004). Furthermore FoxO3 has been shown to directly activate the *atrogin-1* promoter in a mouse model of starvation; conversely, siRNA-mediated knock-down of FoxO proteins prevented *atrogin-1* promoter up-regulation. Thus it is suggested that FoxO transcription factors play a critical role in the progression of skeletal muscle

atrophy (Sandri *et al.* 2004). Therefore it is apparent that the IGF-1/PI3-K/AKT pathway is critical in regulating FoxO protein function; moreover it is suggested that the IGF-1/PI3-K/AKT pathway prevents the induction of the ubiquitin E3 ligases Atrogin-1 and MuRF-1 through AKT-mediated phosphorylation and inactivation of FoxO1 (Stitt *et al.* 2004).

1.3.4.4 *Myostatin*

The secreted growth factor myostatin is involved in the negative regulation of skeletal muscle mass. A number of studies have implicated myostatin in the regulation of skeletal muscle wasting, and recent data has highlighted an involvement of myostatin in ubiquitin-mediated degradation (see Section 1.4.5.4). A detailed review of myostatin biology and physiological effects is discussed in the following section (see Section 1.4).

1.4 Myostatin

1.4.1 The myostatin gene, structure and processing

Myostatin, or growth and differentiation factor-8 (GDF-8), is a TGF-β superfamily member that was initially characterised in 1997 as a specific regulator of skeletal muscle mass in mice (McPherron *et al.* 1997). Targeted disruption of the *myostatin* gene in mice (Figure 1.5A and Figure 1.5B) resulted in a generalised increase in skeletal muscle mass (double-muscling); in particular a 2-3-fold increase in muscle weight was observed with no corresponding increase in adipose tissue (Figure 1.5A and Figure 1.5B). The enhanced muscle phenotype in the *myostatin*-null mice was determined to result from a combination of both muscle hyperplasia and hypertrophy (McPherron *et al.* 1997).

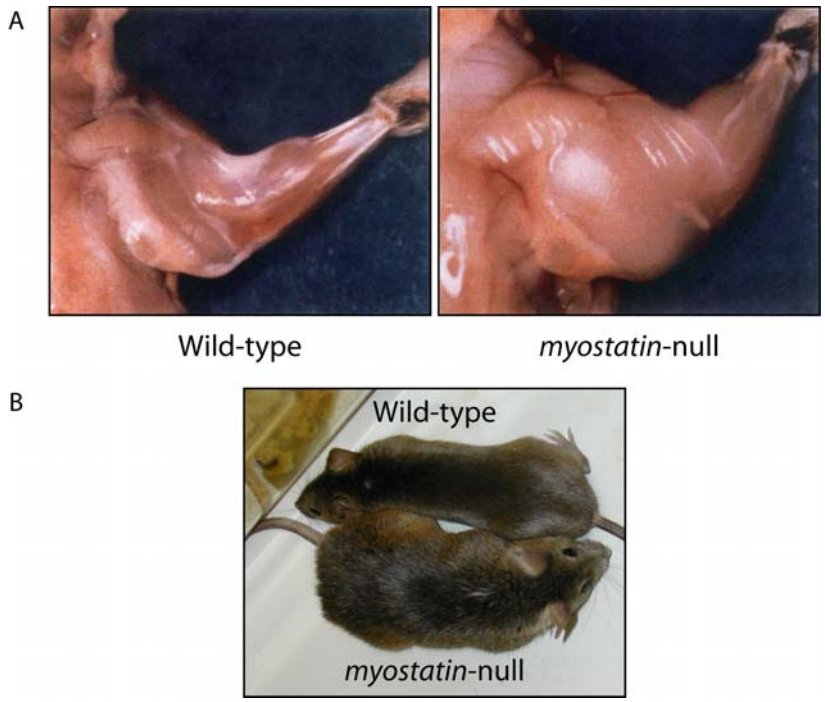

Figure 1.5 *Double-muscling in myostatin-null mice*

A) Photograph showing the difference between the forelimbs of wild-type and *myostatin*-null mice. A dramatic increase in skeletal muscle mass is observed in the *myostatin*-null mice compared to wild-type mice (adapted from McPherron *et al.* 1997). B) Photograph showing the size difference between wild-type and *myostatin*-null mice at the same age. *Myostatin*-null mice were generated by McPherron *et al.* (1997).

Myostatin has a number of characteristics common to the TGF-β superfamily (Figure 1.6). In particular, the precursor Myostatin molecule contains an N-terminal (NH2) core of hydrophobic amino acids that functions as a signal sequence for secretion (McPherron *et al.* 1997). In addition, the C-terminal (COOH) region of Myostatin contains nine conserved cysteine residues which are critical for homodimerisation and for the formation of the "cysteine knot" structure, a characteristic feature of the TGF-β superfamily (McPherron and Lee 1996; McPherron *et al.* 1997). Furthermore, Myostatin is synthesised as a 376 amino acid precursor protein which, like other members of the TGF-β superfamily, is proteolytically cleaved at the RSRR site (Figure 1.6), a process which may occur within the Golgi apparatus under the control of the serine protease furin or other members of the proprotein convertase family (McPherron *et al.* 1997; Sharma *et al.* 1999; Lee and McPherron 2001). The importance of proteolytic processing is clear, as generation of a dominant-negative form of Myostatin, through mutation of the RSRR site to the amino acids GLDG, results in widespread skeletal muscle hypertrophy (Zhu *et al.* 2000). Cleavage of the 52 kDa precursor protein at the RSRR site has been reported to result in the formation of a 36/40 kDa Latency-Associated Peptide (LAP) and a 12.5/26 kDa mature portion, which is suggested to correspond to a C-terminal monomer or dimer respectively (Thomas *et al.* 2000; Lee and McPherron 2001; McFarlane *et al.* 2005).

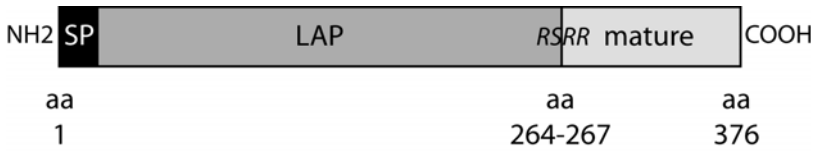

Figure 1.6 *The structure of myostatin*

Schematic representation of the structure of Myostatin. Myostatin shares characteristics common to the TGF-β superfamily, including a signal peptide (SP) for secretion and a RSRR proteolytic processing site. Proteolytic processing of Myostatin gives rise to LAP and mature Myostatin regions. Adapted from Joulia-Ekaza and Cabello (Joulia-Ekaza and Cabello 2006).

1.4.2 Expression of myostatin

Myostatin is first detected in mice embryos at day 9.5 post-coitum, where it is specifically located within the most rostral somites (McPherron *et al.* 1997). By day 10.5 post-coitum, myostatin is expressed in the majority of the somites, specifically located in the myotome layer of developing somites (McPherron *et al.* 1997). In cattle, low levels of *myostatin* mRNA are detected in day 15 to day 29 embryos with increasing expression detected from day 31 onwards (Kambadur *et al.* 1997; Bass *et al.* 1999; Oldham *et al.* 2001). Furthermore, in the pig foetus *myostatin* mRNA expression is abundant at days 21 and 35 of gestation, with an increase in expression by day 49 (Ji *et al.* 1998). In the chicken *myostatin* expression is first detected as early as embryonic day 0 (the blastoderm stage) with relatively low levels detected through to embryonic day 6. From day 7, *myostatin* mRNA levels rapidly increase and level off through to day 16 (Kocamis *et al.* 1999). Post-natal skeletal muscle continues to express *myostatin*, although variation in *myostatin* expression is observed between individual muscles (Kambadur *et al.* 1997; McPherron *et al.* 1997). The expression of *myostatin* is primarily restricted to skeletal muscle (Kambadur *et al.* 1997; McPherron *et al.* 1997; Ji *et al.* 1998; Bass *et al.* 1999; Carlson *et al.* 1999; Kocamis *et al.* 1999; Sazanov *et al.* 1999; Jeanplong *et al.* 2001; Oldham *et al.* 2001), however, low levels of myostatin expression have been detected in various other tissues; in particular in the secretory lobules of lactating mammary glands (Ji *et al.* 1998), in adipose tissue (McPherron *et al.* 1997), and in cardiomyocytes and Purkinje fibres of the heart (Sharma *et al.* 1999). More recently it has been shown that both myostatin mRNA and protein are expressed in human placental tissue. The presence of myostatin in the placenta is suggested to be involved with uptake of glucose (Mitchell *et al.* 2006).

Myostatin expression may also be associated with specific fibre types in skeletal muscle. Carlson *et al*. have shown that higher amounts of myostatin mRNA and protein are detected in fast-twitch muscle (type-II fibres) as compared to slow-twitch muscle (type-I fibres) (Carlson *et al.* 1999). Furthermore, it has been shown that in *myostatin*-null mice there is an increase in fast fibres (type-II) in the typically slow fibre-dominated *M. soleus* muscle, and a switch from oxidative (type-IIA) to glycolytic fibres (type-IIB) in the predominantly fast-twitch EDL

muscle (Girgenrath *et al.* 2005). Therefore, suggesting a fibre type-specific role for Myostatin in regulation of muscle physiology.

1.4.3 *Regulation of myostatin*

Myostatin is synthesised as a precursor protein, proteolytically processed and secreted to elicit its biological function. Studies have highlighted the importance of several proteins that interact with myostatin to regulate its action. Myostatin has been shown to interact with the sarcomeric protein Titin-cap (Nicholas *et al.* 2002); specifically, titin-cap interacts with the C-terminal mature portion of Myostatin (Nicholas *et al.* 2002). Over-expression of titin-cap had no effect on Myostatin synthesis and processing, however, increased titin-cap expression results in enhanced cell proliferation and accumulation of processed Myostatin within myoblasts. Thus titin-cap appears to function by regulating the secretion of mature Myostatin (Nicholas *et al.* 2002). In addition, human small glutamine-rich tetratricopeptide repeat-containing protein (hSGT) has been shown to associate with intracellular myostatin (Wang *et al.* 2003). The C-terminal region of hSGT and the N-terminal signal peptide region of Myostatin were shown to be critical for this interaction. It is suggested that hSGT likely plays a role in mediating Myostatin secretion and activation (Wang *et al.* 2003). Latent TGF-β binding proteins (LTBPs) are extracellular matrix proteins which have been previously identified to interact with the TGF-β superfamily (Saharinen *et al.* 1999). LTBPs associate with TGF-β superfamily members to allow for secretion; once secreted, removal of LTBPs from the latent complex is essential for TGF-β activation (Saharinen *et al.* 1999). Although LTBPs play an essential role in the secretion and activation of TGF-β superfamily members, published results from this thesis suggest that LTBPs do not play a role in the regulation of myostatin (McFarlane *et al.* 2005). Following secretion, the majority of Myostatin (>70%), like TGF-β, has been shown to exist in an inactive latent complex both *in vitro* and *in vivo,* whereby the mature processed portion of Myostatin is bound non-covalently to the propeptide (LAP) region of Myostatin (Lee and McPherron 2001; Thies *et al.* 2001; Yang *et al.* 2001). Recently it has been demonstrated that members of the bone morphogenetic protein-1/tolloid (BMP-1/TLD) family can cleave the Myostatin LAP region from the latent Myostatin complex, thus

resulting in activation of mature Myostatin (Wolfman *et al.* 2003). Furthermore, Wolfman *et al*. demonstrated that a mutation of LAP to confer resistance to cleavage by BMP/TLD resulted in enhanced muscle mass *in vivo*. Previous studies have demonstrated that follistatin is capable of binding and inhibiting various members of the TGF-β superfamily (Michel *et al.* 1993; Hemmati-Brivanlou *et al.* 1994; Fainsod *et al.* 1997). Follistatin has been shown to bind directly to the mature portion of Myostatin blocking the ability of Myostatin to bind with the ActRIIB receptor (Lee and McPherron 2001). Furthermore, interaction with follistatin interferes with the intrinsic ability of myostatin to inhibit muscle differentiation (Amthor *et al.* 2004) (reviewed in Section 1.4.5.2). In support, mice over-expressing follistatin show a drastic increase in muscle mass, significantly greater than that of *myostatin*-null animals (Lee and McPherron 2001). Additionally, *follistatin*-null mice demonstrate reduced muscle mass at birth (Matzuk *et al.* 1995), consistent with increased myostatin activity. Follistatin-related gene (FLRG), like follistatin, is able to bind and inhibit members of the TGF-β superfamily (Tsuchida *et al.* 2000; Schneyer *et al.* 2001; Tsuchida *et al.* 2001). In addition, FLRG has been shown to interact directly with the mature portion of Myostatin, resulting in a dose-dependent reduction in the activity of myostatin, as assessed through reporter gene assay analysis (Hill *et al.* 2002). Growth and differentiation factor-associated serum protein-1 (GASP-1) has been shown to associate with Myostatin in circulation; specifically associating with both mature and LAP regions of Myostatin. Functionally GASP-1 has been shown to interfere with the activity of myostatin as determined by reporter gene analysis (Hill *et al.* 2003). More recently, decorin, a leucine-rich repeat extracellular proteoglycan, has been shown to interact with the mature region of Myostatin, in a Zn^{2+}-dependent manner (Miura *et al.* 2006). This interaction was demonstrated to relieve the inhibitory effect of myostatin on myoblast proliferation *in vitro*. One of the intrinsic features of myostatin is its ability to negatively auto-regulate its expression. In particular, exogenous addition of recombinant Myostatin protein results in both a decrease in *myostatin* mRNA and repression of *myostatin* promoter activity (Forbes *et al.* 2006). Furthermore, myostatin appears to signal through Smad7 to regulate its own activity (Zhu *et al.* 2004; Forbes *et al.* 2006). In support, addition of Myostatin resulted in enhanced Smad7 expression, while over-expression of Smad7 resulted in repression of

myostatin promoter activity and mRNA, an effect abolished through incubation with siRNA specific for Smad7 (Zhu *et al.* 2004; Forbes *et al.* 2006).

1.4.4 *Mutations in myostatin*

In addition to the targeted disruption of *myostatin* in mice, several naturally occurring mutations have been identified in various double-muscled cattle breeds including Belgian Blue (Figure 1.7A) and Piedmontese (Kambadur *et al.* 1997; McPherron and Lee 1997; Grobet *et al.* 1998). Specifically two separate mutations in the coding region of the *myostatin* gene have been reported to result in a non-functional Myostatin product. The phenotype seen in Belgian Blue cattle (Figure 1.7A) is caused by an 11-nucleotide deletion, which ultimately results in expression of a non-functional truncated protein product (Kambadur *et al.* 1997). Conversely, the Piedmontese cattle express a non-functional Myostatin protein through a missense mutation in the gene sequence, resulting in a G to A transition and substitution of cysteine for tyrosine (Kambadur *et al.* 1997; Berry *et al.* 2002). Furthermore, a mutation in the *myostatin* gene has been reported to result in the hyper-muscularity observed in compact (*Cmpt*) mice (Szabo *et al.* 1998). More recently, the heavy muscled phenotype of the Texel sheep breed has been traced to a mutation in the *myostatin* gene resulting in a G to A transition in the 3' untranslated region (UTR) (Clop *et al.* 2006). This mutation creates a target site for two microRNAs abundant in skeletal muscle, namely *mir1* and *mir206* (Clop *et al.* 2006). MicroRNAs are short non-coding RNAs which diminish gene activity post-transcriptionally by binding to target genes, resulting in destabilisation of mRNA and/or inhibition of protein translation (Tsuchiya *et al.* 2006).

A mutation in the *myostatin* gene has recently been shown to result in dramatic hypertrophy in a human child (Schuelke *et al.* 2004) (Figure 1.7B). Cross-sectional measurements determined that the *M. quadriceps* muscle was more than two-fold larger than age- and sex-matched controls, while the thickness of the sub-cutaneous fat pad was significantly lower than controls. The mutation was shown to result from a G to A transition within intron 1 of the *myostatin* gene. This transition resulted in mis-splicing of the precursor mRNA and insertion of the first 108 base pairs of intron 1 (Schuelke *et al.* 2004).

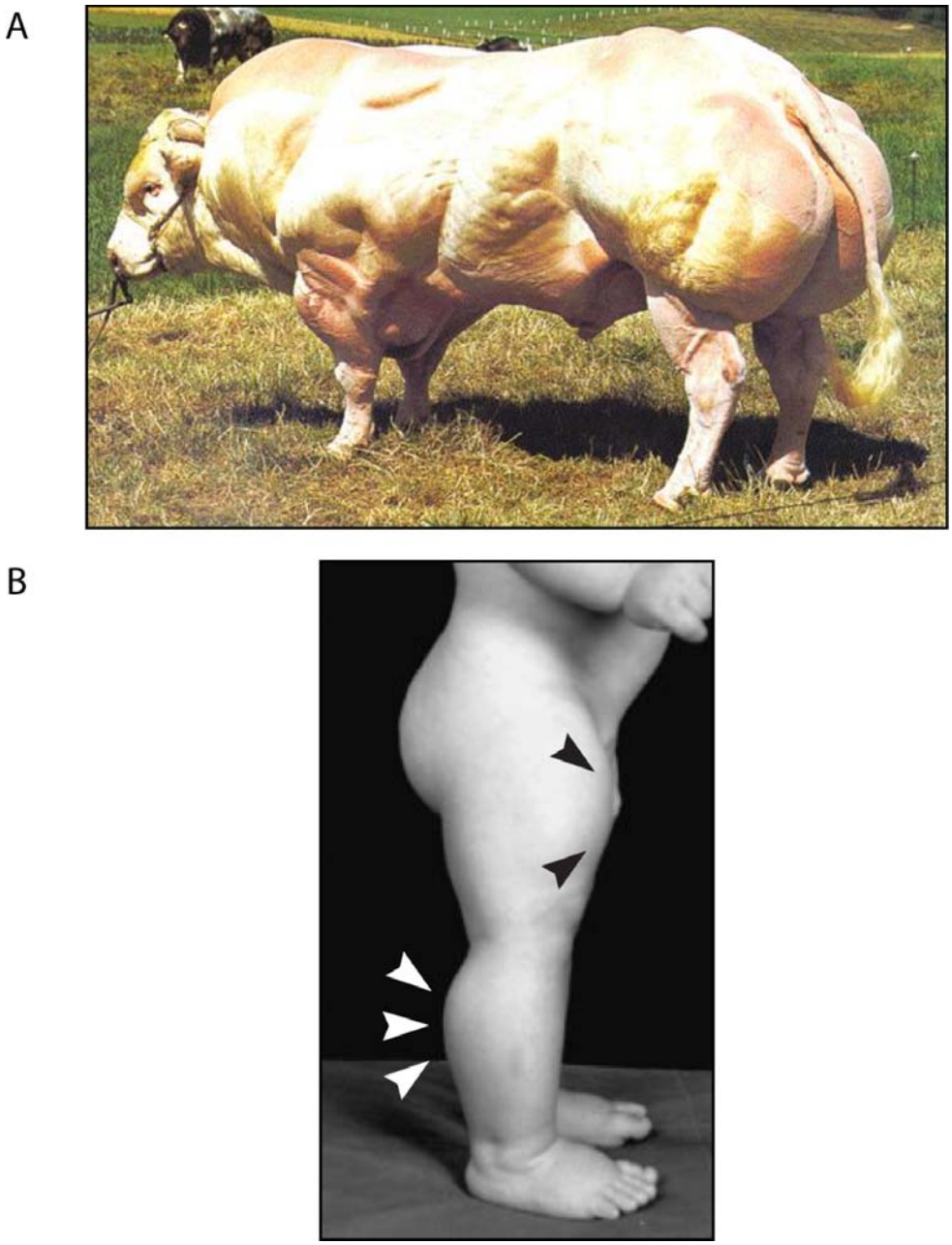

Figure 1.7 *Natural mutations in myostatin*

A) Photograph showing the heavy muscling observed in the Belgian Blue cattle breed (reproduced from Haliba '96 Catalogue). B) Photograph of a human child at 7 months of age possessing a G to A transition mutation in the *myostatin* gene, resulting in a non functional Myostatin protein product. Arrows highlight protruding muscles from the boy's calf and thigh regions. Modified from Schuelke *et al*. (Schuelke *et al.* 2004).

1.4.5 Physiological actions of myostatin

1.4.5.1 Myostatin signaling

Members of the TGF-β superfamily elicit biological functions by binding to specific type-I and type-II serine/threonine kinase receptors. Studies have shown that Myostatin specifically binds to the activin type-IIB (ActRIIB) receptor (Lee and McPherron 2001; Rebbapragada *et al.* 2003). Indeed, transgenic mice that over-express a dominant-negative form of the ActRIIB show a drastic increase in muscle weights, similar to that seen in *myostatin*-null mice (Lee and McPherron 2001). Myostatin-mediated type-II receptor activation results in the phosphorylation of the type-I receptor, either activin receptor-like kinase 4 (ALK4) or ALK5, which in turn initiates downstream signaling events (Rebbapragada *et al.* 2003).

TGF-β superfamily signalling is primarily mediated through substrates known as Smads (Piek *et al.* 1999). Smad proteins can be separated into three sub-groups: the receptor Smads (R-Smads; Smads 1, 2, 3, 5 and 8), the common Smad (Co-Smad; Smad 4) and the inhibitory Smads (I-Smads; Smads 6 and 7) (Piek *et al.* 1999). Phosphorylation of the R-Smads occurs at the type-I receptor, the now active R-Smad heterodimerises with the Co-Smad and translocates to the nucleus to regulate transcription (Nakao *et al.* 1997b; Souchelnytskyi *et al.* 1997; Zhang *et al.* 1997). Inhibitory Smads can compete with R-Smads for receptor binding and Co-Smad heterodimerisation, thus blocking Smad-mediated signaling (Hayashi *et al.* 1997; Nakao *et al.* 1997a; Hata *et al.* 1998). Consistent with other members of the TGF-β superfamily, myostatin has been shown to signal specifically through Smads 2/3 with the involvement of Smad 4 (Zhu *et al.* 2004). In addition, it appears that myostatin-mediated Smad signaling is negatively regulated by Smad 7 but not Smad 6 (Zhu *et al.* 2004). Furthermore, myostatin has also been shown to induce the expression of Smad 7. Interestingly, this induction of Smad 7 appears to provide an auto-regulatory mechanism through which myostatin negatively regulates its own activity (Zhu *et al.* 2004; Forbes *et al.* 2006).

1.4.5.2 Regulation of proliferation and differentiation

It has been previously shown that myostatin is a negative regulator of skeletal muscle growth, in support, naturally occurring mutations or targeted disruption of the *myostatin* gene result in increased muscle mass (Kambadur *et al.* 1997; McPherron *et al.* 1997). Several cell culture based studies have analysed the role of myostatin in the regulation of cell proliferation. Myostatin has been shown to negatively regulate skeletal muscle growth through inhibiting the proliferation of myoblast cell lines in a dose-dependent, reversible manner (Thomas *et al.* 2000). In support, primary myoblasts isolated from *myostati*n-null mice proliferate significantly faster than myoblast cultures from wild-type mice (McCroskery *et al.* 2003). More recently, myostatin has been demonstrated to reversibly inhibit the proliferation of Pax7-positive myogenic precursor cells in embryos injected with Myostatin-coated beads (Amthor *et al.* 2006). Mechanistically, myostatin appears to interact with the cell cycle machinery, resulting in cell cycle exit during the gap phases (G_1 and G_2) (Thomas *et al.* 2000). Specifically, treatment with Myostatin results in up-regulation of the cyclin-dependent kinase inhibitor (CKI), p21 (Thomas *et al.* 2000). p21 is a member of the Cip/Kip family of CKIs which, as their name suggests, block the action of cyclin-dependent kinases and their cyclin partners (Harper *et al.* 1993; Xiong *et al.* 1993). Consistent with this, treatment with recombinant Myostatin protein has been shown to decrease the expression and activity of cyclin-dependent kinase 2 (cdk2) (Thomas *et al.* 2000). The myostatin-mediated loss in cdk2 activity resulted in accumulation of hypophosphorylated retinoblastoma (Rb), which in turn induces cell cycle arrest in the G_1 phase. A recent report has highlighted a role for the p38 mitogen-activated protein kinase (MAPK) signaling pathway in myostatin regulation of myogenesis (Philip *et al.* 2005). In particular, myostatin has been shown to activate p38 MAPK; moreover this activation was shown to augment myostatin-mediated transcription. Furthermore, p38 MAPK was shown to play an important role in myostatin-mediated up-regulation of p21 and subsequent inhibition of cell proliferation (Philip *et al.* 2005). More recently, myostatin has been shown to inhibit the proliferation of the rhabdomyosarcoma cell line, RD (Langley *et al.* 2004). However, unlike normal myoblasts, treatment with Myostatin did not up-regulate the expression of p21 or alter the phosphorylation or activity of Rb. Langley *et al.* demonstrated that treatment with Myostatin resulted in a reduction

in expression and activity of cdk2 and cyclin E. NPAT is a substrate of cdk2/cyclinE and is critical for the continuation of the cell cycle at the G1/S checkpoint. Thus treatment of the RD cell line with Myostatin also reduced the phosphorylation of NPAT, concomitant with a reduction in the expression of the NPAT target histone-H4 (Langley *et al.* 2004).

In addition to the intrinsic ability of myostatin to regulate myoblast proliferation, myostatin has been shown to negatively regulate myogenic differentiation. (Langley *et al.* 2002; Rios *et al.* 2002). In particular, treatment of myoblasts with recombinant Myostatin protein resulted in a dose-dependent reversible inhibition of differentiation (Langley *et al.* 2002). Furthermore, treatment of differentiating myoblasts with Myostatin inhibited the mRNA and protein expression of MyoD, Myf5, myogenin and MHC (Langley *et al.* 2002; Rios *et al.* 2002). Langley *et al.* further demonstrated that during differentiation, treatment with Myostatin increased the phosphorylation of Smad 3 and enhanced Smad 3•MyoD interaction. MyoD is critical for the successful commitment to myogenic differentiation, and furthermore MyoD has been shown to induce cell cycle arrest and induce differentiation through up-regulation of p21. Thus, Langley *et al* proposed that myostatin blocked myogenic differentiation by inhibiting the expression and activity of MyoD in a Smad 3-dependent manner. Recently a role for the extracellular signal-regulated kinase 1/2 (Erk1/2) MAPK signaling pathway has been identified in myostatin regulation of myogenesis (Yang *et al.* 2006). Indeed, inhibition of the Erk1/2 pathway suppressed myostatin-mediated inhibition of myoblast proliferation and differentiation and further interfered with the ability of myostatin to inhibit the expression of genes critical to myogenic differentiation, including MyoD, myogenin and MHC (Yang *et al.* 2006).

1.4.5.3 *Post-natal muscle growth and repair*

Myostatin expression is detected during embryonic and foetal growth and is maintained through into adult muscle tissue, thus myostatin may be an important mediator of skeletal muscle mass throughout myogenesis. Indeed myostatin appears to play a critical role in the regulation of post-natal muscle growth and repair. Several studies have analysed the effect of post-natal modification of myostatin on skeletal muscle mass. Over-expression of a dominant-negative

Myostatin, whereby the RSRR processing site was mutated to GLDG, resulted in a 25-30% increase in skeletal muscle mass in mice; specifically resulting from increased hypertrophy rather than hyperplasia (Zhu *et al.* 2000). In contrast, recapitulation of the Piedmontese cattle C313Y mis-sense mutation in mice results in skeletal muscle hyperplasia without muscle hypertrophy (Nishi *et al.* 2002). Furthermore, injection of the JA16 monoclonal Myostatin-neutralising antibody into mice resulted in an increase in skeletal muscle mass (Whittemore *et al.* 2003). It was determined that incubation with the JA16 antibody for 2-4 weeks was sufficient to induce an increase in muscle mass as compared to control mice. Concomitant to an effect on muscle mass, injection of the neutralising antibody increased the grip strength of treated mice, specifically a 10% increase in peak force was observed (Whittemore *et al.* 2003). Another study focussed on the effect of conditionally targeting *myostatin* for inactivation using the cre-lox system. Subsequent inactivation of *myostatin* resulted in skeletal muscle hypertrophy phenotypically similar to that observed in *myostatin*-null mice (Grobet *et al.* 2003). More recently, an increase in muscle mass was observed following injection of a myostatin-specific short interfering RNA (siRNA) directly into the *M. tibialis anterior* (TA) muscle of rats (Magee *et al.* 2006). The siRNA-mediated knock-down resulted in a 27% drop in *myostatin* mRNA and a 48% drop in Myostatin protein expression. Furthermore, myostatin inhibition resulted in an increase in TA muscle weight and myofibre area. Satellite cell number was also increased 2-fold, as quantified by the number of Pax7-positive cells (Magee *et al.* 2006). Thus inhibitors directed against myostatin may have therapeutic benefit in circumstances where skeletal muscle wasting enhances the morbidity or mortality of a disease.

Myostatin has been demonstrated to be involved in the regulation of skeletal muscle regeneration. A recent study has compared the regeneration process of skeletal muscle in *myostatin*-null mice versus wild-type controls following injection of the myotoxin, notexin (McCroskery *et al.* 2005). Following injury, satellite cell-derived myoblasts migrate to the site of injury to help repair the damage (Watt *et al.* 1987; Watt *et al.* 1994). Muscle damage is closely followed by a localised inflammatory response resulting in the influx of macrophages to the site of injury (Tidball 1995). Interestingly, McCroskery *et al.* found that lack of *myostatin* increased the rate of myogenic cell migration and the rate of

macrophage infiltration to the site of injury, resulting in enhanced numbers of both. Furthermore, presence of recombinant Myostatin protein *in vitro* significantly reduced the migration of both myoblasts and macrophages in chemotaxis chambers (McCroskery *et al.* 2005). The formation of scar tissue is a prominent feature of skeletal muscle injury. However, during the process of regeneration the presence of scar tissue was greatly reduced in regenerated muscle from *myostatin*-null as compared with muscle from wild-type mice. Thus, in addition to regulating the involvement of satellite cells and macrophages in muscle regeneration, myostatin may also contribute to skeletal muscle fibrosis (McCroskery *et al.* 2005).

Satellite cells are responsible for maintaining and repairing skeletal muscle mass following injury (reviewed in Section 1.2). Recently myostatin has been shown to play a role in regulating satellite cell activation, growth and self-renewal (McCroskery *et al.* 2003). Myostatin is expressed within muscle satellite cells and satellite cell-derived primary myoblasts. Specifically, satellite cells, characterised through positive Pax7 staining, were also positive for Myostatin by immunocytochemistry. Furthermore, *in situ* hybridisation confirmed high expression of both *pax7* and *myostatin* mRNA in satellite cells (McCroskery *et al.* 2003). In addition, McCroskery *et al.* also demonstrated that abundant expression of myostatin could be detected by both RT-PCR and Western Blot analysis in isolated satellite cells and satellite cell-derived myoblasts. Functionally, myostatin appears to negatively regulate the activation and proliferation of satellite cells. In particular, increased satellite cell activation, quantified by percentage of BrdU positive cells, is observed in satellite cells isolated from *myostatin*-null mice as compared to wild-type controls (McCroskery *et al.* 2003; Siriett *et al.* 2006). In support, treatment of isolated single fibres with recombinant Myostatin protein results in a dose-dependent decrease in BrdU-positive satellite cells, concomitant with a decrease in satellite cell migration (McCroskery *et al.* 2003; McCroskery *et al.* 2005). Furthermore, treatment of satellite cell-derived myoblasts with Myostatin results in inhibition of proliferation (Thomas *et al.* 2000; McCroskery *et al.* 2003; McFarland *et al.* 2006). Conversely, primary myoblasts isolated from *myostatin*-null mice proliferate at a faster rate compared with cultures isolated from wild-type mice (McCroskery *et al.* 2003).

Satellite cells, consistent with the term muscle stem cell, are able to self-renew their population (reviewed in Section 1.2.1.3). Myostatin has been implicated in regulation of satellite cell self-renewal; in fact, single fibres isolated from *myostatin*-null mice contain a greater proportion of satellite cells as compared with wild-type controls (McCroskery *et al.* 2003). In addition, a recent report has demonstrated that injection of myostatin-specific short hairpin interfering RNA (shRNA) into the TA muscle of rats results in an increase in satellite cell number, as assessed by Pax7 immunostaining (Magee *et al.* 2006). McCroskery *et al.* suggested that increased proliferation and increased satellite cell number per muscle fibre, in the *myostatin*-null mice, is indicative of increased self-renewal. Recently presented results from this thesis further highlight the mechanism behind myostatin regulation of satellite cell self-renewal (McFarlane *et al.* 2006a). Pax7 is thought to play a role in the induction of satellite cell self-renewal. Treatment of primary myoblasts with recombinant Myostatin protein resulted in a significant down-regulation of Pax7, while expression of Pax7 was induced in primary cultures from *myostatin*-null mice as compared to wild-type controls (McFarlane *et al.* 2006a). Furthermore, absence of *myostatin* increased the pool of quiescent reserve cells, a group of cells which share several characteristics with self-renewed satellite cells. It is thus suggested that myostatin may regulate satellite self-renewal through negatively regulating Pax7 (McFarlane *et al.* 2006a).

1.4.5.4 *Myostatin and muscle wasting*

In addition to the inhibitory role of myostatin on skeletal muscle myogenesis, a plethora of evidence now exists to implicate myostatin in the induction of skeletal muscle wasting. Myostatin has been associated with the induction of cachexia, a severe form of muscle wasting that manifests as a result of disease. HIV-infected men undergoing muscle wasting have increased intramuscular and serum concentrations of Myostatin protein as compared with healthy controls (Gonzalez-Cadavid *et al.* 1998). Thus myostatin may contribute to the muscle wasting pathology observed as a result of HIV-infection. Myostatin has also been associated with muscle wasting resulting from liver cirrhosis; Dasarathey *et al.* used the portacaval anastamosis rat, a model of human liver cirrhosis, to study the involvement of myostatin in the muscle wasting associated with this disease.

Gene expression analysis demonstrated an increase in the mRNA and protein levels of myostatin and the myostatin receptor, activin type-IIb (Dasarathy *et al.* 2004). Patients suffering from Addison's disease (adrenal insufficiency) commonly experience skeletal muscle atrophy. Recently it was shown that active Myostatin serum levels increased over time in adrenalectomised rats, a model of Addison's disease (Hosoyama *et al.* 2005). This increase in serum Myostatin correlated with a decrease in muscle weights as compared with controls (Hosoyama *et al.* 2005). Cushing's syndrome is associated with an excessive increase in glucocorticoid production resulting in skeletal muscle wasting (Shibli-Rahhal *et al.* 2006). Ma *et al.* has demonstrated that injection of the glucocorticoid dexamethasone into rats induces skeletal muscle atrophy, concomitant with a dose-dependent up-regulation of myostatin mRNA and protein. The dexamethasone-induced up-regulation of myostatin was inhibited in the presence of glucocorticoid antagonist RU-486 (Ma *et al.* 2003). A separate study has demonstrated that, in addition to mRNA and protein, *myostatin* promoter activity is induced following Dex-induced muscle wasting (Salehian *et al.* 2006). The amino acid glutamine has been previously shown to antagonise glucocorticoid-induced skeletal muscle atrophy (Hickson *et al.* 1995; Hickson *et al.* 1996). Consistent with this, injection of glutamine in conjunction with Dex into rats significantly reduced the muscle atrophy phenotype, concomitant with a down-regulation of myostatin expression (Salehian *et al.* 2006). In addition to an associative role in cachexia, myostatin has been shown to induce cachexia following administration to mice, specifically injection of CHO-control cells and CHO cells over-expressing myostatin (CHO-myostatin) resulted in the formation of tumours. However, in contrast to the gain in body weight observed in CHO-control mice, injection of CHO-myostatin cells resulted in a 33% reduction in total body weight within 16 days (Zimmers *et al.* 2002). This severe body mass reduction was ameliorated by injection of CHO cells expressing the Myostatin propeptide (LAP) region or follistatin, two identified antagonists of myostatin function. Furthermore, injection of CHO-myostatin cells resulted in a significant reduction in fat pad mass, consistent with cachexia (Zimmers *et al.* 2002). Published work from this thesis further delineates the mechanism behind myostatin-mediated induction of cachexia. Specifically over-expression of myostatin *in vitro* and *in vivo* resulted in the up-regulation of genes involved with

the ubiquitin-proteasome proteolytic pathway including *atrogin-1*, *MuRF-1* and $E2_{14k}$ (McFarlane *et al.* 2006b). Treatment of C2C12 myotubes with recombinant Myostatin antagonised the IGF-1/PI3-K/AKT pathway, resulting in enhanced activation of the transcription factor FoxO1 and subsequent activation of atrophy-related genes (McFarlane *et al.* 2006b). It was further shown that myostatin signals independently of NF-κB during the induction of cachexia. In support, myostatin and NF-κB have been previously shown to signal through separate pathways to regulate myogenesis (Bakkar *et al.* 2005). Recently it has been demonstrated that FoxO1 can regulate the expression of myostatin; in particular, over-expression of constitutively active FoxO1 increased the expression of *myostatin* mRNA and promoter reporter activity. Allen and Unterman suggest that FoxO1 up-regulation of myostatin may contribute to skeletal muscle atrophy (Allen and Unterman 2006).

Muscle disuse or inactivity, such as that experienced during periods of prolonged bed rest, also contributes to skeletal muscle atrophy. Several studies have implicated myostatin in the muscle atrophy associated with disuse. The expression of myostatin was measured in a mouse model of hindlimb unloading. Carlson *et al.* showed that *myostatin* mRNA was significantly increased following 1 day of hindlimb unloading, however, no detectable difference in *myostatin* expression was observed at days 3 and 7 of unloading, as compared with controls (Carlson *et al.* 1999). In a separate study, hindlimb unloading in the rat resulted in a 16% decrease in *M. plantaris* muscle weight, concomitant with a 110% increase in *myostatin* mRNA and a 35% increase in Myostatin protein (Wehling *et al.* 2000). A dramatic 30-fold increase in *myostatin* mRNA was observed in patients suffering from disuse atrophy as a result of chronic osteoarthritis of the hip (Reardon *et al.* 2001). In addition, a significant negative correlation was observed between expression of *myostatin* and type-IIA and type-IIB fibre area, suggesting that myostatin may target type-IIA and IIB fibres during disuse atrophy (Reardon *et al.* 2001). Furthermore, a 25 day period of bedrest increased the levels of serum Myostatin-immunoreactive protein to 12% above that observed in baseline measurements (Zachwieja *et al.* 1999). In addition, myostatin has been associated with skeletal muscle loss during space flight (Lalani *et al.* 2000). In particular, exposing rats to the microgravity environment

of space resulted in muscle weight loss, with an associated increase in both myostatin mRNA and protein (Lalani *et al.* 2000).

Sarcopenia is the skeletal muscle atrophy observed as a result of the normal ageing process (Marzetti and Leeuwenburgh 2006). There are several conflicting reports on the expression pattern of myostatin during age-related muscle atrophy. *myostatin* mRNA expression has been shown to be unaltered during ageing in human males (Marcell *et al.* 2001; Welle *et al.* 2002); in contrast, studies have shown that *myostatin* mRNA decreases in aged rats (Baumann *et al.* 2003; Haddad and Adams 2006). Furthermore, Myostatin protein serum levels in humans, and intramuscular protein expression of Myostatin in rats, have been shown to increase during atrophy associated with old age (Schulte and Yarasheski 2001; Yarasheski *et al.* 2002; Baumann *et al.* 2003). However, Kawada *et al.* measured myostatin expression in muscle during ageing in mice and observed no increase in Myostatin protein (Kawada *et al.* 2001). To further delineate the role of myostatin in old age muscle wasting a recent study has analysed the phenomenon of sarcopenia between *myostatin*-null and wild-type mice (Siriett *et al.* 2006). During the ageing process muscle fibres tend to switch to an oxidative state (Alnaqeeb and Goldspink 1987; Allen and Unterman 2006). Interestingly, comparison of fibre-type in young and old *myostatin*-null mice revealed that no fibre switching occurred, whereas muscle fibres from wild-type controls became progressively more oxidative with age (Siriett *et al.* 2006). Although satellite cell activation declined dramatically in both wild-type and *myostatin*-null mice during ageing, satellite cell number remained steady. However, satellite cell number was consistently higher in *myostatin*-null mice as compared with wild-type controls irrespective of age. Furthermore, the ensuing skeletal muscle regeneration, subsequent to notexin-induced muscle injury, was greatly enhanced in old age (24-month) *myostatin*-null mice as compared with wild-type controls (Siriett *et al.* 2006). Thus, myostatin appears to play a critical role in sarcopenia. Therefore methods to target and antagonise the action of myostatin may prove beneficial in reducing the effects of muscle wasting during age.

The most common forms of muscular dystrophy are Duchenne muscular dystrophy (DMD) and Becker muscular dystrophy (BMD) (Zhou *et al.* 2006). Both DMD and BMD are X-linked recessive disorders which can be traced back to mutations in the *dystrophin* gene (*DMD*) (Flanigan *et al.* 2003; Sironi *et al.*

2003). BMD results from in-frame mutations in the *DMD* gene, resulting in a partially functional protein product (Hoffman *et al.* 1988; Koenig *et al.* 1989), however in DMD patients, frame-shift mutations result in very low levels or complete absence of the dystrophin (Hoffman *et al.* 1987; Koenig *et al.* 1987). DMD and BMD afflict about 1 in every 3500 and 1 in 18500 newborn males respectively (Emery 1991; Peterlin *et al.* 1997; Siciliano *et al.* 1999; Darin and Tulinius 2000; Zhou *et al.* 2006). Myostatin is a well characterised negative regulator of skeletal muscle mass: as such, several studies have been performed looking at the role of myostatin in the severe muscular dystrophy phenotype. The expression of myostatin has been shown to decrease by 4-fold in regenerated *mdx* muscle (Tseng *et al.* 2002). It is suggested that a reduction in myostatin may be an adaptive response to aid in the maintenance and rescue of *mdx* skeletal muscle. Antibody-mediated blockade of Myostatin results in both enhanced body mass and skeletal muscle hypertrophy in the *mdx* mouse model of DMD (Bogdanovich *et al.* 2002). Furthermore, antagonising myostatin resulted in increased muscle strength, as measured through grip strength experiments. Bogdanovich *et al.* further demonstrated that blocking Myostatin, through injection of an Fc-fusion stabilised Myostatin propeptide region (LAP), resulted in improvement of the *mdx* DMD phenotype. Consistent with antibody-mediated Myostatin blockade, propeptide injection resulted in enhanced growth, increased muscle mass and grip strength (Bogdanovich *et al.* 2005). They further showed that this blockade resulted in enhanced muscle specific force, over and above that shown by antibody-mediated inhibition of Myostatin. Recently, transgenic *mdx* mice containing a dominant negative activin type-IIB receptor gene (ActRIIB) showed phenotypic improvement over wild-type *mdx* mice (Benabdallah *et al.* 2005). Indeed, increased skeletal muscle mass was observed in conjunction with increased resistance to exercise-induced muscle damage. More recently, Minetti *et al.* have examined the effect of deacetylase inhibitors on the *mdx* phenotype. Treatment of *mdx* mice with deacetylase inhibitors resulted in an improvement in muscle quality and function with an increase in myofibre size (Minetti *et al.* 2006). Interestingly, addition of the deacetylase inhibitors TSA or MS 27-275 resulted in enhanced expression of the myostatin antagonist follistatin (Minetti *et al.* 2006). In addition to disruption in dystrophin, muscular dystrophy can result from mutations in several genes involved in the formation of the dystrophin-

associated protein complex, including laminin-II. Crossing of the *myostatin*-null mice with the *dy* mice, a model of laminin-II-associated dystrophy, resulted in increased muscle mass and enhanced regeneration (Li *et al.* 2005b). However, elimination of *myostatin* in the *dy* mice was unable to correct the severe dystrophic pathology associated with loss of laminin-II, moreover, loss of *myostati*n resulted in an increase in post-natal mortality (Li *et al.* 2005b). Thus, the validity of myostatin as a target for treatment of all forms of dystrophy remains a matter of contention.

1.5 Aims and objectives

Myostatin, a member of the TGF-β superfamily, is now widely accepted as a potent and specific inhibitor of skeletal muscle growth. In support, naturally occurring mutations or targeted inactivation of the *myostatin* gene results in a dramatic increase in skeletal muscle mass. Mechanistically myostatin functions by inhibiting myoblast proliferation and differentiation, which is indeed true with respect to satellite cells and satellite cell-derived myoblast cultures. Satellite cells, which are occasionally referred to as skeletal muscle stem cells, form the basis of the regenerative capacity of skeletal muscle. With the innate ability to inhibit satellite cell activation, proliferation and self-renewal, myostatin may have a negative effect on the ability of skeletal muscle to regenerate. Indeed, it has been recently shown that in the absence of *myostatin* the process of skeletal muscle regeneration is enhanced. The potent inhibitory effect of myostatin begs the question whether or not myostatin functions as a skeletal muscle wasting-inducing factor. Most certainly, elevated myostatin expression is associated with a plethora of skeletal muscle wasting inducing conditions including AIDS, diabetes and liver cirrhosis. Moreover, systemic over-expression of Myostatin results in a severe form of muscle wasting, termed cachexia. Although a role for myostatin is now established in regulation of post-natal muscle growth much of the mechanism behind this regulation remains to be elucidated. Thus the overall aim of this thesis is to enhance the current knowledge of myostatin in the regulation of post-natal muscle growth and repair, with emphasis on satellite cell functionality and skeletal muscle proteolysis. With such a potent negative regulator of skeletal muscle mass, therapies aimed at neutralising active Myostatin may help to alleviate the severe symptoms of skeletal muscle loss associated with disease. The aims of this thesis were studied with the following objectives.

Objective 1: To study regulation of myostatin through proteolytic processing.

Objective 2: To delineate the role of myostatin in satellite cell self-renewal to enable the characterisation of a mechanism through which myostatin acts to regulate this process.

Objective 3: To characterise in detail the functional role of myostatin in skeletal muscle wasting and delineate a potential mechanism through which myostatin signals to promote muscle degradation.

Objective 4: To study and characterise the function of a novel myostatin downstream target gene during the induction of cachexia.

1.6 References

Acharyya, S., K. J. Ladner, L. L. Nelsen, J. Damrauer, P. J. Reiser, S. Swoap and D. C. Guttridge (2004). "Cancer cachexia is regulated by selective targeting of skeletal muscle gene products." J Clin Invest **114**(3): 370-8.

Allen, D. L. and T. G. Unterman (2006). "Regulation of Myostatin Expression and Myoblast Differentiation by FoxO and SMAD Transcription Factors." Am J Physiol Cell Physiol.

Alnaqeeb, M. A. and G. Goldspink (1987). "Changes in fibre type, number and diameter in developing and ageing skeletal muscle." J Anat **153**: 31-45.

Amthor, H., G. Nicholas, I. McKinnell, C. F. Kemp, M. Sharma, R. Kambadur and K. Patel (2004). "Follistatin complexes Myostatin and antagonises Myostatin-mediated inhibition of myogenesis." Dev Biol **270**(1): 19-30.

Amthor, H., A. Otto, R. Macharia, I. McKinnell and K. Patel (2006). "Myostatin imposes reversible quiescence on embryonic muscle precursors." Dev Dyn **235**(3): 672-80.

Anderson, J. E. (2000). "A role for nitric oxide in muscle repair: nitric oxide-mediated activation of muscle satellite cells." Mol Biol Cell **11**(5): 1859-74.

Argiles, J. M., B. Alvarez and F. J. Lopez-Soriano (1997). "The metabolic basis of cancer cachexia." Med Res Rev **17**(5): 477-98.

Argiles, J. M., S. Busquets, A. Felipe and F. J. Lopez-Soriano (2006a). "Muscle wasting in cancer and ageing: cachexia versus sarcopenia." Adv Gerontol **18**: 39-54.

Argiles, J. M., S. Busquets and F. J. Lopez-Soriano (2005). "The pivotal role of cytokines in muscle wasting during cancer." Int J Biochem Cell Biol.

Argiles, J. M., S. Busquets and F. J. Lopez-Soriano (2006b). "Cytokines as mediators and targets for cancer cachexia." Cancer Treat Res **130**: 199-217.

Argiles, J. M., R. Moore-Carrasco, G. Fuster, S. Busquets and F. J. Lopez-Soriano (2003). "Cancer cachexia: the molecular mechanisms." Int J Biochem Cell Biol **35**(4): 405-9.

Auclair, D., D. R. Garrel, A. Chaouki Zerouala and L. H. Ferland (1997). "Activation of the ubiquitin pathway in rat skeletal muscle by catabolic doses of glucocorticoids." Am J Physiol **272**(3 Pt 1): C1007-16.

Bagshaw, C. R. (1993). Muscle Contraction. Dordrecht, Kluwer Academic Publishers.

Bakkar, N., H. Wackerhage and D. C. Guttridge (2005). "Myostatin and NF-κB Regulate Skeletal Myogenesis Through Distinct Signaling Pathways." Signal Transduction **5**(4): 202-210.

Baracos, V. E., C. DeVivo, D. H. Hoyle and A. L. Goldberg (1995). "Activation of the ATP-ubiquitin-proteasome pathway in skeletal muscle of cachectic rats bearing a hepatoma." Am J Physiol **268**(5 Pt 1): E996-1006.

Barthel, A., D. Schmoll and T. G. Unterman (2005). "FoxO proteins in insulin action and metabolism." Trends Endocrinol Metab **16**(4): 183-9.

Bartoli, M. and I. Richard (2005). "Calpains in muscle wasting." Int J Biochem Cell Biol **37**(10): 2115-33.

Barton, E. R., L. Morris, A. Musaro, N. Rosenthal and H. L. Sweeney (2002). "Muscle-specific expression of insulin-like growth factor I counters muscle decline in mdx mice." J Cell Biol **157**(1): 137-48.

Bass, J., J. Oldham, M. Sharma and R. Kambadur (1999). "Growth factors controlling muscle development." Domest Anim Endocrinol **17**(2-3): 191-7.

Baumann, A. P., C. Ibebunjo, G. W. A. and V. M. Paralkar (2003). "Myostatin expression in age and denervation-induced skeletal muscle atrophy." J Musculoskel Neuron Interact **3**(1): 8-16.

Beauchamp, J. R., L. Heslop, D. S. Yu, S. Tajbakhsh, R. G. Kelly, A. Wernig, M. E. Buckingham, T. A. Partridge and P. S. Zammit (2000). "Expression of CD34 and Myf5 defines the majority of quiescent adult skeletal muscle satellite cells." J Cell Biol **151**(6): 1221-34.

Bechet, D., A. Tassa, D. Taillandier, L. Combaret and D. Attaix (2005). "Lysosomal proteolysis in skeletal muscle." Int J Biochem Cell Biol **37**(10): 2098-114.

Belec, L., R. Gherardi, C. Payan, T. Prazuck, J. E. Malkin, C. Tevi-Benissan and J. Pillot (1995). "Proinflammatory cytokine expression in cervicovaginal secretions of normal and HIV-infected women." Cytokine **7**(6): 568-74.

Benabdallah, B. F., M. Bouchentouf and J. P. Tremblay (2005). "Improved success of myoblast transplantation in mdx mice by blocking the myostatin signal." Transplantation **79**(12): 1696-702.

Berry, C., M. Thomas, B. Langley, M. Sharma and R. Kambadur (2002). "Single cysteine to tyrosine transition inactivates the growth inhibitory function of Piedmontese myostatin." Am J Physiol (in press).

Bischoff, R. (1986). "Proliferation of muscle satellite cells on intact myofibers in culture." Dev Biol **115**(1): 129-39.

Bischoff, R. (1994a). The embryonic origin of muscle. New York, McGraw-Hill.

Bischoff, R. (1994b). The satellite cell and muscle regeneration. Myology: Basic and Clinical. A. G. Engel and C. Franzini-Armstrong, McGraw-Hill. **1:** 97-112.

Bischoff, R. and C. Heintz (1994). "Enhancement of skeletal muscle regeneration." Dev Dyn **201**(1): 41-54.

Bodine, S. C., E. Latres, S. Baumhueter, V. K. Lai, L. Nunez, B. A. Clarke, W. T. Poueymirou, F. J. Panaro, E. Na, K. Dharmarajan, Z. Q. Pan, D. M. Valenzuela, T. M. DeChiara, T. N. Stitt, G. D. Yancopoulos and D. J. Glass (2001). "Identification of ubiquitin ligases required for skeletal muscle atrophy." Science **294**(5547): 1704-8.

Bogdanovich, S., T. O. Krag, E. R. Barton, L. D. Morris, L. A. Whittemore, R. S. Ahima and T. S. Khurana (2002). "Functional improvement of dystrophic muscle by myostatin blockade." Nature **420**(6914): 418-21.

Bogdanovich, S., K. J. Perkins, T. O. Krag, L. A. Whittemore and T. S. Khurana (2005). "Myostatin propeptide-mediated amelioration of dystrophic pathophysiology." Faseb J **19**(6): 543-9.

Boonyarom, O. and K. Inui (2006). "Atrophy and Hypertrophy of skeletal muscles: structural and functional aspects." Acta Physiologica **188**: 77-89.

Bossola, M., M. Muscaritoli, P. Costelli, R. Bellantone, F. Pacelli, S. Busquets, J. Argiles, F. J. Lopez-Soriano, I. M. Civello, F. M. Baccino, F. Rossi Fanelli and G. B. Doglietto (2001). "Increased muscle ubiquitin mRNA levels in gastric cancer patients." Am J Physiol Regul Integr Comp Physiol **280**(5): R1518-23.

Brand-Saberi, B. and B. Christ (1999). "Genetic and epigenetic control of muscle development in vertebrates." Cell Tissue Res **296**(1): 199-212.

Brand-Saberi, B., J. Wilting, C. Ebensperger and B. Christ (1996). "The formation of somite compartments in the avian embryo." Int J Dev Biol **40**(1): 411-20.

Braun, T., G. Buschhausen-Denker, E. Bober, E. Tannich and H. H. Arnold (1989). "A novel human muscle factor related to but distinct from MyoD1 induces myogenic conversion in 10T1/2 fibroblasts." Embo J **8**(3): 701-9.

Braun, T., M. A. Rudnicki, H. H. Arnold and R. Jaenisch (1992). "Targeted inactivation of the muscle regulatory gene Myf-5 results in abnormal rib development and perinatal death." Cell **71**(3): 369-82.

Broussard, S. R., R. H. McCusker, J. E. Novakofski, K. Strle, W. H. Shen, R. W. Johnson, R. Dantzer and K. W. Kelley (2004). "IL-1beta impairs insulin-like growth factor i-induced differentiation and downstream activation signals of the insulin-like growth factor i receptor in myoblasts." J Immunol **172**(12): 7713-20.

Brunet, A., A. Bonni, M. J. Zigmond, M. Z. Lin, P. Juo, L. S. Hu, M. J. Anderson, K. C. Arden, J. Blenis and M. E. Greenberg (1999). "Akt promotes cell survival by phosphorylating and inhibiting a Forkhead transcription factor." Cell **96**(6): 857-68.

Buckingham, M. (1992). "Making muscle in mammals." Trends Genet **8**(4): 144-8.

Buckingham, M. (2001). "Skeletal muscle formation in vertebrates." Curr Opin Genet Dev **11**(4): 440-8.

Buckingham, M., L. Bajard, T. Chang, P. Daubas, J. Hadchouel, S. Meilhac, D. Montarras, D. Rocancourt and F. Relaix (2003). "The formation of skeletal muscle: from somite to limb." J Anat **202**(1): 59-68.

Cai, D., J. D. Frantz, N. E. Tawa, Jr., P. A. Melendez, B. C. Oh, H. G. Lidov, P. O. Hasselgren, W. R. Frontera, J. Lee, D. J. Glass and S. E. Shoelson (2004). "IKKbeta/NF-kappaB Activation Causes Severe Muscle Wasting in Mice." Cell **119**(2): 285-98.

Cariuk, P., M. J. Lorite, P. T. Todorov, W. N. Field, S. J. Wigmore and M. J. Tisdale (1997). "Induction of cachexia in mice by a product isolated from the urine of cachectic cancer patients." Br J Cancer **76**(5): 606-13.

Carlson, C. J., F. W. Booth and S. E. Gordon (1999). "Skeletal muscle myostatin mRNA expression is fiber-type specific and increases during hindlimb unloading." Am J Physiol **277**(2 Pt 2): R601-6.

Chen, Z. J. (2005). "Ubiquitin signalling in the NF-kappaB pathway." Nat Cell Biol **7**(8): 758-65.

Christ, B. and C. P. Ordahl (1995). "Early stages of chick somite development." Anat Embryol (Berl) **191**(5): 381-96.

Clavel, S., A. S. Coldefy, E. Kurkdjian, J. Salles, I. Margaritis and B. Derijard (2006). "Atrophy-related ubiquitin ligases, atrogin-1 and MuRF1 are up-regulated in aged rat Tibialis Anterior muscle." Mech Ageing Dev **127**(10): 794-801.

Clop, A., F. Marcq, H. Takeda, D. Pirottin, X. Tordoir, B. Bibe, J. Bouix, F. Caiment, J. M. Elsen, F. Eychenne, C. Larzul, E. Laville, F. Meish, D. Milenkovic, J. Tobin, C. Charlier and M. Georges (2006). "A mutation creating a potential illegitimate microRNA target site in the myostatin gene affects muscularity in sheep." Nat Genet **38**(7): 813-8.

Collins, C. A., I. Olsen, P. S. Zammit, L. Heslop, A. Petrie, T. A. Partridge and J. E. Morgan (2005). "Stem cell function, self-renewal, and behavioral heterogeneity of cells from the adult muscle satellite cell niche." Cell **122**(2): 289-301.

Conboy, I. M. and T. A. Rando (2002). "The regulation of notch signaling controls satellite cell activation and cell fate determination in postnatal myogenesis." Dev Cell **3**(3): 397-409.

Cornelison, D. D., M. S. Filla, H. M. Stanley, A. C. Rapraeger and B. B. Olwin (2001). "Syndecan-3 and syndecan-4 specifically mark skeletal muscle satellite cells and are implicated in satellite cell maintenance and muscle regeneration.PG - 79-94." Dev Biol **239**(1).

Cornelison, D. D. and B. J. Wold (1997). "Single-cell analysis of regulatory gene expression in quiescent and activated mouse skeletal muscle satellite cells." Dev Biol **191**(2): 270-83.

Cossu, G., S. Tajbakhsh and M. Buckingham (1996). "How is myogenesis initiated in the embryo?" Trends Genet **12**(6): 218-23.

Costelli, P., M. Bossola, M. Muscaritoli, G. Grieco, G. Bonelli, R. Bellantone, G. B. Doglietto, F. M. Baccino and F. R. Fanelli (2002). "Anticytokine

treatment prevents the increase in the activity of ATP-ubiquitin- and Ca(2+)-dependent proteolytic systems in the muscle of tumour-bearing rats." Cytokine **19**(1): 1-5.

Costelli, P., M. Muscaritoli, M. Bossola, F. Penna, P. Reffo, A. Bonetto, S. Busquets, G. Bonelli, F. J. Lopez-Soriano, G. B. Doglietto, J. M. Argiles, F. M. Baccino and F. R. Fanelli (2006). "IGF-1 is downregulated in experimental cancer cachexia." Am J Physiol Regul Integr Comp Physiol **291**(3): R674-83.

Costelli, P., P. Reffo, F. Penna, R. Autelli, G. Bonelli and F. M. Baccino (2005). "Ca(2+)-dependent proteolysis in muscle wasting." Int J Biochem Cell Biol **37**(10): 2134-46.

Dardevet, D., C. Sornet, D. Taillandier, I. Savary, D. Attaix and J. Grizard (1995). "Sensitivity and protein turnover response to glucocorticoids are different in skeletal muscle from adult and old rats. Lack of regulation of the ubiquitin-proteasome proteolytic pathway in aging." J Clin Invest **96**(5): 2113-9.

Darin, N. and M. Tulinius (2000). "Neuromuscular disorders in childhood: a descriptive epidemiological study from western Sweden." Neuromuscul Disord **10**(1): 1-9.

Dasarathy, S., M. Dodig, S. M. Muc, S. C. Kalhan and A. J. McCullough (2004). "Skeletal muscle atrophy is associated with an increased expression of myostatin and impaired satellite cell function in the portacaval anastamosis rat." Am J Physiol Gastrointest Liver Physiol.

Davis, R. L., H. Weintraub and A. B. Lassar (1987). "Expression of a single transfected cDNA converts fibroblasts to myoblasts." Cell **51**(6): 987-1000.

De Angelis, L., L. Berghella, M. Coletta, L. Lattanzi, M. Zanchi, M. G. Cusella-De Angelis, C. Ponzetto and G. Cossu (1999). "Skeletal myogenic progenitors originating from embryonic dorsal aorta coexpress endothelial and myogenic markers and contribute to postnatal muscle growth and regeneration." J Cell Biol **147**(4): 869-78.

Deval, C., S. Mordier, C. Obled, D. Bechet, L. Combaret, D. Attaix and M. Ferrara (2001). "Identification of cathepsin L as a differentially expressed

message associated with skeletal muscle wasting." Biochem J **360**(Pt 1): 143-50.

DeVol, D. L., P. Rotwein, J. L. Sadow, J. Novakofski and P. J. Bechtel (1990). "Activation of insulin-like growth factor gene expression during work-induced skeletal muscle growth." Am J Physiol **259**(1 Pt 1): E89-95.

Dhawan, J. and T. A. Rando (2005). "Stem cells in postnatal myogenesis: molecular mechanisms of satellite cell quiescence, activation and replenishment." Trends Cell Biol **15**(12): 666-73.

Di Francia, M., D. Barbier, J. L. Mege and J. Orehek (1994). "Tumor necrosis factor-alpha levels and weight loss in chronic obstructive pulmonary disease." Am J Respir Crit Care Med **150**(5 Pt 1): 1453-5.

Dogra, C., H. Changotra, S. Mohan and A. Kumar (2006). "Tumor necrosis factor-like weak inducer of apoptosis inhibits skeletal myogenesis through sustained activation of nuclear factor-kappaB and degradation of MyoD protein." J Biol Chem **281**(15): 10327-36.

Dreyfus, P. A., F. Chretien, B. Chazaud, Y. Kirova, P. Caramelle, L. Garcia, G. Butler-Browne and R. K. Gherardi (2004). "Adult bone marrow-derived stem cells in muscle connective tissue and satellite cell niches." Am J Pathol **164**(3): 773-9.

Edgerton, V. R., R. R. Roy, D. L. Allen and R. J. Monti (2002). "Adaptations in skeletal muscle disuse or decreased-use atrophy." Am J Phys Med Rehabil **81**(11 Suppl): S127-47.

Edmondson, D. G. and E. N. Olson (1989). "A gene with homology to the myc similarity region of MyoD1 is expressed during myogenesis and is sufficient to activate the muscle differentiation program." Genes Dev **3**(5): 628-40.

Emery, A. E. (1991). "Population frequencies of inherited neuromuscular diseases--a world survey." Neuromuscul Disord **1**(1): 19-29.

Enomoto, A., M. C. Rho, A. Fukami, O. Hiraku, K. Komiyama and M. Hayashi (2004). "Suppression of cancer cachexia by 20S,21-epoxy-resibufogenin-3-acetate-a novel nonpeptide IL-6 receptor antagonist." Biochem Biophys Res Commun **323**(3): 1096-102.

Fainsod, A., K. Deissler, R. Yelin, K. Marom, M. Epstein, G. Pillemer, H. Steinbeisser and M. Blum (1997). "The dorsalizing and neural inducing gene follistatin is an antagonist of BMP-4." Mech Dev **63**(1): 39-50.

Fang, C. H., B. G. Li, C. J. Wray and P. O. Hasselgren (2002). "Insulin-like growth factor-I inhibits lysosomal and proteasome-dependent proteolysis in skeletal muscle after burn injury." J Burn Care Rehabil **23**(5): 318-25.

Fareed, M. U., A. R. Evenson, W. Wei, M. Menconi, V. Poylin, V. Petkova, B. Pignol and P. O. Hasselgren (2006). "Treatment of rats with calpain inhibitors prevents sepsis-induced muscle proteolysis independent of atrogin-1/MAFbx and MuRF1 expression." Am J Physiol Regul Integr Comp Physiol **290**(6): R1589-97.

Fernandez, A. M., J. Dupont, R. P. Farrar, S. Lee, B. Stannard and D. Le Roith (2002). "Muscle-specific inactivation of the IGF-I receptor induces compensatory hyperplasia in skeletal muscle." J Clin Invest **109**(3): 347-55.

Flanigan, K. M., A. von Niederhausern, D. M. Dunn, J. Alder, J. R. Mendell and R. B. Weiss (2003). "Rapid direct sequence analysis of the dystrophin gene." Am J Hum Genet **72**(4): 931-9.

Forbes, D., M. Jackman, A. Bishop, M. Thomas, R. Kambadur and M. Sharma (2006). "Myostatin auto-regulates its expression by feedback loop through Smad7 dependent mechanism." J Cell Physiol **206**(1): 264-72.

Franz, T., R. Kothary, M. A. Surani, Z. Halata and M. Grim (1993). "The Splotch mutation interferes with muscle development in the limbs." Anat Embryol (Berl) **187**(2): 153-60.

Fukada, S., S. Higuchi, M. Segawa, K. Koda, Y. Yamamoto, K. Tsujikawa, Y. Kohama, A. Uezumi, M. Imamura, Y. Miyagoe-Suzuki, S. Takeda and H. Yamamoto (2004). "Purification and cell-surface marker characterization of quiescent satellite cells from murine skeletal muscle by a novel monoclonal antibody." Exp Cell Res **296**(2): 245-55.

Fung, Y. C. (1981). Biomechanics: mechanical properties of living tissues. New York, Springer-Verlag.

Galvez, B. G., M. Sampaolesi, S. Brunelli, D. Covarello, M. Gavina, B. Rossi, G. Constantin, Y. Torrente and G. Cossu (2006). "Complete repair of

dystrophic skeletal muscle by mesoangioblasts with enhanced migration ability." J Cell Biol **174**(2): 231-43.

Garcia-Martinez, C., N. Agell, M. Llovera, F. J. Lopez-Soriano and J. M. Argiles (1993). "Tumour necrosis factor-alpha increases the ubiquitinization of rat skeletal muscle proteins." FEBS Lett **323**(3): 211-4.

Garry, D. J., Q. Yang, R. Bassel-Duby and R. S. Williams (1997). "Persistent expression of MNF identifies myogenic stem cells in postnatal muscles." Dev Biol **188**(2): 280-94.

Gibson, M. C. and E. Schultz (1982). "The distribution of satellite cells and their relationship to specific fiber types in soleus and extensor digitorum longus muscles." Anat Rec **202**(3): 329-37.

Gibson, M. C. and E. Schultz (1983). "Age-related differences in absolute numbers of skeletal muscle satellite cells." Muscle Nerve **6**(8): 574-80.

Girgenrath, S., K. Song and L. A. Whittemore (2005). "Loss of myostatin expression alters fiber-type distribution and expression of myosin heavy chain isoforms in slow- and fast-type skeletal muscle." Muscle Nerve **31**(1): 34-40.

Glass, D. J. (2005). "Skeletal muscle hypertrophy and atrophy signaling pathways." Int J Biochem Cell Biol **37**(10): 1974-84.

Goll, D. E., V. F. Thompson, H. Li, W. Wei and J. Cong (2003). "The calpain system." Physiol Rev **83**(3): 731-801.

Gomes, M. D., S. H. Lecker, R. T. Jagoe, A. Navon and A. L. Goldberg (2001). "Atrogin-1, a muscle-specific F-box protein highly expressed during muscle atrophy." Proc Natl Acad Sci U S A **98**(25): 14440-5.

Gonzalez-Cadavid, N. F., W. E. Taylor, K. Yarasheski, I. Sinha-Hikim, K. Ma, S. Ezzat, R. Shen, R. Lalani, S. Asa, M. Mamita, G. Nair, S. Arver and S. Bhasin (1998). "Organization of the human myostatin gene and expression in healthy men and HIV-infected men with muscle wasting." Proc Natl Acad Sci U S A **95**(25): 14938-43.

Goodell, M. A., K. Brose, G. Paradis, A. S. Conner and R. C. Mulligan (1996). "Isolation and functional properties of murine hematopoietic stem cells that are replicating in vivo." J Exp Med **183**(4): 1797-806.

Goulding, M. D., G. Chalepakis, U. Deutsch, J. R. Erselius and P. Gruss (1991). "Pax-3, a novel murine DNA binding protein expressed during early neurogenesis." Embo J **10**(5): 1135-47.

Grobet, L., D. Pirottin, F. Farnir, D. Poncelet, L. J. Royo, B. Brouwers, E. Christians, D. Desmecht, F. Coignoul, R. Kahn and M. Georges (2003). "Modulating skeletal muscle mass by postnatal, muscle-specific inactivation of the myostatin gene." Genesis **35**(4): 227-38.

Grobet, L., D. Poncelet, L. J. Royo, B. Brouwers, D. Pirottin, C. Michaux, F. Menissier, M. Zanotti, S. Dunner and M. Georges (1998). "Molecular definition of an allelic series of mutations disrupting the myostatin function and causing double-muscling in cattle." Mamm Genome **9**(3): 210-3.

Gros, J., M. Manceau, V. Thome and C. Marcelle (2005). "A common somitic origin for embryonic muscle progenitors and satellite cells." Nature **435**(7044): 954-8.

Gross, J. G. and J. E. Morgan (1999). "Muscle precursor cells injected into irradiated mdx mouse muscle persist after serial injury." Muscle Nerve **22**(2): 174-85.

Grounds, M. D. (1998). "Age-associated changes in the response of skeletal muscle cells to exercise and regeneration." Ann N Y Acad Sci **854**: 78-91.

Grounds, M. D. and Z. Yablonka-Reuveni (1993). "Molecular and cell biology of skeletal muscle regeneration." Mol Cell Biol Hum Dis Ser **3**: 210-56.

Gullberg, D., T. Velling, L. Lohikangas and C. F. Tiger (1998). "Integrins during muscle development and in muscular dystrophies." Front Biosci **3**: D1039-50.

Gussoni, E., Y. Soneoka, C. D. Strickland, E. A. Buzney, M. K. Khan, A. F. Flint, L. M. Kunkel and R. C. Mulligan (1999). "Dystrophin expression in the mdx mouse restored by stem cell transplantation." Nature **401**(6751): 390-4.

Guttinger, M., E. Tafi, M. Battaglia, M. Coletta and G. Cossu (2006). "Allogeneic mesoangioblasts give rise to alpha-sarcoglycan expressing fibers when transplanted into dystrophic mice." Experimental cell research **15**(312): 3872-3879.

Guttridge, D. C., M. W. Mayo, L. V. Madrid, C. Y. Wang and A. S. Baldwin, Jr. (2000). "NF-kappaB-induced loss of MyoD messenger RNA: possible role in muscle decay and cachexia." Science **289**(5488): 2363-6.

Haddad, F. and G. R. Adams (2006). "Aging-sensitive cellular and molecular mechanisms associated with skeletal muscle hypertrophy." J Appl Physiol **100**(4): 1188-203.

Haddad, F., F. Zaldivar, D. M. Cooper and G. R. Adams (2005). "IL-6-induced skeletal muscle atrophy." J Appl Physiol **98**(3): 911-7.

Halevy, O., Y. Piestun, M. Z. Allouh, B. W. Rosser, Y. Rinkevich, R. Reshef, I. Rozenboim, M. Wleklinski-Lee and Z. Yablonka-Reuveni (2004). "Pattern of Pax7 expression during myogenesis in the posthatch chicken establishes a model for satellite cell differentiation and renewal." Dev Dyn **231**(3): 489-502.

Harper, J. W., G. R. Adami, N. Wei, K. Keyomarsi and S. J. Elledge (1993). "The p21 Cdk-interacting protein Cip1 is a potent inhibitor of G1 cyclin-dependent kinases." Cell **75**(4): 805-16.

Harris, A. J., M. J. Duxson, R. B. Fitzsimons and F. Rieger (1989). "Myonuclear birthdates distinguish the origins of primary and secondary myotubes in embryonic mammalian skeletal muscles." Development **107**(4): 771-84.

Hasselgren, P. O. and J. E. Fischer (2001). "Muscle cachexia: current concepts of intracellular mechanisms and molecular regulation." Ann Surg **233**(1): 9-17.

Hasty, P., A. Bradley, J. H. Morris, D. G. Edmondson, J. M. Venuti, E. N. Olson and W. H. Klein (1993). "Muscle deficiency and neonatal death in mice with a targeted mutation in the myogenin gene [see comments]." Nature **364**(6437): 501-6.

Hata, A., G. Lagna, J. Massague and A. Hemmati-Brivanlou (1998). "Smad6 inhibits BMP/Smad1 signaling by specifically competing with the Smad4 tumor suppressor." Genes Dev **12**(2): 186-97.

Hawke, T. J. and D. J. Garry (2001). "Myogenic satellite cells: physiology to molecular biology." J Appl Physiol **91**(2): 534-51.

Hawke, T. J., A. P. Meeson, N. Jiang, S. Graham, K. Hutcheson, J. M. DiMaio and D. J. Garry (2003). "p21 is essential for normal myogenic progenitor

cell function in regenerating skeletal muscle." Am J Physiol Cell Physiol **285**(5): C1019-27.

Hayashi, H., S. Abdollah, Y. Qiu, J. Cai, Y. Y. Xu, B. W. Grinnell, M. A. Richardson, J. N. Topper, M. A. Gimbrone, Jr., J. L. Wrana and D. Falb (1997). "The MAD-related protein Smad7 associates with the TGFbeta receptor and functions as an antagonist of TGFbeta signaling." Cell **89**(7): 1165-73.

Hellerstein, M. K., S. N. Meydani, M. Meydani, K. Wu and C. A. Dinarello (1989). "Interleukin-1-induced anorexia in the rat. Influence of prostaglandins." J Clin Invest **84**(1): 228-35.

Hemmati-Brivanlou, A., O. G. Kelly and D. A. Melton (1994). "Follistatin, an antagonist of activin, is expressed in the Spemann organizer and displays direct neuralizing activity." Cell **77**(2): 283-95.

Heslop, L., J. R. Beauchamp, S. Tajbakhsh, M. E. Buckingham, T. A. Partridge and P. S. Zammit (2001). "Transplanted primary neonatal myoblasts can give rise to functional satellite cells as identified using the Myf5nlacZl+ mouse." Gene Ther **8**(10): 778-83.

Heszele, M. F. and S. R. Price (2004). "Insulin-like growth factor I: the yin and yang of muscle atrophy." Endocrinology **145**(11): 4803-5.

Hickson, R. C., S. M. Czerwinski and L. E. Wegrzyn (1995). "Glutamine prevents downregulation of myosin heavy chain synthesis and muscle atrophy from glucocorticoids." Am J Physiol **268**(4 Pt 1): E730-4.

Hickson, R. C., L. E. Wegrzyn, D. F. Osborne and I. E. Karl (1996). "Alanyl-glutamine prevents muscle atrophy and glutamine synthetase induction by glucocorticoids." Am J Physiol **271**(5 Pt 2): R1165-72.

Hill, J. J., M. V. Davies, A. A. Pearson, J. H. Wang, R. M. Hewick, N. M. Wolfman and Y. Qiu (2002). "The myostatin propeptide and the follistatin-related gene are inhibitory binding proteins of myostatin in normal serum." J Biol Chem **277**(43): 40735-41.

Hill, J. J., Y. Qiu, R. M. Hewick and N. M. Wolfman (2003). "Regulation of myostatin in vivo by growth and differentiation factor-associated serum protein-1: a novel protein with protease inhibitor and follistatin domains." Mol Endocrinol **17**(6): 1144-54.

Hoffman, E. P., R. H. Brown, Jr. and L. M. Kunkel (1987). "Dystrophin: the protein product of the Duchenne muscular dystrophy locus." Cell **51**(6): 919-28.

Hoffman, E. P., K. H. Fischbeck, R. H. Brown, M. Johnson, R. Medori, J. D. Loike, J. B. Harris, R. Waterston, M. Brooke, L. Specht and et al. (1988). "Characterization of dystrophin in muscle-biopsy specimens from patients with Duchenne's or Becker's muscular dystrophy." N Engl J Med **318**(21): 1363-8.

Hollway, G. and P. Currie (2005). "Vertebrate myotome development." Birth Defects Res C Embryo Today **75**(3): 172-9.

Holterman, C. E. and M. A. Rudnicki (2005). "Molecular regulation of satellite cell function." Semin Cell Dev Biol **16**(4-5): 575-84.

Hopf, F. W., P. R. Turner, W. F. Denetclaw, Jr., P. Reddy and R. A. Steinhardt (1996). "A critical evaluation of resting intracellular free calcium regulation in dystrophic mdx muscle." Am J Physiol **271**(4 Pt 1): C1325-39.

Hosoyama, T., C. Tachi, K. Yamanouchi and M. Nishihara (2005). "Long term adrenal insufficiency induces skeletal muscle atrophy and increases the serum levels of active form myostatin in rat serum." Zoolog Sci **22**(2): 229-36.

Huang, J. and N. E. Forsberg (1998). "Role of calpain in skeletal-muscle protein degradation." Proc Natl Acad Sci U S A **95**(21): 12100-5.

Hudson, N. J. and C. E. Franklin (2003). "Preservation of three-dimensional capillary structure in frog muscle during aestivation." J Anat **202**(5): 471-4.

Irintchev, A., M. Zeschnigk, A. Starzinski-Powitz and A. Wernig (1994). "Expression pattern of M-cadherin in normal, denervated, and regenerating mouse muscles." Dev Dyn **199**(4): 326-37.

Jackman, R. W. and S. C. Kandarian (2004). "The molecular basis of skeletal muscle atrophy." Am J Physiol Cell Physiol **287**(4): C834-43.

Jagoe, R. T., C. P. Redfern, R. G. Roberts, G. J. Gibson and T. H. Goodship (2002). "Skeletal muscle mRNA levels for cathepsin B, but not components of the ubiquitin-proteasome pathway, are increased in patients

with lung cancer referred for thoracotomy." Clin Sci (Lond) **102**(3): 353-61.

Janssen, S. P., G. Gayan-Ramirez, A. Van den Bergh, P. Herijgers, K. Maes, E. Verbeken and M. Decramer (2005). "Interleukin-6 causes myocardial failure and skeletal muscle atrophy in rats." Circulation **111**(8): 996-1005.

Jeanplong, F., M. Sharma, W. G. Somers, J. J. Bass and R. Kambadur (2001). "Genomic organization and neonatal expression of the bovine myostatin gene." Mol Cell Biochem **220**(1-2): 31-7.

Ji, S., R. L. Losinski, S. G. Cornelius, G. R. Frank, G. M. Willis, D. E. Gerrard, F. F. Depreux and M. E. Spurlock (1998). "Myostatin expression in porcine tissues: tissue specificity and developmental and postnatal regulation." Am J Physiol **275**(4 Pt 2): R1265-73.

Johnson, S. E. and R. E. Allen (1995). "Activation of skeletal muscle satellite cells and the role of fibroblast growth factor receptors." Exp Cell Res **219**(2): 449-53.

Joulia-Ekaza, D. and G. Cabello (2006). "Myostatin regulation of muscle development: molecular basis, natural mutations, physiopathological aspects." Exp Cell Res **312**(13): 2401-14.

Kambadur, R., M. Sharma, T. P. Smith and J. J. Bass (1997). "Mutations in myostatin (GDF8) in double-muscled Belgian Blue and Piedmontese cattle." Genome Res **7**(9): 910-6.

Karayiannakis, A. J., K. N. Syrigos, A. Polychronidis, M. Pitiakoudis, A. Bounovas and K. Simopoulos (2001). "Serum levels of tumor necrosis factor-alpha and nutritional status in pancreatic cancer patients." Anticancer Res **21**(2B): 1355-8.

Kardon, G., J. K. Campbell and C. J. Tabin (2002). "Local extrinsic signals determine muscle and endothelial cell fate and patterning in the vertebrate limb." Dev Cell **3**(4): 533-45.

Kassar-Duchossoy, L., B. Gayraud-Morel, D. Gomes, D. Rocancourt, M. Buckingham, V. Shinin and S. Tajbakhsh (2004). "Mrf4 determines skeletal muscle identity in Myf5:Myod double-mutant mice." Nature **431**(7007): 466-71.

Kassar-Duchossoy, L., E. Giacone, B. Gayraud-Morel, A. Jory, D. Gomes and S. Tajbakhsh (2005). "Pax3/Pax7 mark a novel population of primitive myogenic cells during development." Genes Dev **19**(12): 1426-31.

Katz, F. (1961). "The termination of the afferent nerve fiber in the muslce spindle of the frog." Phil trans Roy Soc Lond **243**: 221-225.

Kawada, S., C. Tachi and N. Ishii (2001). "Content and localization of myostatin in mouse skeletal muscles during aging, mechanical unloading and reloading." J Muscle Res Cell Motil **22**(8): 627-33.

Khal, J., A. V. Hine, K. C. Fearon, C. H. Dejong and M. J. Tisdale (2005). "Increased expression of proteasome subunits in skeletal muscle of cancer patients with weight loss." Int J Biochem Cell Biol **37**(10): 2196-206.

Kitzmann, M., G. Carnac, M. Vandromme, M. Primig, N. J. Lamb and A. Fernandez (1998). "The muscle regulatory factors MyoD and myf-5 undergo distinct cell cycle-specific expression in muscle cells." J Cell Biol **142**(6): 1447-59.

Kocamis, H., D. C. Kirkpatrick-Keller, J. Richter and J. Killefer (1999). "The ontogeny of myostatin, follistatin and activin-B mRNA expression during chicken embryonic development." Growth Dev Aging **63**(4): 143-50.

Koenig, M., A. H. Beggs, M. Moyer, S. Scherpf, K. Heindrich, T. Bettecken, G. Meng, C. R. Muller, M. Lindlof, H. Kaariainen and et al. (1989). "The molecular basis for Duchenne versus Becker muscular dystrophy: correlation of severity with type of deletion." Am J Hum Genet **45**(4): 498-506.

Koenig, M., E. P. Hoffman, C. J. Bertelson, A. P. Monaco, C. Feener and L. M. Kunkel (1987). "Complete cloning of the Duchenne muscular dystrophy (DMD) cDNA and preliminary genomic organization of the DMD gene in normal and affected individuals." Cell **50**(3): 509-17.

Kramerova, I., E. Kudryashova, G. Venkatraman and M. J. Spencer (2005). "Calpain 3 participates in sarcomere remodeling by acting upstream of the ubiquitin-proteasome pathway." Hum Mol Genet **14**(15): 2125-34.

Krawiec, B. J., R. A. Frost, T. C. Vary, L. S. Jefferson and C. H. Lang (2005). "Hindlimb casting decreases muscle mass in part by proteasome-dependent proteolysis but independent of protein synthesis." Am J Physiol Endocrinol Metab **289**(6): E969-80.

Kuang, S., S. B. Charge, P. Seale, M. Huh and M. A. Rudnicki (2006). "Distinct roles for Pax7 and Pax3 in adult regenerative myogenesis." J Cell Biol **172**(1): 103-13.

Kurzrock, R., J. Redman, F. Cabanillas, D. Jones, J. Rothberg and M. Talpaz (1993). "Serum interleukin 6 levels are elevated in lymphoma patients and correlate with survival in advanced Hodgkin's disease and with B symptoms." Cancer Res **53**(9): 2118-22.

LaBarge, M. A. and H. M. Blau (2002). "Biological progression from adult bone marrow to mononucleate muscle stem cell to multinucleate muscle fiber in response to injury." Cell **111**(4): 589-601.

Lalani, R., S. Bhasin, F. Byhower, R. Tarnuzzer, M. Grant, R. Shen, S. Asa, S. Ezzat and N. F. Gonzalez-Cadavid (2000). "Myostatin and insulin-like growth factor-I and -II expression in the muscle of rats exposed to the microgravity environment of the NeuroLab space shuttle flight." J Endocrinol **167**(3): 417-28.

Lang, C. H., D. Huber and R. A. Frost (2006). "Burn-Induced Increase in Atrogin-1 and MuRF-1 in Skeletal Muscle is Glucocorticoid-Independent but Down Regulated by IGF-I." Am J Physiol Regul Integr Comp Physiol.

Langley, B., M. Thomas, A. Bishop, M. Sharma, S. Gilmour and R. Kambadur (2002). "Myostatin inhibits myoblast differentiation by down regulating MyoD expression." J Biol Chem **18**: 18.

Langley, B., M. Thomas, C. McFarlane, S. Gilmour, M. Sharma and R. Kambadur (2004). "Myostatin inhibits rhabdomyosarcoma cell proliferation through an Rb-independent pathway." Oncogene **23**(2): 524-34.

Laviano, A., C. Cangiano, A. Fava, M. Muscaritoli, G. Mulieri and F. Rossi Fanelli (1999). "Peripherally injected IL-1 induces anorexia and increases brain tryptophan concentrations." Adv Exp Med Biol **467**: 105-8.

Lecker, S. H., R. T. Jagoe, A. Gilbert, M. Gomes, V. Baracos, J. Bailey, S. R. Price, W. E. Mitch and A. L. Goldberg (2004). "Multiple types of skeletal muscle atrophy involve a common program of changes in gene expression." Faseb J **18**(1): 39-51.

Lee, S. J. and A. C. McPherron (2001). "Regulation of myostatin activity and muscle growth." Proc Natl Acad Sci U S A **98**(16): 9306-11.

Li, Y. P., Y. Chen, J. John, J. Moylan, B. Jin, D. L. Mann and M. B. Reid (2005a). "TNF-alpha acts via p38 MAPK to stimulate expression of the ubiquitin ligase atrogin1/MAFbx in skeletal muscle." Faseb J **19**(3): 362-70.

Li, Y. P. and M. B. Reid (2000). "NF-kappaB mediates the protein loss induced by TNF-alpha in differentiated skeletal muscle myotubes." Am J Physiol Regul Integr Comp Physiol **279**(4): R1165-70.

Li, Y. P., R. J. Schwartz, I. D. Waddell, B. R. Holloway and M. B. Reid (1998). "Skeletal muscle myocytes undergo protein loss and reactive oxygen-mediated NF-kappaB activation in response to tumor necrosis factor alpha." Faseb J **12**(10): 871-80.

Li, Z. F., G. D. Shelton and E. Engvall (2005b). "Elimination of myostatin does not combat muscular dystrophy in dy mice but increases postnatal lethality." Am J Pathol **166**(2): 491-7.

Lipford, J. R. and R. J. Deshaies (2003). "Diverse roles for ubiquitin-dependent proteolysis in transcriptional activation." Nat Cell Biol **5**(10): 845-50.

Llovera, M., N. Carbo, C. Garcia-Martinez, P. Costelli, L. Tessitore, F. M. Baccino, N. Agell, G. J. Bagby, F. J. Lopez-Soriano and J. M. Argiles (1996). "Anti-TNF treatment reverts increased muscle ubiquitin gene expression in tumour-bearing rats." Biochem Biophys Res Commun **221**(3): 653-5.

Lorite, M. J., P. Cariuk and M. J. Tisdale (1997). "Induction of muscle protein degradation by a tumour factor." Br J Cancer **76**(8): 1035-40.

Lorite, M. J., H. J. Smith, J. A. Arnold, A. Morris, M. G. Thompson and M. J. Tisdale (2001). "Activation of ATP-ubiquitin-dependent proteolysis in skeletal muscle in vivo and murine myoblasts in vitro by a proteolysis-inducing factor (PIF)." Br J Cancer **85**(2): 297-302.

Lorite, M. J., M. G. Thompson, J. L. Drake, G. Carling and M. J. Tisdale (1998). "Mechanism of muscle protein degradation induced by a cancer cachectic factor." Br J Cancer **78**(7): 850-6.

Ma, K., C. Mallidis, S. Bhasin, V. Mahabadi, J. Artaza, N. Gonzalez-Cadavid, J. Arias and B. Salehian (2003). "Glucocorticoid-induced skeletal muscle atrophy is associated with upregulation of myostatin gene expression." Am J Physiol Endocrinol Metab **285**(2): E363-71.

Magee, T. R., J. N. Artaza, M. G. Ferrini, D. Vernet, F. I. Zuniga, L. Cantini, S. Reisz-Porszasz, J. Rajfer and N. F. Gonzalez-Cadavid (2006). "Myostatin short interfering hairpin RNA gene transfer increases skeletal muscle mass." J Gene Med.

Mansouri, A., A. Stoykova, M. Torres and P. Gruss (1996). "Dysgenesis of cephalic neural crest derivatives in Pax7-/- mutant mice." Development **122**(3): 831-8.

Marcell, T. J., S. M. Harman, R. J. Urban, D. D. Metz, B. D. Rodgers and M. R. Blackman (2001). "Comparison of GH, IGF-I, and testosterone with mRNA of receptors and myostatin in skeletal muscle in older men." Am J Physiol Endocrinol Metab **281**(6): E1159-64.

Martini, F. H. (2001). Fundamentals of Anatomy and Physiology. New Jersey, Prentice Hall International Inc.

Marzetti, E. and C. Leeuwenburgh (2006). "Skeletal muscle apoptosis, sarcopenia and frailty at old age." Exp Gerontol **41**(12): 1234-1238.

Matthys, P., R. Dijkmans, P. Proost, J. Van Damme, H. Heremans, H. Sobis and A. Billiau (1991). "Severe cachexia in mice inoculated with interferon-gamma-producing tumor cells." Int J Cancer **49**(1): 77-82.

Matzuk, M. M., N. Lu, H. Vogel, K. Sellheyer, D. R. Roop and A. Bradley (1995). "Multiple defects and perinatal death in mice deficient in follistatin." Nature **374**(6520): 360-3.

Mauro, A. (1961). "Satellite cell of skeletal fibers." Journal of Biophysical & Biochemistry Cytology **9**: 493-498.

McCroskery, S., M. Thomas, L. Maxwell, M. Sharma and R. Kambadur (2003). "Myostatin negatively regulates satellite cell activation and self-renewal." J Cell Biol **162**(6): 1135-47.

McCroskery, S., M. Thomas, L. Platt, A. Hennebry, T. Nishimura, L. McLeay, M. Sharma and R. Kambadur (2005). "Improved muscle healing through enhanced regeneration and reduced fibrosis in myostatin-null mice." J Cell Sci **118**(Pt 15): 3531-41.

McDevitt, T. M., P. T. Todorov, S. A. Beck, S. H. Khan and M. J. Tisdale (1995). "Purification and characterization of a lipid-mobilizing factor associated with cachexia-inducing tumors in mice and humans." Cancer Res **55**(7): 1458-63.

McFarland, D. C., S. G. Velleman, J. E. Pesall and C. Liu (2006). "Effect of myostatin on turkey myogenic satellite cells and embryonic myoblasts." Comp Biochem Physiol A Mol Integr Physiol **144**(4): 501-8.

McFarlane, C., A. Hennebry, M. Thomas, M. Sharma and R. Kambadur (2006a). Myostatin signals through Pax7 to regulate post-natal myogenesis. Frontiers in Myogenesis, Society for Muscle Biology, Pine Mountain, Grorgia, U.S.A.

McFarlane, C., B. Langley, M. Thomas, A. Hennebry, E. Plummer, G. Nicholas, C. McMahon, M. Sharma and R. Kambadur (2005). "Proteolytic processing of myostatin is auto-regulated during myogenesis." Dev Biol **283**(1): 58-69.

McFarlane, C., E. Plummer, M. Thomas, A. Hennebry, M. Ashby, N. Ling, H. Smith, M. Sharma and R. Kambadur (2006b). "Myostatin induces cachexia by activating the ubiquitin proteolytic system through an NF-kappaB-independent, FoxO1-dependent mechanism." J Cell Physiol **209**(2): 501-514.

McPherron, A. C., A. M. Lawler and S. J. Lee (1997). "Regulation of skeletal muscle mass in mice by a new TGF-beta superfamily member." Nature **387**(6628): 83-90.

McPherron, A. C. and S. Lee (1996). "The transforming growth factor-b superfamily." Growth Factors Cytokines Health Dis **1B**: 357-393.

McPherron, A. C. and S. J. Lee (1997). "Double muscling in cattle due to mutations in the myostatin gene." Proc Natl Acad Sci U S A **94**(23): 12457-61.

Medina, R., S. S. Wing and A. L. Goldberg (1995). "Increase in levels of polyubiquitin and proteasome mRNA in skeletal muscle during starvation and denervation atrophy." Biochem J **307 (Pt 3)**: 631-7.

Michel, U., P. Farnworth and J. K. Findlay (1993). "Follistatins: more than follicle-stimulating hormone suppressing proteins." Mol Cell Endocrinol **91**(1-2): 1-11.

Minetti, G. C., C. Colussi, R. Adami, C. Serra, C. Mozzetta, V. Parente, S. Fortuni, S. Straino, M. Sampaolesi, M. Di Padova, B. Illi, P. Gallinari, C. Steinkuhler, M. C. Capogrossi, V. Sartorelli, R. Bottinelli, C. Gaetano and P. L. Puri (2006). "Functional and morphological recovery of dystrophic

muscles in mice treated with deacetylase inhibitors." Nat Med **12**(10): 1147-50.

Mitch, W. E., J. L. Bailey, X. Wang, C. Jurkovitz, D. Newby and S. R. Price (1999). "Evaluation of signals activating ubiquitin-proteasome proteolysis in a model of muscle wasting." Am J Physiol **276**(5 Pt 1): C1132-8.

Mitch, W. E. and A. L. Goldberg (1996). "Mechanisms of muscle wasting. The role of the ubiquitin-proteasome pathway." N Engl J Med **335**(25): 1897-905.

Mitchell, M. D., C. C. Osepchook, K. C. Leung, C. D. McMahon and J. J. Bass (2006). "Myostatin is a human placental product that regulates glucose uptake." J Clin Endocrinol Metab **91**(4): 1434-7.

Mitchell, P. O. and G. K. Pavlath (2001). "A muscle precursor cell-dependent pathway contributes to muscle growth after atrophy." Am J Physiol Cell Physiol **281**(5): C1706-15.

Miura, T., Y. Kishioka, J. Wakamatsu, A. Hattori, A. Hennebry, C. J. Berry, M. Sharma, R. Kambadur and T. Nishimura (2006). "Decorin binds myostatin and modulates its activity to muscle cells." Biochem Biophys Res Commun **340**(2): 675-80.

Montanaro, F., K. Liadaki, J. Schienda, A. Flint, E. Gussoni and L. M. Kunkel (2004). "Demystifying SP cell purification: viability, yield, and phenotype are defined by isolation parameters." Exp Cell Res **298**(1): 144-54.

Montarras, D., J. Morgan, C. Collins, F. Relaix, S. Zaffran, A. Cumano, T. Partridge and M. Buckingham (2005). "Direct isolation of satellite cells for skeletal muscle regeneration." Science **309**(5743): 2064-7.

Morgan, J., J. Beauchamp, C. Pagel, M. Peckham, P. Ataliotis, P. Jat, M. Noble, K. Farmer and T. Partridge (1994). "Myogenic cell lines derived from transgenic mice carrying a thermolabile T antigen: a model system for the derivation of tissue-specific and mutation-specific cell lines." Developmental Biology **162**(2): 486-98.

Musaro, A., K. McCullagh, A. Paul, L. Houghton, G. Dobrowolny, M. Molinaro, E. R. Barton, H. L. Sweeney and N. Rosenthal (2001). "Localized Igf-1 transgene expression sustains hypertrophy and regeneration in senescent skeletal muscle." Nat Genet **27**(2): 195-200.

Nabeshima, Y., K. Hanaoka, M. Hayasaka, E. Esumi, S. Li and I. Nonaka (1993). "Myogenin gene disruption results in perinatal lethality because of severe muscle defect [see comments]." Nature **364**(6437): 532-5.

Nagata, Y., H. Kobayashi, M. Umeda, N. Ohta, S. Kawashima, P. S. Zammit and R. Matsuda (2006). "Sphingomyelin levels in the plasma membrane correlate with the activation state of muscle satellite cells." J Histochem Cytochem **54**(4): 375-84.

Nakao, A., M. Afrakhte, A. Moren, T. Nakayama, J. L. Christian, R. Heuchel, S. Itoh, M. Kawabata, N. E. Heldin, C. H. Heldin and P. ten Dijke (1997a). "Identification of Smad7, a TGFbeta-inducible antagonist of TGF-beta signalling." Nature **389**(6651): 631-5.

Nakao, A., T. Imamura, S. Souchelnytskyi, M. Kawabata, A. Ishisaki, E. Oeda, K. Tamaki, J. Hanai, C. H. Heldin, K. Miyazono and P. ten Dijke (1997b). "TGF-beta receptor-mediated signalling through Smad2, Smad3 and Smad4." Embo J **16**(17): 5353-62.

Nakashima, J., M. Tachibana, M. Ueno, A. Miyajima, S. Baba and M. Murai (1998). "Association between tumor necrosis factor in serum and cachexia in patients with prostate cancer." Clin Cancer Res **4**(7): 1743-8.

Nandi, D., P. Tahiliani, A. Kumar and D. Chandu (2006). "The ubiquitin-proteasome system." J Biosci **31**(1): 137-55.

Nicholas, G., M. Thomas, B. Langley, W. Somers, K. Patel, C. F. Kemp, M. Sharma and R. Kambadur (2002). "Titin-cap associates with, and regulates secretion of, Myostatin." J Cell Physiol **193**(1): 120-31.

Nishi, M., A. Yasue, S. Nishimatu, T. Nohno, T. Yamaoka, M. Itakura, K. Moriyama, H. Ohuchi and S. Noji (2002). "A missense mutant myostatin causes hyperplasia without hypertrophy in the mouse muscle." Biochem Biophys Res Commun **293**(1): 247-51.

Oldham, J. M., J. A. Martyn, M. Sharma, F. Jeanplong, R. Kambadur and J. J. Bass (2001). "Molecular expression of myostatin and MyoD is greater in double-muscled than normal-muscled cattle fetuses." Am J Physiol Regul Integr Comp Physiol **280**(5): R1488-93.

Olguin, H. C. and B. B. Olwin (2004). "Pax-7 up-regulation inhibits myogenesis and cell cycle progression in satellite cells: a potential mechanism for self-renewal." Dev Biol **275**(2): 375-88.

Oliff, A., D. Defeo-Jones, M. Boyer, D. Martinez, D. Kiefer, G. Vuocolo, A. Wolfe and S. H. Socher (1987). "Tumors secreting human TNF/cachectin induce cachexia in mice." Cell **50**(4): 555-63.

Olson, E. N., H. H. Arnold, P. W. Rigby and B. J. Wold (1996). "Know your neighbors: three phenotypes in null mutants of the myogenic bHLH gene MRF4." Cell **85**(1): 1-4.

Ott, M. O., E. Bober, G. Lyons, H. Arnold and M. Buckingham (1991). "Early expression of the myogenic regulatory gene, myf-5, in precursor cells of skeletal muscle in the mouse embryo." Development **111**(4): 1097-107.

Oustanina, S., G. Hause and T. Braun (2004). "Pax7 directs postnatal renewal and propagation of myogenic satellite cells but not their specification." Embo J **23**(16): 3430-9.

Peterlin, B., J. Zidar, M. Meznaric-Petrusa and N. Zupancic (1997). "Genetic epidemiology of Duchenne and Becker muscular dystrophy in Slovenia." Clin Genet **51**(2): 94-7.

Philip, B., Z. Lu and Y. Gao (2005). "Regulation of GDF-8 signaling by the p38 MAPK." Cell Signal **17**(3): 365-75.

Piek, E., C. H. Heldin and P. Ten Dijke (1999). "Specificity, diversity, and regulation in TGF-beta superfamily signaling." Faseb J **13**(15): 2105-24.

Polesskaya, A., P. Seale and M. A. Rudnicki (2003). "Wnt signaling induces the myogenic specification of resident CD45+ adult stem cells during muscle regeneration." Cell **113**(7): 841-52.

Porter, J. D., S. Khanna, H. J. Kaminski, J. S. Rao, A. P. Merriam, C. R. Richmonds, P. Leahy, J. Li, W. Guo and F. H. Andrade (2002). "A chronic inflammatory response dominates the skeletal muscle molecular signature in dystrophin-deficient mdx mice." Hum Mol Genet **11**(3): 263-72.

Pownall, M. E., M. K. Gustafsson and C. P. Emerson, Jr. (2002). "Myogenic regulatory factors and the specification of muscle progenitors in vertebrate embryos." Annu Rev Cell Dev Biol **18**: 747-83.

Reardon, K. A., J. Davis, R. M. Kapsa, P. Choong and E. Byrne (2001). "Myostatin, insulin-like growth factor-1, and leukemia inhibitory factor mRNAs are upregulated in chronic human disuse muscle atrophy." Muscle Nerve **24**(7): 893-9.

Rebbapragada, A., H. Benchabane, J. L. Wrana, A. J. Celeste and L. Attisano (2003). "Myostatin signals through a transforming growth factor beta-like signaling pathway to block adipogenesis." Mol Cell Biol **23**(20): 7230-42.

Relaix, F., D. Montarras, S. Zaffran, B. Gayraud-Morel, D. Rocancourt, S. Tajbakhsh, A. Mansouri, A. Cumano and M. Buckingham (2006). "Pax3 and Pax7 have distinct and overlapping functions in adult muscle progenitor cells." J Cell Biol **172**(1): 91-102.

Relaix, F., D. Rocancourt, A. Mansouri and M. Buckingham (2005). "A Pax3/Pax7-dependent population of skeletal muscle progenitor cells." Nature **435**(7044): 948-53.

Rhodes, S. J. and S. F. Konieczny (1989). "Identification of MRF4: a new member of the muscle regulatory factor gene family." Genes Dev **3**(12B): 2050-61.

Rios, R., I. Carneiro, V. M. Arce and J. Devesa (2002). "Myostatin is an inhibitor of myogenic differentiation." Am J Physiol Cell Physiol **282**(5): C993-9.

Rommel, C., S. C. Bodine, B. A. Clarke, R. Rossman, L. Nunez, T. N. Stitt, G. D. Yancopoulos and D. J. Glass (2001). "Mediation of IGF-1-induced skeletal myotube hypertrophy by PI(3)K/Akt/mTOR and PI(3)K/Akt/GSK3 pathways." Nat Cell Biol **3**(11): 1009-13.

Rosenblatt, J. D., A. I. Lunt, D. J. Parry and T. A. Partridge (1995). "Culturing satellite cells from living single muscle fiber explants." In Vitro Cell Dev Biol Anim **31**(10): 773-9.

Rosenblatt, J. D., D. Yong and D. J. Parry (1994). "Satellite cell activity is required for hypertrophy of overloaded adult rat muscle." Muscle Nerve **17**(6): 608-13.

Rosenblatt, S., G. H. Clowes, Jr., B. C. George, E. Hirsch and B. Lindberg (1983). "Exchange of amino acids by muscle and liver in sepsis." Arch Surg **118**(2): 167-75.

Rudnicki, M. A., T. Braun, S. Hinuma and R. Jaenisch (1992). "Inactivation of MyoD in mice leads to up-regulation of the myogenic HLH gene Myf-5 and results in apparently normal muscle development." Cell **71**(3): 383-90.

Rudnicki, M. A., P. N. Schnegelsberg, R. H. Stead, T. Braun, H. H. Arnold and R. Jaenisch (1993). "MyoD or Myf-5 is required for the formation of skeletal muscle." Cell **75**(7): 1351-9.

Sacheck, J. M., A. Ohtsuka, S. C. McLary and A. L. Goldberg (2004). "IGF-I stimulates muscle growth by suppressing protein breakdown and expression of atrophy-related ubiquitin ligases, atrogin-1 and MuRF1." Am J Physiol Endocrinol Metab **287**(4): E591-601.

Saharinen, J., M. Hyytiainen, J. Taipale and J. Keski-Oja (1999). "Latent transforming growth factor-beta binding proteins (LTBPs)-- structural extracellular matrix proteins for targeting TGF-beta action." Cytokine Growth Factor Rev **10**(2): 99-117.

Salehian, B., V. Mahabadi, J. Bilas, W. E. Taylor and K. Ma (2006). "The effect of glutamine on prevention of glucocorticoid-induced skeletal muscle atrophy is associated with myostatin suppression." Metabolism **55**(9): 1239-47.

Sampaolesi, M., Y. Torrente, A. Innocenzi, R. Tonlorenzi, G. D'Antona, M. A. Pellegrino, R. Barresi, N. Bresolin, M. G. De Angelis, K. P. Campbell, R. Bottinelli and G. Cossu (2003). "Cell therapy of alpha-sarcoglycan null dystrophic mice through intra-arterial delivery of mesoangioblasts." Science **301**(5632): 487-92.

Sandri, M., C. Sandri, A. Gilbert, C. Skurk, E. Calabria, A. Picard, K. Walsh, S. Schiaffino, S. H. Lecker and A. L. Goldberg (2004). "Foxo transcription factors induce the atrophy-related ubiquitin ligase atrogin-1 and cause skeletal muscle atrophy." Cell **117**(3): 399-412.

Sassoon, D., G. Lyons, W. E. Wright, V. Lin, A. Lassar, H. Weintraub and M. Buckingham (1989). "Expression of two myogenic regulatory factors myogenin and MyoD1 during mouse embryogenesis." Nature **341**(6240): 303-7.

Sazanov, A., D. Ewald, J. Buitkamp and R. Fries (1999). "A molecular marker for the chicken myostatin gene (GDF8) maps to 7p11." Anim Genet **30**(5): 388-9.

Schienda, J., K. A. Engleka, S. Jun, M. S. Hansen, J. A. Epstein, C. J. Tabin, L. M. Kunkel and G. Kardon (2006). "Somitic origin of limb muscle satellite and side population cells." Proc Natl Acad Sci U S A **103**(4): 945-50.

Schneyer, A., D. Tortoriello, Y. Sidis, H. Keutmann, T. Matsuzaki and W. Holmes (2001). "Follistatin-related protein (FSRP): a new member of the follistatin gene family." Mol Cell Endocrinol **180**(1-2): 33-8.

Schuelke, M., K. R. Wagner, L. E. Stolz, C. Hubner, T. Riebel, W. Komen, T. Braun, J. F. Tobin and S. J. Lee (2004). "Myostatin mutation associated with gross muscle hypertrophy in a child." N Engl J Med **350**(26): 2682-8.

Schulte, J. N. and K. E. Yarasheski (2001). "Effects of resistance training on the rate of muscle protein synthesis in frail elderly people." Int J Sport Nutr Exerc Metab **11 Suppl**: S111-8.

Schultz, E. and K. M. McCormick (1994). "Skeletal muscle satellite cells." Rev Physiol Biochem Pharmacol **123**: 213-57.

Scott, H. R., D. C. McMillan, A. Crilly, C. S. McArdle and R. Milroy (1996). "The relationship between weight loss and interleukin 6 in non-small-cell lung cancer." Br J Cancer **73**(12): 1560-2.

Seale, P., J. Ishibashi, A. Scime and M. A. Rudnicki (2004). "Pax7 is necessary and sufficient for the myogenic specification of CD45+:Sca1+ stem cells from injured muscle." PLoS Biol **2**(5): E130.

Seale, P. and M. A. Rudnicki (2000). "A new look at the origin, function, and "stem-cell" status of muscle satellite cells." Dev Biol **218**(2): 115-24.

Seale, P., L. A. Sabourin, A. Girgis-Gabardo, A. Mansouri, P. Gruss and M. A. Rudnicki (2000). "Pax7 is required for the specification of myogenic satellite cells." Cell **102**(6): 777-86.

Sharma, M., R. Kambadur, K. G. Matthews, W. G. Somers, G. P. Devlin, J. V. Conaglen, P. J. Fowke and J. J. Bass (1999). "Myostatin, a transforming growth factor-beta superfamily member, is expressed in heart muscle and is upregulated in cardiomyocytes after infarct." J Cell Physiol **180**(1): 1-9.

Shefer, G., D. P. Van de Mark, J. B. Richardson and Z. Yablonka-Reuveni (2006). "Satellite-cell pool size does matter: defining the myogenic potency of aging skeletal muscle." Dev Biol **294**(1): 50-66.

Sherwood, R. I., J. L. Christensen, I. M. Conboy, M. J. Conboy, T. A. Rando, I. L. Weissman and A. J. Wagers (2004). "Isolation of adult mouse myogenic progenitors: functional heterogeneity of cells within and engrafting skeletal muscle." Cell **119**(4): 543-54.

Shibli-Rahhal, A., M. Van Beek and J. A. Schlechte (2006). "Cushing's syndrome." Clin Dermatol **24**(4): 260-5.

Shinin, V., B. Gayraud-Morel, D. Gomes and S. Tajbakhsh (2006). "Asymmetric division and cosegregation of template DNA strands in adult muscle satellite cells." Nat Cell Biol **8**(7): 677-87.

Siciliano, G., A. Tessa, M. Renna, M. L. Manca, M. Mancuso and L. Murri (1999). "Epidemiology of dystrophinopathies in North-West Tuscany: a molecular genetics-based revisitation." Clin Genet **56**(1): 51-8.

Siriett, V., L. Platt, M. S. Salerno, N. Ling, R. Kambadur and M. Sharma (2006). "Prolonged absence of myostatin reduces sarcopenia." J Cell Physiol **209**(3): 866-73.

Sironi, M., R. Cagliani, G. P. Comi, U. Pozzoli, A. Bardoni, R. Giorda and N. Bresolin (2003). "Trans-acting factors may cause dystrophin splicing misregulation in BMD skeletal muscles." FEBS Lett **537**(1-3): 30-4.

Smith, H. J., M. J. Lorite and M. J. Tisdale (1999). "Effect of a cancer cachectic factor on protein synthesis/degradation in murine C2C12 myoblasts: modulation by eicosapentaenoic acid." Cancer Res **59**(21): 5507-13.

Solomon, V. and A. L. Goldberg (1996). "Importance of the ATP-ubiquitin-proteasome pathway in the degradation of soluble and myofibrillar proteins in rabbit muscle extracts." J Biol Chem **271**(43): 26690-7.

Song, Y. H., Y. Li, J. Du, W. E. Mitch, N. Rosenthal and P. Delafontaine (2005). "Muscle-specific expression of IGF-1 blocks angiotensin II-induced skeletal muscle wasting." J Clin Invest **115**(2): 451-8.

Souchelnytskyi, S., K. Tamaki, U. Engstrom, C. Wernstedt, P. ten Dijke and C. H. Heldin (1997). "Phosphorylation of Ser465 and Ser467 in the C terminus of Smad2 mediates interaction with Smad4 and is required for transforming growth factor-beta signaling." J Biol Chem **272**(44): 28107-15.

Spencer, M. J., D. E. Croall and J. G. Tidball (1995). "Calpains are activated in necrotic fibers from mdx dystrophic mice." J Biol Chem **270**(18): 10909-14.

Spencer, M. J. and R. L. Mellgren (2002). "Overexpression of a calpastatin transgene in mdx muscle reduces dystrophic pathology." Hum Mol Genet **11**(21): 2645-55.

Stewart, C. E., P. V. Newcomb and J. M. Holly (2004). "Multifaceted roles of TNF-alpha in myoblast destruction: a multitude of signal transduction pathways." J Cell Physiol **198**(2): 237-47.

Stitt, T. N., D. Drujan, B. A. Clarke, F. Panaro, Y. Timofeyva, W. O. Kline, M. Gonzalez, G. D. Yancopoulos and D. J. Glass (2004). "The IGF-1/PI3K/Akt pathway prevents expression of muscle atrophy-induced ubiquitin ligases by inhibiting FOXO transcription factors." Mol Cell **14**(3): 395-403.

Szabo, G., G. Dallmann, G. Muller, L. Patthy, M. Soller and L. Varga (1998). "A deletion in the myostatin gene causes the compact (Cmpt) hypermuscular mutation in mice." Mamm Genome **9**(8): 671-2.

Szalay, K., Z. Razga and E. Duda (1997). "TNF inhibits myogenesis and downregulates the expression of myogenic regulatory factors myoD and myogenin." Eur J Cell Biol **74**(4): 391-8.

Taillandier, D., E. Aurousseau, D. Meynial-Denis, D. Bechet, M. Ferrara, P. Cottin, A. Ducastaing, X. Bigard, C. Y. Guezennec, H. P. Schmid and et al. (1996). "Coordinate activation of lysosomal, Ca 2+-activated and ATP-ubiquitin-dependent proteinases in the unweighted rat soleus muscle." Biochem J **316 (Pt 1)**: 65-72.

Tajbakhsh, S. and M. Buckingham (2000). "The birth of muscle progenitor cells in the mouse: spatiotemporal considerations." Curr Top Dev Biol **48**: 225-68.

Tajbakhsh, S., D. Rocancourt, G. Cossu and M. Buckingham (1997). "Redefining the genetic hierarchies controlling skeletal myogenesis: Pax- 3 and Myf-5 act upstream of MyoD." Cell **89**(1): 127-38.

Tamaki, T., A. Akatsuka, K. Ando, Y. Nakamura, H. Matsuzawa, T. Hotta, R. R. Roy and V. R. Edgerton (2002). "Identification of myogenic-endothelial progenitor cells in the interstitial spaces of skeletal muscle." J Cell Biol **157**(4): 571-7.

Tang, E. D., G. Nunez, F. G. Barr and K. L. Guan (1999). "Negative regulation of the forkhead transcription factor FKHR by Akt." J Biol Chem **274**(24): 16741-6.

Tatsumi, R., J. E. Anderson, C. J. Nevoret, O. Halevy and R. E. Allen (1998). "HGF/SF is present in normal adult skeletal muscle and is capable of activating satellite cells." Dev Biol **194**(1): 114-28.

Tatsumi, R., A. Hattori, Y. Ikeuchi, J. E. Anderson and R. E. Allen (2002). "Release of hepatocyte growth factor from mechanically stretched skeletal muscle satellite cells and role of pH and nitric oxide." Mol Biol Cell **13**(8): 2909-18.

Tatsumi, R., X. Liu, A. Pulido, M. Morales, T. Sakata, S. Dial, A. Hattori, Y. Ikeuchi and R. E. Allen (2006). "Satellite cell activation in stretched skeletal muscle and the role of nitric oxide and hepatocyte growth factor." Am J Physiol Cell Physiol **290**(6): C1487-94.

Temparis, S., M. Asensi, D. Taillandier, E. Aurousseau, D. Larbaud, A. Obled, D. Bechet, M. Ferrara, J. M. Estrela and D. Attaix (1994). "Increased ATP-ubiquitin-dependent proteolysis in skeletal muscles of tumor-bearing rats." Cancer Res **54**(21): 5568-73.

Thies, R. S., T. Chen, M. V. Davies, K. N. Tomkinson, A. A. Pearson, Q. A. Shakey and N. M. Wolfman (2001). "GDF-8 propeptide binds to GDF-8 and antagonizes biological activity by inhibiting GDF-8 receptor binding." Growth Factors **18**(4): 251-9.

Thomas, M., B. Langley, C. Berry, M. Sharma, S. Kirk, J. Bass and R. Kambadur (2000). "Myostatin, a negative regulator of muscle growth, functions by inhibiting myoblast proliferation." J Biol Chem **275**(51): 40235-43.

Tidball, J. G. (1995). "Inflammatory cell response to acute muscle injury." Med Sci Sports Exerc **27**(7): 1022-32.

Tidball, J. G. and M. J. Spencer (2002). "Expression of a calpastatin transgene slows muscle wasting and obviates changes in myosin isoform expression during murine muscle disuse." J Physiol **545**(Pt 3): 819-28.

Tintignac, L. A., J. Lagirand, S. Batonnet, V. Sirri, M. P. Leibovitch and S. A. Leibovitch (2005). "Degradation of MyoD Mediated by the SCF (MAFbx) Ubiquitin Ligase." J Biol Chem **280**(4): 2847-56.

Tisdale, M. J. (2005). "The ubiquitin-proteasome pathway as a therapeutic target for muscle wasting." J Support Oncol **3**(3): 209-17.

Tolosa, L., M. Morla, A. Iglesias, X. Busquets, J. Llado and G. Olmos (2005). "IFN-gamma prevents TNF-alpha-induced apoptosis in C2C12 myotubes

through down-regulation of TNF-R2 and increased NF-kappaB activity." Cell Signal **17**(11): 1333-42.

Tracey, K. J., S. Morgello, B. Koplin, T. J. Fahey, 3rd, J. Fox, A. Aledo, K. R. Manogue and A. Cerami (1990). "Metabolic effects of cachectin/tumor necrosis factor are modified by site of production. Cachectin/tumor necrosis factor-secreting tumor in skeletal muscle induces chronic cachexia, while implantation in brain induces predominantly acute anorexia." J Clin Invest **86**(6): 2014-24.

Tremblay, P., S. Dietrich, M. Mericskay, F. R. Schubert, Z. Li and D. Paulin (1998). "A crucial role for Pax3 in the development of the hypaxial musculature and the long-range migration of muscle precursors." Dev Biol **203**(1): 49-61.

Tseng, B. S., P. Zhao, J. S. Pattison, S. E. Gordon, J. A. Granchelli, R. W. Madsen, L. C. Folk, E. P. Hoffman and F. W. Booth (2002). "Regenerated mdx mouse skeletal muscle shows differential mRNA expression." J Appl Physiol **93**(2): 537-45.

Tsuchida, K., K. Y. Arai, Y. Kuramoto, N. Yamakawa, Y. Hasegawa and H. Sugino (2000). "Identification and characterization of a novel follistatin-like protein as a binding protein for the TGF-beta family." J Biol Chem **275**(52): 40788-96.

Tsuchida, K., T. Matsuzaki, N. Yamakawa, Z. Liu and H. Sugino (2001). "Intracellular and extracellular control of activin function by novel regulatory molecules." Mol Cell Endocrinol **180**(1-2): 25-31.

Tsuchiya, S., Y. Okuno and G. Tsujimoto (2006). "MicroRNA: biogenetic and functional mechanisms and involvements in cell differentiation and cancer." J Pharmacol Sci **101**(4): 267-70.

Vermaelen, M., J. F. Marini, A. Chopard, Y. Benyamin, J. Mercier and C. Astier (2005). "Ubiquitin targeting of rat muscle proteins during short periods of unloading." Acta Physiol Scand **185**(1): 33-40.

Vivanco, I. and C. L. Sawyers (2002). "The phosphatidylinositol 3-Kinase AKT pathway in human cancer." Nat Rev Cancer **2**(7): 489-501.

Volonte, D., Y. Liu and F. Galbiati (2005). "The modulation of caveolin-1 expression controls satellite cell activation during muscle repair." Faseb J **19**(2): 237-9.

Wang, H., Q. Zhang and D. Zhu (2003). "hSGT interacts with the N-terminal region of myostatin." Biochem Biophys Res Commun **311**(4): 877-83.

Wang, W., L. Nacusi, R. J. Sheaff and X. Liu (2005). "Ubiquitination of p21Cip1/WAF1 by SCFSkp2: substrate requirement and ubiquitination site selection." Biochemistry **44**(44): 14553-64.

Watt, D. J., J. Karasinski, J. Moss and M. A. England (1994). "Migration of muscle cells." Nature **368**(6470): 406-7.

Watt, D. J., J. E. Morgan, M. A. Clifford and T. A. Partridge (1987). "The movement of muscle precursor cells between adjacent regenerating muscles in the mouse." Anat Embryol (Berl) **175**(4): 527-36.

Wehling, M., B. Cai and J. G. Tidball (2000). "Modulation of myostatin expression during modified muscle use." Faseb J **14**(1): 103-10.

Weissman, I. L., D. J. Anderson and F. Gage (2001). "Stem and progenitor cells: origins, phenotypes, lineage commitments, and transdifferentiations." Annu Rev Cell Dev Biol **17**: 387-403.

Welle, S., K. Bhatt, B. Shah and C. Thornton (2002). "Insulin-like growth factor-1 and myostatin mRNA expression in muscle: comparison between 62-77 and 21-31 yr old men." Exp Gerontol **37**(6): 833-9.

Wernig, G., V. Janzen, R. Schafer, M. Zweyer, U. Knauf, O. Hoegemeier, R. R. Mundegar, S. Garbe, S. Stier, T. Franz, M. Wernig and A. Wernig (2005). "The vast majority of bone-marrow-derived cells integrated into mdx muscle fibers are silent despite long-term engraftment." Proc Natl Acad Sci U S A **102**(33): 11852-7.

Whitehouse, A. S. and M. J. Tisdale (2003). "Increased expression of the ubiquitin-proteasome pathway in murine myotubes by proteolysis-inducing factor (PIF) is associated with activation of the transcription factor NF-kappaB." Br J Cancer **89**(6): 1116-22.

Whitman, S. A., M. J. Wacker, S. R. Richmond and M. P. Godard (2005). "Contributions of the ubiquitin-proteasome pathway and apoptosis to human skeletal muscle wasting with age." Pflugers Arch **450**(6): 437-46.

Whittemore, L. A., K. Song, X. Li, J. Aghajanian, M. Davies, S. Girgenrath, J. J. Hill, M. Jalenak, P. Kelley, A. Knight, R. Maylor, D. O'Hara, A. Pearson, A. Quazi, S. Ryerson, X. Y. Tan, K. N. Tomkinson, G. M. Veldman, A. Widom, J. F. Wright, S. Wudyka, L. Zhao and N. M. Wolfman (2003).

"Inhibition of myostatin in adult mice increases skeletal muscle mass and strength." Biochem Biophys Res Commun **300**(4): 965-71.

Williams, A., X. Sun, J. E. Fischer and P. O. Hasselgren (1999a). "The expression of genes in the ubiquitin-proteasome proteolytic pathway is increased in skeletal muscle from patients with cancer." Surgery **126**(4): 744-9; discussion 749-50.

Williams, A. B., G. M. Decourten-Myers, J. E. Fischer, G. Luo, X. Sun and P. O. Hasselgren (1999b). "Sepsis stimulates release of myofilaments in skeletal muscle by a calcium-dependent mechanism." Faseb J **13**(11): 1435-43.

Wing, S. S. (2005). "Control of ubiquitination in skeletal muscle wasting." Int J Biochem Cell Biol **37**(10): 2075-87.

Wolfman, N. M., A. C. McPherron, W. N. Pappano, M. V. Davies, K. Song, K. N. Tomkinson, J. F. Wright, L. Zhao, S. M. Sebald, D. S. Greenspan and S. J. Lee (2003). "Activation of latent myostatin by the BMP-1/tolloid family of metalloproteinases." Proc Natl Acad Sci U S A **100**(26): 15842-6.

Wyke, S. M., J. Khal and M. J. Tisdale (2005). "Signalling pathways in the induction of proteasome expression by proteolysis-inducing factor in murine myotubes." Cell Signal **17**(1): 67-75.

Wyke, S. M. and M. J. Tisdale (2005). "NF-kappaB mediates proteolysis-inducing factor induced protein degradation and expression of the ubiquitin-proteasome system in skeletal muscle." Br J Cancer **92**(4): 711-21.

Xiong, Y., G. J. Hannon, H. Zhang, D. Casso, R. Kobayashi and D. Beach (1993). "p21 is a universal inhibitor of cyclin kinases." Nature **366**(6456): 701-4.

Yablonka-Reuveni, Z. and A. J. Rivera (1994). "Temporal expression of regulatory and structural muscle proteins during myogenesis of satellite cells on isolated adult rat fibers." Dev Biol **164**(2): 588-603.

Yablonka-Reuveni, Z., R. Seger and A. J. Rivera (1999). "Fibroblast growth factor promotes recruitment of skeletal muscle satellite cells in young and old rats." J Histochem Cytochem **47**(1): 23-42.

Yan, Z., S. Choi, X. Liu, M. Zhang, J. J. Schageman, S. Y. Lee, R. Hart, L. Lin, F. A. Thurmond and R. S. Williams (2003). "Highly coordinated gene regulation in mouse skeletal muscle regeneration." J Biol Chem **278**(10): 8826-36.

Yang, J., T. Ratovitski, J. P. Brady, M. B. Solomon, K. D. Wells and R. J. Wall (2001). "Expression of myostatin pro domain results in muscular transgenic mice." Mol Reprod Dev **60**(3): 351-61.

Yang, W., Y. Chen, Y. Zhang, X. Wang, N. Yang and D. Zhu (2006). "Extracellular signal-regulated kinase 1/2 mitogen-activated protein kinase pathway is involved in myostatin-regulated differentiation repression." Cancer Res **66**(3): 1320-6.

Yarasheski, K. E., S. Bhasin, I. Sinha-Hikim, J. Pak-Loduca and N. F. Gonzalez-Cadavid (2002). "Serum myostatin-immunoreactive protein is increased in 60-92 year old women and men with muscle wasting." J Nutr Health Aging **6**(5): 343-8.

Yoshida, N., S. Yoshida, K. Koishi, K. Masuda and Y. Nabeshima (1998). "Cell heterogeneity upon myogenic differentiation: down-regulation of MyoD and Myf-5 generates 'reserve cells'." J Cell Sci **111**(Pt 6)): 769-79.

Yu, Z. K., J. L. Gervais and H. Zhang (1998). "Human CUL-1 associates with the SKP1/SKP2 complex and regulates p21(CIP1/WAF1) and cyclin D proteins." Proc Natl Acad Sci U S A **95**(19): 11324-9.

Zachwieja, J. J., S. R. Smith, I. Sinha-Hikim, N. Gonzalez-Cadavid and S. Bhasin (1999). "Plasma myostatin-immunoreactive protein is increased after prolonged bed rest with low-dose T3 administration." J Gravit Physiol **6**(2): 11-5.

Zaki, M. H., J. A. Nemeth and M. Trikha (2004). "CNTO 328, a monoclonal antibody to IL-6, inhibits human tumor-induced cachexia in nude mice." Int J Cancer **111**(4): 592-5.

Zammit, P. S., J. P. Golding, Y. Nagata, V. Hudon, T. A. Partridge and J. R. Beauchamp (2004). "Muscle satellite cells adopt divergent fates: a mechanism for self-renewal?" J Cell Biol **166**(3): 347-57.

Zammit, P. S., T. A. Partridge and Z. Yablonka-Reuveni (2006a). "The skeletal muscle satellite cell: the stem cell that came in from the cold." J Histochem Cytochem **54**(11): 1177-91.

Zammit, P. S., F. Relaix, Y. Nagata, A. P. Ruiz, C. A. Collins, T. A. Partridge and J. R. Beauchamp (2006b). "Pax7 and myogenic progression in skeletal muscle satellite cells." J Cell Sci **119**(Pt 9): 1824-32.

Zhang, Y., T. Musci and R. Derynck (1997). "The tumor suppressor Smad4/DPC 4 as a central mediator of Smad function." Curr Biol **7**(4): 270-6.

Zhao, S. P. and L. H. Zeng (1997). "Elevated plasma levels of tumor necrosis factor in chronic heart failure with cachexia." Int J Cardiol **58**(3): 257-61.

Zhou, G. Q., H. Q. Xie, S. Z. Zhang and Z. M. Yang (2006). "Current understanding of dystrophin-related muscular dystrophy and therapeutic challenges ahead." Chin Med J (Engl) **119**(16): 1381-91.

Zhu, X., M. Hadhazy, M. Wehling, J. G. Tidball and E. M. McNally (2000). "Dominant negative myostatin produces hypertrophy without hyperplasia in muscle." FEBS Lett **474**(1): 71-5.

Zhu, X., S. Topouzis, L. F. Liang and R. L. Stotish (2004). "Myostatin signaling through Smad2, Smad3 and Smad4 is regulated by the inhibitory Smad7 by a negative feedback mechanism." Cytokine **26**(6): 262-72.

Zimmers, T. A., M. V. Davies, L. G. Koniaris, P. Haynes, A. F. Esquela, K. N. Tomkinson, A. C. McPherron, N. M. Wolfman and S. J. Lee (2002). "Induction of cachexia in mice by systemically administered myostatin." Science **296**(5572): 1486-8.

Chapter 2 Materials and Methods

This Chapter reviews the relevant materials and methods utilised throughout this project, including all reagents, chemicals and solutions. Also it includes an overview of all the general methods, with the specific methods being detailed in the relevant results chapters.

2.1 Materials

This section outlines general materials used in this thesis. Specific laboratory equipment required and the relevant commercially-available kits used during this study will be outlined in Section 2.2 of this Chapter.

2.1.1 Enzymes

All restriction endonuclease enzymes were acquired from either Invitrogen (Invitrogen, Carlsbad, CA) or Roche (Roche Diagnostics Corporation, Indianapolis, IN). Restriction enzyme buffers are supplied with all restriction enzymes. The remaining enzymes used in this study are listed in Table 2.1

Table 2.1 *Enzymes*

Enzyme	Source
DNase1	Invitrogen
Proteinase K	Roche
RNase H	Invitrogen
Superscript II Reverse Transcriptase	Invitrogen
T4 DNA ligase	Invitrogen
Taq DNA Polymerase	Roche
ThermalAce DNA Polymerase	Invitrogen

2.1.2 *Radioactive isotopes*

dCTP [α-^{32}P] with a specific activity of 3000 Ci/mM was used for labelling cDNA probes. This isotope was purchased from GE Healthcare Bio-Sciences.

2.1.3 *Antibodies*

Antibodies used in this thesis were purchased from the following companies: BD Pharmingen (BD Pharmingen, San Diego, CA), Boston Biochem (Boston Biochem, Cambridge, MA), DSHB (Developmental Studies Hybridoma Bank , Iowa City, IA), Santa Cruz Biotechology Inc. (Santa Cruz Biotechnology Inc, Santa Cruz, CA), Dako (Dako, Glostrup, Denmark), Sigma (Sigma, St Louis, MO), GE Healthcare Bio-Sciences (GE Healthcare Bio-Sciences Corp. Piscataway, NJ) and Research Diagnostics (Research Diagnostics, Concord, MA). All antibodies and associated information including dilution and incubation times are outlined in the Material and Methods sections of the results Chapters 3, 4, 5 and 6 where they were used.

Rabbit anti-Myostatin antibodies were produced by Dr Ravi Kambadur and Dr Mridula Sharma, Functional Muscle Genomics, AgResearch, Hamilton, New Zealand.

The Atrogin-1 antibody was a gift from Dr Cam Patterson, Department of Medicine, Division of Cardiology, University of North Carolina, School of Medicine, NC, USA.

2.1.4 *Plasmid DNA*

Plasmid DNA and their sources are listed in Table 2.2, commercial plasmids are listed in Table 2.3 The DNA was stored at -20ºC or 4ºC in TE buffer or MQ water.

Table 2.2 *Plasmid DNA*

Name	Species	Size (bp) Approx	Source
CXXC5 (MM1)	Mouse	1000	Bridgette Wilson[1,2] (Wilson 2006)
Pax3 Promoter	Mouse	1600	Dr J.A. Epstein[3] (Li *et al.* 1999)
MyoD Enhancer	Human	6500	Dr J.P. Capone[4] (Hunter *et al.* 2001)
P1 Furin promoter	Human	3700	Dr Claire Dubois[5] (Blanchette *et al.* 2001)
Pax7	Mouse	3000	Dr Michael Rudnicki[6]
RP23-48C24	Mouse	>100,000	BACPAC Resources[7]
RP24-337A16	Mouse	>100,000	BACPAC Resources[7]

[1]Functional Muscle Genomics, AgResearch, Hamilton, New Zealand.

[2]Department of Biological Sciences, University of Waikato, Hamilton, New Zealand.

[3]University of Pennsylvania School of Medicine, University of Pennsylvania, PA, USA.

[4]Department of Biochemistry, McMaster University, Hamilton, Ontario L8N 3Z5, Canada.

[5]Immunology Division, Faculty of Medicine, Université de Sherbrooke, Sherbrooke QC, Canada.

[6]Molecular Medicine Program and Center for Stem Cell and Gene Therapy, Ottawa Health Research Institute, Ottawa, ON, Canada.

[7]BACPAC Resources, Children's Hospital Oakland, Oakland, CA, USA.

Table 2.3 *Commercial plasmids*

Name	Description	Source
pcDNA3	5.446 bp, Amp^r, Neo^r, CMV, T7 and Sp6 RNA pol initiation sites, bGH p(A)	Invitrogen
pGEM-T Easy	3018 bp, Amp^r, T3 and T7 RNA pol initiation sites, LacZ	Promega
pGL3b	4818 bp, Amp^r, Luciferase gene-SV40 late p(A)	Promega
pCH110	7128 bp, Amp^r, SV40 Early promoter-lacZ	GE Healthcare Bio-Sciences
pBACe3.6	11612 bp, CM^r, T7 and SP6, SacB gene promoter, loxP	BACPAC Resources

2.1.5 Common solutions

Common solutions were made using the recipes described by Ausubel (Ausubel 1988) or Sambrook *et al*. (Sambrook *et al.* 1989) unless otherwise stated. Common solutions and their composition are listed in Table 2.4.

Table 2.4 *Common solutions*

Solution	Composition
Apoptosis lysis buffer	10 mM Tris-HCL (pH) 10nM EDTA 0.5% Triton X-100 0.1 mg/mL RNase A
Chicken embryo extract	see Section 2.2.8.4
Church and Gilbert hybridisation buffer	0.5 M Na_2HPO_4 (pH 7.2) 7% SDS 1 mM EDTA
DEPC treated water	Add 2 mL DEPC (0.1%) to 2 L of MQ water Autoclave

DNA loading dye	15% ficoll 0.25% bromophenol blue 0.25% xylene cyanol 1% SDS 1 mM EDTA (pH 8.0)
LB broth (with ampicillin)	20g/L Lennox LB broth base (Invitrogen) Add 1g/L of glucose MilliQ water to 1 L Autoclave. When cool add 1ml/litre of 50 mg/mL ampicillin.
LB agar (with ampicillin)	32 g/L Lennox LB agar base (Invitrogen) Add 1 g/L of glucose MilliQ water to 1 L Autoclave. When cool add 1ml/litre of 50 mg/mL ampicillin. Pour onto Petri dish
Lysis Buffer (protein extraction buffer)	50 mM Tris (pH 7.5) 250 mM NaCl 5 mM EDTA 0.1% NP-40 1x Protease inhibitor (Complete; Roche)
MOPS (10x)	41.8% MOPS 50 mM NaOAc 10 mM EDTA
PBS	1 Phosphate Buffered Saline tablet (Oxoid) 100 mL H_2O
Protein Sample buffer (2x)	1.5 M Tris (pH 6.8) 30% glycerol 20 % SDS

	2 M β-mercaptoethanol 0.0018% bromophenol blue
RNA loading dye	10% MOPS (10x) 20% deionised formaldehyde 50% deionised formamide 0.02% bromophenol blue 5% glycerol 1 mM EDTA (pH 8.0) 40 μg/mL ethidium bromide
Running buffer (DNA Agarose)	1x TAE diluted in MilliQ water
Running buffer (RNA Agarose)	1x MOPS diluted in DEPC treated water
Running buffer (SDS-PAGE; Western Blot)	25 mM Tris 190 mM glycine 1% SDS
Scott's tapwater	2 g Sodium Bicarbonate 20 g Magnesium Sulphate 1L MQ water 1 Crystal of Thymol
SSC (20x)	3 M NaCl 0.3 M sodium citrate (pH 7.0)
TAE	40 mM Tris-acetate 2 mM EDTA (pH 8.0)
TBS (Tris-buffered saline)	50 mM Tris (pH 7.5) 150 mM NaCl
TBST	50 mM Tris (pH 7.5) 150 mM NaCl 0.1% Tween 20

TE	10 mM Tris-Cl (at desired pH) 1 mM EDTA (pH 8.0)
Transfer buffer (Western transfer)	25 mM Tris 190 mM Glycine 20% methanol
Western Blocking Solution (Milk)	5% solution of low fat milk in TBST
Western Blocking Solution (BSA)	1% PVP 10,000, 1% PEG 4000 and 0.3% BSA in TBST
10x Trypsin	2.5% Trypsin in PBS

2.1.6 *Common laboratory chemicals and reagents*

All common laboratory chemicals and reagents are specified in Table 2.5. All chemicals and reagents are Analar grade unless otherwise stated.

Table 2.5 *Chemicals and reagents*

Chemical or Reagent	**Source**
Hybond-N+ membrane; radiographic cassettes	GE Healthcare Bio-Sciences
Ethanol; formaldehyde; glycerol; hydrochloric acid; methanol; sodium chloride; Tween-20; EDTA; sodium hydroxide (pelleted); chloroform; isopropanol; glucose	BDH Ltd
Bradford protein assay	Bio-Rad
Ultrapure agarose; low melting point	Invitrogen (Gibco BRL)

agarose (LMP); ethidium bromide; formamide; sodium dodecyl sulphate (SDS); dNTPs; TRIZOL reagent; tris; Benchmark prestained protein ladder; glycine; LB broth base; LB agar base; IPTG (isopropyl thio-β-galactoside); urea; NuPAGE 4-12% Bis Tris precast protein gels; phenol; DMEM (Dulbeccos Modified Eagle Medium); geneticin	
Kodak imaging film (XOMAT XAR)	Radiographic Supplies
DEPC (Diethyl pyrocarbonate); βMe (Beta-mercaptoethanol); Trizma base; MOPs (3-[N-Morpholino] propanesulfonic acid); ampicillin; phenol red.	Sigma-Aldrich

2.1.7 *Bacterial strains*

The bacterial strains used in this project are outlined in Table 2.6. The bacterial strains were kept at -80ºC in a 50% glycerol, 50% LB solution.

Table 2.6 *Bacterial strains*

Species	**Strain**	**Source**
E. coli	DH5α	Invitrogen
E. coli	JM109	Promega

2.1.8 *Oligonucleotides*

All oligonucleotides used during the course of this study were synthesised by Invitrogen. All oligonucleotides were stored at -20ºC and resuspended in TE at a concentration of 100 μM. Primers were further diluted in MQ water to generate working concentrations of 10 μM for each primer. While primers used for specific work will be documented in the relevant results chapters, Table 2.7 contains a list of primers, their associated annealing temperatures and product sizes.

Table 2.7 *Oligonucleotides*

Gene name	**Primer sequence (5' - 3')**	**Temp (°C)**	**Size (bp)**
Myostatin	Fwd: GGTATTTGGCAGAGTATTGATGTG	52	514
	Rev: GTCTACTACCATGGCTGGAAT		
MyoD	Fwd: GGATCCTAAGACGACTCTCAC	52	1047
	Rev: GGATCCAGTGCCTACGGTGG		
Pax3	Fwd: GCAAGATGGAGGAAACAAGC	60	676
	Rev: CGTTCTCAAGCAAGAGGTG		
NF-κB	Fwd: GGATCCATGGACGATCTGTTTCCCCT	55	1651
	Rev: GGATCCTTAGGAGCTGATCTGACTC		
FoxO1	Fwd: TTCAAGGATAAGGGCGACAG	60	300
	Rev: ACTCGCAGGCCACTTAGAAA		
CXXC5	Fwd: AACATGTGGGTGTATCGG	60	954
	Rev: TCTTGAGGGGAAAGTGAG		
Atrogin-1	Fwd: AACATGTGGGTGTATCGG	52	465
	Rev: TCTTGAGGGGAAAGTGAG		
MuRF-1	Fwd: GTTAAACCAGAGGTTCGAG	52	343
	Rev: ATGGTTCGCAACATTTCGG		

$E2_{14k}$	Fwd: ATGTCGCCCCGGCCCGGAGGCTCATG	45	453
	Rev: ATGAATCATTCCAGCTTTGTTCAAC		
$E2_{20k}$	Fwd: GGCGACACCATGTCATC	52	552
	Rev: ATGTCCTGGGCCTCATC		
RC2	Fwd: TCCAAACCTGCCCATCTGCTAACT	45	305
	Rev: AGGCTGTGCTTTTCTCTGTGGTCT		
Atrogin-1 promoter	Fwd: GGGGTACCCTTCTCCAGGCCAGTAGGTG	60	3500
	Rev: GGAAGATCTTGGTACAGAGCGCGGACGC		
FoxO1 promoter	Fwd: GGTACCAGTGCCCATGAAGTTTGGAG	60	4000
	Rev: GCTAGCCCCACCAGCAGAGAAGTACC		
GAPDH	Fwd: GTGGCAAAGTGGAGATTGTTGCC	60	289
	Rev: GATGATGACCCGTTTGGCTCC		

2.1.9 *Mammalian cell lines*

The established mammalian cell lines used in this thesis are listed below in Table 2.8. Mammalian cell stocks were stored in DMEM 10% Foetal bovine serum (FBS) medium with 10% DMSO in liquid Nitrogen.

Table 2.8 *Mammalian cell lines*

Line	**Species**	**Cell type**	**Source**
C2C12	Mouse	Myoblast	ATCC (Yaffe and Saxel 1977)
C3H10T1/2	Mouse	Fibroblast	ATCC (Reznikoff *et al.* 1973)
CHO	Hamster	Ovary	Dr Se-Jin Lee[1] (Zimmers *et al.* 2002)
IκBα SR C2C12	Mouse	Myoblasts	Dr Denis Guttridge[2] (Guttridge *et al.* 1999)

[1]Dr Se-Jin Lee, Johns Hopkins University School of Medicine, Baltimore, MD, USA.

[2]Dr Denis C. Guttridge, Ohio State University, OH, USA.

2.1.10 *Bovine skeletal muscle*

The bovine skeletal muscle used in this study had been collected previously by Dr Sonnie Kirk, Dr Julie Martyn and Mr Mark Thomas; myoblast extraction and tissue culture by Mr Mark Thomas, Animal Genomics, AgResearch, Hamilton, New Zealand.

The AgResearch Ruakura Animal Ethics Committee gave prior approval to the animal manipulations. Standard superovulation and embryo transfer techniques were used to generate bovine foetuses (Kambadur *et al.* 1997) Foetuses were Hereford/Friesian crossbreeds. The *M. semitendinosus* and *M. vastus lateralis* muscles were excised from the foetus and stored at -80°C or were cut into small pieces, placed in Minimal Essential Medium (MEM) containing 20% FBS and 10% DMSO, and frozen in liquid nitrogen for subsequent myoblast culture generation.

2.1.11 *Recombinant myostatin protein*

The recombinant Myostatin protein (Mstn) used in all the experiments was generated and purified by Mrs Carole Berry, Animal Genomics, AgResearch, Hamilton, New Zealand.

The generation of recombinant Myostatin is overviewed below, the pET protein expression system (Novagen) was used to express and purify recombinant myostatin. Bovine *myostatin* cDNA (amino acids 267-375) was PCR amplified and cloned into the pGEM-T easy vector (Promega). After *Bam*H1 digestion, the myostatin cDNA was sub-cloned into the pET 16-B vector (Novagen) in-frame with the 10-histidine residues. An overnight BL21 *E. coli* culture transformed with the recombinant *myostatin* expression vector was diluted and grown to an

OD of 0.8 (600 nm) in 1 L of Lennox Luria Broth (LB) medium plus ampicillin (50 mg/L). Expression of the Myostatin fusion protein was then induced by 0.5 mM isopropyl thio-β-galactoside (IPTG) for 2-3 hr. The bacteria were then harvested by centrifugation and resuspended in 40 mL of lysis buffer (6 M guanidine hydrochloride; 20 mM Tris pH 8.0; 5 mM β-mercaptoethanol), sonicated and centrifuged at 10,000 x g for 30 min. Myostatin was purified from the supernatant by Ni-Agarose affinity chromatography (Qiagen), according to the manufacturer's protocol. Soluble fractions containing myostatin were pooled and dialysed at 4ºC against two changes of 50 mM Tris-HCl (pH 8.0) containing 500 mM NaCl and 10% glycerol for 6 hr. Coommassie Blue stained SDS-PAGE gels and Western Blot analyses were performed using specific anti-Myostatin antibodies to verify purification.

2.2 Methods

Standard molecular biology techniques utilised in this study can be found in Ausubel (Ausubel 1988) or Sambrook *et al*. (Sambrook *et al.* 1989). Experiments were all performed with MQ purified water. DEPC-treated solutions, including water, were used for any work involving RNA. Unless otherwise stated, experimental reactions were carried out at room temperature. All cell culture work performed was carried out in PC1 laminar flow hoods located in a tissue culture suit.

2.2.1 *Electrophoresis*

2.2.1.1 *DNA gel electrophoresis*

Agarose gels ranged from 0.8-2% agarose (Invitrogen), depending on the size of the fragments to be separated. DNA gels were made up in 1 x TAE, with ethidium bromide added for visualisation of the DNA bands at a concentration of 300 ng/mL. The DNA gels were cast and run in specific gel boxes (either Owl [Biolab Scientific] or Horizon [Invitrogen] boxes) containing 1 x TAE as the

running buffer. DNA samples were mixed with a 10 x concentrated DNA loading dye before loading. DNA molecular markers were run beside the DNA samples. Electrophoresis was carried out between 30-100 V until the desired separation of bands was obtained. The separated DNA was then visualised under ultraviolet (UV) light (312 nm) using the Gel Doc system (Bio-Rad Laboratories, Hercules, CA) and photos were printed as a record.

2.2.1.2 *RNA gel electrophoresis*

Formaldehyde/Agarose gels contained between 1-2% agarose, 1 x MOPS and 0.66 M Formaldehyde. Total RNA was quantified using the NanoDrop spectrophotometer (ND-1000; NanoDrop Technologies Inc., Wilmington, DE, USA) to ensure accurate amounts for Northern analysis and RT-PCR reactions. Total RNA (10-15 μg) was mixed with an equal volume of RNA loading dye and incubated at 65^{o}C for 5 min prior to loading. Electrophoresis of RNA was between 40-80 V until the desired separation was achieved. The RNA loading dye contained ethidium bromide and allowed the visualisation of the RNA by UV illumination. A Gel Doc system (Bio-Rad) was used to photograph gels. The integrity of the RNA was monitored by observing the state of the 28S and 18S ribosomal bands.

2.2.1.3 *SDS polyacrylamide gel electrophoresis*

Total protein was estimated for Western Blot analysis using Bradford's protein assay reagent (Bio-Rad) analysed against BSA standards read at 595 nm. Samples were boiled for 5 min in the presence of loading dye and β-mercaptoethanol (βMe) before loading. Samples were run with the SeeBlue Plus 2 Pre-Stained Standard (Invitrogen) to give a guide to the size of the proteins on the gel. Separation of proteins was achieved using SDS-PAGE gels. SDS-PAGE gels were run in the XCell Surelock Electrophoresis cell (Invitrogen). NuPage 4-12% gradient Bis-Tris pre cast polyacrylamide gels (Invitrogen) were used for protein separation. 4 x NuPage sample buffer (Invitrogen) and a 1 x NuPage MES SDS running buffer were used with this system.

2.2.2 Nucleic acid purification

2.2.2.1 Purification after enzymatic manipulation

Infrequently, plasmid DNA and DNA resulting from PCR amplification needed to be purified after enzymatic reactions; removing protein and contaminants by phenol-chloroform extraction. DNA was extracted two times with a mix of Buffer-saturated phenol:chloroform at a ratio of 1:1, followed by a single extraction with chloroform alone. Purified DNA was then precipitated in 1 μL of Glycogen, 1/10 volume of 0.3 M NaOAc and three volumes of 100% ethanol at –20°C for at least 30 min. The DNA was pelleted by centrifugation (>10,000 x g for 10-15 min). The DNA pellet was washed two times in 70% ethanol, dried and resuspended in an appropriate volume of TE or MQ-H_2O.

2.2.2.2 The Wizard DNA purification system (Promega) for recovery of DNA

DNA was initially separated by DNA gel electrophoresis (see 2.2.1.1) using low melting point (LMP) agarose (Invitrogen). The DNA band of interest was excised from the gel using a razor blade, placed in an eppendorf tube and then incubated at 65ºC until the agarose was melted (5 min). Purification resin (1 mL) was added to the melted gel slice and mixed by inverting the tube. The resin/DNA mix was then passed through a wizard minicolumn using a syringe, followed by a wash with 80% isopropanol (2 mL). The minicolumns were removed from the syringes and centrifuged (10,000 x g for 2 min). DNA was then eluted from the column with 30 μL of TE buffer (1 min incubation) and centrifugation (10,000 x g for 20 s).

2.2.3 Enzymatic reactions

2.2.3.1 Restriction endonuclease digestions

Restriction endonuclease digests were performed with 5-10 U of required enzyme per µg of DNA with the amount of enzyme not exceeding 10% of the total reaction volume. The digests were performed with the appropriate restriction endonuclease buffers supplied at an initial 10 x concentration. Digests were performed at 37ºC (unless manufacturer guidelines specified otherwise) for 1-2 hr. Restriction digests were then either visualised using gel electrophoresis (see Section 2.2.1.1) or purified using the Wizard kit (see Section 2.2.2.2) for further manipulations.

2.2.3.2 Ligation of DNA

Separate restriction endonuclease digestions were performed on DNA inserts and vector DNA to generate complementary 3' or 5' extensions for cloning. The digested DNA was separated by gel electrophoresis (see Section 2.2.1.1) on LMP agarose gels and purified (see Section 2.2.2.2), with the desired vector or insert DNA excised from the gel. Ligation reactions contained 25-50 ng of vector DNA with a 3-fold molar excess of insert DNA, 1 µL of 10 x ligation buffer (Invitrogen) and 1 U T4 DNA ligase. The ligation reactions were performed at 16ºC for 18 hr.

2.2.4 Transformation and growth of bacteria

2.2.4.1 Transformation of competent cells

Transformation of DH5α or JM109 competent cells was achieved by addition of 1-20 ng of either vector DNA or ligation mixture to 50 µL of the cells. The DNA/competent cell mixture was incubated on ice for 20 min, followed by a heat shock at 42ºC for 48 s, then a further 2 min incubation on ice. Following this, 950 µL of room temperature LB broth (without antibiotic) was added to the mixture and the transformed cells were incubated at 37ºC for 90 min with gentle shaking

(~150 rpm). The culture was spread over LB agar plates, which contain ampicillin (50 μg/mL), and grown overnight for 16-24 hr at 37ºC.

2.2.4.2 *Culturing of bacteria*

Single colonies, from LB agar plates grown overnight or from frozen bacterial strains in the form of glycerol stocks, were seeded in 4 mL (miniprep) or 100 mL (maxiprep) of LB broth with ampicillin (50 μg/mL). Miniprep cultures were grown in 50 mL plastic tubes (Nalge Nunc International, Rochester, NY) and maxiprep cultures were grown in 1 L plastic flasks (Nalge Nunc). The cultures were grown at 37ºC with shaking (~250 rpm) for 12-18 hr.

2.2.5 *Isolation of plasmid DNA from bacteria*

2.2.5.1 *Miniprep (Small scale plasmid isolation)*

Plasmid DNA from miniprep cultures was extracted and purified using the QIAprep spin miniprep system (Qiagen), according to the manufacturer's protocol. Bacteria were harvested by centrifugation at 3500 rpm for 5 min in a 1.5 mL eppendorf tube. The bacterial pellet was resuspended in 250 μL of Buffer P1 followed by 250 μL Buffer P2, the sample was then mixed by inverting four-six times and allowed to incubate at room temperature for no more than 5 min. After incubation 350 μL buffer P3 was added. After the addition of Buffer P3 the tube was again inverted four-six times to mix. The extract was centrifuged (20,000 x g for 10 min) and the supernatant removed to a QIAprep spin column. The spin column was centrifuged (20,000 x g for 1 min), washed with 0.75 mL Buffer PE and centrifuged twice to remove any traces of Buffer PE. Plasmid DNA was eluted in 50 μL Buffer EB by centrifugation (20,000 x g for 1 min) after a 1 min incubation time.

2.2.5.2 Maxipreps (Large scale plasmid isolation)

Large scale purification of plasmid DNA was performed using the Qiagen Plasmid Maxi kit (Qiagen) as per the protocol. Briefly, 250 mL of overnight culture was harvested by centrifugation at 6000 x g for 15 min. The pellet was then resuspended in 10 mL of buffer P1, mixed with 10 mL of Buffer P2 and incubated on ice for 20 min on addition of Buffer P3. The mix was then centrifuged for 30 min at 20,000 x g followed by a second spin at 20,000 x g for 15 min to remove any contaminants. The plasmid DNA containing supernatant was passed through a pre-equilibrated Qiagen-column by gravity flow. Plasmid DNA bound to the column was washed twice with Qiagen Buffer QC and eluted with Qiagen elution buffer. The eluted DNA was precipitated with 0.7 volumes of isopropanol and pelleted by centrifugation at 20,000 x g for 10 min. The pellet was washed twice with 70% ethanol, dried and resuspended in an appropriate volume of TE buffer.

2.2.6 Polymerase Chain Reaction (PCR)

2.2.6.1 First-strand synthesis using SuperScript II Reverse Transcriptase (Invitrogen)

First-strand synthesis was performed using the SuperScript First-Strand Synthesis System (Invitrogen). SuperScript II reverse transcriptase (RT) reactions were performed as described in the manufacturer's protocol. For the RT reaction, 0.5 µg of Oligo$(dT)_{12-18}$ was annealed to 1-5 µg of total RNA in a 10 µL reaction containing 1 µL dNTPs (10 mM). This reaction was incubated at 65^{o}C for 5 min than placed on ice for 1 min. A separate 9 µL reaction containing 2 µL of 10 x RT Buffer, 4 µL of 25 mM $MgCl_2$, 2 µL of 0.1 M DTT and 1 µL RNaseOUT recombinant RNase inhibitor was added to the RNA/primer mixture mixed and incubated at 42 ^{o}C for 2 min. SuperScript II RT (50 U) was added to the mixture and incubated at 42 ^{o}C for 50 min. The reaction was subsequently terminated by incubation at 70 ^{o}C for 15 min, followed by treatment with 1 µL of RNase H at 37^{o}C for 20 min. The RT synthesised cDNA were used in subsequent PCR reactions.

2.2.6.2 *PCR using Taq DNA polymerase*

Routine laboratory PCR reactions were carried out with *Taq* DNA Polymerase (Roche) and were performed as described in the manufacturer's protocol. PCR reactions (50 µL) contained 0.5 µL of *Taq*, 0.2 mM of each dNTP, 0.1 µM Fwd primer, 0.1 µM Rev primer, 5 µL of a 10 x PCR buffer, which included $MgCl_2$ at a final concentration of 1.5 mM. The reactions were carried out with various concentrations of DNA template. The Hybaid MultiBlock System (MBS) utilising the 0.5S block (Hybaid) was used for all PCR thermocycling. Specific PCR cycling temperatures and times are described in the Materials and Methods of the relevant results Chapters where PCR was used.

2.2.6.3 *PCR using ThermalAce DNA polymerase (Invitrogen)*

ThermalAce DNA polymerase was used to generate the PCR products for subsequent cloning into the pGL3b vector for future cell culture work, as this enzyme contains 3'-5' exonuclease (proofreading) activity. PCR amplifications were performed as described in the manufacturer's protocol. *ThermalAce* reactions were prepared as one mix with components added in the following order. DNA template (1 µL) at varying concentrations, 0.2 µM of Fwd primer and 0.2 µM of Rev primer, 0.2 mM of each dNTP, 5 µL of a 10 x *ThermalAce* buffer which includes $MgSO_4$ at a final concentration of 1.5 mM, sterile water up to 49 µL, and 2 U (1 µL) of the *ThermalAce* DNA polymerase. The reaction was mixed and stored on ice until ready for cycling. The Hybaid MultiBlock System (MBS) utilising the 0.5S block (Hybaid) was used for all PCR thermocycling. Specific PCR cycling temperatures and times are described in the Materials and Methods of the relevant results Chapters in which *ThermalAce* DNA polymerase was used. Due to the 3'-5' exonuclease (proofreading) activity of *ThermalAce* the PCR products had to be A-tailed before cloning into pGEM-T easy. This reaction contained 43 µL of PCR product, 1 µL of *Taq* polymerase, 1 µL of 10 mM dATP, and 5 µL of 10 x PCR buffer. This reaction was incubated at 72ºC for 30 min.

2.2.7 Radio-labelling of cDNA probes

cDNA probes were labelled using a Rediprime II random prime labelling system (GE Healthcare Bio-Sciences Corp. Piscataway, NJ). Labelling was performed as described in the manufacturer's protocol. DNA was diluted to 25 ng in a final volume of 12.5 µL. The DNA was denatured by heating to 100°C for 5 min, cooled for 5 min on ice, and added to 10 µL (half of the total mix) of the Rediprime random priming mix. In addition, 2.5 µL of (25 µCi) [α-^{32}P]-dCTP was added and mixed. The reaction was incubated at 37°C for 45 min. The reaction was denatured using 5 µL of 4 M NaOH for 10 min at room temperature before incubation with the membrane.

2.2.8 Mammalian cell culture

2.2.8.1 Media components and the culturing of bovine and murine primary and C2C12 myoblasts.

Bovine primary myoblast cultures were grown in minimum essential medium (MEM) Proliferation Medium containing, 10% FBS (Invitrogen), 7.22 nM Phenol red (Sigma), 1 x 10^5 IU/L penicillin (Sigma), 100 mg/L streptomycin (Sigma). The medium was buffered with 41.9 mM $NaHCO_3$ (Sigma) and gaseous CO_2. All media and constituents were filter sterilised with 0.22 µm pore filters. Bovine primary myoblasts were cultured on gelatin-coated plates at 37°C, in 5% CO_2 in a Forma Scientific Water Jacketed Incubator 3250. Plates were gelatinised by the method of Quinn and Nameroff (Quinn and Nameroff 1983).

Murine myoblast cultures were maintained in proliferation medium containing DMEM supplemented with 20% FBS, 10% horse serum (HS) and 1% Chicken Embryo Extract (CEE) (see Section 2.2.8.4), 7.22 nM Phenol red, 1 x 10^5 IU/L penicillin, 100 mg/L streptomycin on 10% matrigel-coated plates. The medium was buffered with 41.9 mM $NaHCO_3$ and gaseous CO_2. All media and constituents were filter-sterilised with 0.22 µm pore filters. Murine myoblasts were cultured at 37°C, in 5% CO_2.

C2C12 myoblasts were cultured in Proliferation Medium which contained DMEM, 10% FBS, 7.22 nM Phenol red, 1 x 10^5 IU/L penicillin, 100 mg/L streptomycin. The medium was buffered with 41.9 mM $NaHCO_3$ and gaseous CO_2. All media and constituents were filter-sterilised with 0.22 μm pore filters. C2C12 myoblasts were cultured at 37°C, in 5% CO_2.

The culture dishes, seeding densities and treatments for specific experiments are described in the relevant Materials and Methods sections of the Result Chapters.

2.2.8.2 *Murine primary myoblast extraction*

Murine primary myoblasts were cultured from the hindlimb muscle of 4 to 6 week old mice, according to published protocols (Allen *et al.* 1997; Partridge 1997). Briefly, muscles were minced and then digested in 0.2% collagenase type-1A (Sigma) for 90 min. Following digestion the cultures were centrifuged to pellet digested muscle, resuspended in PBS and triturated vigorously for 5 min. The resulting slurry was then passed though a 100 μM cell strainer, centrifuged and the pellet resuspended in proliferation medium. The cultures were enriched for myoblasts by pre-plating on uncoated plates for 3 hr. Myoblast cultures were maintained in proliferation medium containing DMEM supplemented with 20% FBS, 10% HS and 1% CEE on plates coated with 10% Matrigel (BD; Becton Dickinson, Franklin Lakes, NJ), at 37°C/5% CO_2. This method is well established in our laboratory and yields cultures of high (95%) myogenic purity (McCroskery *et al.* 2003).

2.2.8.3 *Bovine primary myoblast extraction*

Bovine primary myoblasts were generated from bovine muscle tissues by Mark Thomas, Animal Genomics, AgResearch, Hamilton, New Zealand.

Briefly, mixed cultures containing both myoblasts and fibroblasts were liberated from thawed *M. Semitendinosus* by mincing muscle and then digesting with 0.25% trypsin (Sigma) for 45 min at 37°C. Medium for subsequent culture consisted of MEM, 10% FBS, 1x10^5 IU/L penicillin and 100 mg/L streptomycin.

Medium was buffered with 41.9 mM $NaHCO_3$ and gaseous CO_2 and 7.22 nM Phenol red (Sigma) was used as a pH indicator.

The method of O'Malley *et al.* (O'Malley *et al.* 1996) was used to enrich cultures for myoblasts. A total of 1 x 10^6 liberated cells were added to Matrigel coated 10 cm dishes (Nalge Nunc). Matrigel-coated dishes were prepared by adding 10 mL of 5.0 mL/L Matrigel in Earle's Balanced Salt Solution (EBSS; obtained as a 10 x concentrate) (Invitrogen) to each 10 cm dish and then incubating at 37°C for 16 hr. Cultures were grown on Matrigel for 3 days, and then digested with 0.5 g/L type-IA collagenase for 10 min to preferentially detach fibroblasts. Cultures were washed twice with EBSS before, and three times after collagenase digestion. When cultured under differentiating conditions, 90% of cells stained positive for the muscle-specific marker desmin, indicating a high purity of myoblasts (Thomas *et al.* 2000).

2.2.8.4 *Chicken embryo extract*

Fertilised Cobb eggs (Bromley Park Hatcheries) were incubated at 37.5°C and 65-70% humidity for 9 days. The eggs shells were wiped clean with sterile water, followed by 2 x washes with 70% ethanol. With sterile scissors, the wide end of the shell was cut open and the embryo was removed with a sterile surgical spoon. The embryos were weighed and 1 mL 1 x EBSS (Invitrogen) per gram of embryo weight was added. The solution was blended on a high speed for 15 s, 3 times, with 15 s rests on ice between blending. The solution was then centrifuged at 3,000 x g for 15 min at 4°C. The supernatant was later aliquoted into 1 mL, 0.5 mL and 0.25 mL lots and stored at -80°C. Sterility of the CEE was checked by preparing DMEM + 10% FBS + 1% CEE medium which was incubated for 48 hr at 37°C and observed for any bacterial or fungal growth.

2.2.8.5 *Media components and the culturing of C3H10T1/2 fibroblasts and Chinese Hamster Ovary (CHO) cells.*

C3H10T1/2 fibroblasts were cultured in Proliferation Medium which contained Eagle's Basal Medium (BME; Invitrogen), 10% FBS, 7.22 nM Phenol red, 1 x 10^5

IU/L penicillin, 100 mg/L streptomycin. The medium was buffered with 41.9 mM $NaHCO_3$ and gaseous CO_2. All media and constituents were filter-sterilised with 0.22 μm pore filters. C3H10T1/2 fibroblasts were cultured at 37°C, in 5% CO_2 incubator.

Chinese Hamster Ovary (CHO) cells were cultured in Proliferation Medium which contained DMEM/F12 (Invitrogen), 10% FBS, 7.22 nM Phenol red, 1 x 10^5 IU/L penicillin, 100 mg/L streptomycin. The medium was buffered with 41.9 mM $NaHCO_3$ and gaseous CO_2. All media and constituents were filter-sterilised with 0.22 μm pore filters. CHO were cultured at 37°C, in 5% CO_2 incubator.

2.2.8.6 *Differentiation of myoblasts.*

Myoblast differentiation was induced in murine primary, bovine primary and C2C12 myoblasts by the switching the cells from Proliferation Medium to Differentiation Medium. Differentiation Media were the same as described for Proliferation Media except the 10% FBS was replaced with 2% HS.

2.2.8.7 *The passage and trypsinisation of mammalian cells*

The passage and harvesting of cells was achieved by the removal of medium, followed by two washes with phosphate buffered saline (PBS). Trypsin (1 x, volume dependent on the size of the culture dish) was added to the cells and incubated at 37°C until cells had lifted off (~10 min). After the cells had detached from the plastic, fresh medium was added and cells were aliquoted into new dishes at the required densities and returned to the incubator. Cells to be harvested were washed off the culture dishes with Proliferation Medium depending on conditions at the time of extraction. The cells were then transferred to a centrifuge tube, pelleted by centrifugation (4000 x g) and the pellets washed with PBS.

2.2.8.8 *Transfection of mammalian cells on 10 cm cell culture plates*

Mammalian cells were transfected with the mammalian expression vectors described in the relevant Materials and Methods sections of the Results Chapters. Transfection of the constructs was performed using Lipofectamine 2000 (LF2000) reagent (Invitrogen) according to the manufacturer's protocol. Cells cultured on 10 cm plates were approximately 80-90% confluent when transfected. In separate tubes, 12.5 μg DNA and 40 μL LF2000 reagent were diluted in 800 μL serum-free DMEM each. The diluted DNA and LF2000 were then complexed by the dropwise addition of LF2000 to the DNA and incubation at room temperature. After 20 min incubation, the DNA/LF2000 transfection mix was added to 6.4 mL of Proliferation Medium and added to pre-washed cells. Cells were incubated with the transfection mix/Proliferation Medium at 37^{o}C, in 5% CO_2 overnight, after which the medium was replaced with straight Proliferation Medium and other relevant treatments.

2.2.8.9 *Transfection of C2C12 myoblast cells on 6 well cell culture plates*

C2C12 myoblast cells were transfected with the mammalian expression vectors described in the relevant Materials and Methods sections of the Results Chapters. Transfection of the constructs was performed using LF2000 reagent according to the manufacturer's protocol. Cells cultured on 6 well plates were transfected at densities dependent on the relevant medium to be used or the time interval for which the cells were to be treated, to prevent the cells reaching confluence prior to extraction. In separate tubes, 2.0 μg of each DNA and 8 μL LF2000 reagent were diluted in 250 μL serum-free DMEM per well. The diluted DNA and LF2000 were then complexed by the dropwise addition of LF2000 to the DNA and incubation at room temperature. After 20 min incubation, the DNA/LF2000 transfection mix was added dropwise to 2 mL of Proliferation Medium contained within the relevant well(s), at the same time the plate was being rocked. Myoblasts were incubated with the transfection mix/Proliferation Medium at 37^{o}C, in 5% CO_2 overnight, after which the medium was replaced with Proliferation Medium or Differentiation Medium and relevant treatments.

2.2.8.10 *Transfection of C2C12 myoblasts with siRNA using HiPerFect*

C2C12 myoblast cells were transfected with the siRNA described in the relevant Materials and Methods sections of Chapter 5. Transfection of siRNA was performed according to the manufacturer's protocol (Qiagen). Cells were cultured on 6 well plates in Proliferation Medium prior to transfection. In a tube, 7.5 ng of each siRNA was diluted in 100 µL of DMEM (no serum) medium to a final concentration of 1 nM per well. HiPerFect reagent (3 µL) was added to the diluted siRNA, mixed by vortexing, and incubated at room temperature for 5-10 min. The complexes were subsequently added drop-wise to the cells while the plates were gently swirled. The cells were incubated with the transfection complexes for an appropriate time as per the experimental requirements.

2.2.8.11 *Selection of myoblasts containing stable integration of transfected constructs*

Mammalian cells were transfected as described in Section 2.2.8.8. Following 48 hr of incubation with Proliferation Medium, the antibiotic Geneticin (Invitrogen) was added to the medium at 400 µg/mL. Cells were incubated as before for 24 hr and passaged to two 10 cm plastic dishes (Falcon). Passaged cells were maintained in duplicate lines, with separate medium to safeguard against the loss of cell line by contamination. Selection with Geneticin was continued for 20 days, adding fresh Proliferation Medium when needed. Negative control cells (not transfected, neomycin sensitive) had all died before day ten. Resistant cells (expressing the neomycin resistance cassette) had formed individual colonies (at least 100), which were pooled to overcome individual variation and integration effects. Clonal cell lines were generated by plating transfected cells at a clonal density of 25 cells/cm^2, individual neomycin resistant colonies were isolated and further expanded to allow for expression analysis of the gene of interest. Based on expression analysis, stable over-expressing clonal cell lines were selected for further study.

2.2.9 Harvesting of protein, the luciferase assay and β-gal assay

C2C12 myoblasts grown on 6 well plates were transfected (see Section 2.2.8.9) and harvested following 2 washes with 5 mL PBS. Harvesting occurred by scraping the cells off the wells using 300 µL of Reporter Lysis Buffer (Promega), the resulting lysate was transferred to a 1.5 mL eppendorf. Following a vortex for 10 s, the lysate was rapidly frozen on dry ice, directly followed by thawing to room temperature. The lysates were subjected to a second 10 s vortex before they were centrifuged at 20,000 x g for 15 s to pellet cell debris. The supernatant was then transferred to a new tube to be used in the subsequent luciferase or β-gal assay.

The Luciferase Assay System (Promega) was used to measure the level of luciferase expression in C2C12 cells that had been transfected with promoter-luciferase constructs. The luciferase assays were performed according to the manufacturer's protocol. Relative luciferase activity of each of the extracted protein samples was measured by addition of 10 µL of each protein to 1.5 mL eppendorfs in triplicate. Fifty µL of Luciferase Assay Reagent was then added to the protein and the subsequent luciferase activity measured using a Luminometer (TD-20/20 Turner Designs) with a delay time of 3 s and an integration time of 20 s.

Transfections of C2C12 myoblasts with 1 µg the pCH110 vector per well allowed for analyses of β-gal expression, which was used to normalise the luciferase values as a measure of transfection efficiency. β-gal expression levels were detected using the β-Galactosidase Enzyme Asssay System (Promega) according to the manufacturer's protocol. Cell lysates were analysed using a 96 Well Plate Assay, where 50 µL of the extract was pipetted into the 96 well plate (Nalge Nunc). Standards were also used which varied from 0-5.0 mU of β-gal. All standards and samples were plated in duplicate. Fifty µL of 2 x Assay Buffer was added to each well with pipetting to mix, followed by an incubation period at 37ºC for 30 min. Finally, 150 µL of 1 M Na_2CO_3 was added to each well to stop the reaction. The absorbance of each sample was then measured using the EL-311 microplate autoreader (Bio-Tek Instruments) at 420 nm. The β-gal activity of each sample was determined by comparing each sample to the generated standard curve.

2.2.10 RNA extraction from cultured C2C12 myoblasts and muscle tissue

Total RNA was isolated from cultured cells using TRIZOL as per the manufacturer's protocol. Proliferation Medium was removed from the culture dishes and the cells were washed twice with PBS to remove any cell debris. Cells were lysed by the addition of TRIZOL (Invitrogen) reagent (2 mL per 10 cm plate) and the subsequent repeated passing of the lysates through a pipette. The cell lysates were removed from the plate and placed in a 10 mL tube. Following 5 min incubation at room temperature 400 µL of Chloroform was added and the tubes were shaken vigorously for 15 s. After 3 min incubation at room temperature the samples were centrifuged at 12,000 x g for 15 min. The upper clear aqueous phase was then removed to a new tube and the RNA was precipitated with 1 mL of isopropyl alcohol. Following 10 min incubation at room temperature the samples were centrifuged at 12,000 x g for 10 min. The total RNA was then washed with 2 mL of 75 % ethanol and finally pelleted at 7,500 x g for 5 min and resuspended in an appropriate volume of DEPC-treated MQ water.

Total RNA was isolated from muscle tissue using TRIZOL as per the manufacturer's protocol. For every 50-100 mg of muscle tissue 1 mL TRIZOL was added and the sample was homogenised using an Ultraturrex (IKA). After 5 min incubation at room temperature, 200 µL of chloroform was added, and the tubes were shaken for 15 s. Following incubation at room temperature for a further 3 min, the samples were centrifuged at 12,000 x g for 15 min. The aqueous phase was removed to a new tube and total RNA precipitated with 0.5 mL of isopropanol for 10 min at room temperature. Total RNA was pelleted by centrifugation at 14,000 x g for 10 min. The pellet was washed with 1 mL of 75% ethanol and resuspended in an appropriate volume of DEPC-treated MQ water. RNA isolated from cells and muscle was quantified using the NanoDrop spectrophotometer to measure concentration and purity. In addition, RNA was subjected to electrophoresis (see Section 2.2.1.2) to check RNA quality. All RNA samples were stored at -80°C prior to use.

2.2.11 RNA purification using the RNeasy midi kit (Qiagen)

RNA was purified using the RNeasy kit for subsequent microarray analysis (Chapter 5 and Chapter 6). RNA was initially isolated using TRIZOL reagent as per the manufacturer's protocol (see Section 2.2.10). Following isolation, the volume of the RNA solution (0.5-1.0 mg) was adjusted to 1 mL with DEPC-treated water. To the diluted RNA sample 4 mL of Buffer RLT along with 2.8 mL of 100% ethanol was added. The sample was subsequently applied to an RNeasy midi column and centrifuged for 5 min at 5000 x g with flowthrough discarded. Buffer RW1 (2 mL) was then added to the column followed by centrifugation at 5000 x g for 4 min. Two 2.5 mL volumes of Buffer RPE were subsequently applied to the column followed by centrifugation at 5000 x g for 4 min and 10 min respectively. The RNA was eluted from the column with 2 x 250 µL applications of RNase-free water and centrifugation for 3 min at 5000 x g. The RNA was subsequently precipitated overnight with 1:10 volume of 0.3 M NaCl and three volumes of 100% ethanol at -20^{o}C. The DNA was then pelleted by centrifugation (>10,000 x g for 10-15 min). The DNA pellet was washed twice in 70% ethanol, dried and resuspended in an appropriate volume of DEPC-treated MQ water. The RNA was quantified using the NanoDrop spectrophotometer to measure concentration and purity. In addition, the RNA was subjected to electrophoresis (see Section 2.2.1.2) to check RNA quality. RNA samples were stored at -80°C prior to use.

2.2.12 Northern Blotting

Northern Blot analyses were performed to quantify gene expression changes in the relevant Results Chapters. RNA samples were run out using formaldehyde gel electrophoresis as described in Section 2.2.1.2. The gel was then soaked in 10 x SSC for 30 min to remove any contaminating formaldehyde. The RNA was transferred to Hybond N+ (GE Healthcare Bio-Sciences) membrane by capillary action. Following transfer, the blots were washed and the RNA was covalently cross-linked to the membrane using a UV light Stratalinker 1800 (Stratagene). Efficiency of the transfer and quality of the RNA was assessed by examining the membrane under UV light.

Cross-linked membranes were prehybridised in glass Hybaid bottles with 20 mL of Church and Gilbert hybridisation buffer at 55°C for approximately 1 hr prior to hybridisation. Radiolabelled cDNA probes (see Section 2.2.7) were added to the hybridisation bottles (avoiding contact with the membrane) with fresh Church and Gilbert hybridisation buffer after the probes had been denatured with 0.2 volumes (5 µL) of 4 M NaOH for 5 min. Hybridisation was performed in a hybridisation oven (Hybaid) for 16 hr. Hybridisation temperatures and washing procedures are listed in the relevant Materials and Methods section of the Results Chapter where they were used. Membranes were heat sealed in plastic and exposed to XAR film for the required time.

2.2.13 *Protein extraction from cultured mammalian cells and muscle tissue*

Total protein was extracted from myoblasts and C3H10T1/2 fibroblasts for immunoprecipitation and Western Blot analyses. Harvesting of the cells was undertaken as described in Section 2.2.8.7 with the cell pellet resuspended in 200 µL of Lysis Buffer (protein extraction buffer). The cell lysate was either sonicated (1 s pulses for 30 s) using a Vibra Cell Sonicator (Sonics and Materials Inc.), or passed through as 26 gauge syringe needle 10 times. To pellet cell debris the lysate was centrifuged at 12,000 x g for 10 min with the supernatant (protein extract) removed and transferred to a new 1.5 mL eppendorf tube for storage at -80ºC until needed.

Total proteins were extracted from muscle tissue for Western Blot analyses. For muscle tissue protein extraction, whole muscle tissues were homogenised in at least 1 mL Lysis Buffer (protein extraction buffer) using an Ultraturrex (IKA). The homogenised sample was centrifuged (14,000 x g for 5 min) to pellet cell debris and the supernatant (protein extract) was stored at -80°C until needed.

2.2.14 *Bradford Assay*

The Bradford Assay (Bradford 1976) was used to provide an estimation of the total protein concentrations in protein extract samples. Total protein (2 µL) was added to PBS to give a final volume of 100 µL Bradford Reagent concentrate

(Bio-Rad) was diluted 1 in 5 with MQ water and 1.2 mL was added to the diluted protein. Samples were then mixed and the absorbance at 595 nm was measured using a UV spectrophotometer (Thermo Spectronic). The absorbances of BSA standards (0 to 10 μg) were measured to generate a standard curve with which the unknown sample protein was compared.

2.2.15 *Western Blotting*

Western Blot analyses were performed to quantify gene expression changes in the relevant Results Chapters. SDS-PAGE electrophoresis was undertaken as described in Section 2.2.1.3. Following electrophoresis, the pre-cast gels were washed in Western Blot Transfer Buffer. The protein was transferred to Trans-Blot (Bio-Rad) Nitrocellulose membrane by electroblotting using the XCell II Blot Module (Invitrogen). The membranes were then blocked overnight at 4ºC using a solution of TBST/5% low fat milk. Alternatively, membranes were blocked for 1 hr at room temperature in 0.3% BSA solution. Once blocking was complete, the membranes were ready for probing with the primary and secondary antibodies corresponding to the gene of interest.

Antibodies used, concentrations and the detection of specific proteins is described in the Materials and Methods section of the Results Chapters where Western Blot analysis was used. The secondary antibody (conjugated to Horseradish Peroxidase; HRP; Dako) was detected using Western Lightning (PerkinElmer) Western Blot Chemiluminescence Reagent.

2.2.16 *MHC immunocytochemistry*

Myoblasts were fixed with 70% ethanol:formaldehyde:glacial acetic acid (20:2:1) for 30 s, and then rinsed three times with PBS. Cells were blocked overnight at 4^{o}C in 0.35% Carrageenen λ (Cλ) containing 5% normal sheep serum (NSS). Cells were incubated with primary antibody, 1:200 dilution mouse anti-MHC (MF20; DSHB), in Cλ/5% NSS for 1 hr. Cells were washed (3 x 5 min) with TBST and incubated with secondary antibody, 1:300 dilution sheep anti-mouse IgG (RPN1001; GE Healthcare Bio-Sciences), in Cλ/5% NSS for 30 min. Cells

were washed as before and incubated with tertiary antibody, 1:300 dilution of streptavidin-biotin peroxidase complex (RPN1051; GE Healthcare Bio-Sciences), in Cλ/5% NSS for 30 min. MHC immunostaining was visualised using 3,3-diaminobenzidine tetrahydrochloride (DAB; Invitrogen) enhanced with 0.0375 % CoCl. MHC-immunostained cultures were counterstained with Gill's haematoxylin and/or 1% eosin, dehydrated and mounted as described in Section 2.2.17.

2.2.17 *Haematoxylin and eosin cell staining*

Cells were fixed with 70% ethanol:formaldehyde:glacial acetic acid (20:2:1) prior to staining. Haematoxylin and eosin staining was performed as described below. Cells were incubated with 1:1 Gill's haematoxylin for 2-4 min, rinsed with tapwater, then incubated for 2 min with Scott's tapwater before counterstaining with 1% eosin for 2 min. Following a rinse with tapwater the cells were dehydrated with washes of increasing concentrations of ethanol (1 x 50%, 1 x 70%, 1 x 95%, and 2 x 100%) for 2 min each. The cells were then incubated in Xylene for 2 x 5 min before mounting onto slides with DPX solution (BDH).

2.2.18 *Calculations used*

2.2.18.1 *RNA quantification from absorbance*

$$\mu g\ RNA = 40 \times (A_{260} / dilution)$$

2.2.18.2 *DNA quantification from absorbance*

$$\mu g\ DNA = 50 \times (A_{260} / dilution)$$

2.2.18.3 *DNA concentration conversion from pM to µg and vice versa*

$$pM\ of\ dsDNA = \mu g\ (of\ dsDNA) \times \frac{10^6\ pg}{1\ \mu g} \times \frac{1\ pM}{660\ pg} \times \frac{1}{n_{(bp)}} = \frac{\mu g\ (of\ dsDNA) \times 1{,}515}{n_{(bp)}}$$

$$\mu g \text{ of dsDNA} = pM \text{ (of dsDNA)} \times \frac{660 \text{ pg}}{1 \text{ pM}} \times \frac{1 \mu g}{10^6 \text{ pg}} \times n_{(bp)} = pM \text{ (of dsDNA)} \times n_{(bp)} \times 6.6 \times 10^{-4}$$

2.2.18.4 *Insert:vector ratio calculation*

$$\frac{\text{ng of vector} \times \text{kb size of insert}}{\text{kb size of vector}} \times \text{insert:vector molar ratio} = \text{ng insert}$$

2.2.19 *Statistics*

Statistical analyses performed throughout this thesis are described in the specific results Chapters, 3, 4, 5 and 6.

2.3 References

Allen, R. E., C. J. Temm-Grove, S. M. Sheehan and G. Rice (1997). "Skeletal muscle satellite cell cultures." Methods Cell Biol **52**: 155-76.

Ausubel, F. M. (1988). Curent protocols in molecular biology. New York, Published by Greene Pub. Associates and Wiley- Interscience: J. Wiley.

Blanchette, F., P. Rudd, F. Grondin, L. Attisano and C. M. Dubois (2001). "Involvement of Smads in TGFbeta1-induced furin (fur) transcription." J Cell Physiol **188**(2): 264-73.

Bradford, M. M. (1976). "A rapid and sensitive method for the quantitation of microgram quantities of protein utilizing the principle of protein-dye binding." Anal Biochem **72**: 248-54.

Guttridge, D. C., C. Albanese, J. Y. Reuther, R. G. Pestell and A. S. Baldwin, Jr. (1999). "NF-kappaB controls cell growth and differentiation through transcriptional regulation of cyclin D1." Mol Cell Biol **19**(8): 5785-99.

Hunter, J. G., M. F. van Delft, R. A. Rachubinski and J. P. Capone (2001). "Peroxisome Proliferator-activated Receptor gamma Ligands Differentially Modulate Muscle Cell Differentiation and MyoD Gene Expression via Peroxisome Proliferator-activated Receptor gamma - dependent and - independent Pathways." J Biol Chem **276**(41): 38297-306.

Kambadur, R., M. Sharma, T. P. Smith and J. J. Bass (1997). "Mutations in myostatin (GDF8) in double-muscled Belgian Blue and Piedmontese cattle." Genome Res **7**(9): 910-6.

Li, J., K. C. Liu, F. Jin, M. M. Lu and J. A. Epstein (1999). "Transgenic rescue of congenital heart disease and spina bifida in Splotch mice." Development **126**(11): 2495-503.

McCroskery, S., M. Thomas, L. Maxwell, M. Sharma and R. Kambadur (2003). "Myostatin negatively regulates satellite cell activation and self-renewal." J Cell Biol **162**(6): 1135-47.

O'Malley, J. P., I. Greenberg and M. M. Salpeter (1996). "The production of long-term rat muscle cell cultures on a Matrigel substrate and the removal of fibroblast contamination by collagenase." Meth. Cell Sci. **18**: 19-23.

Partridge, T. A. (1997). "Tissue culture of skeletal muscle." Methods Mol Biol **75**: 131-44.

Quinn, L. S. and M. Nameroff (1983). "Analysis of the myogenic lineage in chick embryos. III. Quantitative evidence for discrete compartments of precursor cells." Differentiation **24**(2): 111-23.

Reznikoff, C. A., D. W. Brankow and C. Heidelberger (1973). "Establishment and characterization of a cloned line of C3H mouse embryo cells sensitive to postconfluence inhibition of division." Cancer Res **33**(12): 3231-8.

Sambrook, J., E. F. Fritsch and T. Maniatis (1989). Molecular cloning: A labatory manual, 2nd ed. N.Y., Cold Spring Harbour Laboratory Press.

Thomas, M., B. Langley, C. Berry, M. Sharma, S. Kirk, J. Bass and R. Kambadur (2000). "Myostatin, a negative regulator of muscle growth, functions by inhibiting myoblast proliferation." J Biol Chem **275**(51): 40235-43.

Wilson, B. (2006). Cloning and Characterisation of a Novel Muscle Wasting Gene: *menos musculo-1* (*mm1*). Department of Biological Sciences. Hamilton, University of Waikato**:** 147.

Yaffe, D. and O. Saxel (1977). "Serial passaging and differentiation of myogenic cells isolated from dystrophic mouse muscle." Nature **270**(5639): 725-7.

Zimmers, T. A., M. V. Davies, L. G. Koniaris, P. Haynes, A. F. Esquela, K. N. Tomkinson, A. C. McPherron, N. M. Wolfman and S. J. Lee (2002). "Induction of cachexia in mice by systemically administered myostatin." Science **296**(5572): 1486-8.

Chapter 3 Proteolytic processing of myostatin

The results in this Chapter are published in Developmental Biology vol. 283 pages 58-69 (2005). See CD attached to the back cover of this thesis (Appendix 1) for a PDF copy of this paper.

Available online at www.sciencedirect.com

SCIENCE DIRECT

Developmental Biology 283 (2005) 58 – 69

DEVELOPMENTAL BIOLOGY

www.elsevier.com/locate/ydbio

Proteolytic processing of myostatin is auto-regulated during myogenesis

Craig McFarlane[a,b,1], Brett Langley[a,1], Mark Thomas[a], Alex Hennebry[a], Erin Plummer[a], Gina Nicholas[a], Chris McMahon[a], Mridula Sharma[a], Ravi Kambadur[a,*]

[a]*AgResearch, East Street, Hamilton, New Zealand*
[b]*Department of Biological Sciences, University of Waikato, Hamilton, New Zealand*

Received for publication 18 August 2004, revised 19 March 2005, accepted 23 March 2005
Available online 3 May 2005

Abstract

Myostatin, a potent negative regulator of myogenesis is proteolytically processed by furin proteases into active mature myostatin before secretion from myoblasts. Here it is show that mature myostatin auto-regulates its processing during myogenesis. In a cell culture model of myogenesis, Northern Blot analysis revealed no appreciable change in *myostatin* mRNA levels between proliferating myoblasts and differentiated myotubes. However, Western Blot analysis confirmed a relative reduction in myostatin processing and secretion by differentiated myotubes as compared to proliferating myoblasts. Furthermore, *in vivo* results demonstrate a lower level of myostatin processing during foetal muscle development when compared to post-natal adult muscle. Consequently, high levels of circulatory mature Myostatin were detected in post-natal serum, while foetal circulatory Myostatin levels were undetectable. Furin proteases are important for proteolytically processing members of the TGF-β superfamily, therefore the ability of myostatin to control the transcription of furin and auto-regulate the extent of its processing was investigated. Transfection experiments

indicated that mature Myostatin indeed regulates furin protease promoter activity. Based on these results, it is proposed that myostatin negatively regulates its proteolytic processing during foetal development, ultimately facilitating the differentiation of myoblasts by controlling both furin protease gene expression and subsequent active concentrations of mature Myostatin peptide.

3.1 Introduction

Myostatin is a secreted growth factor and a member of TGF-β superfamily. While lack of myostatin leads to increased muscle growth (Kambadur *et al.* 1997; McPherron *et al.* 1997), systemic injection of Myostatin leads to muscle wasting (Zimmers *et al.* 2002) indicating that myostatin acts as a potent negative regulator of skeletal muscle growth. Myostatin expression is detected in embryonic, foetal, and post-natal myogenic cells suggesting it plays a role in all stages of myogenesis. It is first detected in the myogenic precursor cells of the myotome compartment of developing somites (McPherron *et al.* 1997). Myostatin expression continues throughout myogenesis and is detected post-natally at varying levels in different axial and paraxial muscles (Kambadur *et al.* 1997; McPherron *et al.* 1997). Myostatin expression has also been detected at low levels in other mammalian tissues (McPherron *et al.* 1997; Ji *et al.* 1998; Sharma *et al.* 1999).

The primary structure of myostatin contains several features shared with all members of the TGF-β superfamily. These features include a hydrophobic core of amino acids near the N-terminus that functions as a secretory signal and a putative proteolytic processing site (RSRR) in the C-terminal half of the precursor protein (McPherron and Lee 1996). The proteolytic processing of Myostatin is carried out by a calcium-dependent serine protease called furin (Lee and McPherron 2001). Furin belongs to a family of mammalian processing enzymes called proprotein convertases (PCs), of which seven members have so far been identified (Thomas 2002). All PCs have overlapping cleavage site specificity and tissue distribution (Seidah and Chretien 1997; Steiner 1998). In particular, furin is highly concentrated in the trans-Golgi network (Molloy *et al.* 1994; Molloy *et al.* 1999). Importantly, several TGF-β superfamily precursor proteins have been

shown to be cleaved by furin, including TGF-β1 (Dubois *et al.* 2001) and BMP-4 (Cui *et al.* 1998; Constam and Robertson 1999; Cui *et al.* 2001). The proteolytic processing of Myostatin results in both a N-terminal Latency-Associated Peptide (LAP, also referred to as pro-peptide) and a C-terminal mature Myostatin peptide (Thomas *et al.* 2000). The mature Myostatin is secreted into circulation as a high molecular weight protein in association with various interacting proteins. Titin cap and human Small Glutamine-rich Tetratricopeptide repeat-containing protein (hSGT) have been shown to associate with intracellular forms of myostatin (Nicholas *et al.* 2002; Wang *et al.* 2003). While follistatin, Follistatin-Related Gene (FLRG) and Growth And differentiation factor-associated Serum Protein-1 (GASP-1) have been shown to bind to the extracellular circulatory form of Myostatin (Lee and McPherron 2001; Hill *et al.* 2002; Hill *et al.* 2003). Recently, it is shown that the circulatory latency Myostatin protein is activated by the BMP-1/tolloid family of metalloproteinases (Wolfman *et al.* 2003) to release the mature Myostatin peptide. The mature Myostatin presumably elicits its biological function by binding to its receptor, the Activin type-IIB receptor (Lee and McPherron 2001). While the mature Myostatin can bind to the receptor, the N-terminal LAP appears to be required for the correct folding, dimerisation and secretion of the mature peptide (Gray and Mason 1990).

Mechanistically, myostatin appears to function by regulating myoblast cell cycle progression and differentiation. During the active proliferation phase of myoblast growth, myostatin negatively regulates the G1 to S phase transition of the cell cycle through both Rb-dependent and -independent pathways (Thomas *et al.* 2000; Langley *et al.* 2004). In addition, excess myostatin also inhibits myoblast terminal differentiation by inactivating MyoD (Langley *et al.* 2002). Although the function of myostatin is well defined, the significance of Myostatin processing and secretion during myogenesis has yet to be investigated. Thus in this Chapter, myostatin expression, processing and secretion during myogenesis is investigated. The results presented here indicate that Myostatin processing and secretion is reduced during myogenesis. An auto-regulatory loop, whereby myostatin self-regulates its own converting enzyme appears to be a possible mechanism for the regulation of Myostatin processing during development.

3.2 Materials and Methods

3.2.1 *Cell culture*

Comprehensive methods covering cell culture and primary myoblast extraction are detailed previously (Thomas *et al.* 2000) (see Section 2.2.8). Briefly, C2C12 myoblasts were grown prior to assay in Proliferation Medium (Dulbecco's modified Eagle's medium, (DMEM; Invitrogen, Carlsbad, CA) containing 10% foetal bovine serum (FBS, Invitrogen) on uncoated plates, while primary bovine myoblasts were grown in minimum essential medium-Proliferation Medium (MEM, Invitrogen) containing 10% FBS on gelatin (Sigma, St Louis, MO) coated plates. Differentiation was induced in the C2C12 myoblasts by culture in Differentiation Medium (DMEM) containing 2% horse serum (HS, Invitrogen) for 24, 48, or 72 hr, and in primary bovine myoblasts by culture in MEM-Differentiation Medium (with 2% HS) for 24, 48, or 72 hr.

3.2.2 *Transfections and luciferase assays*

For transfections C2C12 cells were seeded at a density of 15,000 cells/cm^2 in 6-well plates (Nalge Nunc International, Rochester, NY) with DMEM medium containing 10% FBS. After a 24 hr attachment period the cells were transfected with 3 μg total plasmid DNA (2 μg of P1 Furin promoter (Blanchette *et al.* 2001) construct and 1 μg of SV40-β-galactosidase (β-gal) control vector, pCH110 (GE Healthcare Bio-Sciences Corp. Piscataway, NJ) using Lipofectamine 2000 (Invitrogen) according to the manufacturer's recommendations (see Section 2.2.8.9). The cultures were then incubated in an atmosphere of 5% CO_2/37^{o}C for a further 18 hr. The medium was removed and replaced with either proliferation or differentiation medium. Cultures were incubated in 5% CO_2/37^{o}C for a further 24 hr. Medium was then removed and cells rinsed twice with PBS (pH 7.4) and lysed in 300 μL of 1 x Reporter lysis buffer (Promega Corporation, Madison, WI). Lysates were collected and vortexed for 10 s. After a quick freeze-thaw the lysates were centrifuged at 12,000 x g for 15 s and 10 μL of the supernatant was analysed for luciferase reporter gene activity (Promega) in a Turner Designs Luminometer

(Model TD-20/20). To control for variations in transfection efficiency, the transfections were performed in triplicate and each experiment repeated a minimum of three times. The individual luciferase value for each assay was normalised against β-galactosidase expression.

3.2.3 *Myostatin indirect immunofluorescence microscopy and photography*

C2C12 myoblasts were grown prior to immunostaining in Proliferation Medium and seeded on Thermonox coverslips (Nalge Nunc) at a density of 15,000 cells/cm^2 for proliferation studies or 25,000 cells/cm^2 for differentiation studies. Following a 16 hr attachment period, medium was changed to either Proliferation Medium (for the maintenance of actively proliferating myoblasts) or Differentiation Medium (for the induction of differentiation and formation of myotubes). After 72 hr of incubation, cells were rinsed once with PBS and then fixed with 70% ethanol:formaldehyde:glacial acetic acid (20:2:1) for 30 s, rinsed three times with PBS and blocked overnight at 4^{o}C in TBS containing 1% normal sheep serum (NSS). Cells were incubated with the specific primary antibody; 1:100 dilution anti-Myostatin antibody (Sharma *et al.* 1999) in TBS containing 1% NSS for 1 hr. Rabbit IgG (5 μg/mL; Dako, Copenhagen, Denmark) was used as a negative control. Cells were washed (3 x 5 min) with TBS containing 0.1% Tween 20 (TBST) and incubated with secondary antibody; 1:150 dilution biotinylated donkey anti-rabbit IgG (RPN1004; GE Healthcare Bio-Sciences) in TBS/1% NSS for 30 min. Cells were washed as before and incubated with tertiary antibody; 1:100 dilution of streptavidin-biotin fluorescein isothiocynate complex (FITC; RPN1232; GE Healthcare Bio-Sciences) in TBS/1% NSS for 30 minutes. Cells were again washed. Myostatin-immunofluorescence was visualised using an UV emission wavelength of 520 nm (U-MWIG) filter, BH2-RFL-T3 burner; Olympus Optical Co., Germany). Cell nuclei were visualised by the addition of 0.3 μM 4, 6-diamidino-2-phenylindole, dihydrochloride (DAPI, Invitrogen) to the cells for 5 minutes followed by TBST wash (3 x 5 min), and an UV emission wavelength of 420 nm (U-MWU2 filter, BH2-RFL-T3 burner; Olympus). FITC and DAPI fluorescence was photographed using an Olympus BX50 microscope (Olympus) fitted with a DAGE-MTI DC-330 colour camera (DAGE-MTI) and Scion Image Capture software.

3.2.4 Detection of Myostatin secreted into cell culture medium

Mouse C2C12 myoblasts were seeded at the density mentioned above in 6-well plates and cultured in either Proliferation Medium or induced to differentiate in Differentiation Medium for 72 hr. The formation of myotubes in Differentiation Medium cultured cells was confirmed by light microscopy. After washing three times with PBS, the cultured myoblasts and myotubes were incubated with methionine-free Proliferation or Differentiation medium, respectively. After 30 min the cells were washed, followed by the addition of test medium. Test medium consisted of methionine-free Proliferation or Differentiation Medium supplemented with 0.5 mCi/mL of L-[^{35}S]-methionine (1 mCi = 37 MBq; GE Healthcare Bio-Sciences). Cells were incubated in precisely 2 mL of this medium for 24 hr. Conditioned media were collected for the immunoprecipitation of proteins, while the cells were harvested for the quantification of DNA content (Hoechst assay).

3.2.5 Immunoprecipitation of Myostatin from conditioned medium.

The conditioned media (300 µL) were pre-cleared prior to myostatin immunoprecipitation by incubating with 0.3 µg of anti-rabbit IgG HRP conjugate (P0448; Dako) for 30 minutes at 4°C. Conditioned media were then incubated with 100 µL of 50% Protein A-Agarose (Invitrogen), washed twice with Lysis Buffer for 1 hr at 4°C, centrifuged and the supernatant (precleared medium) collected. The precleared media were then incubated with 4 µL anti-Myostatin antibody for 1 hr at 4°C, incubated with 50% Protein A-Agarose (Invitrogen) (washed twice with Lysis Buffer) for 1 hr at 4°C and centrifuged to pellet the immunoprecipitated complexes. Pellets were washed five times with lysis buffer. Pellets were then resuspended in 20 µL 4 x NuPAGE sample buffer (Invitrogen). Western Blot analysis for Myostatin was performed as described in Section 3.2.6.

3.2.6 *Protein isolation and Western Blot analysis*

C2C12 and bovine primary myoblasts were cultured in Proliferation or Differentiation medium as outlined above (see Section 3.2.1). Protein was isolated from the cultured cells as previously described (see Section 2.2.13). Briefly, myoblasts were resuspended in 200 μL lysis buffer (50 mM Tris pH 7.6; 250 mM NaCl; 5 mM EDTA; 0.1% Nonidet P-40; Complete protease inhibitor (Roche Diagnostics Corporation, Indianapolis, IN) and passed through a 26 gauge needle 10 times. Protein was isolated from muscle tissue as previously described (see Section 2.2.13). Briefly, skeletal muscle tissue from *M. vastus lateralis* and *M. semitendinosus* were resuspended in 500 μL of lysis buffer and homogenised. The cell and muscle tissue extracts were then centrifuged to pellet cell debris with protein containing supernatant recovered. Bradford Reagent (Bio-Rad Laboratories, Hercules, CA) was used to estimate total protein content to ensure equal loadings (see Section 2.2.14). Total protein (15 μg) was separated by 4-12% SDS-PAGE (Invitrogen) electrophoresis and transferred to nitrocellulose membrane by electroblotting. The membranes were blocked in 5% milk in TBST overnight at 4ºC, followed by incubation with 1:2000 dilution of rabbit anti-Myostatin antibody (Sharma *et al.* 1999) for 3 hr at room temperature. The membranes were washed (5 x 5 min) with TBST and further incubated with 1:2,000 dilution anti-rabbit IgG Horseradish Peroxidase (HRP) conjugate (P0448; Dako, Glostrup, Denmark) secondary antibody for 1 hr at room temperature. The membranes were washed as above, and HRP activity was detected using Western Lightning Chemiluminescence Reagent Plus (NEL104; PerkinElmer Life And Analytical Sciences, Inc., Wellesley, MA) and exposure to XOMAT XAR film (Eastman Kodak Company, Rochester, NY).

3.2.7 *Hoechst assay for the quantification of DNA*

After the removal of the conditioned medium from the cultures, cells were washed in PBS and detached from the culture dishes by incubating with 0.25% Trypsin (Sigma) in PBS. Cells were washed again with PBS and transferred to eppendorf tubes with 800 μL Phosphate buffered saline EDTA (PBSE; 40 mM $Na_2HPO_4.H_2O$, 10 mM $NaH_2PO_4.H_2O$, 2 M NaCl, 2 mM EDTA, pH7.4)

incubated on ice and sonicated twice for 15 s. In a 96 well plate (Nalge Nunc), 15 µL of each sample was added to 35 µL PBSE in triplicate. Standards, (50 µL of 0 to 20 µg/mL DNA) were also added to the 96-well plate (Nalge Nunc). Freshly made Hoechst buffer (250 µL of 0.5 µg/mL Hoechst in PBSE) was added to each well and the plates read using a microplate reader (model 3550; Bio-Rad, Hercules, CA, USA) at 360 nm excitation and 460 nm emission wavelengths.

3.2.8 *Northern Blot analysis*

For Northern Blot analysis, mouse C2C12 or bovine primary myoblasts were cultured as described in Section 3.2.1 in either Proliferation Medium or Differentiation Medium. RNA was isolated from cultured cells and skeletal muscle tissue using TRIZOL Reagent (Invitrogen) as per the manufacturer's protocol (see Section 2.2.10). Northern Blot analysis was performed as described in Section 2.2.12, using 12 µg total RNA and 0.66 M formaldehyde-1% agarose gel electrophoresis. The membranes were hybridised with a ^{32}P-labelled *myostatin* cDNA probe in Church and Gilbert Hybridisation Buffer at 60°C, overnight. The membrane was washed at 60°C for 15 min each with 2 x SSC, 0.5% SDS, and then 1 x SSC, 0.5% SDS. The *myostatin* cDNA was obtained by RT-PCR. First-strand cDNA was synthesised in a 20 µL reverse transcriptase (RT) reaction from 5 µg total RNA (from C2C12 cells) using the SuperScript II First-Strand Synthesis System (Invitrogen), according to the manufacturer's protocol (see Section 2.2.6.1). PCR was performed with 2 µL of the RT reaction at 94°C for 20 s, 52°C for 20 s, and 72°C for 1 min for 35 cycles using *Taq* polymerase (Roche). This was followed by a single 72°C extension step for 5 min. The primers used for the amplification were 5'-GGT ATT TGG CAG AGT ATT GAT GTG-3' and 5'-GTC TAC TAC CAT GGC TGG AAT-3' (514 bp). The *myostatin* cDNA was radioactively labelled using α^{32}P-(dCTP) (GE Healthcare Bio-Sciences) and Rediprime II labelling kit (GE Healthcare Bio-Sciences) as described in Section 2.2.7.

3.2.9 Detection of circulating levels of Myostatin.

Bovine serum samples were obtained from foetal days 70, 90, 138, 150, 165, 240 through to adult. 2 μL of serum from each sample was loaded onto a 4-12% Bis-Tris pre-cast gel (Invitrogen). Subsequent Western Blot analysis for Myostatin was performed as described in Section 3.2.6.

3.2.10 Detection of myostatin in wild-type and myostatin-null mice.

One mL of lysis buffer (PBS, pH 7.2) with 0.05% IGEPAL detergent (Sigma) and an enzyme inhibitor (Roche) was added to 100 mg of muscle from each animal. Samples were homogenised on ice, then centrifuged at 11,000 x g for 10 min. Supernatant was recovered, mixed with Laemmli loading buffer (Laemmli 1970), boiled for 5 min, then stored at -20°C until analysis. The protein concentration of the supernatant was determined using the bicinchoninic acid assay (Sigma).

Twenty μg of protein from each muscle sample was loaded and separated in a 10% SDS-polyacrylamide gel under reducing conditions, then transferred to a nitrocellulose membrane. After transfer, membranes were stained with Ponceau S to verify transfer of protein. Membranes were blocked and incubated in 0.05 M tris buffered saline with 0.05% Tween 20 (TBST, pH 7.6), containing 0.3% BSA, 1% polyethylene glycol (3,350 Mw), 1% polyvinylpyrrolidone (10,000 Mw). Membranes were incubated with either rabbit anti-Myostatin, or goat anti-Myostatin (1:5000, sc-6884, Santa Cruz Biotechnology Inc.). Twenty four hr later, membranes were washed in TBST, then incubated for 2 hr with either 1:10,000 dilution of HRP conjugated anti-rabbit antibody (A0545; Sigma), or 1:5,000 dilution of HRP conjugated anti-goat antibody (P0160; Dako. Glostrup, Denmark) against respective primary antibodies, then washed again in TBST. Bound HRP activity was detected with enhanced chemiluminescence and then blots were exposed to XOMAT XAR film (Eastman Kodak Company).

3.2.11 *Biological activity of circulating Myostatin*

The AgResearch Ruakura Animal Ethics Committee approved all animal manipulations described in this paper. Standard superovulation and embryo transfer techniques were used to generate bovine Hereford x Friesian crossbreed foetuses as described by Kambadur *et al*. (Kambadur *et al.* 1997). Cows were slaughtered at the Ruakura abattoir when foetuses were at gestational age 120, 210 and 260 days. Foetal blood was collected via cardiac puncture and allowed to clot at 4^{o}C overnight. Serum was then separated from the clot via centrifugation at 4200 rpm for 20 min. Serum was then filtered through a sterile 0.22 μm membrane.

Serum was then added to test medium at a concentration of 10%. This test medium consisted of DMEM (Invitrogen), buffered with $NaHCO_3$ (41.9 mmol/l, Sigma) and gaseous CO_2. Phenol red (7.22 nmol/L, Sigma) was used as a pH indicator. Penicillin (1 x 10^5 IU/l) and Streptomycin (100 mg/l, Sigma) were also included in the medium.

Cell proliferation assays were then conducted to test the biological activity of the serum. C2C12 (Yaffe and Saxel 1977) cultures were seeded at 1,000 cells/well (3 x 10^3 cells/cm^2) in Nalge Nunc 96 well dishes in Proliferation Medium. After a 24 hr attachment period medium was decanted and test medium described above added back to the plates. Test samples were randomly distributed over the plate in order to avoid possible edge effects.

Plates wrapped in parafilm then incubated in an atmosphere of 37^{o}C 5% CO_2. The plate was fixed at 72 hr post medium change, and assayed for proliferation by the method of Oliver et al. (1989) (Oliver *et al.* 1989). Briefly, Proliferation Medium was decanted and cells washed once with PBS then fixed for 30 min in 10% formol saline. The fixed cells were then stained for 30 min with 10 g/L methylene blue in 0.01 M borate buffer (pH 8.5). Excess stain was then removed by four sequential washes in borate buffer. Methylene blue was then eluted off the fixed cells by the addition of 100 μL of 1:1 (v/v) ethanol and 0.1 M HCL. The plates were then gently shaken for 30 s and absorbance at 655 nm measured for each well by a microplate photometer (Bio-Rad model 3550 microplate reader, Bio-Rad, Hercules, CA). Absorbance is directly proportional to cell number in this assay.

3.2.12 Statistics

For the transfection experiments, the mean luciferase values were calculated per well and the three means averaged over three independent experiments. Myostatin secretion was measured by densitometry analysis of Autoradiographs, which were adjusted for background and normalised to total DNA content of the cells. The ratio between three replicates was calculated. To determine the significance level of differences between two groups Student's-T test was used. Statistical analysis was performed in Excel. A P value of <0.05 was deemed significant for all experiments.

3.3 Results

3.3.1 *Intracellular localisation of Myostatin*

Indirect immunofluorescence microscopy was performed on myoblasts and myotubes to investigate if there are any qualitative changes in Myostatin distribution during myogenesis. C2C12 cell cultures were used for immunostaining. The immunofluorescence microscopy studies show that Myostatin protein was detected in actively proliferating C2C12 myoblasts (Figure 3.1A and Figure 3.1C). Specifically, Myostatin immunofluorescence was mainly localised in a peri-nuclear pattern, often showing the characteristic reticular morphology seen for TGF-β1 (Figure 3.1C) (Miyazono *et al.* 1992; Mizoi *et al.* 1993; Roth-Eichhorn *et al.* 1998). In contrast to actively proliferating myoblasts, Myostatin immunostaining in differentiated myotubes was mainly localised throughout the cytoplasm (Figure 3.1E).

3.3.2 *Myostatin processing is regulated during differentiation*

Myostatin protein is synthesised and secreted from myoblasts and it is shown that secreted Myostatin regulates myoblast growth and differentiation systemically (Zimmers *et al.* 2002). Thus processing and/or secretion of Myostatin play a critical role in the myogenesis. To investigate if changes in either transcription or post transcription events regulate active levels of myostatin during myogenesis, the levels of *myostatin* mRNA and the level of Myostatin processing was examined during the differentiation of myoblasts in a cell culture system. In this experiment, bovine primary myoblasts were grown in either Proliferation Medium or induced to differentiate in Differentiation Medium for 24, 48 and 72 hr before being harvested for total RNA and protein. Northern Blot analysis revealed that *myostatin* mRNA (2.9 kb) was present in all of the total RNA extracts, with no appreciable change in the levels between myoblasts cultured in Proliferation Medium and myoblasts undergoing differentiation in Differentiation Medium (Figure 3.2A).

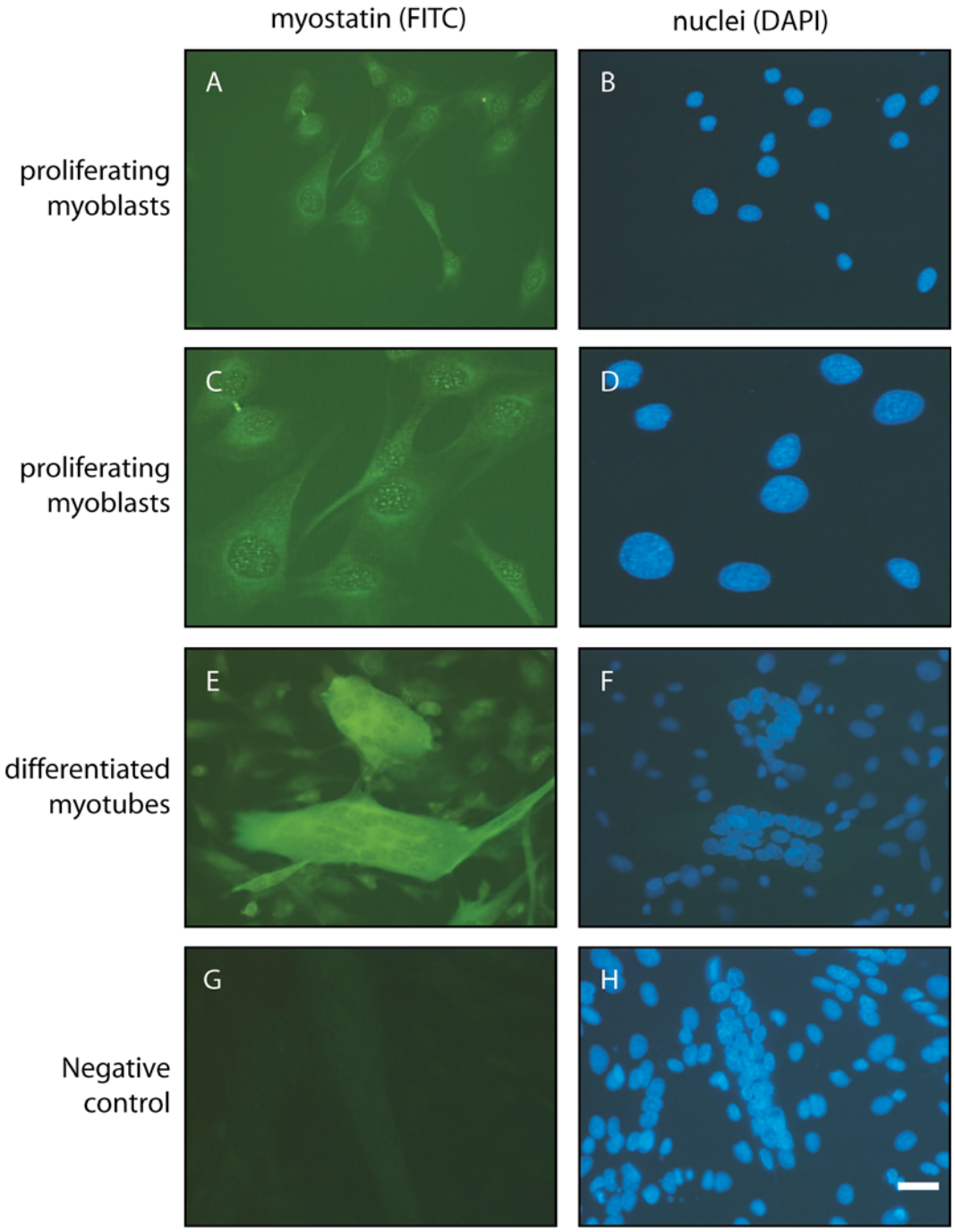

Figure 3.1 *Myostatin intracellular localisation is altered between C2C12 myoblast and myotube populations*

Immunofluorescence microscopy showing Myostatin localisation in (A) proliferating C2C12 myoblasts and (E) differentiated C2C12 myotubes. Myostatin-immunoreactive protein was detected using anti-Myostatin antibodies and FITC staining. (G) Anti-rabbit IgG negative-control on differentiated C2C12 myotubes. (B), (D), (F) and (H) DAPI stained cell nuclei of plates (A), (C), (E) and (G) respectively. Bar equals 50 μM. Panels (C) and (D) are larger inserts of (A) and (B) respectively.

In the Western Blot analysis using Myostatin-specific antibodies, no precursor Myostatin was observed in the myoblasts cultured in Proliferation Medium. In the myoblasts undergoing differentiation, however, a relatively high level of precursor Myostatin was detected (Figure 3.2B). In contrast to the precursor Myostatin, the level of LAP and mature Myostatin appeared to be slightly higher in actively proliferating myoblasts than in the differentiating myoblasts (Figure 3.2B). In addition, Western Blot analysis was performed using our in-house Myostatin-specific antibody and a commercially available GDF-8 antibody (sc-6884, Santa Cruz), using muscle protein extracts from wild-type and *myostatin*-null mice. As shown in Figure 3.2C the myostatin-specific antibodies fail to detect the strong 26-kDa protein band, which is observed in the wild-type controls. Therefore this supports the assignment of the 26-kDa band to mature Myostatin.

In addition to the bovine primary myoblasts, mouse C2C12 myoblasts were cultured in either Proliferation Medium or Differentiation Medium for 24 hr and myostatin processing was examined by Western Blot analysis. In the C2C12 myoblasts cultured in Proliferation Medium, the majority of Myostatin protein that was detected was the 26-kDa mature and 40-kDa LAP forms. Only a relatively low level of precursor Myostatin was detected (Figure 3.3A). In myotubes by contrast, relatively high levels of the 52-kDa precursor Myostatin were detected, while low levels of the 40-kDa LAP and no 26-kDa mature Myostatin were detected (Figure 3.3A). These results suggest that there is a change in the in the level of proteolytic processing of Myostatin during myogenic differentiation.

3.3.3 *Myoblasts and myotubes secrete Myostatin protein*

Northern and Western Blot analysis performed on myoblast extracts indicated that while there is no change in *myostatin* mRNA during myogenic differentiation, there is a dramatic difference in proteolytic processing of Myostatin protein. Since proteolytic processing of the TGF-β superfamily members must occur for secretion, it is possible that more Myostatin protein is retained in myotubes compared to myoblasts where the majority of Myostatin is processed and

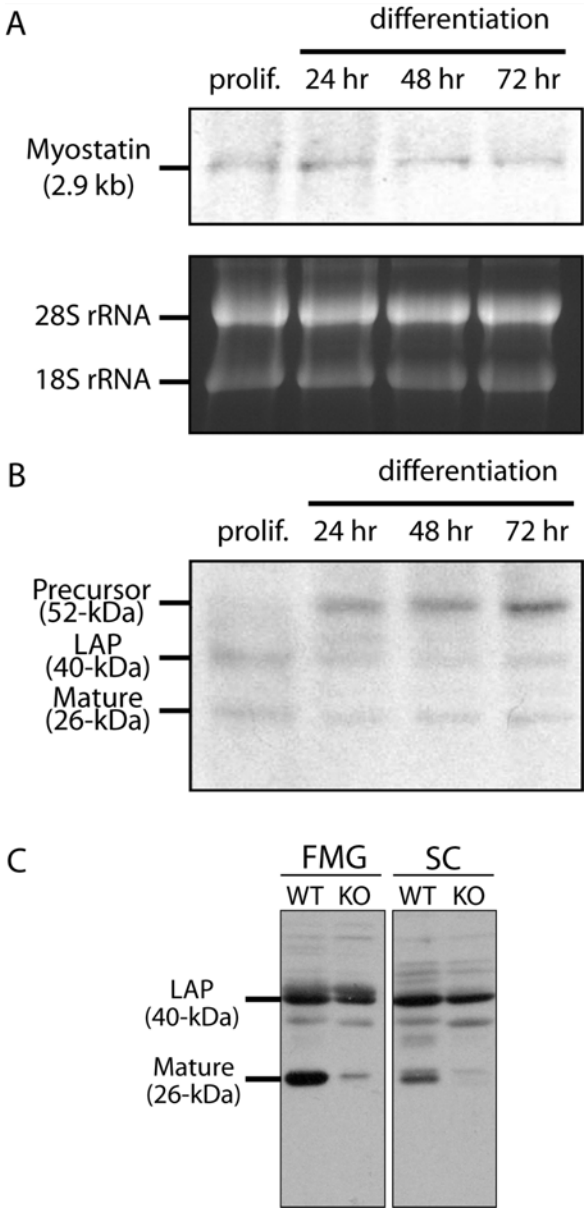

Figure 3.2 *Myostatin processing is regulated during myogenic differentiation*

A) Northern Blot showing *myostatin* mRNA levels in primary bovine myoblasts cultured from foetal day 70 hindlimb muscle in Proliferation Medium (prolif.) or Differentiation Medium for 24, 48 or 72 hr. The Northern Blot was probed with a 514 bp *myostatin* cDNA probe. The 2.9 kb *myostatin* transcript is indicated. Ethidium bromide stained formaldehyde/agarose gel showing 28S and 18S rRNA is also included. B) Western Blot showing the levels of precursor, LAP and mature Myostatin in primary bovine myoblasts cultured from foetal day 70 hindlimb muscle in Proliferation Medium (prolif.) or Differentiation Medium for 24, 48 or 72 hr. C) Western Blot showing the levels of LAP and mature Myostatin between muscle samples obtained from wild type (WT) and *myostatin*-null mice (KO). Two different antibodies were used, our in house anti-Myostatin antibody (FMG) and a commercially available GDF-8 antibody from Santa Cruz (SC).

presumably secreted. To investigate if the rate of Myostatin secretion differs between myoblasts and differentiated myotubes, C2C12 myoblasts or myotubes were cultured for 72 hr and Myostatin protein was immunoprecipitated from the conditioned medium. To distinguish between exogenous Myostatin in the medium serum (10% and 2% in proliferating and differentiated cultures, respectively) and endogenous Myostatin secreted from the cells, the cultures were pulsed with S^{35}-methionine for a period of 24 hr. Myostatin labelled with S^{35}-methionine therefore represented *de novo* synthesised and secreted Myostatin. A Hoechst Assay was also performed on the cultured cells to normalise the detected myostatin to DNA content. As can be seen in Figure 3.3B and Figure 3.3C, less mature and LAP Myostatin protein was detected, per DNA content, in the myotube conditioned medium than in the proliferating myoblast conditioned medium. This result supports the above observations that there is greater proteolytically processing of precursor Myostatin to LAP and mature forms in proliferating myoblasts than in differentiated tubes. Thus an increase in processing results in more secretion of Myostatin by the myoblasts, while unprocessed precursor Myostatin is retained intracellularly in the myotubes.

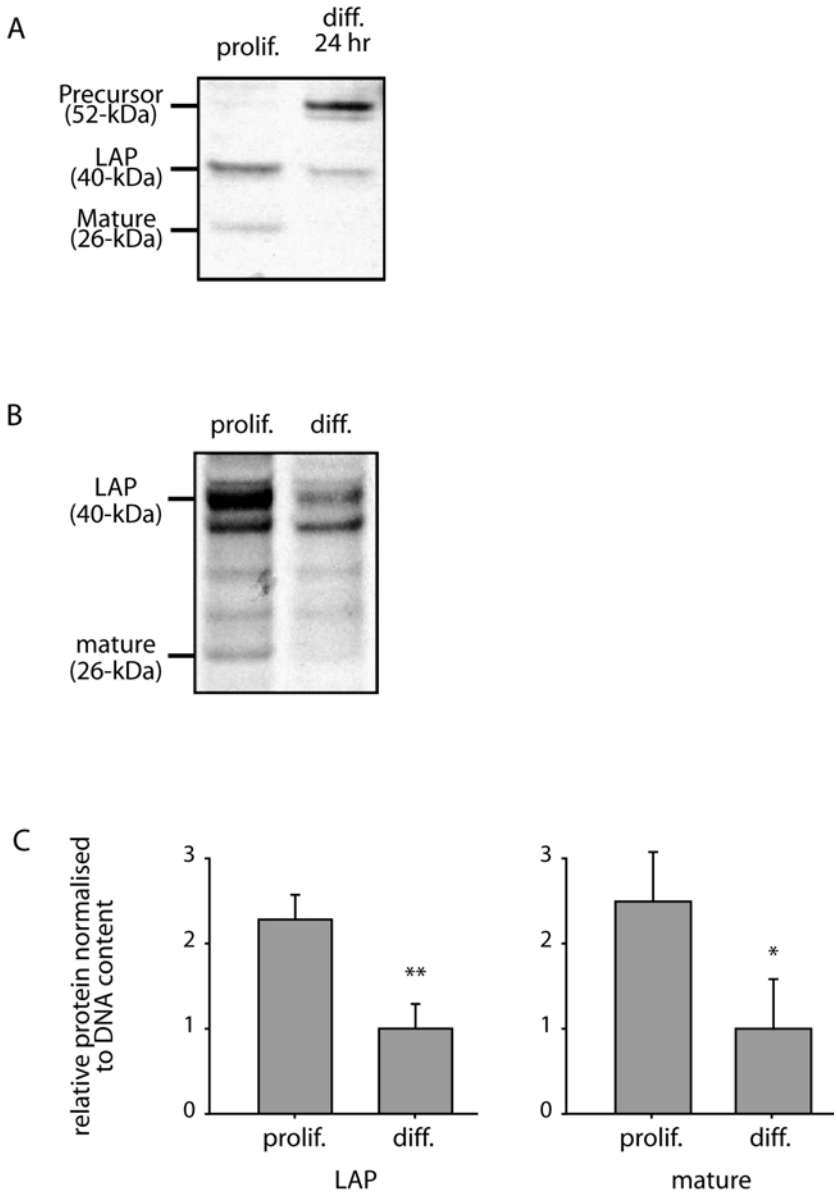

Figure 3.3 *Secretion of Myostatin is regulated during myogenic differentiation*

A) Western Blot showing the levels of precursor, LAP and mature Myostatin in C2C12 myoblasts cultured in Proliferation Medium (prolif.) or Differentiation Medium (diff.) for 24 hr. Myostatin-immunoreactive protein was detected using anti-Myostatin antibodies. B) Autoradiograph of metabolically-labelled LAP and mature Myostatin immunoprecipitated from the conditioned medium of proliferating C2C12 myoblasts (prolif.) or differentiated C2C12 myoblasts (diff.). Myostatin-immunoreactive protein was immunoprecipitated using anti-Myostatin antibodies and fractionated by SDS-polyacrylamide gel electrophoresis. C) Graph showing the ratio of Myostatin secretion between proliferating and differentiated myoblasts for the LAP and Processed forms. Myostatin secretion was measured by densitometry analysis of Autoradiographs in (B), adjusted for background and normalised to total DNA content of the cells. Bars represent the average ratio of three replicates. Statistical differences determined by Student's-T test are indicated, $P<0.01$ (**) and $P<0.05$ (*) compared to Prolif. sample.

3.3.4 Myostatin processing is regulated during development

Previously it has been demonstrated that precursor Myostatin protein is synthesised in myoblasts and proteolytically processed prior to secretion as a mature form (Thomas *et al.* 2000). Since mature Myostatin is the active signaling peptide, proteolytic processing plays a significant role in the regulation of myostatin function during myogenesis. Although it has been shown that Myostatin protein is present in myoblasts and adult muscle fibres, the pattern of myostatin processing during myogenic development is not yet known. Hence, Western Blot analysis was performed on protein extracts from bovine foetal day 61 hind limb, as well as *M. vastus lateralis* (*vl.*) and bovine *M. semitendinosus* (*st.*) muscles collected from various time points (foetal day 120 to post-natal day 14). Myostatin protein was detected in the precursor (52-kDa) and LAP (40-kDa) forms in nearly all of the bovine *vl.* muscle extracts (Figure 3.4A). In the foetal day 61 muscle extract, a relatively high level of precursor Myostatin was observed. No LAP was detected, even with a longer exposure of the Western Blot to autoradiography film (Figure 3.4A). As the foetal age increased (foetal days 120-260) a decrease in the amount of precursor Myostatin and a corresponding increase in LAP was observed (Figure 3.4A). Post-natally, the predominant form of Myostatin present was LAP, with very little precursor Myostatin being detected (Figure 3.4A). To determine the level of *myostatin* mRNA expression, Northern Blot analysis was performed on total RNA extracted from the same source (Bovine hindlimb muscle, foetal day 61 and *vl.* Muscle, foetal day 120 to post-natal day 14) used in the Western Blot analyses. As shown in Figure 3.4B, *myostatin* mRNA of 2.9 kb was detected in all of the bovine muscle samples from foetal day 61 through to post-natal day 14. At foetal days 61 and 120, *myostatin* mRNA was relatively abundant. At foetal days 160 to 260 and full-term (280/post-natal day 1) the relative levels of *myostatin* mRNA were increased, peaking at the day 260 and full-term time points. Post-natally, *myostatin* mRNA levels dramatically declined, as seen by the relatively low level of *myostatin* mRNA in post-natal days 8 to adult (Figure 3.4B). In addition to the *vl.* muscle, myostatin processing during development was also examined in the *M. semitendinosis* muscle. A similar overall pattern of processing that is seen in the *vl*. muscle was also observed in the *st.* muscle (Figure 3.4C). The observed increase in Myostatin processing during gestation suggests that the extent of

Myostatin processing is regulated during embryonic and foetal bovine myogenesis.

Like other TGF-β superfamily members, proteolytic processing of the Myostatin precursor molecule results in the formation of two distinct peptides, the LAP peptide and the C-terminal mature peptide (McPherron *et al.* 1997). Following processing both The LAP and mature Myostatin dimer are maintained in a circulatory latent complex (Lee and McPherron 2001). Thus, to investigate if the extent of Myostatin processing at the site of synthesis correlated with the amount of circulatory Myostatin, the levels of Myostatin in foetal blood during development was analysed. The results show that mature Myostatin was virtually undetectable during early embryonic and foetal growth. However, post-natally high levels of 26-kDa mature Myostatin was detected, confirming that reduced processing indeed results in low systemic levels of Myostatin (Figure 3.4D). These results, investigating the expression of myostatin, suggest that there is an increase in *myostatin* mRNA and an increase in the proteolytic processing of myostatin during foetal development. Post-natally however, *myostatin* mRNA expression declines but a high level of processing is still maintained.

To determine if the increase in myostatin processing during foetal development is significant with respect to myostatin function, the biological activity of circulating Myostatin was measured. As shown in Figure 3.5, C2C12 cells treated with serum obtained from day 260 bovine foetuses showed a 13% decrease in proliferation when compared to cells treated with serum obtained from earlier gestational time points. This decrease in proliferation coincides with the large increase in Myostatin processing seen from day 260 onwards (Figure 3.4).

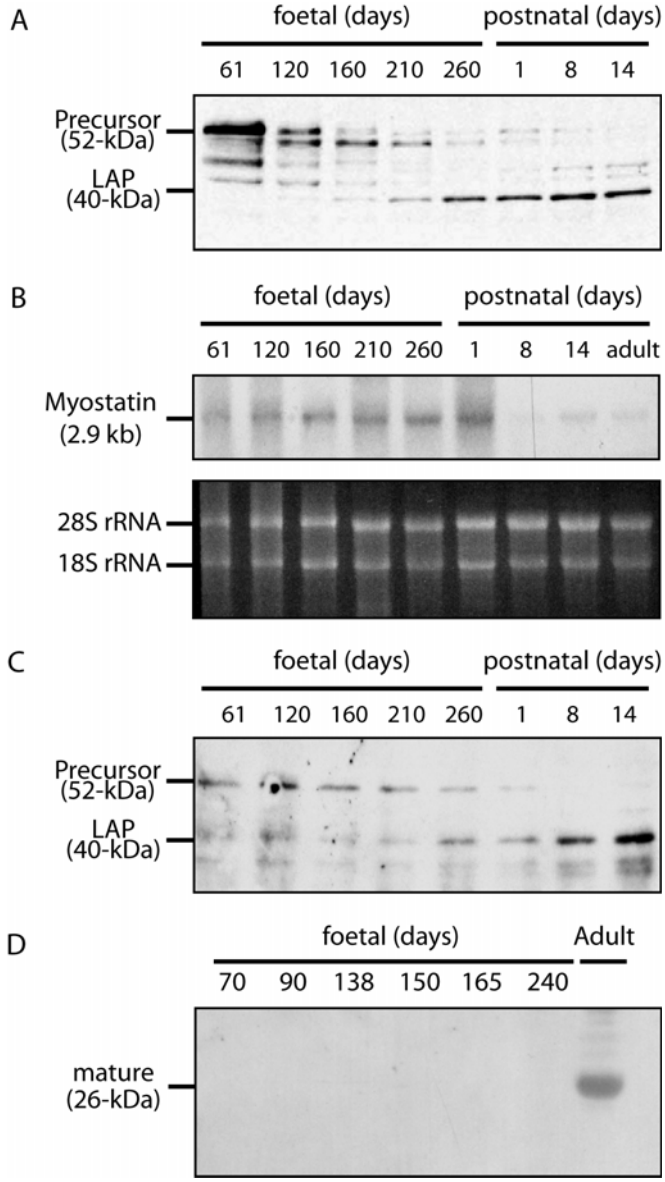

Figure 3.4 *Myostatin processing is regulated during development*

A) Western Blot showing the levels of Myostatin precursor and Latency-Associated Peptide (LAP) in *M. vastus lateralis*. B) Northern Blot showing *myostatin* expression in *M. vastus lateralis* from foetal days 61, 120, 160, 210, 260 and post-natal 1, 8, 14 and adult cattle. The Northern Blot was probed with a 514 bp *myostatin* cDNA probe. The 2.9 kb *myostatin* transcript is indicated. Ethidium bromide stained formaldehyde/agarose gel showing 28S and 18S rRNA is also included. C) Western Blot showing the levels of Myostatin precursor and LAP in *M. semitendinosus* from foetal days 61, 120, 160, 210, 260 and post-natal 1, 8 and 14 cattle. Myostatin-immunoreactive protein was detected using anti-Myostatin antibodies. D) Western Blot showing the serum levels of mature Myostatin from foetal days 70, 90, 138, 150, 165, 240 to adult. 2 µL of total serum was loaded and analysed for Myostatin expression using specific anti-Myostatin antibodies.

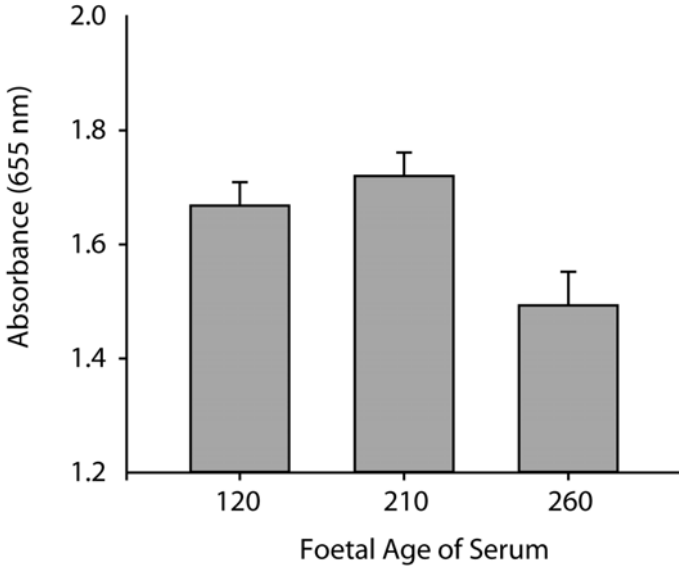

Figure 3.5 *Biological activity of circulating Myostatin is altered during foetal development*

The biological activity of Myostatin in circulating foetal blood was assessed by collecting blood from known age bovine foetuses. This blood was then used to make serum and the biological activity of the serum assessed by its ability to promote the proliferation of C2C12 myoblasts in a 72 hr methylene blue cell staining proliferation assay. Absorbance at 655 nm is directly proportional to cell number at the conclusion of the assay.

3.3.5 Mature Myostatin regulates furin promoter activity

Results shown above clearly indicate that differentiation somehow reduces processing of Myostatin. Furin proteases are responsible for proteolytically processing TGF-β superfamily members; therefore the observed reduction in the processing may be due to reduced furin expression. To prove this, the P1 *furin* promoter-luciferase reporter construct was transfected into C2C12 myoblasts, with subsequent promoter reporter activity measured during proliferating and differentiating conditions. Consistent with the reduction in processing of Myostatin protein, *furin* promoter activity is also reduced in differentiated tubes as compared to actively growing myoblasts (Figure 3.6A). This result indirectly suggested that furin gene expression could be regulated by myostatin. Thus *furin* promoter-luciferase reporter activity was measured in the presence and in the absence of Myostatin. As shown in Figure 3.6B, treatment of the P1 *furin* promoter with Myostatin decreases the promoter activity in a concentration dependent manner. This result indicates that the *furin* promoter is negatively regulated by myostatin.

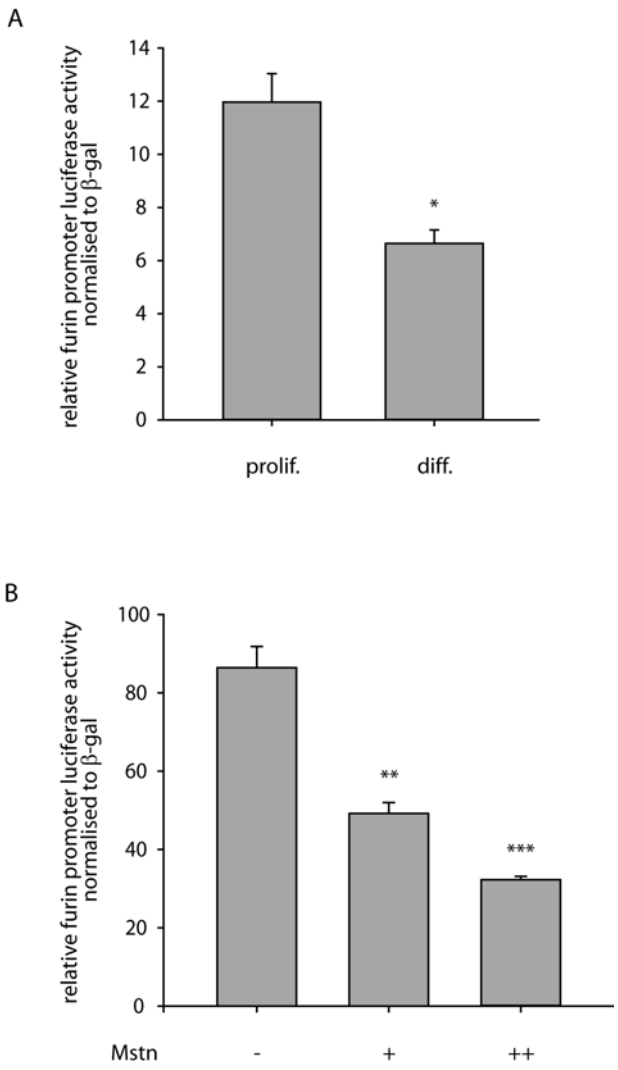

Figure 3.6 *Mature Myostatin regulates furin promoter activity*

A) *in vitro* analysis of the *furin* promoter during proliferation and differentiation conditions. The *furin* promoter and β-galactosidase (β-gal) expression plasmids were transfected into C2C12 myoblasts. The cells were grown for a further 24 hr in either Proliferation or Differentiation Medium after which luciferase and β-gal activity was measured. Results reflect relative *furin* promoter-luciferase activity normalised to β-gal. Bars indicate means ± standard error of three independent experiments. Statistical differences determined by Student's-T test are indicated, $P<0.05$ (*) compared to Prolif. control. B) *in vitro* analysis of the effect of myostatin on *furin* promoter activity during proliferation conditions. The *furin* promoter and β-galactosidase (β-gal) expression plasmids were transfected into C2C12 myoblasts. The cells were grown for a further 24 hr in Proliferation medium after which luciferase and β-gal activity was measured. Results reflect relative change in furin promoter luciferase activity with increasing Myostatin concentration (+ 0.5 μg/mL, ++ 3 μg/mL) as compared to the un-treated control (-). Luciferase values were normalised to β-gal and the bars indicate means ± standard error of three independent experiments. Statistical differences determined by Student's-T test are indicated, $P<0.001$ (***) and $P<0.01$ (**) compared to un-treated control (-).

3.4 Discussion

Previously published results have shown that *myostatin* is synthesised in both myoblasts and in muscle fibres, proteolytically processed, and secreted as a mature Myostatin peptide (Thomas *et al.* 2000). However, the processing and secretion during myogenesis has not been widely investigated. In this Chapter, it is demonstrated that the processing and secretion of Myostatin is reduced upon differentiation or during foetal fibre formation stages. Furthermore it is shown that myostatin auto-regulates the extent of processing by regulating the gene expression of its converting enzyme, furin.

Myostatin expression during development - Northern Blot analysis revealed that *myostatin* expression is developmentally regulated (Figure 3.4B). *Myostatin* mRNA was abundant during early foetal development (days 61 and 160), increasing at foetal day 160. A relatively high level of *myostatin* mRNA was observed in each gestational time point from day 160 onward, the peak expression being observed in the day 260 sample. After birth, the levels of *myostatin* mRNA declined dramatically and remained low in all the post-natal days (8, 14 and adult) observed. These results are predominantly in agreement with other results published from our laboratory in which *myostatin* expression is examined by RT-PCR in bovine *M. semitendinosus* muscle over the same time period (Oldham *et al.* 2001). In the published results, a dramatic and transient increase in *myostatin* expression is also observed at foetal day 90; which lies between the two foetal time points, day 61 and 120, examined by Northern Blot analysis in this study. This peak expression of myostatin coincides with the peak expression of MyoD. In addition, published results from our laboratory has demonstrated that the bovine *myostatin* promoter is a downstream target gene of MyoD (Spiller *et al.* 2002). Thus it is quite possible that the developmental expression pattern of myostatin is predominately regulated by MyoD.

Myostatin indirect immunofluorescence microscopy experiments on myoblasts and myotubes confirmed that myostatin is synthesised in muscle cells (Figure 3.1). Myostatin-immunoreactive protein was detected in both proliferating myoblasts and nascent myotubes; localised in a perinuclear pattern (Figure 3.1). In addition, Myostatin was localised throughout the cytoplasm in the myotubes

(Figure 3.1). These findings are consistent with studies examining TGF-β in several cell types, whereby TGF-β1 is localised to a perinuclear region, sometimes showing a characteristic reticular morphology (Miyazono *et al.* 1992; Mizoi *et al.* 1993; Roth-Eichhorn *et al.* 1998). In one of these studies, the subcellular localisation of TGF-β1 was determined by immunoelectron microscopy to be in the lumen of the rER and perinuclear cisternae of fibroblasts, macrophages, and endothelial cells, indicating the biosynthetic process of the protein (Mizoi *et al.* 1993). In another study, immunofluorescence microscopy of human erythroleukemia cells (HEL) revealed that TGF-β co-localises with mannosidase II, an integral Golgi protein (Miyazono *et al.* 1992). Taken together these studies indicate TGF-β is synthesised and secreted via the endoplasmic reticulum and Golgi, respectively (Miyazono *et al.* 1992; Mizoi *et al.* 1993; Roth-Eichhorn *et al.* 1998). Based on these reports, it is possible that the perinuclear localisation of Myostatin reflects its synthesis and processing in the endoplasmic reticulum and Golgi. However, co-localisation studies using Golgi-specific markers, such as mannosidase II, would be required to determine this for certain. In addition to the perinuclear localisation of Myostatin, a diffuse immunofluorescence was detected in the cytoplasm of the nascent myotubes supporting the observation that less Myostatin is secreted in myotubes. Intracellular retention has also been observed for other members of the TGF-β superfamily, including Activin A, TGF-β1 (Miyazono *et al.* 1992; Roth-Eichhorn *et al.* 1998), TGF-β2 (Jakowlew *et al.* 1991; Roth-Eichhorn *et al.* 1998) and TGF-β3 (Roth-Eichhorn *et al.* 1998). Latent TGF-β binding proteins (LTBPs) have been proposed to play a role in the cytoplasmic retention of TGF-β1, -β2 and -β3 (Oklu and Hesketh 2000). It is unlikely that LTBPs would regulate Myostatin secretion, since yeast two hybrid and co-immunoprecipitation studies did not detect any interaction between LTBPs and Myostatin (data not shown). However, previously published results from our laboratory suggest that the protein Titin-Cap (T-cap) could regulate the intracellular levels of Myostatin, due to the fact that over-expression of T-cap leads to reduced secretion of Myostatin (Nicholas *et al.* 2002). Further myostatin-interacting proteins, including follistatin, FLRG and GASP-1, appear to be unlikely candidates since they have been shown to interact with Myostatin in circulation, following secretion (Lee and McPherron 2001; Hill *et al.* 2002; Hill *et al.* 2003).

Processing and secretion of myostatin during myogenic differentiation - Changes in the extent of Myostatin proteolytic processing and secretion were observed between actively proliferating myoblasts and differentiated myotubes (Figure 3.2 and 3.3). In actively proliferating mouse C2C12 and bovine primary myoblasts, the predominating forms of Myostatin detected were the mature Myostatin and/or LAP suggesting that the Myostatin precursor protein is being proteolytically processed. In differentiating and nascent myotubes by contrast, Myostatin was observed predominantly in the precursor form. Consistent with the processing results, relatively more Myostatin was secreted in proliferating myoblasts as compared to fully differentiated myotubes. Since the Myostatin that was detected was metabolically labeled, it likely reflects the *de novo* synthesis from the cells and not Myostatin introduced by medium differences. Although the processing of myostatin is altered during myogenesis, no appreciable change in *myostatin* mRNA expression was observed in the bovine primary myoblasts. Levels of LAP and mature Myostatin were measured between muscle tissues from wild-type and *myostatin*-null mice. A dramatic loss of the 26-kDa mature Myostatin protein band was observed in *myostatin*-null mice when using two different Myostatin-specific antibodies (Figure 3.2C), thus providing evidence for the validity of the protein bands assigned to Myostatin. However, a faint band running at 26-kDa is observed in the *myostatin*-null muscle tissue, this could be attributed to antibody cross reactivity with GDF-11 as GDF-11 shares a high homology with the mature region of Myostatin.

Processing and secretion of myostatin during myogenesis - Lowered levels of Myostatin processing occur during foetal muscle development when compared to post-natal adult muscle (Figure 3.4). The primary observation in the examination of Myostatin expression by Western Blot analysis is the progressive shift in Myostatin expression from precursor protein to LAP (Figure 3.4A & Figure 3.4C). At foetal day 61 most of the Myostatin detected was present in the precursor form. Between foetal days 160 and 210, relatively more processing resulted in reduced precursor Myostatin and increased LAP. From foetal day 260 onward, the majority of observed Myostatin was present in the LAP form suggesting almost all of the synthesised Myostatin is processed. Since the processing of TGF-β superfamily members is required for secretion, and moreover secretion occurs rapidly after processing (Miyazono *et al.* 1992; Roth-

Eichhorn *et al.* 1998), this observation suggests that during late foetal development more Myostatin is secreted. This increase in myostatin secretion, in conjunction with an up-regulation of *myostatin* gene expression, implies that there is a large increase in mature Myostatin from day 210 in the developing foetus. This is indeed supported by western analysis results of foetal systemic Myostatin levels (Figure 3.4D). While virtually all the secreted Myostatin is undetectable during early foetal development, during post-natal adult stages abundant levels of Myostatin were present. Myostatin systemic expression was not detected during days 165 and 240 despite processing occurring. This could be due to the fact that Myostatin circulatory levels during these time points were below the limits of detection for Western Blot analysis. The dramatic increase in mature Myostatin from day 210 in the foetus may result in the production of biologically active Myostatin. To examine this a well characterised bioassay for myostatin was performed (Thomas *et al.* 2000). The results show there is a 13% drop in C2C12 proliferation rate in cells treated with serum obtained from foetal day 260 cattle compared to cells treated with foetal day 210 serum (Figure 3.5). This drop in proliferation rate is consistent with known myostatin function and interestingly, coincides with the dramatic increase in Myostatin processing observed during foetal day 260 (Figure 3.4).

Low levels of circulatory Myostatin during early foetal development may allow for the differentiation of primary and secondary waves of myoblasts to occur during myogenesis, due to the fact that excess amounts of mature Myostatin have been shown to cause a down-regulation of MyoD expression, resulting in the inhibition of myogenic differentiation of C2C12 myoblasts (Langley *et al.* 2002). Thus to reduce the availability of biologically active Myostatin and facilitate the process of post-mitotic differentiation, myoblasts could facilitate a reduction in processing of Myostatin by an auto-regulatory mechanism. For such an auto-regulatory mechanism to be feasible, ligands involved in the functioning of TGF-β family members should be able to directly regulate proteolytic processing enzymes. Furin has been shown to cleave several TGF-β family members including bone morphogenetic protein-4 (BMP-4) and TGF-β1 (Cui *et al.* 1998; Dubois *et al.* 2001). Previously, it has been shown that TGF-β up-regulates its own converting enzyme furin (Blanchette *et al.* 1997). In contrast, the results presented here demonstrate that myostatin can negatively regulate furin protease

promoter expression (Figure 3.6B). Recently it has been demonstrated that *myostatin* expression peaks at the onset of primary bovine myoblast fusion with a subsequent reduction during differentiation (Deveaux *et al.* 2003). Therefore it is quite possible that the reduced processing of Myostatin seen during differentiation is due to down-regulation of furin protease activity by an increase in *myostatin* expression prior to differentiation. In other words, a peak in Myostatin levels during the onset of differentiation results in lowered furin protein expression and subsequent reduction in Myostatin processing during differentiation. This novel mechanism of negative auto-regulation allows for timely myogenic differentiation during development leading to the formation of myogenic fibres.

An analysis of the *furin* P1 promoter has identified several consensus E-Box sequences (data not shown), which could indicate the involvement of bHLH transcription factors in the regulation of *furin* gene expression. MyoD is an important bHLH transcription factor involved in regulating myogenesis. Previously published results from our laboratory have shown that myostatin can cause a down-regulation of MyoD expression, resulting in an inhibition of C2C12 myoblast differentiation (Langley *et al.* 2002). Therefore increased myostatin expression may cause a decrease in furin promoter activation by down-regulating MyoD expression.

Collectively this study demonstrates that there is reduced proteolytic processing of Myostatin protein during myogenesis and that myostatin negatively regulates the transcription of its own converting enzyme, furin. Given that myostatin is a negative regulator of myogenesis, it is hypothesised that myostatin auto-regulates its processing, thereby regulating the process of myoblast terminal differentiation.

3.5 Acknowledgments

Thanks to the Functional Muscle Genomics Group, AgResearch, Hamilton, New Zealand. Thanks also to Dr Claire Dubois for the gift of the P1 Furin promoter construct used in this study. Further thanks to both the Royal Society of New Zealand (Marsden) and the Foundation of Research and Technology (New Zealand) for financial support. Thanks to Dr Brett Langley for instructing me on the molecular biological techniques used in this paper. Further thanks to Mark Thomas for plating the myoblast cell lines and maintaining fresh medium. Thanks also to Alex Hennebry for contributing to the Western Blot analysing serum levels of Myostatin. Further thanks to Erin Plummer for help with *furin* promoter DNA purification. Thanks also to Dr Gina Nicholas for contributing to Western Blotting. Also thanks to Dr Chris McMahon for contributing to the characterisation of Myostatin bands by Western Blot.

3.6 References

Blanchette, F., R. Day, W. Dong, M. H. Laprise and C. M. Dubois (1997). "TGFbeta1 regulates gene expression of its own converting enzyme furin." J Clin Invest **99**(8): 1974-83.

Blanchette, F., P. Rudd, F. Grondin, L. Attisano and C. M. Dubois (2001). "Involvement of Smads in TGFbeta1-induced furin (fur) transcription." J Cell Physiol **188**(2): 264-73.

Constam, D. B. and E. J. Robertson (1999). "Regulation of bone morphogenetic protein activity by pro domains and proprotein convertases." J Cell Biol **144**(1): 139-49.

Cui, Y., R. Hackenmiller, L. Berg, F. Jean, T. Nakayama, G. Thomas and J. L. Christian (2001). "The activity and signaling range of mature BMP-4 is regulated by sequential cleavage at two sites within the prodomain of the precursor." Genes Dev **15**(21): 2797-802.

Cui, Y., F. Jean, G. Thomas and J. L. Christian (1998). "BMP-4 is proteolytically activated by furin and/or PC6 during vertebrate embryonic development." Embo J **17**(16): 4735-43.

Deveaux, V., B. Picard, J. Bouley and I. Cassar-Malek (2003). "Location of myostatin expression during bovine myogenesis in vivo and in vitro." Reprod Nutr Dev **43**(6): 527-42.

Dubois, C. M., F. Blanchette, M. H. Laprise, R. Leduc, F. Grondin and N. G. Seidah (2001). "Evidence that furin is an authentic transforming growth factor-beta1- converting enzyme." Am J Pathol **158**(1): 305-16.

Gray, A. M. and A. J. Mason (1990). "Requirement for activin A and transforming growth factor--beta 1 pro- regions in homodimer assembly." Science **247**(4948): 1328-30.

Hill, J. J., M. V. Davies, A. A. Pearson, J. H. Wang, R. M. Hewick, N. M. Wolfman and Y. Qiu (2002). "The myostatin propeptide and the follistatin-related gene are inhibitory binding proteins of myostatin in normal serum." J Biol Chem **277**(43): 40735-41.

Hill, J. J., Y. Qiu, R. M. Hewick and N. M. Wolfman (2003). "Regulation of myostatin in vivo by GASP-1: a novel protein with protease inhibitor and follistatin domains." Mol Endocrinol.

Jakowlew, S. B., P. J. Dillard, T. S. Winokur, K. C. Flanders, M. B. Sporn and A. B. Roberts (1991). "Expression of transforming growth factor-beta s 1-4 in chicken embryo chondrocytes and myocytes." Dev Biol **143**(1): 135-48.

Ji, S., R. L. Losinski, S. G. Cornelius, G. R. Frank, G. M. Willis, D. E. Gerrard, F. F. Depreux and M. E. Spurlock (1998). "Myostatin expression in porcine tissues: tissue specificity and developmental and postnatal regulation." Am J Physiol **275**(4 Pt 2): R1265-73.

Kambadur, R., M. Sharma, T. P. Smith and J. J. Bass (1997). "Mutations in myostatin (GDF8) in double-muscled Belgian Blue and Piedmontese cattle." Genome Res **7**(9): 910-6.

Laemmli, U. K. (1970). "Cleavage of structural proteins during the assembly of the head of bacteriophage T4." Nature **227**(5259): 680-5.

Langley, B., M. Thomas, A. Bishop, M. Sharma, S. Gilmour and R. Kambadur (2002). "Myostatin Inhibits Myoblast Differentiation by Down-regulating MyoD Expression." J Biol Chem **277**(51): 49831-40.

Langley, B., M. Thomas, C. McFarlane, S. Gilmour, M. Sharma and R. Kambadur (2004). "Myostatin inhibits rhabdomyosarcoma cell proliferation through an Rb-independent pathway." Oncogene **23**(2): 524-34.

Lee, S. J. and A. C. McPherron (2001). "Regulation of myostatin activity and muscle growth." Proc Natl Acad Sci U S A **98**(16): 9306-11.

McPherron, A. C., A. M. Lawler and S. J. Lee (1997). "Regulation of skeletal muscle mass in mice by a new TGF-beta superfamily member." Nature **387**(6628): 83-90.

McPherron, A. C. and S. Lee (1996). "The transforming growth factor-b superfamily." Growth Factors Cytokines Health Dis **1B**: 357-393.

Miyazono, K., J. Thyberg and C. H. Heldin (1992). "Retention of the transforming growth factor-beta 1 precursor in the Golgi complex in a latent endoglycosidase H-sensitive form." J Biol Chem **267**(8): 5668-75.

Mizoi, T., H. Ohtani, K. Miyazono, M. Miyazawa, S. Matsuno and H. Nagura (1993). "Immunoelectron microscopic localization of transforming growth factor beta 1 and latent transforming growth factor beta 1 binding protein

in human gastrointestinal carcinomas: qualitative difference between cancer cells and stromal cells." Cancer Res **53**(1): 183-90.

Molloy, S. S., E. D. Anderson, F. Jean and G. Thomas (1999). "Bi-cycling the furin pathway: from TGN localization to pathogen activation and embryogenesis." Trends Cell Biol **9**(1): 28-35.

Molloy, S. S., L. Thomas, J. K. VanSlyke, P. E. Stenberg and G. Thomas (1994). "Intracellular trafficking and activation of the furin proprotein convertase: localization to the TGN and recycling from the cell surface." Embo J **13**(1): 18-33.

Nicholas, G., M. Thomas, B. Langley, W. Somers, K. Patel, C. F. Kemp, M. Sharma and R. Kambadur (2002). "Titin-cap associates with, and regulates secretion of, Myostatin." J Cell Physiol **193**(1): 120-31.

Oklu, R. and R. Hesketh (2000). "The latent transforming growth factor beta binding protein (LTBP) family." Biochem J **352 Pt 3**: 601-10.

Oldham, J. M., J. A. Martyn, M. Sharma, F. Jeanplong, R. Kambadur and J. J. Bass (2001). "Molecular expression of myostatin and MyoD is greater in double-muscled than normal-muscled cattle fetuses." Am J Physiol Regul Integr Comp Physiol **280**(5): R1488-93.

Oliver, M. H., N. K. Harrison, J. E. Bishop, P. J. Cole and G. J. Laurent (1989). "A rapid and convenient assay for counting cells cultured in microwell plates: application for assessment of growth factors." J Cell Sci **92**(Pt 3): 513-8.

Roth-Eichhorn, S., K. Kuhl and A. M. Gressner (1998). "Subcellular localization of (latent) transforming growth factor beta and the latent TGF-beta binding protein in rat hepatocytes and hepatic stellate cells." Hepatology **28**(6): 1588-96.

Seidah, N. G. and M. Chretien (1997). "Eukaryotic protein processing: endoproteolysis of precursor proteins." Curr Opin Biotechnol **8**(5): 602-7.

Sharma, M., R. Kambadur, K. G. Matthews, W. G. Somers, G. P. Devlin, J. V. Conaglen, P. J. Fowke and J. J. Bass (1999). "Myostatin, a transforming growth factor-beta superfamily member, is expressed in heart muscle and is upregulated in cardiomyocytes after infarct." J Cell Physiol **180**(1): 1-9.

Spiller, M. P., R. Kambadur, F. Jeanplong, M. Thomas, J. K. Martyn, J. J. Bass and M. Sharma (2002). "The myostatin gene is a downstream target gene

of basic helix-loop-helix transcription factor MyoD." Mol Cell Biol **22**(20): 7066-82.

Steiner, D. F. (1998). "The proprotein convertases." Curr Opin Chem Biol **2**(1): 31-9.

Thomas, G. (2002). "Furin at the cutting edge: from protein traffic to embryogenesis and disease." Nat Rev Mol Cell Biol **3**(10): 753-66.

Thomas, M., B. Langley, C. Berry, M. Sharma, S. Kirk, J. Bass and R. Kambadur (2000). "Myostatin, a negative regulator of muscle growth, functions by inhibiting myoblast proliferation." J Biol Chem **275**(51): 40235-43.

Wang, H., Q. Zhang and D. Zhu (2003). "hSGT interacts with the N-terminal region of myostatin." Biochem Biophys Res Commun **311**(4): 877-83.

Wolfman, N. M., A. C. McPherron, W. N. Pappano, M. V. Davies, K. Song, K. N. Tomkinson, J. F. Wright, L. Zhao, S. M. Sebald, D. S. Greenspan and S. J. Lee (2003). "Activation of latent myostatin by the BMP-1/tolloid family of metalloproteinases." Proc Natl Acad Sci U S A **100**(26): 15842-6.

Yaffe, D. and O. Saxel (1977). "Serial passaging and differentiation of myogenic cells isolated from dystrophic mouse muscle." Nature **270**(5639): 725-7.

Zimmers, T. A., M. V. Davies, L. G. Koniaris, P. Haynes, A. F. Esquela, K. N. Tomkinson, A. C. McPherron, N. M. Wolfman and S. J. Lee (2002). "Induction of cachexia in mice by systemically administered myostatin." Science **296**(5572): 1486-8.

Chapter 4 Pax7, myostatin and post-natal myogenesis

This Chapter has been submitted to the Journal of Biological Chemistry and is currently under peer review.

MYOSTATIN SIGNALS THROUGH PAX7 TO REGULATE SATELLITE CELL SELF-RENEWAL

Craig McFarlane[1, 2], Nicholas Ling[2], Mridula Sharma[1], and Ravi Kambadur[1*]
[1] AgResearch, Functional Muscle Genomics, Hamilton, New Zealand
[2] Department of Biological Sciences, University of Waikato, Hamilton, New Zealand
Running Title: Myostatin signals through Pax7
Address correspondence to: Dr Ravi Kambadur, Program Leader, Animal Genomics, AgResearch, East Street, Hamilton, New Zealand, Tel. 0064 7 838 5193; Fax. 0064 7 838 5536; Email: ravi.kambadur@agresearch.co.nz

Abstract

The paired-box transcription factor Pax7 has been implicated in satellite cell biology. In this Chapter the role of Pax7 in myogenesis and regulation of satellite cell growth has been further characterised. Over-expression of Pax7 in C3H10T1/2 multipotent cells resulted in enhanced expression of MyoD concomitant with increased myogenic specification of these cells. However, when Pax7 was over-expressed in myogenic C2C12 cells delayed differentiation was observed, this was accompanied by an increase in the proportion of quiescent reserve cells. These reserve cells may form a population analogous to self-renewed satellite cells; indeed Pax7 expression was higher in reserve cells as compared to that of either actively growing C2C12 cells or myotube populations. Myostatin, a Transforming Growth Factor-beta (TGF-β) superfamily member, has been well characterised as a negative regulator of post-natal myogenesis, and in fact myostatin has previously been shown to inhibit satellite cell activation and self-renewal. Thus the ability of myostatin to signal through Pax7 to regulate satellite cell function was investigated. Treatment with recombinant Myostatin protein down-regulated the expression of Pax7, while Pax7 expression was higher in *myostatin*-null myoblasts as compared to wild-type myoblast cultures. Furthermore, absence of *myostatin* altered cell heterogeneity, resulting in a

reduction in $Pax7^+/MyoD^+$ cells, concomitant with an increase in the population of $Pax7^+/MyoD^-$ cells. Pax7 expression persisted through differentiation in cultured primary myoblasts from *myostatin*-null animals when compared to wild-type counterparts. Therefore, the reserve cell population was measured and, consistent with increased expression of Pax7, there was an increased pool of quiescent "self-renewed" reserve cells in differentiated cultures from *myostatin*-null mice as compared with wild-type cultures. Taken together, these results suggest that increased expression of Pax7 regulates the self-renewal process of satellite cells, and furthermore, growth factors such as myostatin signal through Pax7 to regulate the self-renewed pool of satellite cells.

4.1 Introduction

Skeletal muscle is primarily involved with active force production, resulting in voluntary movement of the skeletal system. Repair and maintenance of skeletal muscle is attributed to the skeletal muscle stem cell pool, the satellite cells. Satellite cells represent a unique population of muscle precursor cells that are located between the basal lamina and sarcolemma of adult myofibres (Grounds and Yablonka-Reuveni 1993; Bischoff and Heintz 1994). In response to several stimuli including muscle injury, quiescent satellite cells activate, proliferate and differentiate to repair damaged skeletal muscle (Bischoff 1989).

MyoD and Myf-5 are myogenic regulatory factors (MRFs) critical for myogenic specification. However, recent evidence has implicated the paired-box transcription factor Pax7 in specification of the myogenic lineage, as observed with enhanced myogenic conversion of $CD45^+$:$Sca1^+$ stem cells following over-expression of Pax7 (Seale *et al.* 2004). MyoD, Myf-5 and Pax7 appear to play critical roles during satellite cell activation, proliferation and differentiation. In fact Myf-5 expression is present in the majority of quiescent satellite cells (Beauchamp *et al.* 2000). Similarly, Pax7 is expressed in quiescent satellite cells and moreover is transcriptionally active in these quiescent cells (Seale *et al.* 2000; Zammit *et al.* 2006). Following activation, satellite cells co-express Pax7 and MyoD (Yablonka-Reuveni and Rivera 1994; Seale *et al.* 2000; Asakura *et al.*

2001), proliferate and then down-regulate Pax7 prior to differentiation (Olguin and Olwin 2004; Zammit *et al.* 2004).

Within healthy skeletal muscle quiescent satellite cell number remains constant irrespective of repeated cycles of degeneration and regeneration, thus indicating that mechanisms exist which maintain the satellite cell pool, such as self-renewal (Schmalbruch and Lewis 2000; Heslop *et al.* 2001; Yoshida 2004). Pax7 has been implicated in the regulation of satellite cell self-renewal. Indeed *pax7*-null mice have impaired regenerative capacity concomitant with a progressive loss in satellite cell number due to cell cycle defects and increased apoptosis (Oustanina *et al.* 2004; Kuang *et al.* 2006; Relaix *et al.* 2006). Further evidence for a role of Pax7 in self-renewal is observed in satellite cell cultures whereby populations of cells express Pax7 but lose MyoD and adopt a phenotype similar to quiescent satellite cells (Halevy *et al.* 2004; Zammit *et al.* 2004). In addition, over-expression of Pax7 has also been shown to inhibit MyoD, block myogenin and induce cell cycle exit without commitment to differentiation (Olguin and Olwin 2004). Although evidence strongly supports a role for Pax7 in myogenic specification and satellite cell self-renewal, the mechanism(s) through which Pax7 regulates these processes remains a matter of contention.

Myostatin, a member of the Transforming Growth Factor-beta (TGF-β) superfamily, has been shown to be a negative regulator of skeletal muscle myogenesis. While addition of Myostatin inhibits myoblast proliferation and differentiation (Thomas *et al.* 2000; Langley *et al.* 2002), a lack functional *myostatin in vivo* results in a heavy muscled phenotype (Kambadur *et al.* 1997; McPherron *et al.* 1997; McPherron and Lee 1997; Schuelke *et al.* 2004). Myostatin expression is detected during embryonic and post-natal stages of growth, thus myostatin may play an important role throughout myogenesis (Kambadur *et al.* 1997; McPherron *et al.* 1997). Indeed myostatin has been implicated in several forms of muscle wasting, including severe cachexia, observed as a result of conditions such as AIDS and liver cirrhosis (Gonzalez-Cadavid *et al.* 1998; Dasarathy *et al.* 2004). Furthermore, over-expression of Myostatin has been shown to induce cachexia (Zimmers *et al.* 2002) through regulation of the ubiquitin-proteasome pathway (McFarlane *et al.* 2006). Conversely, loss of *myostatin* enhances the regenerative capacity of skeletal muscle following injury (McCroskery *et al.* 2005). The dramatic effect of

myostatin on post-natal growth is primarily due to the ability of myostatin to negatively regulate skeletal muscle satellite cell activation, proliferation and satellite cell self-renewal (McCroskery *et al.* 2003); however little is known about the mechanism(s) behind the intrinsic ability of Myostatin to regulate satellite cell physiology.

In this Chapter *in vitro* models have been used to study the role of Pax7 in myogenic specification and satellite cell self-renewal. In addition, the ability of myostatin to regulate Pax7 was assessed in an effort to further delineate the complex mechanism behind myostatin regulation of post-natal myogenesis. It is proposed that Pax7 is capable of promoting the conversion of non-myogenic cell lines to the myogenic lineage. Furthermore, results from this Chapter suggest that over-expression of Pax7 in a committed myoblast cell line results in increased self-renewal, thus supporting a role for Pax7 in the maintenance of the quiescent satellite cell pool primed for activation and contribution to skeletal muscle regeneration. It is further proposed that myostatin negatively regulates satellite cell expansion and self-renewal through preceding regulation of Pax7.

4.2 Materials and Methods

4.2.1 *Cell culture*

C2C12 myoblasts (American Type Culture Collection; ATCC, Manassas, VA) (Yaffe and Saxel 1977), C3H10T1/2 fibroblasts (ATCC) (Reznikoff *et al.* 1973) and primary myoblasts were utilised in this Chapter. C2C12 cells were cultured in Dulbecco's Modified Eagle Medium (DMEM; Invitrogen, Carlsbad, CA), while C3H10T1/2 cells were cultured in Eagle's Basal Medium (BME; Invitrogen). Foetal Bovine Serum (FBS, 10%, Invitrogen) was added to the medium for culturing cells under growth conditions. Following the method of Taylor and Jones (1979) (Taylor and Jones 1979), myogenic conversion of C3H10T1/2 cells was induced by the addition of 0.3 nM 5-Aza-2'-deoxycytidine in Proliferation Medium for 24 hr, C3H10T1/2 cultures were then maintained for 16 days in Proliferation Medium in the absence of 5-Aza-2'-deoxycytidine. For differentiation studies C2C12 cells were plated at a density of 25,000 cells/cm^2, following an overnight attachment period, the cells were induced to differentiate under low serum conditions in DMEM 2% Horse Serum (HS, Invitrogen) and grown for periods as experimentally required. The AgResearch Ruakura Animal Ethics Committee approved all animal manipulations described in this paper. Primary myoblasts were cultured from the hindlimb muscle of 4 to 6 week old mice, according to published protocols (Allen *et al.* 1997; Partridge 1997). Briefly, muscles were minced and then digested in 0.2% collagenase type 1A for 90 min. Cultures were enriched for myoblasts by pre-plating on uncoated plates for 3 hr. Myoblast cultures were maintained in DMEM supplemented with 20% FBS, 10% HS and 1% Chicken Embryo Extract (CEE) on 10% matrigel-coated plates, at 37°C/5% CO_2. This method is well established in our laboratory and yields cultures of high (95%) myogenic purity (McCroskery *et al.* 2003). The recombinant Myostatin protein (Mstn) used in these *in vitro* experiments was generated and purified in our laboratory (Sharma *et al.* 1999).

4.2.2 Stable transfection and generation of clonal cell lines

Pax7 over-expressing C3H10T1/2 and C2C12 cells were generated by stable transfection of a pcDNA3-Pax7 construct encoding full-length murine Pax7 driven by a CMV promoter and including neomycin and ampicillin resistance cassettes. The Pax7 cassette was kindly gifted by Dr Michael Rudnicki. Stable cell lines were generated by stable transfection with 12.5 μg of pcDNA3-Pax7 or pcDNA3 in 0.8 mL DMEM (no serum) mixed with 40 μL of Lipofectamine 2000 (Invitrogen) in 0.8 mL DMEM (no serum). After 20 min at room temperature the transfection mixture was added to the appropriate plates and incubated for 24 hr at 37˚C. Cells were then subjected to neomycin treatment at a concentration of 0.6 mg/mL and selected based on their ability to grow in the presence of neomycin. After 21 days, neomycin resistant cells were taken for further analysis or frozen in liquid nitrogen for later use. Clonal cell lines were generated by plating Pax7 transfected cells at a clonal density of 25 cells/cm^2, individual neomycin-resistant colonies were isolated and further expanded to allow for analysis of Pax7 expression. Two Pax7 over-expressing clonal cell lines were selected for further study.

4.2.3 Limited trypsinisation to obtain myotubes and reserve cells

The protocol of Kitzmann *et al* (1998) (Kitzmann *et al.* 1998) was used to separate myotube and reserve cell populations. C2C12 cells were plated at a density of 25,000 cells/cm^2, allowed to attach overnight, then induced to differentiate under low serum conditions in DMEM 2% HS for 96 hr. Following incubation, a short trypsinisation period (5 min, 0.15% trypsin) and two phosphate buffered saline (PBS) washes were used to preferentially detach myotubes. Reserve cells, which remained attached to the culture dish, were then removed with 10 min incubation in 0.25% trypsin.

4.2.4 Detection of MHC, Myf-5, Pax7 and MyoD by immunocytochemistry

Detection of Myosin Heavy Chain (MHC) in C3H10T1/2 cells was performed as previously described (see Section 2.2.16). MHC (MF-20, Developmental Studies

Hybridoma Bank; DSHB, University of Iowa, Iowa City, IA) was used at a final dilution of 1:100. Detection of Myf-5, Pax7 and MyoD is outlined below. Myoblast and myotube cultures grown on Permanox chamber slides (Nalge Nunc International, Rochester, NY) were fixed with 70% ethanol:formaldehyde:glacial acetic acid (20:2:1) for 30 s, then rinsed three times with PBS. Cells were permeabilised with 0.1% triton X-100 in PBS for 10 min at room temperature then washed with PBS. Cells were then blocked in 5% NGS in 0.35% Carrageenen λ (Sigma, St. Louis, MO) in PBS for 1 hr at room temperature; the same solution was used for subsequent antibody and fluorophore dilutions. Cells were incubated with primary antibodies overnight at 4˚C. Rabbit polyclonal anti-Myf-5 antibody (sc-302, Santa Cruz Biotechnology, Santa Cruz, CA), rabbit polyclonal anti-MyoD antibody (sc-304, Santa Cruz Biotechnology) and mouse monoclonal anti-Pax7 antibody (DSHB) were added at a dilution of 1:100. The next day, slides were washed 3 times for 5 min in TBST before secondary incubation with biotinylated donkey anti-rabbit IgG (RPN1004; GE Healthcare Bio-Sciences Corp. Piscataway, NJ) at 1:300 for 1 hr at room temperature. Following another 3 washes in TBST, fluorescent complexes Alexa Fluor anti-mouse 546 (A11030; Invitrogen) and Alexa Fluor 488 (S11223; Invitrogen) were added at dilutions of 1:300 and 1:400 respectively and incubated for 1 hr at room temperature. After a further 3 washes in TBST, slides were incubated with DAPI (1:1000 in PBS, Invitrogen) for 5 min at room temperature, rinsed with PBS, and mounted using fluorescent mounting medium (Dako, Glostrup, Denmark). Cells were visualised using an Olympus BX50 microscope (Olympus Optical Co, Germany) with a SPOT RT camera (Diagnostic Instruments Inc, Sterling Heights, MI) and the Windows Version 4.0.1 SPOT Basic software program (Diagnostic Instruments Inc).

4.2.5 *Cell staining*

To assess Pax7 clone myotube formation during differentiation, cultures were grown on Thermanox coverslips (Nalge Nunc) under low serum conditions (DMEM 2% HS), fixed with 20:2:1 and stained with Gill's haematoxylin followed by 1% eosin, photographed as above, and myotube number counted. To quantitate the number of myotubes present in C3H10T1/2 cultures, a six-well

culture plate (Nalge Nunc) of each cell type was grown and treated with 5-Aza-2'-deoxycytidine as above. Following treatment, cultures were stained with methylene blue. Briefly, cells were covered in 1% methylene blue in 0.01M borate buffer, pH8, and left at room temperature for 2 min. The methylene blue stain was then removed and plates washed twice for 2 min with 0.01M borate buffer (pH8) in order to remove all unbound dye. Cells were photographed as above and myotube number counted.

4.2.6 *Proliferation assay*

Myoblast proliferation was assessed as described previously (Thomas *et al.* 2000). Briefly, C2C12 cultures were seeded on 96 well plates (Nalge Nunc) at a density of 1,000 cells per well in Proliferation Medium. After an overnight attachment period, cells were supplemented with fresh Proliferation Medium (DMEM 10% FBS). Cultures were subsequently fixed at 24 hr intervals. Cells were fixed in 100 μL of 10% formal saline (0.17% saline, 10% formaldehyde). Following the incubation periods, proliferation was assessed using the methylene blue photometric end-point assay, as previously described (Oliver *et al.* 1989). Briefly, the fixative was removed, 100 μL of stain (1% methylene blue, 0.01 M Borate buffer, pH 8.5) was added to each well and the cells were incubated for 30 min at room temperature. The stain solution was removed and the cells washed four times with 200 μL Borate buffer, followed by the addition of 200 μL 0.1 N HCl:70% ethanol, (1:1). The absorbance of the cells was read on a microplate reader (model 3550; Bio-Rad), at 655 nm. In this assay absorbance at 655 nm is directly proportional to final cell number. Samples were run in replicates of eight with the results representing two independent experiments.

4.2.7 *Protein isolation and Western Blot analysis*

C2C12 and C3H10T1/2 cells were resuspended in 200 μL lysis buffer (50 mM Tris pH 7.6; 250 mM NaCl; 5 mM EDTA; 0.1% Nonidet P-40; Complete protease inhibitor [Roche Diagnostics Corporation, Indianapolis, IN]) and passed through a 26 gauge needle 10 times. The cell extracts were then centrifuged to pellet cell

debris. Bradford Reagent (Bio-Rad Laboratories, Hercules, CA) was used to estimate total protein content to ensure equal loadings. Total protein (15 μg) was separated by 4-12% SDS-PAGE (Invitrogen) electrophoresis and transferred to nitrocellulose membrane by electroblotting. The membranes were blocked in 5% milk in TBST overnight at 4ºC, followed by incubation with specific primary antibodies for 3 hr at room temperature. The following primary antibodies were used for immunoblotting; 1:500 dilution of purified mouse monoclonal anti-Pax7 antibody (DSHB, Iowa City, IA); 1:400 dilution of rabbit polyclonal anti-MyoD antibody (sc-304; Santa Cruz Biotechnology Inc, Santa Cruz, CA); 1:400 dilution of purified rabbit polyclonal anti-Myf-5 antibody (sc-302; Santa Cruz Biotechnology Inc.); 1:400 dilution of purified rabbit polyclonal anti-myogenin antibody (sc-576; Santa Cruz Biotechnology Inc.); 1:400 dilution of purified mouse monoclonal anti-p21 antibody (556430; BD Pharmingen, San Diego, CA); 1:10,000 dilution of purified mouse monoclonal α-Tubulin antibody (T-9026; Sigma); 1:10,000 dilution of purified mouse monoclonal anti-GAPDH antibody (RDI-TRK5G4-6C5, Research Diagnostics, Concord, MA). The membranes were washed (5 x 5 min) with TBST and further incubated with 1:2,000 dilution anti-rabbit IgG Horseradish Peroxidase (HRP) conjugate (P0448; Dako, Glostrup, Denmark) or 1:2,000 dilution anti-mouse IgG HRP conjugate (P0447; Dako) secondary antibodies for 1 hr at room temperature. The membranes were washed as above, and HRP activity was detected using Western Lightning Chemiluminescence Reagent Plus (NEL104; PerkinElmer Life And Analytical Sciences, Inc., Wellesley, MA) and exposure to autoradiography film. Blots were quantified by densitometry analysis using the GS-800 densitometer (Bio-Rad).

4.2.8 *Statistics*

For quantification, the number of cells in each category (i.e. $Pax7^{+}/MyoD^{-}$, $Pax7^{+}/MyoD^{+}$, or Myf-5 positives) were counted and expressed as a percentage of the total cell pool (DAPI stained cells), and the data from multiple wells were pooled to give a population mean (±SEM). For C3H10T1/2 myotube assessment, six wells per culture were counted, with the mean number of myotubes ±SEM calculated. For Pax7 over-expressing clone and control myotube assessment, average myotube number (±SEM) over 3 coverslips per timepoint was calculated.

Total myotubes were counted in 5 random images per coverslip. To determine the significance level of differences between two groups, comparisons were made using Student's-T test. Statistical analysis was performed in Excel. A P value of <0.05 was deemed significant for all experiments.

4.3 Results

4.3.1 *Pax7 over-expression enhances myogenic conversion of the mesenchymal multipotent C3H10T1/2 cell line*

Previously published data has highlighted a role for Pax7 in the specification of the myogenic lineage (Seale *et al.* 2004). In particular, Pax7 over-expression has been shown to convert $CD45^{+}$:$Sca1^{+}$ muscle-derived cells to the myogenic lineage as supported by the up-regulation of markers specific to the myogenic lineage, such as Myf-5 and MyoD, and by the formation of MHC positive myotubes (Seale *et al.* 2004). In contrast, Pax7 over-expression in the multipotent mesenchymal C3H10T1/2 fibroblast cell line fails to induce myogenic conversion (Seale *et al.* 2004). Furthermore, Pax7 over-expression has been shown to inhibit MyoD-mediated myogenic conversion of the C3H10T1/2 cell line (Olguin and Olwin 2004). To study this in further detail we analysed the ability of Pax7 to enhance myogenic conversion of C3H10T1/2 cells following treatment with 5-Aza-2'-deoxycytidine, a well-characterised compound which causes DNA demethylation. Pax7 expression was quantified by Western Blot analysis to ensure over-expression of Pax7 was achieved (Figure 4.1A). Following 5-Aza-2'-deoxycytidine treatment, we found that C3H10T1/2 cells stably over-expressing Pax7 adopted an enhanced myogenic program, whereby the expression of the myogenic marker MyoD was significantly increased (Figure 4.1B). As expected, treatment of C3H10T1/2 cells with 5-Aza-2'-deoxycytidine resulted in the formation of MHC positive myotubes (Figure 4.1C). Methylene blue stained myotubes were counted, and consistent with enhanced myogenesis, Pax7 over-expression increased myotube formation with an ~8-fold increase in myotube number following Pax7 over-expression as compared to control empty vector transfected cells (Figure 4.1D). These data further confirm a role for Pax7 in the specification of cells to a myogenic lineage and highlight the ability of Pax7 to control the expression of MyoD, a key regulatory factor during the induction of the myogenic program.

Figure 4.1 *Pax7 enhances C3H10T1/2 myogenic conversion*

A) Western Blot examining Pax7 expression between control C3H10T1/2 cells (Control C3H) and Pax7 over-expressing C3H10T1/2 cells (Pax7 C3H). Tubulin levels were measured to ensure equal loadings. B) Western Blot showing MyoD expression in control C3H10T1/2 cells (Control C3H) compared to Pax7 over-expressing C3H10T1/2 cells (Pax7 C3H) at day 0 (d0) and day 8 (d8) following treatment with 5-Aza-2'-deoxycytidine. GAPDH levels were measured to ensure equal loadings. C) Myosin Heavy Chain (MHC) immunostained myotubes formed in day 15 control C3H10T1/2 (Control C3H) and Pax7 over-expressing C3H10T1/2 (Pax7 C3H) cultures following treatment with 5-Aza-2'-deoxycytidine, cells were counterstained with Gill's haematoxylin. Scale bar represents 10 μm. D) Methylene blue staining of day 15 control C3H10T1/2 (Control C3H) and Pax7 over-expressing C3H10T1/2 (Pax7 C3H) cultures, following treatment with 5-Aza-2'-deoxycytidine. Scale bar represents 20 μm; arrows indicate methylene blue positive myotubes. The corresponding graph represents the number of myotubes for control C3H10T1/2 (Control C3H) and Pax7 over-expressing C3H10T1/2 (Pax7 C3H) cultures, determined by counting methylene blue stained myotubes. Six wells per culture were counted, with the mean number of myotubes ±SEM represented graphically as counts per well. Statistical differences determined by Student's-T test are indicated, $P<0.001$ (***) compared to Control C3H.

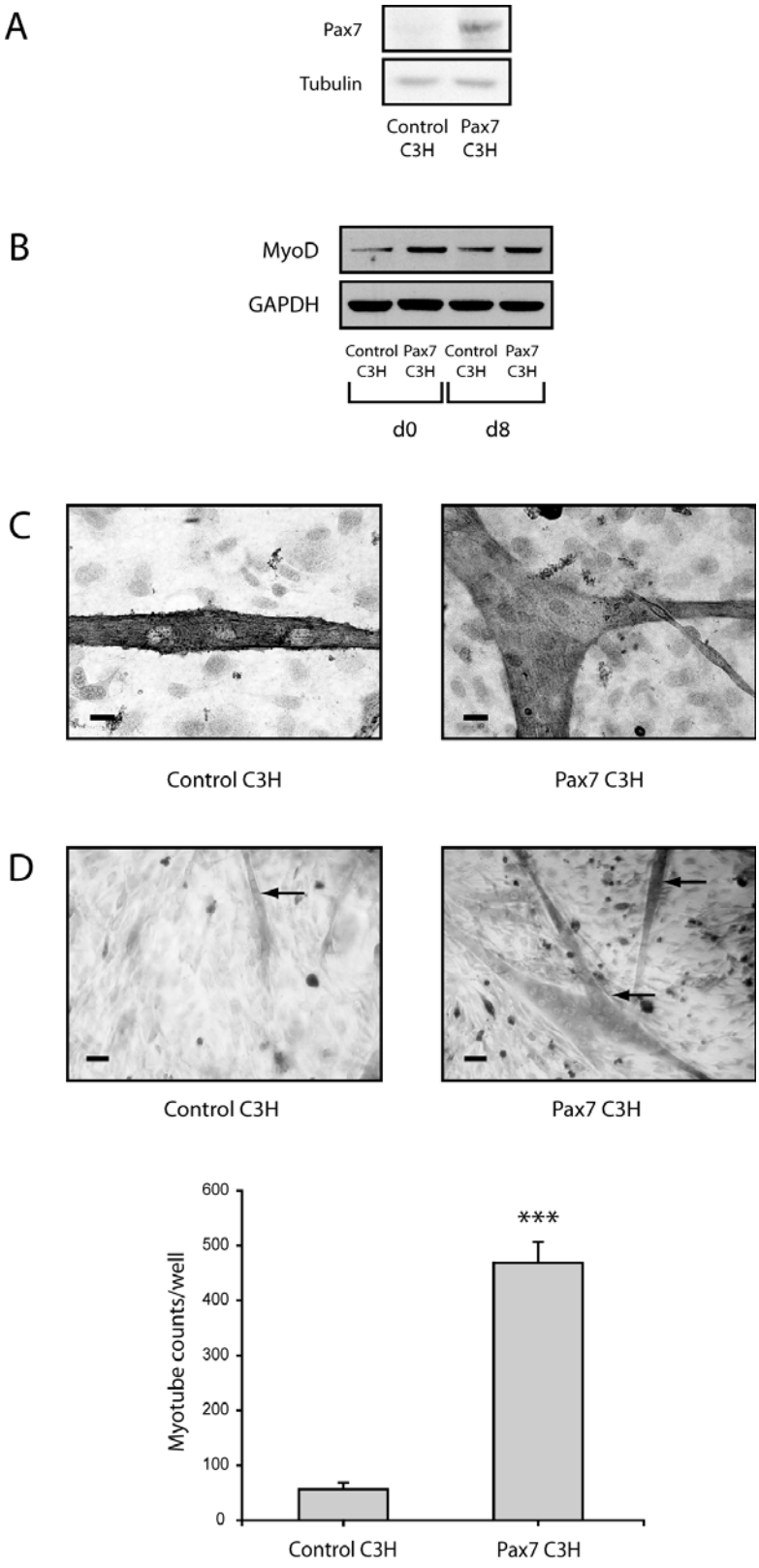
A
Pax7
Tubulin
Control C3H
Pax7 C3H
B
MyoD
GAPDH
Control C3H
Pax7 C3H
Control C3H
Pax7 C3H
d0
d8
C
Control C3H
Pax7 C3H
D
Control C3H
Pax7 C3H
Myotube counts/well
600
500
400
300
200
100
0
***
Control C3H
Pax7 C3H

4.3.2 Pax7 over-expression in C2C12 myoblasts impairs myogenesis

Previous published results have indicated that Pax7 over-expression in the C2C12 and MM14 adult myoblast cell lines is refractory to myogenesis (Olguin and Olwin 2004). In particular, Pax7 over-expression in MM14 myoblasts resulted in reduced MyoD levels, prevented myogenin expression, and promoted cell cycle exit to a quiescent, differentiation-resistant phenotype (Olguin and Olwin 2004). Furthermore, it has been stated that Pax7 over-expression in C2C12 cells inhibited the formation of MHC positive myotubes (Seale *et al.* 2004). To better understand the effect of Pax7 on adult myoblast growth we generated two stable clonal C2C12 cell lines over-expressing Pax7, termed Pax7 Clone 1 and Pax7 Clone 2. Initially we measured the expression of Pax7 by Western Blot to ensure over-expression of Pax7, and as shown in Figure 4.2A, both Pax7 clonal cell lines have greatly increased expression of Pax7. In addition, we compared the proliferation capacity of the Pax7 clonal cell lines to that of control cell lines. As shown in Figure 4.2B, both Pax7 clonal cell lines had a reduced rate of proliferation compared to that of control C2C12 cells, as determined by methylene blue assay. Pax7 over-expression has been documented to inhibit the differentiation of C2C12 myoblasts (Seale *et al.* 2004; Zammit *et al.* 2006), thus we analysed the ability of the Pax7 clonal cell lines to undergo myogenic differentiation. Up-regulation of Pax7 in C2C12 cells did not inhibit myogenic differentiation; rather an extreme delay in differentiation phenotype was observed, with a small number of myotubes present in the Pax7 over-expressing cell lines at 96 hr differentiation (Figure 4.2C). In fact, at 48 hr differentiation, control C2C12 cultures contained at least 7-fold more myotubes as compared to Pax7 clonal cell lines (Figure 4.2D). This variation in myotube number continued with the progression of differentiation, with comparable differences at 72 hr and 96 hr differentiation.

Next we analysed gene expression changes during differentiation in the Pax7 clones compared to control cells. MyoD levels were similar between control and Pax7 over-expressing clones at Time 0, however during the induction of differentiation MyoD levels appeared to be significantly reduced in both of the Pax7 clonal cell lines as compared to controls (Figure 4.3A, Figure 4.3B and Figure 4.3C). MyoD is an important myogenic regulatory factor which is capable

of promoting and maintaining cell cycle arrest through regulation of the cyclin-dependent kinase inhibitor p21 (Guo *et al.* 1995; Halevy *et al.* 1995). Thus p21 levels were measured, and as expected p21 expression appeared to closely follow the expression of MyoD and was considerably lower in the Pax7 clonal cell lines as compared to controls during the induction of differentiation (Figure 4.3A, Figure 4.3B and Figure 4.3C). Interestingly, the expression of p21 appeared to be higher in both of the Pax7 clones at Time 0 (Figure 4.3A, Figure 4.3B and Figure 4.3C). Myf-5, like MyoD, is an important myogenic regulatory factor involved with the specification of the myogenic lineage (Rudnicki *et al.* 1993; Tajbakhsh *et al.* 1996). Interestingly, elevated levels of Myf-5 were detected in the Pax7 clonal cell lines at Time 0 (Figure 4.3A, Figure 4.3B and Figure 4.3C), and although Myf-5 expression decreased during differentiation, levels were consistently higher than in control cell lines (Figure 4.3A and Figure 4.3B and Figure 4.3C). As stated above, both Pax7 clones differentiated considerably slower than controls. Consistent with this, myogenin expression was significantly delayed in the Pax7 clones (Figure 4.3A, Figure 4.3B and Figure 4.3C). However, myogenin expression gradually increased as differentiation proceeded, which coincides with the eventual formation of myotubes in the Pax7 clonal cells (Figure 4.3A, Figure 4.3B and Figure 4.3C). Thus Pax7 appears to play a critical role in controlling the ability of myogenic cell lines to undergo differentiation, and as shown, Pax7 has the ability to down-regulate several key myogenic regulatory factors including MyoD and myogenin, both critical to the successful adoption of a myotube phenotype. This gene regulation may form the underlying basis of Pax7 regulation of myogenic progression.

Figure 4.2 *Pax7 regulates proliferation and differentiation in C2C12 myoblasts*

A) Western Blots showing protein expression of Pax7 during actively growing conditions in Pax7 over-expressing (Pax7 Clone 1 and 2) lysates compared to control (C2C12) lysates. Tubulin expression was analysed to ensure equal loading of samples. B) Methylene blue assay showing proliferation of control (C2C12) cells compared to Pax7 over-expressing clones (Pax7 Clone 1 and 2) over a 72 hr period. Statistical differences determined by Student's-T test are indicated, $P<0.001$ (***) compared to C2C12 at each timepoint. C) Representative images of differentiating cells for Pax7 over-expressing clones (Pax7 Clone 1 and 2) compared to control (C2C12) cells at 48 hr, 72 hr and 96 hr differentiation; cells were stained with Gill's haematoxylin and eosin. Scale bar represents 5 μm. D) The graph shows the average myotube number ±SEM over 3 coverslips per timepoint for Pax7 over-expressing clones (Pax7 Clone 1 and 2) and control (C2C12) cells, total myotubes were counted in 5 random images per coverslip. Statistical differences determined by Student's-T test are indicated, $P<0.05$ (*) and $P<0.01$ (**) as compared to C2C12 at each timepoint.

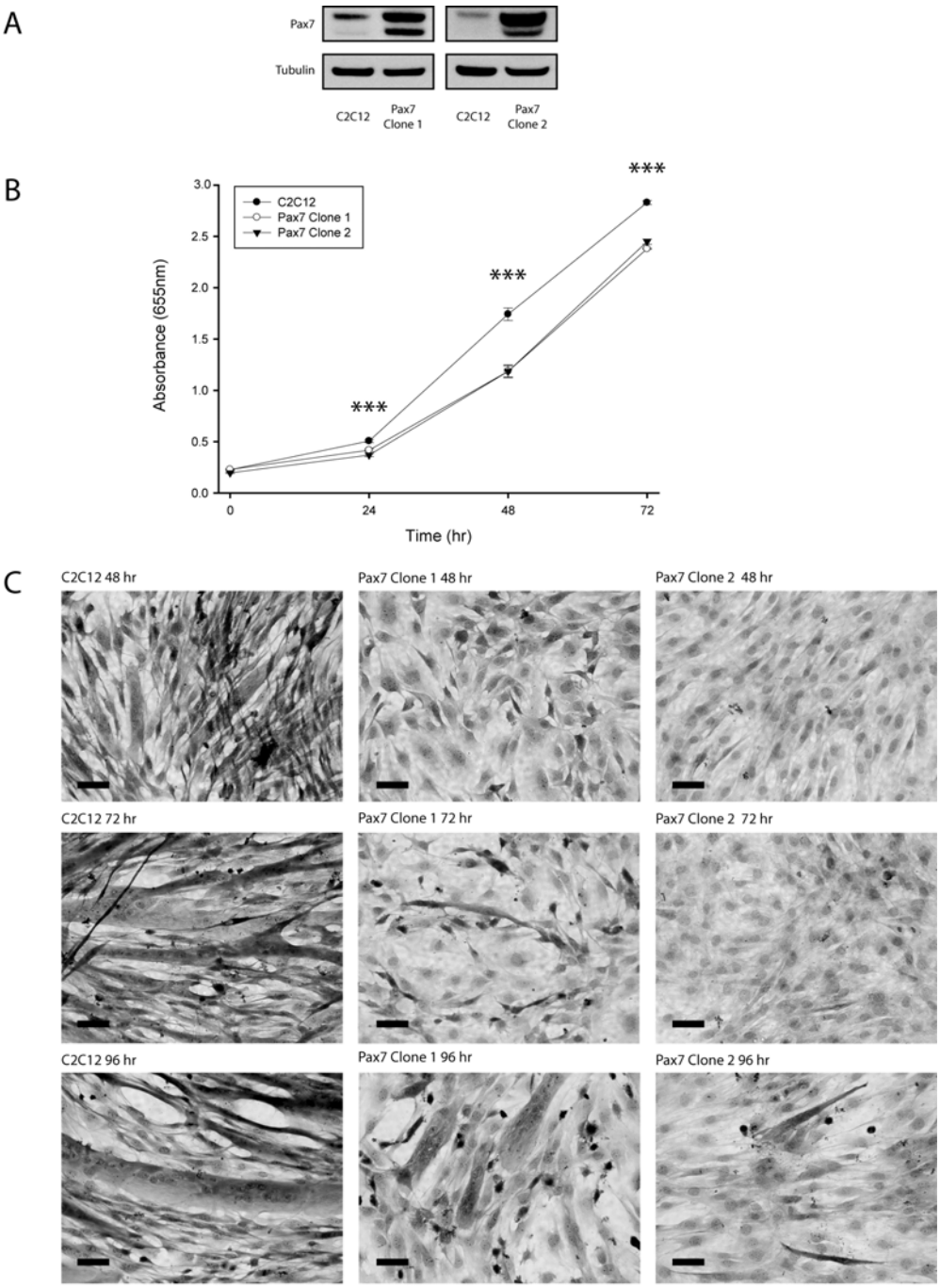
A
Pax7
Tubulin
C2C12
Pax7 Clone 1
C2C12
Pax7 Clone 2
B
C2C12
Pax7 Clone 1
Pax7 Clone 2
Absorbance (655nm)
Time (hr)
***
***
***
C
C2C12 48 hr
Pax7 Clone 1 48 hr
Pax7 Clone 2 48 hr
C2C12 72 hr
Pax7 Clone 1 72 hr
Pax7 Clone 2 72 hr
C2C12 96 hr
Pax7 Clone 1 96 hr
Pax7 Clone 2 96 hr
D
C2C12
Pax7 Clone 1
Pax7 Clone 2
Myotube Number
48 hr
72 hr
96 hr

4.3.3 Pax7 over-expression increases the population of reserve cells in C2C12 myotube cultures

During the induction of differentiation there is a rapid decrease in the expression of Pax7, however in differentiated myotube cultures a small subset of cells retain Pax7 expression (Olguin and Olwin 2004; Zammit *et al.* 2004). When differentiation is induced through serum-withdrawal, two distinct populations of cells arise, differentiated post-mitotic myotubes and quiescent differentiation-resistant reserve cells. Reserve cells share several similarities with skeletal muscle stem cells, for example reserve cells can re-enter the cell cycle, where they proliferate and then differentiate to form new myotubes (Kitzmann *et al.* 1998; Yoshida *et al.* 1998). Reserve cells, much akin to skeletal muscle stem cells, can also renew their population to maintain the reserve cell numbers *in vitro* (Yoshida *et al.* 1998). Furthermore the marker genes Myf-5 and CD34 which are expressed by skeletal muscle stem cells are also expressed at high levels in reserve cell populations (Kitzmann *et al.* 1998; Lindon *et al.* 1998; Beauchamp *et al.* 2000). To study in detail the changes in Pax7 expression during differentiation, C2C12 cultures were enriched for myotube and reserve cell populations by limited trypsinisation. Interestingly, during differentiation Pax7 expression appeared to coincide with Myf-5 expression and became restricted to the reserve cell pool, while MyoD expression was maintained in the myotube population (Figure 4.4A). As stated above, over-expression of Pax7 delayed the induction of differentiation (Figure 4.2C and 4.2D) and increased the expression of Myf-5 (Figure 4.3A, Figure 4.3B and Figure 4.3C), thus we quantified the reserve cell population in the Pax7 over-expressing clones.

Figure 4.3 *Pax7 over-expression alters the expression of several critical myogenic genes*.

A), B) Western Blots showing protein expression of MyoD, p21, Myf-5 and myogenin at Time 0 and after 24, 48, 72 and 96 hr of differentiation in Pax7 over-expressing (Pax7 Clone 1 [A] and Pax7 Clone 2 [B]) lysates compared to control (C2C12) lysates. Tubulin expression was analysed to ensure equal loading of samples. C) Densitometry analysis of protein expression for Western Blots (MyoD, p21, Myf-5, myogenin), normalised to Tubulin expression, for Pax7 over-expressing clones (Clone 1 and 2) compared to control (C2C12) cells.

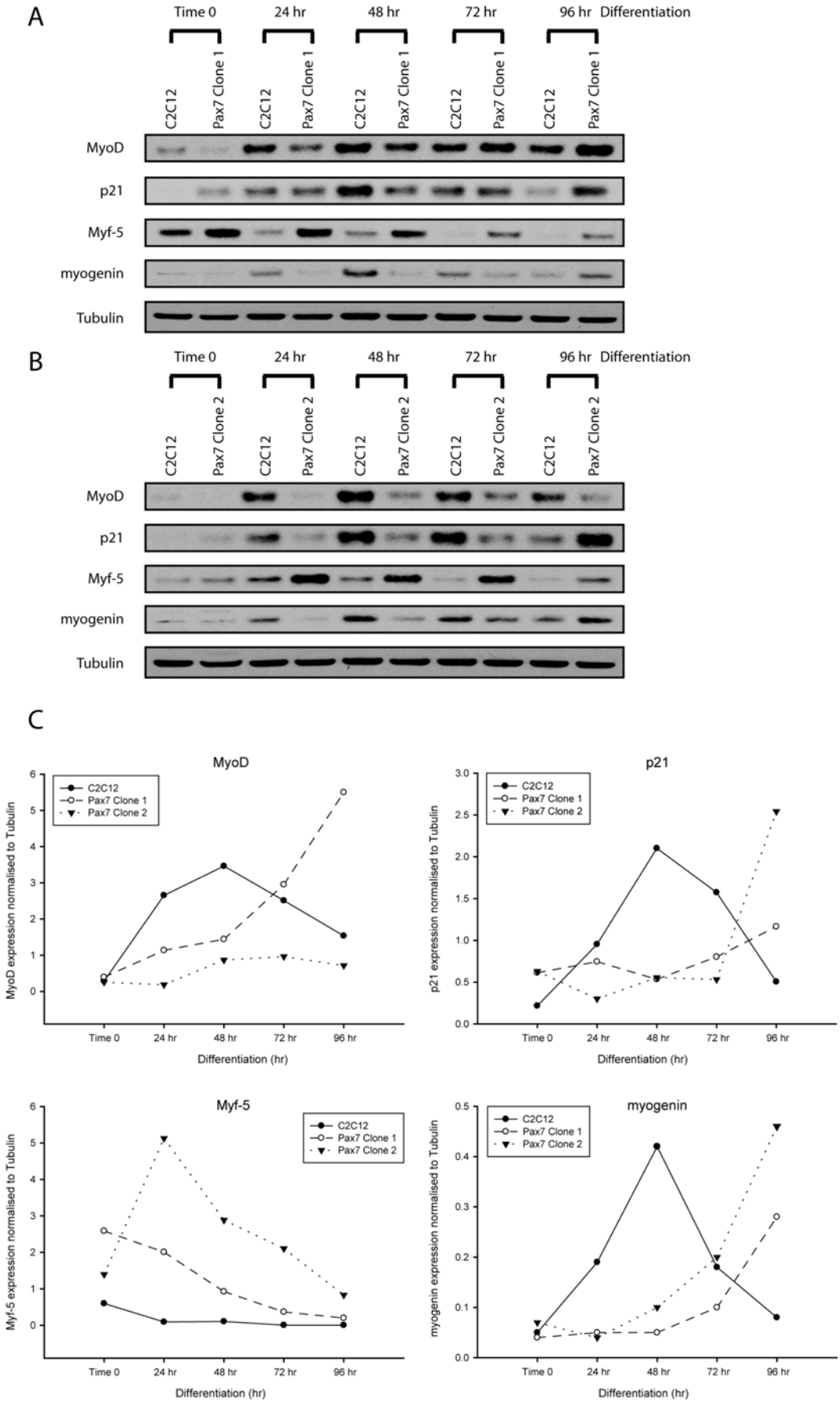
A
Time 0
24 hr
48 hr
72 hr
96 hr Differentiation
C2C12
Pax7 Clone 1
MyoD
p21
Myf-5
myogenin
Tubulin
B
Time 0
24 hr
48 hr
72 hr
96 hr Differentiation
C2C12
Pax7 Clone 2
MyoD
p21
Myf-5
myogenin
Tubulin
C
MyoD
MyoD expression normalised to Tubulin
C2C12
Pax7 Clone 1
Pax7 Clone 2
Time 0
24 hr
48 hr
72 hr
96 hr
Differentiation (hr)
p21
p21 expression normalised to Tubulin
Myf-5
Myf-5 expression normalised to Tubulin
myogenin
myogenin expression normalised to Tubulin

Pax7 clonal cells and control C2C12 cells were differentiated for 144 hr, fixed and analysed for Myf-5 expression by immunocytochemistry. Myf-5 was used to mark the reserve cell populations in both Pax7 clonal and control C2C12 cell lines. As shown in Figure 4.4B, of the total cell number there were 17.5% ± 1.4% Myf-5 positive reserve cells following over-expression of Pax7 as compared with 1.6% ± 0.5% Myf-5 positive reserve cells in the control cell line. Thus there was a ~10-fold increase in the number of reserve cells in C2C12 cells stably over-expressing Pax7 (Pax7 Clone 1) as compared with control C2C12 cells. Therefore, increasing the expression of Pax7 appears to delay differentiation, concomitant with an increase in the quiescent Myf-5 positive reserve cell population in the established C2C12 myogenic cell line. As stated above, reserve cell populations share several characteristics with quiescent satellite cells, and thus over-expression of Pax7 may recapitulate the process of self-renewal seen in skeletal muscle stem cells.

4.3.4 *Myostatin regulates Pax7 expression during myogenesis*

Myostatin is a potent negative regulator of skeletal myogenesis, in fact myostatin functions to block both myoblast proliferation and differentiation (Thomas *et al.* 2000; Langley *et al.* 2002). More recently myostatin has been implicated in the regulation of post-natal muscle growth through, in part, the regulation of satellite cell growth and self-renewal (McCroskery *et al.* 2003). Although myostatin has been shown to negatively regulate satellite cell self-renewal, the mechanism behind this process remains unclear. Pax7 has gained recent interest as an important mediator of satellite cell self-renewal, thus we analysed the ability of myostatin to regulate Pax7. As shown in Figure 4.5A, Myostatin treatment severely down-regulated the expression of Pax7 in actively growing primary myoblast cultures as determined by Western Blot analysis. Consistent with this, Western Blot analysis of Pax7 expression between wild-type and *myostatin*-null primary myoblast cultures revealed a consistently higher expression of Pax7 in the *myostatin*-null cultures (Figure 4.5B).

Figure 4.4 *Over-expression of Pax7 increases the resident reserve cell population*

A) Western Blots for Pax7, Myf-5 and MyoD in C2C12 myotubes (M.T.) compared to reserve cells (R.C.). Ponceau S staining is shown to demonstrate equal loading of protein samples. B) Myf-5 immunocytochemistry (green), with the corresponding DAPI staining (blue), for Pax7 over-expressing cells (Pax7 Clone) compared to Control (C2C12) cells after 144 hr differentiation. Scale bar represents 5 μm. The corresponding graph shows Myf-5 positive cells as a proportion of total cell number (shown by DAPI staining) for Pax7 over-expressing cells (Pax7 Clone) as compared to control (C2C12) cells. Statistical differences determined by Student's-T test are indicated, $P<0.01$ (**) compared to C2C12.

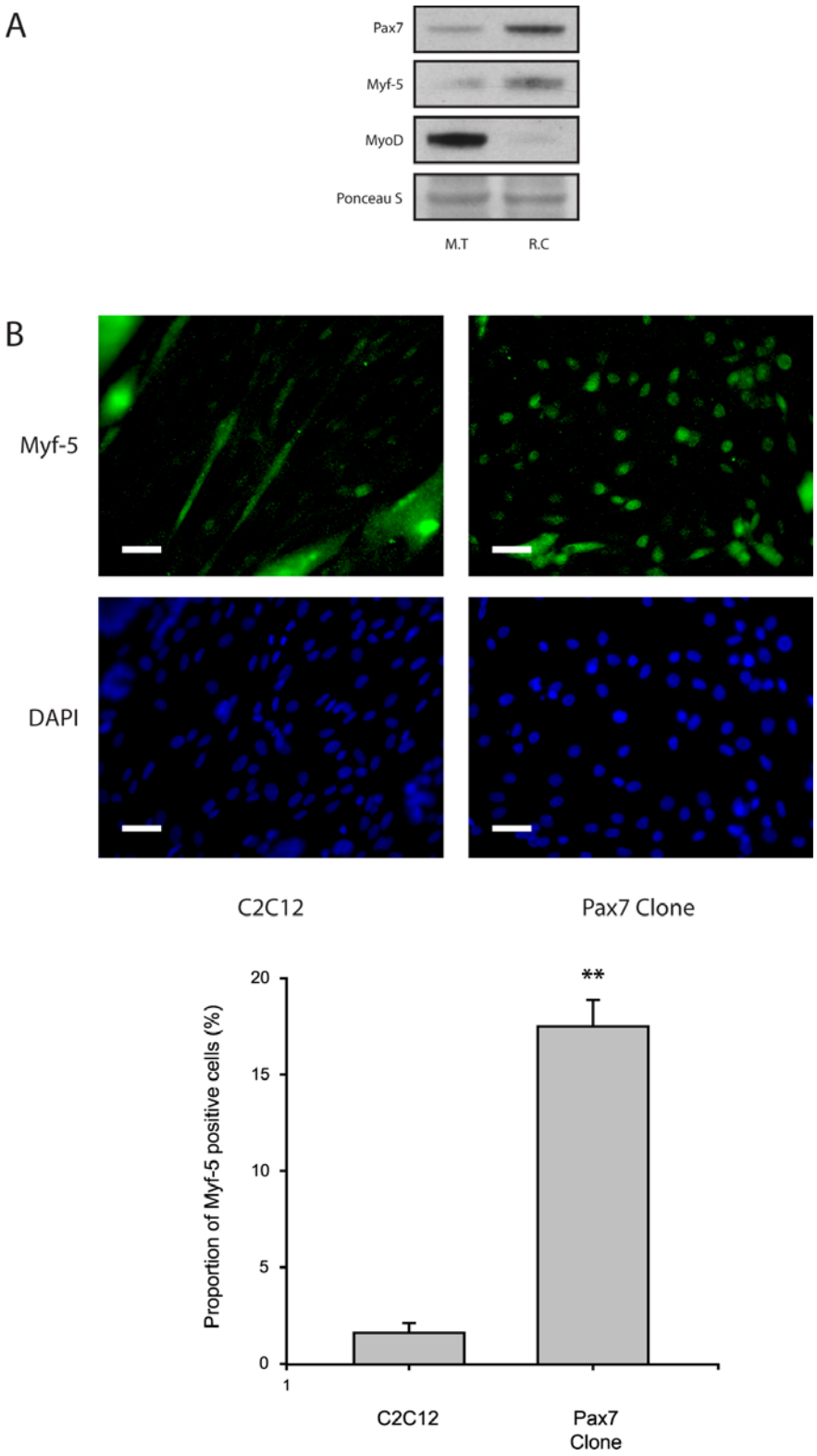
A
Pax7
Myf-5
MyoD
Ponceau S
M.T
R.C
B
Myf-5
DAPI
C2C12
Pax7 Clone
Proportion of Myf-5 positive cells (%)
20
15
10
5
0
1
**
C2C12
Pax7
Clone

Furthermore, analysis of Pax7 expression patterns during differentiation of both wild-type and *myostatin*-null primary cultures highlighted a dramatic difference in the expression profile of Pax7, whereby Pax7 levels are maintained considerably longer in the *myostatin*-null primary myoblasts when compared to wild-type controls (Figure 4.5B). We further analysed the populations of Pax7 and MyoD expressing cells between wild-type and *myostatin*-null cultures by immunofluorescence. Subsequently we observed an increase in the population of $Pax7^{+}/MyoD^{-}$ expressing cells in the *myostatin*-null cultures, specifically there was a significant increase from 2.3% ± 0.94% in wild-type cultures to 9.1% ± 1.3% in *myostatin*-null cultures, an overall increase of ~4-fold (Figure 4.5C). Furthermore, we observed a significant drop in $Pax7^{+}/MyoD^{+}$ populations from 63.9% ± 2.9% in wild-type cultures to 55.3% ± 1.6% in *myostatin*-null cultures (Figure 4.5C). Thus, absence of Myostatin appears to affect cell population heterogeneity, increasing the numbers of $Pax7^{+}/MyoD^{-}$ cells concomitant with a decrease in $Pax7^{+}/MyoD^{+}$ cells. As stated before, increased expression of Pax7 in C2C12 cells increased the resident population of Myf-5 positive reserve cells *in vitro*. Thus we analysed the inherent population of reserve cells in both *myostatin*-null and wild-type cultures. Interestingly, we found that differentiated cultures from *myostatin*-null mice contained a greater proportion of quiescent reserve cells, as determined by Myf-5 immunocytochemistry (Figure 4.5D). Indeed, we found Myf-5 positive reserve cell populations of 8% ± 0.28% in wild-type and 10% ± 0.18% in *myostatin*-null cultures, thus there was a ~20% increase in the number of reserve cells in differentiating *myostatin*-null cultures as compared with wild-type controls. As stated before, Pax7 expression is restricted to reserve cell populations during myoblast differentiation, thus the observed persistent expression of Pax7, the increased $Pax7^{+}/MyoD^{-}$ pool and the enhanced reserve cell populations in *myostatin*-null cultures during differentiation, may highlight a potential Pax7-dependent mechanism behind myostatin regulation of satellite cell self-renewal.

Figure 4.5 *Myostatin regulates Pax7 during myogenesis*

A) Western Blot for Pax7 in primary cell lysates after culture in the absence (-) or presence (+) of recombinant Myostatin protein (Mstn). Cells were treated with 10 μg/mL Mstn for a period of 6 hr. GAPDH expression was analysed to ensure equal loading of samples. B) Western Blot for Pax7 in primary cell cultures from wild-type and *myostatin*-null mice during both actively growing (Ag) and differentiation (Diff 24 hr and Diff 48 hr) conditions. Ponceau S staining is used to ensure equal loading of samples. C) Pax7 (red), MyoD (green) and double-stained (yellow) immunofluorescence in wild-type compared to *myostatin*-null mouse primary cultures. The corresponding images for DAPI (blue) are also shown. Scale bar represents 5 μm. The graph represents the proportions of $Pax7^{+}/MyoD^{-}$ and $Pax7^{+}/MyoD^{+}$ cells between wild-type and *myostatin*-null cultures. Statistical differences determined by Student's-T test are indicated, $P<0.01$ (**) and $P<0.05$ (*) compared to wild-type. D) Myf-5 immunocytochemistry in 72 hr differentiated wild-type and *myostatin*-null mouse myoblast cultures. The corresponding images for DAPI are also shown. Scale bar represents 5 μm. The proportion of Myf-5 positive reserve cells for wild-type and *myostatin*-null cultures is represented graphically. Statistical differences determined by Student's-T test are indicated, $P<0.01$ (**) compared to wild-type.

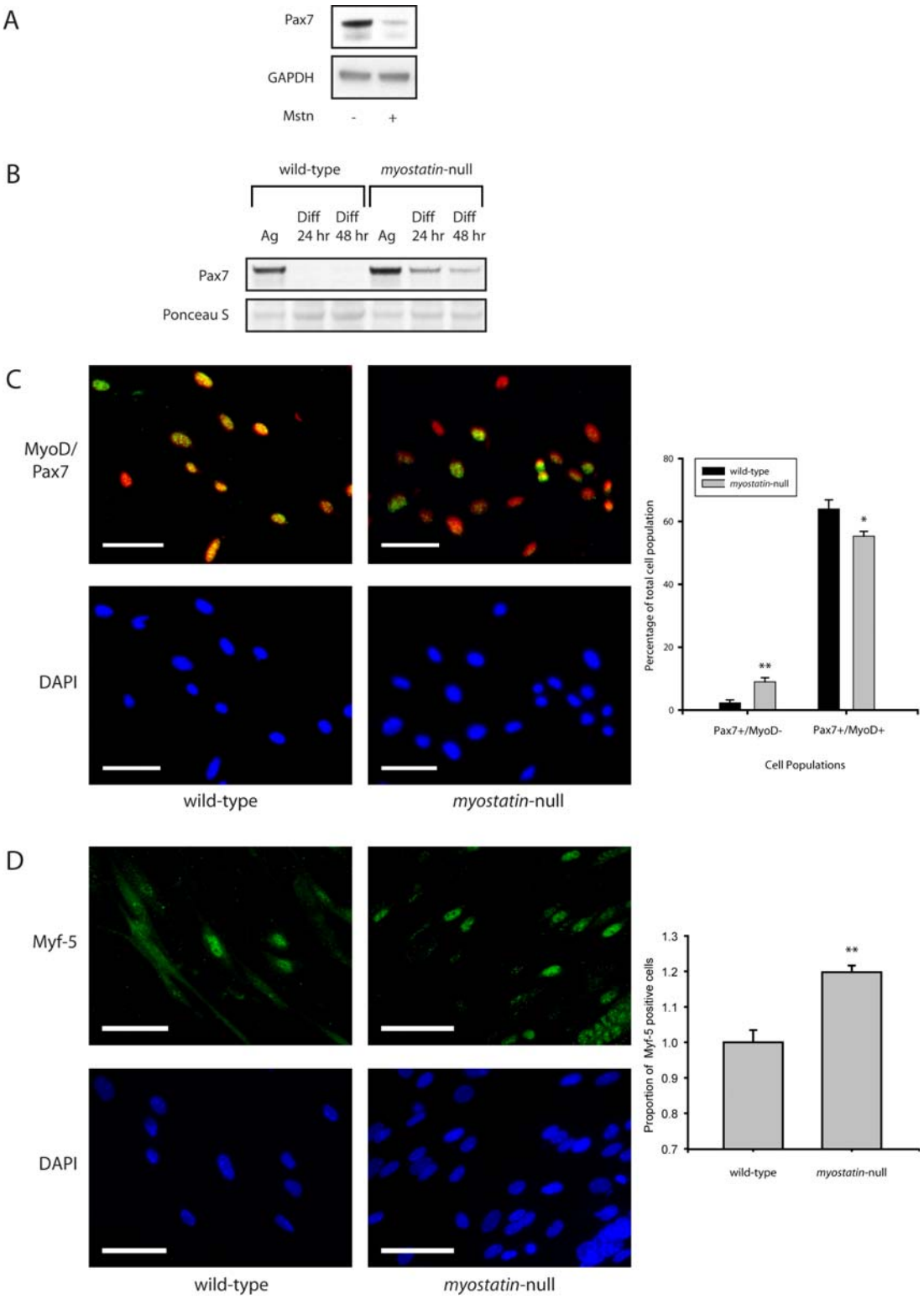
A
Pax7
GAPDH
Mstn - +
B
wild-type
myostatin-null
Ag
Diff 24 hr
Diff 48 hr
Ag
Diff 24 hr
Diff 48 hr
Pax7
Ponceau S
C
MyoD/ Pax7
DAPI
wild-type
myostatin-null
wild-type
myostatin-null
Percentage of total cell population
80
60
40
20
0
**
*
Pax7+/MyoD-
Pax7+/MyoD+
Cell Populations
D
Myf-5
DAPI
wild-type
myostatin-null
Proportion of Myf-5 positive cells
1.3
1.2
1.1
1.0
0.9
0.8
0.7
**
wild-type
myostatin-null

4.4 Discussion

The dynamic paired-box transcription factor Pax7 has been reported to play a role in many processes throughout skeletal muscle myogenesis. Pax7 has been implicated in myogenic commitment (Seale *et al.* 2004) and Pax7 expression appears to be detected, and moreover is transcriptionally active, in quiescent satellite cells (Seale *et al.* 2000; Zammit and Beauchamp 2001; Zammit *et al.* 2006). Furthermore, Pax7 persists during the progression from satellite cell quiescence to activation and is maintained during proliferation (Seale *et al.* 2000; Asakura *et al.* 2001), however, Pax7 expression appears to be progressively lost during myogenic differentiation (Olguin and Olwin 2004; Zammit *et al.* 2004). Pax7 is further thought to be involved with the maintenance of quiescence, satellite cell survival, and the induction of satellite cell self-renewal (Olguin and Olwin 2004; Oustanina *et al.* 2004; Kuang *et al.* 2006; Relaix *et al.* 2006). Although much work has been done to elucidate a role for Pax7 in the regulation of myogenesis, little is known about the underlying mechanism of Pax7 function, and indeed factors which regulate Pax7.

Pax7 has been implicated in the specification of myogenic identity; indeed Pax7 can direct the specification of $CD45^{+}/Sca1^{+}$ stem cells to the myogenic lineage (Seale *et al.* 2004). In contrast however, it has been recently shown that Pax7 over-expression blocks MyoD-dependent myogenic conversion of the C3H10T1/2 multipotent mesenchymal stem cell line (Olguin and Olwin 2004). Previously it has been demonstrated that treatment of the C3H10T1/2 cell line with 5-Aza-2'-deoxycytidine induces the formation of myogenic cells capable of undergoing differentiation into multinucleated myotubes (Konieczny and Emerson 1984; Liu *et al.* 1986), a function that has been attributed to the ability of 5-Aza-2'-deoxycytidine to inhibit DNA methylation (Konieczny and Emerson 1984). To further characterise the role of Pax7 in myogenic specification we have studied the effect of over-expressing Pax7 in the C3H10T1/2 cell line in the presence of 5-Aza-2'-deoxycytidine (Figure 4.1). In Pax7 stably over-expressing C3H10T1/2 cell lines, we observe an increase in the expression of MyoD (Figure 4.1B); this is in agreement with the pre-established idea that Pax7 lies upstream of MyoD. Indeed previously published data whereby over-expression of Pax7 in a C2C12

subclone lacking Pax7, has been reported to result in an increase in MyoD expressing cells (Zammit *et al.* 2006). Furthermore over-expression of a dominant-negative form of Pax7 has been shown to inhibit *myoD* expression in satellite cell cultures (Relaix *et al.* 2006). We also find that over-expression of Pax7 in the C3H10T1/2 cell line enhances the myogenic program, with an increase in the formation of multinucleated myotubes over and above that seen in C3H10T1/2 controls (Figure 4.1D). Thus we conclude that Pax7 over-expression in the non-myogenic C3H10T1/2 cell line results in an enhancement of 5-Aza-2'-deoxycytidine induced myogenic conversion concomitant with an increase in the levels of MyoD, thus Pax7 may regulate adoption of a myogenic program through preceding regulation of MyoD. It is noteworthy to mention that while Pax7 can induce myogenic commitment of $CD45^{+}$:$Sca1^{+}$ stem cells, Pax7 is unable to directly induce myogenic specification of C3H10T1/2 cells (Seale *et al.* 2004). This may indicate that $CD45^{+}$:$Sca1^{+}$ lineages have true stem cell features and as such are more amenable to lineage change as compared to the multipotent C3H10T1/2 cell line. In contrast to Pax7, it is well documented that MyoD is able to directly induce myogenic conversion of the C3H10T1/2 cell line (Edmondson and Olson 1989; Guo *et al.* 1995). One of the salient features of MyoD is its ability to interact with p300 and PCAF, members of the histone acetyl transferase family, which function as critical co-activators of MyoD, regulating key events of myogenesis including myogenic commitment and induction of differentiation (Puri *et al.* 1997a; Puri *et al.* 1997b; Sartorelli *et al.* 1997). Thus it is interesting to surmise that the ability of MyoD to spontaneously direct the C3H10T1/2 cell line to follow a myogenic lineage is in some manner due to the ability of MyoD to function in conjunction with enzymes critical for gene regulation at the chromatin level, a function perhaps beyond the inherent role of Pax7 during myogenesis.

In addition to Pax7 over-expression in a non-myogenic cell line, we analysed the effects of Pax7 exogenous expression on the adult committed myogenic C2C12 cell line. Initially we analysed the proliferative capacity of the Pax7 clonal cell lines as compared with control levels. As shown in Figure 4.2B, both Pax7 clones share a similarly reduced proliferation rate to that of control. However, albeit a statistically significant reduction, the proliferation observed in both Pax7 clones is not dramatically lower than that seen in the control. One point of interest is that we observe significantly increased expression of the cyclin-dependent kinase

inhibitor p21 in both Pax7 clones during proliferation (Time 0) (Figure 4.3A, Figure 4.3B and Figure 4.3C). p21 is a member of the Cip/Kip family of cyclin-dependent kinase inhibitors (CKIs) and as the name suggests CKIs block the action of cyclin-dependent kinases and their obligate partners, the cyclins (Harper *et al.* 1993; Xiong *et al.* 1993). Cyclin-dependent kinases regulate Retinoblastoma (Rb)-mediated cell cycle progression by phosphorylating Rb. Subsequent phosphorylation of Rb results in activation of the E2F transcription factor family which are essential for the induction of genes required for DNA synthesis (S phase) (Guo and Walsh 1997). Thus it is conceivable that the increased expression of p21 we observe in the Pax7 clones may result in a delay in cell cycle transition into the S phase which may in turn affect the cell proliferation rate.

MyoD is critical in the decision to terminally differentiate and in fact, MyoD can induce differentiation through, in part, the up-regulation of p21. However, as differentiation proceeds in the Pax7 clonal cell lines we observe that the up-regulation of both MyoD and p21 is dramatically delayed, as compared with the control cell line (Figure 4.3A, Figure 4.3B and Figure 4.3C). Consistent with these data, we also find a delay in the progression of myogenic differentiation as quantified through myotube counts (Figure 4.2D). It is important to mention that although MyoD expression increased during differentiation in Clone 2, the levels of MyoD did not exceed or equal that observed in the control cell line; this is consistent with the reduced differentiation we observed in Pax7 Clone 2 compared to that of Pax7 Clone 1 (Figure 4.2D). Myogenin, a marker of myoblast differentiation, was also dramatically reduced in the Pax7 over-expressing clones (Figure 4.3A, Figure 4.3B and Figure 4.3C). Thus we conclude that C2C12 myogenic cell lines over-expressing Pax7 are indeed amenable to differentiation, however it appears that the normal progression of differentiation seen in the C2C12 cell line is severely disrupted.

During the onset of differentiation we observe a rapid down-regulation of Pax7 expression, which is consistent with previously published accounts (Olguin and Olwin 2004; Zammit *et al.* 2004). However, we also observe a down-regulation of Pax7 protein expression in the over-expressing cells lines, despite constitutive expression of Pax7 (data not shown). This reduction of Pax7 in the over-expressing clones does indeed coincide with the eventual formation of myotubes

during differentiation (Figure 4.2C and 4.2D). Thus it is feasible that post-transcriptional or post-translational mechanisms may exist which regulate the levels of Pax7 during the progression of myogenic differentiation.

Two protein isoforms of Pax7 have previously been reported (Vorobyov and Horst 2004). It is thus noteworthy to mention that following over-expression of Pax7 in the C2C12 cell line we detect both the 54-kDa and 57-kDa isoforms of Pax7, whereas in C2C12 controls we only observe the 57-kDa band at measurable levels (Figure 4.2A). Interestingly, at early timepoints the predominant Pax7 isoform is the 57-kDa band, however as differentiation continues both isoforms were expressed at similar levels (data not shown). The significance of the two Pax7 isoforms is yet to be determined; however it is interesting to surmise that the two differing Pax7 isoforms may perform separate functions *in vivo*.

Previously it has been reported that during differentiation a subset of cells retain expression of Pax7, lack myogenin expression and remain in an undifferentiated state (Olguin and Olwin 2004). To study this in further detail we enriched cultures of differentiated C2C12 cells into reserve cell and myotube populations. Following Western Blot analysis we identify that Pax7 appears to become restricted to the reserve cell pool along with Myf-5 (Figure 4.4A), a previously identified marker of reserve cells (Kitzmann *et al.* 1998; Lindon *et al.* 1998; Beauchamp *et al.* 2000). In agreement with previously published data (Kitzmann *et al.* 1998; Friday and Pavlath 2001), MyoD expression is retained in the myotube population (Figure 4.4A). Interestingly, examination of Myf-5 expression during differentiation in the Pax7 over-expressing clones demonstrates that Myf-5 is maintained at a considerably higher level during differentiation in the Pax7 over-expressing clones versus control C2C12 cells (Figure 4.3A, Figure 4.3B and Figure 4.3C). Thus we examined the proportion of Myf-5 positive reserve cells following over-expression of Pax7, compared to that of the control C2C12 cell line (Figure 4.4B). In support of gene expression analysis we find that there is a considerable increase (10-fold) in the number of Myf-5 positive reserve cells as a consequence of increased Pax7 expression (Figure 4.4B). Thus these data demonstrate that up-regulation of Pax7 increases the expression of Myf-5 concomitant with an increase in the reserve cell population during differentiation. As previously stated reserve cells share many characteristics with quiescent skeletal muscle stem cells, including reversible quiescence, the ability to renew

their population and the expression of such markers as Myf-5 and CD34. Thus over-expression of Pax7 in the C2C12 cell line may enhance the generation of a cell pool reminiscent of self-renewed satellite cells primed for re-entry into the cell cycle and eventual contribution to the myogenic program.

The utility of myostatin as a growth factor responsible for the control of skeletal muscle mass is well-documented. In support, a multitude of evidence now exists highlighting the important role of myostatin in the negative regulation of myoblast proliferation (Thomas *et al.* 2000; Taylor *et al.* 2001; Joulia *et al.* 2003; McCroskery *et al.* 2003), differentiation (Langley *et al.* 2002; Rios *et al.* 2002; Joulia *et al.* 2003) and more recently, satellite cell activation and self-renewal (McCroskery *et al.* 2003). However, further work is required to carefully define the mechanism(s) behind myostatin regulation of satellite cell growth and post-natal myogenesis.

Given the dual role of Pax7 in enhancing myogenic specification and in the induction of self-renewal as outlined above, we sought to investigate the involvement of myostatin in the regulation of Pax7. In this Chapter we demonstrated that exogenous addition of Myostatin dramatically reduced Pax7 expression in primary cell cultures (Figure 4.5A). In support, we also found an increase in Pax7 expression in primary myoblasts isolated from *myostatin*-null mice as compared with wild-type cultures (Figure 4.5B). This may have importance with respect to satellite cell numbers *in vivo*. Indeed we have previously shown that there is an increase in satellite cell number per unit fibre length in *myostatin*-null mice as compared with wild-type controls and more recently, siRNA-mediated reduction of *myostatin* resulted in an observed increase in Pax7-positive satellite cells (Magee *et al.* 2006). In contrast, recent published data stated that myostatin does not alter the expression of Pax7 during embryonic HH-stage 21-23 in the chick, however, consistent with the known function of Myostatin, the proliferation of Pax7-positive muscle precursor cells was inhibited (Amthor *et al.* 2006). Thus separate mechanisms may exist which regulate Pax7 during embryonic and post-natal myogenesis with myostatin playing a role in the latter.

Increased satellite cell number is in some part due to enhanced satellite cell self-renewal. The critical role of Pax7 in the process of self-renewal is evident in

pax7-null mice, at birth *pax7*-null mice appear normal but fail to thrive, dying between 2-3 weeks of age (Mansouri *et al.* 1996; Seale *et al.* 2000). Although there are large numbers of satellite cells present at birth there appears to be a constant decline in satellite cell number concomitant with impaired muscle regeneration in these mice (Oustanina *et al.* 2004). Further evidence for the involvement of Pax7 in self-renewal is seen in heterogeneous satellite cell populations. Indeed, in mouse myofibre cultures, populations of cells retain high expression of Pax7 but have a down-regulated expression of MyoD (Zammit *et al.* 2004). Interestingly, these cells do not commit to differentiation and in fact proliferate slowly or not at all, thus adopting characteristics of quiescent satellite cells (Zammit *et al.* 2004). Similarly, reserve cell-like populations of $Pax7^{+}/MyoD^{-}$ cells have been identified in the chicken (Halevy *et al.* 2004). Together these data strongly support a role for Pax7 in satellite cell renewal.

In agreement with previously published data (Halevy *et al.* 2004; Olguin and Olwin 2004; Zammit *et al.* 2004), we found heterogeneity in the expression of Pax7 and MyoD in satellite cell cultures. Interestingly, on analysis of wild-type and *myostatin*-null cultures we found a significant increase in $Pax7^{+}/MyoD^{-}$ populations concomitant with a reduction in $Pax7^{+}/MyoD^{+}$ populations in the absence of *myostatin* (Figure 4.5C). Thus it is interesting to surmise that loss of *myostatin* may result in a switch in cell fate determination, thus increasing the $Pax7^{+}/MyoD^{-}$ quiescent reserve cell-like population. Further evidence was observed upon analysis of Myf-5 positive reserve cell populations between wild-type and *myostatin*-null cultures. We saw a significant 20% increase in the number of Myf-5 positive reserve cells, expressed as a percentage of total cell number, in differentiated primary cultures of *myostatin*-null mice compared to wild-type (Figure 4.5D). It is noteworthy to mention that although both the wild-type and *myostatin*-null cultures were plated at the same density for study, *myostatin*-null myoblast numbers quickly overtook those of wild-type cultures (data not shown), presumably due to an enhanced cell proliferation rate as we have previously described (McCroskery *et al.* 2003). Thus, if we then consider total Myf-5 positive reserve cell numbers irrespective of total cell number we found a marked 75% increase in the reserve cell population in differentiated *myostatin*-null cultures as compared to wild-type cultures (data not shown). This increase has importance if we consider *in vivo* situations, whereby enhanced self-

renewal would increase the available pool of quiescent satellite cells primed for activation and subsequent contribution to muscle regeneration, indeed consistent with the enhanced regenerative capacity observed in *myostatin*-null mice (McCroskery *et al.* 2005). Therefore, we have further delineated the mechanism behind myostatin regulation of satellite cell self-renewal. As shown in Figure 4.6, satellite cells become activated, proliferate and form myoblasts, which can either fuse to damaged myofibres or differentiate to form new myotubes. A proportion of these cells can exit the cell cycle, without commitment to differentiation, and self-renew via increased expression of Pax7, a process which is negatively regulated by myostatin. Thus we propose a mechanism whereby myostatin inhibits satellite cell expansion and self-renewal through preceding regulation of Pax7 (Figure 4.6).

In this Chapter we have highlighted a dual function for Pax7, whereby Pax7 enhances commitment of non-myogenic multipotent cells to the myogenic lineage, while retaining the ability to promote the adoption of a quiescent self-renewed phenotype in committed myogenic cell lines. Thus, in agreement with pre-established theories, we suggest that Pax7 promotes myogenic specification, in addition to maintaining muscle stem cell populations through increased self-renewal. In addition, we have further delineated the complex mechanism(s) behind myostatin regulation of satellite cell self-renewal, namely the ability of myostatin to control the replenishment of the skeletal muscle stem cell pool through negative regulation of Pax7.

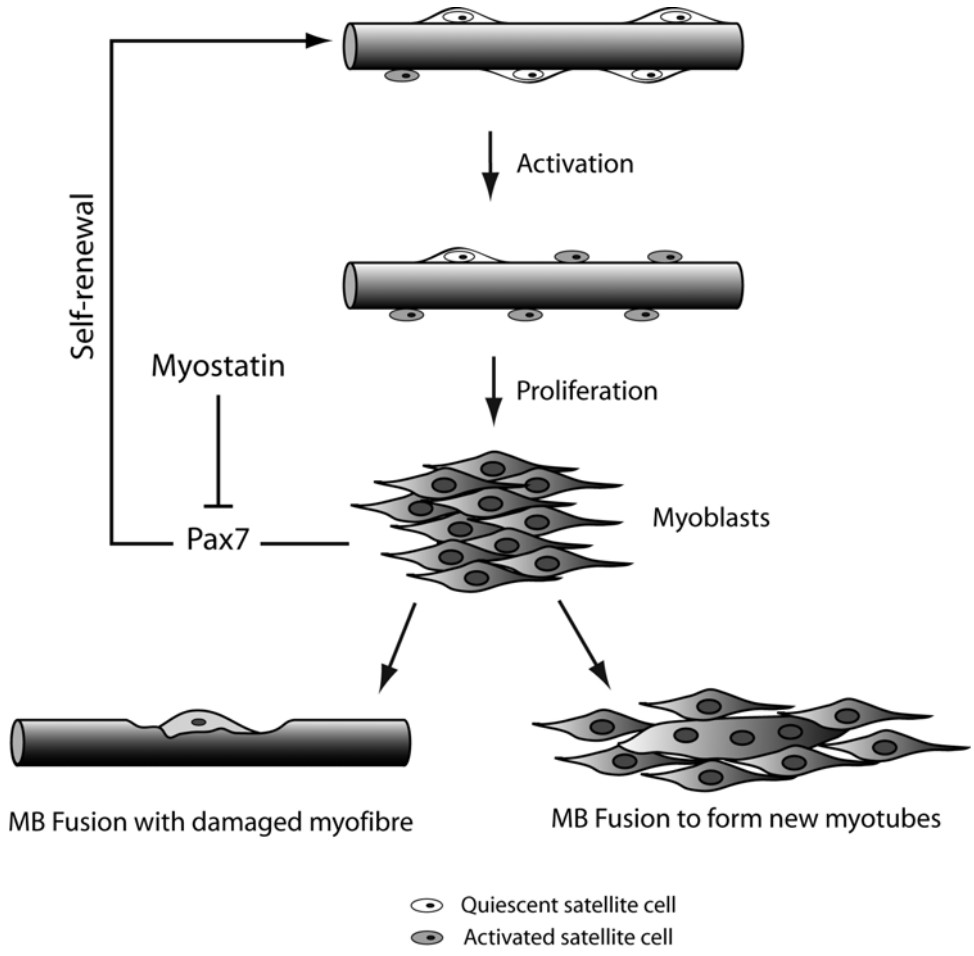

Figure 4.6 *Model of myostatin regulation of Pax7 during myogenesis*

Quiescent satellite cells on muscle fibres are activated in response to various stimuli giving rise to myoblasts (MB). Following subsequent proliferation, myoblasts can fuse with existing damaged myofibres, differentiate to form new myotubes or self-renew to replenish the satellite cell pool via continued expression of Pax7. Myostatin inhibits Pax7 expression during myoblast proliferation, implicating it in the negative regulation of satellite cell self-renewal.

4.5 Acknowledgements

Thanks to Victoria Siriett for help with standardising immunocytochemistry protocols. Further thanks to Dr Michael Rudnicki, for gifting the Pax7 cassette used in this Chapter. The Pax7 monoclonal antibody was obtained from the Developmental Studies Hybridoma Bank developed under the auspices of the NICHD and maintained by The University of Iowa, Department of Biological Sciences, Iowa City, IA 52242.

4.6 References

Allen, R. E., C. J. Temm-Grove, S. M. Sheehan and G. Rice (1997). "Skeletal muscle satellite cell cultures." Methods Cell Biol **52**: 155-76.

Amthor, H., A. Otto, R. Macharia, I. McKinnell and K. Patel (2006). "Myostatin imposes reversible quiescence on embryonic muscle precursors." Dev Dyn **235**(3): 672-80.

Asakura, A., M. Komaki and M. Rudnicki (2001). "Muscle satellite cells are multipotential stem cells that exhibit myogenic, osteogenic, and adipogenic differentiation." Differentiation **68**(4-5): 245-53.

Beauchamp, J. R., L. Heslop, D. S. Yu, S. Tajbakhsh, R. G. Kelly, A. Wernig, M. E. Buckingham, T. A. Partridge and P. S. Zammit (2000). "Expression of CD34 and Myf5 defines the majority of quiescent adult skeletal muscle satellite cells." J Cell Biol **151**(6): 1221-34.

Bischoff, R. (1989). "Analysis of muscle regeneration using single myofibers in culture." Med Sci Sports Exerc **21**(5 Suppl): S164-72.

Bischoff, R. and C. Heintz (1994). "Enhancement of skeletal muscle regeneration." Dev Dyn **201**(1): 41-54.

Dasarathy, S., M. Dodig, S. M. Muc, S. C. Kalhan and A. J. McCullough (2004). "Skeletal muscle atrophy is associated with an increased expression of myostatin and impaired satellite cell function in the portacaval anastamosis rat." Am J Physiol Gastrointest Liver Physiol.

Edmondson, D. G. and E. N. Olson (1989). "A gene with homology to the myc similarity region of MyoD1 is expressed during myogenesis and is sufficient to activate the muscle differentiation program." Genes Dev **3**(5): 628-40.

Friday, B. B. and G. K. Pavlath (2001). "A calcineurin- and NFAT-dependent pathway regulates Myf5 gene expression in skeletal muscle reserve cells." J Cell Sci **114**(Pt 2): 303-10.

Gonzalez-Cadavid, N. F., W. E. Taylor, K. Yarasheski, I. Sinha-Hikim, K. Ma, S. Ezzat, R. Shen, R. Lalani, S. Asa, M. Mamita, G. Nair, S. Arver and S. Bhasin (1998). "Organization of the human myostatin gene and expression

in healthy men and HIV-infected men with muscle wasting." Proc Natl Acad Sci U S A **95**(25): 14938-43.

Grounds, M. D. and Z. Yablonka-Reuveni (1993). "Molecular and cell biology of skeletal muscle regeneration." Mol Cell Biol Hum Dis Ser **3**: 210-56.

Guo, K. and K. Walsh (1997). "Inhibition of myogenesis by multiple cyclin-Cdk complexes. Coordinate regulation of myogenesis and cell cycle activity at the level of E2F." J Biol Chem **272**(2): 791-7.

Guo, K., J. Wang, V. Andres, R. C. Smith and K. Walsh (1995). "MyoD-induced expression of p21 inhibits cyclin-dependent kinase activity upon myocyte terminal differentiation." Mol Cell Biol **15**(7): 3823-9.

Halevy, O., B. G. Novitch, D. B. Spicer, S. X. Skapek, J. Rhee, G. J. Hannon, D. Beach and A. B. Lassar (1995). "Correlation of terminal cell cycle arrest of skeletal muscle with induction of p21 by MyoD." Science **267**(5200): 1018-21.

Halevy, O., Y. Piestun, M. Z. Allouh, B. W. Rosser, Y. Rinkevich, R. Reshef, I. Rozenboim, M. Wleklinski-Lee and Z. Yablonka-Reuveni (2004). "Pattern of Pax7 expression during myogenesis in the posthatch chicken establishes a model for satellite cell differentiation and renewal." Dev Dyn **231**(3): 489-502.

Harper, J. W., G. R. Adami, N. Wei, K. Keyomarsi and S. J. Elledge (1993). "The p21 Cdk-interacting protein Cip1 is a potent inhibitor of G1 cyclin-dependent kinases." Cell **75**(4): 805-16.

Heslop, L., J. R. Beauchamp, S. Tajbakhsh, M. E. Buckingham, T. A. Partridge and P. S. Zammit (2001). "Transplanted primary neonatal myoblasts can give rise to functional satellite cells as identified using the Myf5nlacZl+ mouse." Gene Ther **8**(10): 778-83.

Joulia, D., H. Bernardi, V. Garandel, F. Rabenoelina, B. Vernus and G. Cabello (2003). "Mechanisms involved in the inhibition of myoblast proliferation and differentiation by myostatin." Exp Cell Res **286**(2): 263-75.

Kambadur, R., M. Sharma, T. P. Smith and J. J. Bass (1997). "Mutations in myostatin (GDF8) in double-muscled Belgian Blue and Piedmontese cattle." Genome Res **7**(9): 910-6.

Kitzmann, M., G. Carnac, M. Vandromme, M. Primig, N. J. Lamb and A. Fernandez (1998). "The muscle regulatory factors MyoD and myf-5

undergo distinct cell cycle-specific expression in muscle cells." J Cell Biol **142**(6): 1447-59.

Konieczny, S. F. and C. P. Emerson, Jr. (1984). "5-Azacytidine induction of stable mesodermal stem cell lineages from 10T1/2 cells: evidence for regulatory genes controlling determination." Cell **38**(3): 791-800.

Kuang, S., S. B. Charge, P. Seale, M. Huh and M. A. Rudnicki (2006). "Distinct roles for Pax7 and Pax3 in adult regenerative myogenesis." J Cell Biol **172**(1): 103-13.

Langley, B., M. Thomas, A. Bishop, M. Sharma, S. Gilmour and R. Kambadur (2002). "Myostatin Inhibits Myoblast Differentiation by Down-regulating MyoD Expression." J Biol Chem **277**(51): 49831-40.

Lindon, C., D. Montarras and C. Pinset (1998). "Cell cycle-regulated expression of the muscle determination factor Myf5 in proliferating myoblasts." J Cell Biol **140**(1): 111-8.

Liu, L., M. Harrington and P. A. Jones (1986). "Characterization of myogenic cell lines derived by 5-azacytidine treatment." Dev Biol **117**(2): 331-6.

Magee, T. R., J. N. Artaza, M. G. Ferrini, D. Vernet, F. I. Zuniga, L. Cantini, S. Reisz-Porszasz, J. Rajfer and N. F. Gonzalez-Cadavid (2006). "Myostatin short interfering hairpin RNA gene transfer increases skeletal muscle mass." J Gene Med.

Mansouri, A., A. Stoykova, M. Torres and P. Gruss (1996). "Dysgenesis of cephalic neural crest derivatives in Pax7-/- mutant mice." Development **122**(3): 831-8.

McCroskery, S., M. Thomas, L. Maxwell, M. Sharma and R. Kambadur (2003). "Myostatin negatively regulates satellite cell activation and self-renewal." J Cell Biol **162**(6): 1135-47.

McCroskery, S., M. Thomas, L. Platt, A. Hennebry, T. Nishimura, L. McLeay, M. Sharma and R. Kambadur (2005). "Improved muscle healing through enhanced regeneration and reduced fibrosis in myostatin-null mice." J Cell Sci **118**(Pt 15): 3531-41.

McFarlane, C., E. Plummer, M. Thomas, A. Hennebry, M. Ashby, N. Ling, H. Smith, M. Sharma and R. Kambadur (2006). "Myostatin induces cachexia by activating the ubiquitin proteolytic system through an NF-kappaB-

independent, FoxO1-dependent mechanism." J Cell Physiol **209**(2): 501-514.

McPherron, A. C., A. M. Lawler and S. J. Lee (1997). "Regulation of skeletal muscle mass in mice by a new TGF-beta superfamily member." Nature **387**(6628): 83-90.

McPherron, A. C. and S. J. Lee (1997). "Double muscling in cattle due to mutations in the myostatin gene." Proc Natl Acad Sci U S A **94**(23): 12457-61.

Olguin, H. C. and B. B. Olwin (2004). "Pax-7 up-regulation inhibits myogenesis and cell cycle progression in satellite cells: a potential mechanism for self-renewal." Dev Biol **275**(2): 375-88.

Oliver, M. H., N. K. Harrison, J. E. Bishop, P. J. Cole and G. J. Laurent (1989). "A rapid and convenient assay for counting cells cultured in microwell plates: application for assessment of growth factors." J Cell Sci **92**(Pt 3): 513-8.

Oustanina, S., G. Hause and T. Braun (2004). "Pax7 directs postnatal renewal and propagation of myogenic satellite cells but not their specification." Embo J **23**(16): 3430-9.

Partridge, T. A. (1997). "Tissue culture of skeletal muscle." Methods Mol Biol **75**: 131-44.

Puri, P. L., M. L. Avantaggiati, C. Balsano, N. Sang, A. Graessmann, A. Giordano and M. Levrero (1997a). "p300 is required for MyoD-dependent cell cycle arrest and muscle-specific gene transcription." Embo J **16**(2): 369-83.

Puri, P. L., V. Sartorelli, X. J. Yang, Y. Hamamori, V. V. Ogryzko, B. H. Howard, L. Kedes, J. Y. Wang, A. Graessmann, Y. Nakatani and M. Levrero (1997b). "Differential roles of p300 and PCAF acetyltransferases in muscle differentiation." Mol Cell **1**(1): 35-45.

Relaix, F., D. Montarras, S. Zaffran, B. Gayraud-Morel, D. Rocancourt, S. Tajbakhsh, A. Mansouri, A. Cumano and M. Buckingham (2006). "Pax3 and Pax7 have distinct and overlapping functions in adult muscle progenitor cells." J Cell Biol **172**(1): 91-102.

Reznikoff, C. A., D. W. Brankow and C. Heidelberger (1973). "Establishment and characterization of a cloned line of C3H mouse embryo cells sensitive to postconfluence inhibition of division." Cancer Res **33**(12): 3231-8.

Rios, R., I. Carneiro, V. M. Arce and J. Devesa (2002). "Myostatin is an inhibitor of myogenic differentiation." Am J Physiol Cell Physiol **282**(5): C993-9.

Rudnicki, M. A., P. N. Schnegelsberg, R. H. Stead, T. Braun, H. H. Arnold and R. Jaenisch (1993). "MyoD or Myf-5 is required for the formation of skeletal muscle." Cell **75**(7): 1351-9.

Sartorelli, V., J. Huang, Y. Hamamori and L. Kedes (1997). "Molecular mechanisms of myogenic coactivation by p300: direct interaction with the activation domain of MyoD and with the MADS box of MEF2C." Mol Cell Biol **17**(2): 1010-26.

Schmalbruch, H. and D. M. Lewis (2000). "Dynamics of nuclei of muscle fibers and connective tissue cells in normal and denervated rat muscles." Muscle Nerve **23**(4): 617-26.

Schuelke, M., K. R. Wagner, L. E. Stolz, C. Hubner, T. Riebel, W. Komen, T. Braun, J. F. Tobin and S. J. Lee (2004). "Myostatin mutation associated with gross muscle hypertrophy in a child." N Engl J Med **350**(26): 2682-8.

Seale, P., J. Ishibashi, A. Scime and M. A. Rudnicki (2004). "Pax7 is necessary and sufficient for the myogenic specification of CD45+:Sca1+ stem cells from injured muscle." PLoS Biol **2**(5): E130.

Seale, P., L. A. Sabourin, A. Girgis-Gabardo, A. Mansouri, P. Gruss and M. A. Rudnicki (2000). "Pax7 is required for the specification of myogenic satellite cells." Cell **102**(6): 777-86.

Sharma, M., R. Kambadur, K. G. Matthews, W. G. Somers, G. P. Devlin, J. V. Conaglen, P. J. Fowke and J. J. Bass (1999). "Myostatin, a transforming growth factor-beta superfamily member, is expressed in heart muscle and is upregulated in cardiomyocytes after infarct." J Cell Physiol **180**(1): 1-9.

Tajbakhsh, S., D. Rocancourt and M. Buckingham (1996). "Muscle progenitor cells failing to respond to positional cues adopt non-myogenic fates in myf-5 null mice." Nature **384**(6606): 266-70.

Taylor, S. M. and P. A. Jones (1979). "Multiple new phenotypes induced in 10T1/2 and 3T3 cells treated with 5-azacytidine." Cell **17**(4): 771-9.

Taylor, W. E., S. Bhasin, J. Artaza, F. Byhower, M. Azam, D. H. Willard, Jr., F. C. Kull, Jr. and N. Gonzalez-Cadavid (2001). "Myostatin inhibits cell proliferation and protein synthesis in C2C12 muscle cells." Am J Physiol Endocrinol Metab **280**(2): E221-8.

Thomas, M., B. Langley, C. Berry, M. Sharma, S. Kirk, J. Bass and R. Kambadur (2000). "Myostatin, a negative regulator of muscle growth, functions by inhibiting myoblast proliferation." J Biol Chem **275**(51): 40235-43.

Vorobyov, E. and J. Horst (2004). "Expression of two protein isoforms of PAX7 is controlled by competing cleavage-polyadenylation and splicing." Gene **342**(1): 107-12.

Xiong, Y., G. J. Hannon, H. Zhang, D. Casso, R. Kobayashi and D. Beach (1993). "p21 is a universal inhibitor of cyclin kinases." Nature **366**(6456): 701-4.

Yablonka-Reuveni, Z. and A. J. Rivera (1994). "Temporal expression of regulatory and structural muscle proteins during myogenesis of satellite cells on isolated adult rat fibers." Dev Biol **164**(2): 588-603.

Yaffe, D. and O. Saxel (1977). "Serial passaging and differentiation of myogenic cells isolated from dystrophic mouse muscle." Nature **270**(5639): 725-7.

Yoshida, M. (2004). "Amyotrophic lateral sclerosis with dementia: the clinicopathological spectrum." Neuropathology **24**(1): 87-102.

Yoshida, N., S. Yoshida, K. Koishi, K. Masuda and Y. Nabeshima (1998). "Cell heterogeneity upon myogenic differentiation: down-regulation of MyoD and Myf-5 generates 'reserve cells'." J Cell Sci **111**(Pt 6)): 769-79.

Zammit, P. and J. Beauchamp (2001). "The skeletal muscle satellite cell: stem cell or son of stem cell?" Differentiation **68**(4-5): 193-204.

Zammit, P. S., J. P. Golding, Y. Nagata, V. Hudon, T. A. Partridge and J. R. Beauchamp (2004). "Muscle satellite cells adopt divergent fates: a mechanism for self-renewal?" J Cell Biol **166**(3): 347-57.

Zammit, P. S., F. Relaix, Y. Nagata, A. P. Ruiz, C. A. Collins, T. A. Partridge and J. R. Beauchamp (2006). "Pax7 and myogenic progression in skeletal muscle satellite cells." J Cell Sci **119**(Pt 9): 1824-32.

Zimmers, T. A., M. V. Davies, L. G. Koniaris, P. Haynes, A. F. Esquela, K. N. Tomkinson, A. C. McPherron, N. M. Wolfman and S. J. Lee (2002). "Induction of cachexia in mice by systemically administered myostatin." Science **296**(5572): 1486-8.

Chapter 5 Mechanism of myostatin-mediated cachexia

The results of this Chapter are published in the Journal of Cellular Physiology vol. 209 pages 501-514 (2006). See CD attached to the back cover of this thesis (Appendix 1) for a PDF copy of this paper.

JOURNAL OF CELLULAR PHYSIOLOGY 209:501–514 (2006)

Myostatin Induces Cachexia by Activating the Ubiquitin Proteolytic System Through an NF-κB-Independent, FoxO1-Dependent Mechanism

CRAIG MCFARLANE,[1,2] ERIN PLUMMER,[1,3] MARK THOMAS,[1] ALEX HENNEBRY,[1] MURRAY ASHBY,[1] NICHOLAS LING,[2] HEATHER SMITH,[3] MRIDULA SHARMA,[1] AND RAVI KAMBADUR[1]*

[1]AgResearch, Functional Muscle Genomics, East Street, Hamilton, New Zealand

[2]Department of Biological Sciences, University of Waikato, Hamilton, New Zealand

[3]Department of Sport and Exercise Science, University of Auckland, Auckland, New Zealand

Abstract

Myostatin, a Transforming Growth Factor-beta (TGF-β) superfamily member, has been well characterised as a negative regulator of muscle growth and development. Myostatin has been implicated in several forms of muscle wasting including the severe cachexia observed as a result of conditions such as AIDS and liver cirrhosis. Here it is shown that myostatin induces cachexia by a mechanism independent of NF-κB. Myostatin treatment resulted in a reduction in both myotube number and size *in vitro*, as well as a loss in body mass *in vivo*. Furthermore, the expression of the myogenic genes *myoD* and *pax3* was reduced, while NF-κB (the p65 subunit) localisation and expression remained unchanged. In addition, promoter analysis has confirmed Myostatin inhibition of *myoD* and *pax3*. An increase in the expression of genes involved in ubiquitin-mediated proteolysis is observed during many forms of muscle wasting. Hence the effect of Myostatin treatment on proteolytic gene expression was analysed. The ubiquitin-associated genes atrogin-1, MuRF-1 and $E2_{14k}$ were up-regulated following

Myostatin treatment. The signalling mechanism behind myostatin-induced cachexia was subsequently studied. Myostatin signalling reversed the IGF-1/PI3-K/AKT hypertrophy pathway by inhibiting AKT phosphorylation thereby increasing the levels of active FoxO1, allowing for increased expression of atrophy-related genes. Therefore these data suggest that myostatin induces cachexia through an NF-κB-independent mechanism. Furthermore, increased Myostatin levels appear to antagonise hypertrophy signalling through regulation of the AKT-FoxO1 pathway.

5.1 Introduction

Skeletal muscle cachexia is an all too common disease with up to 50% of all cancer patients experiencing some degree of muscle loss (Tisdale 2003), thus cachexia is a condition which almost certainly contributes to the high morbidity and mortality rates associated with this disease (Nelson 2000; Tisdale 2002).

Proinflammatory cytokines appear to play a critical role during the initiation of cachectic conditions (Moldawer and Copeland 1997). The expression of several cytokines including Interleukin-1 (IL-1), Interleukin-6 (IL-6) and Tumor Necrosis Factor-alpha (TNF-α) have been previously shown to increase during cachexia (Stovroff *et al.* 1989; Moldawer and Copeland 1997) and indeed, TNF-α appears to play an important role in tumour-induced muscle wasting (Torelli *et al.* 1999; Karayiannakis *et al.* 2001). A well studied pathway activated by TNF-α involves the downstream target transcription factor Nuclear Factor-kappa B (NF-κB). TNF-α is a potent regulator of NF-κB and in fact TNF-α induction of NF-κB has been linked to increased proteolysis and reduced expression of Myosin Heavy Chain (Li *et al.* 1998; Guttridge *et al.* 2000; Li and Reid 2000). MyoD, a myogenic basic Helix-Loop-Helix (bHLH) transcription factor, is critically involved in regulating skeletal muscle differentiation and is essential for the repair of damaged skeletal muscle (Megeney *et al.* 1996; Cornelison *et al.* 2000; Guttridge *et al.* 2000; Montarras *et al.* 2000). MyoD expression has been shown to decline dramatically during tumour-associated muscle wasting (Costelli *et al.* 2005). Interestingly, TNF-α signalling through NF-κB results in the inhibition of C2C12

myoblast differentiation through down-regulation of MyoD expression (Guttridge *et al.* 2000). Furthermore, TNF-α in conjunction with the cytokine Interferon-gamma (IFN-γ), functions through NF-κB to inhibit MyoD expression in fully differentiated myotube cultures, thus facilitating myotube degeneration (Guttridge *et al.* 2000).

One of the principal catabolic systems behind the induction of skeletal muscle atrophy in many forms of disease is the ubiquitin-proteasome pathway. Two important muscle-specific ubiquitin E3 ligases, MuRF-1 and Atrogin-1 (MAFbx) (Bodine *et al.* 2001; Gomes *et al.* 2001), have recently been associated with a variety of atrophic conditions. In particular, an up-regulation in the expression of *MuRF-1* and *atrogin-1* was observed in five independent models of skeletal muscle atrophy including immobilisation, denervation, hindlimb suspension, administration of IL-1 and administration of the glucocorticoid dexamethasone (Bodine *et al.* 2001). Furthermore, mice deficient in either *atrogin-1* or *MuRF-1* were found to be resistant to atrophy in a denervation and disuse model (Bodine *et al.* 2001).

The activity of the IGF-1/PI3-K/AKT pathway decreases during muscle atrophy (Sandri *et al.* 2004). Reduced activity of the IGF-1/PI3-K/AKT signalling pathway appears to result in the accumulation of hypo-phosphorylated active forms of the Forkhead box O (FoxO) class of transcription factors (Sandri *et al.* 2004). The FoxO transcription factors have gained recent attention in the field of muscle wasting. Indeed FoxO1 (FKHR) expression is greatly induced during atrophic conditions including fasting, cancer, diabetes mellitus and renal failure (Lecker *et al.* 2004). Furthermore, FoxO transcription factors have recently been shown to induce skeletal muscle wasting through the regulation of atrophy-related genes ("atrogenes") including Atrogin-1 (Sandri *et al.* 2004).

Myostatin, a TGF-β superfamily member, is a secreted growth factor that is well recognised as a negative regulator of muscle growth. Myostatin expression is detected during embryonic, foetal and post-natal stages of development, suggesting that it may play a vital role throughout myogenesis (Kambadur *et al.* 1997; McPherron *et al.* 1997). Myostatin expression is first detected in myogenic precursor cells of the myotome compartment in developing somites (McPherron *et al.* 1997). During prenatal development myostatin appears to function by

negatively regulating myoblast proliferation via control of the G_1 to S transition of the cell cycle through both Retinoblastoma-dependent and -independent mechanisms (Thomas *et al.* 2000; Langley *et al.* 2004). In addition, myostatin blocks myoblast differentiation through the regulation of MyoD activity (Langley *et al.* 2002). Post-natally, myostatin expression has pronounced effects on muscle growth; indeed the expression of a non-functional allele of *myostatin* in cattle (Kambadur *et al.* 1997) and humans (Schuelke *et al.* 2004), or targeted disruption of *myostatin* in mice (McPherron *et al.* 1997), result in severe hyperplasia and extreme muscle growth. In addition, molecular analysis suggests that a lack of *myostatin* results in increased muscle regeneration through enhanced satellite cell activation and self renewal, thereby promoting post-natal muscle growth and repair (McCroskery *et al.* 2003; McCroskery *et al.* 2005). Alternatively, increased myostatin expression has been implicated in atrophic conditions seen during AIDS (Gonzalez-Cadavid *et al.* 1998), sarcopenia (Schulte and Yarasheski 2001; Yarasheski *et al.* 2002) and muscle disuse such as chronic human disuse atrophy (Zachwieja *et al.* 1999; Reardon *et al.* 2001), hindlimb unloading (Carlson *et al.* 1999; Wehling *et al.* 2000) and space flight (Lalani *et al.* 2000). In addition, myostatin expression increases during glucocorticoid-induced muscle atrophy (Ma *et al.* 2003). Furthermore, systemic administration of Myostatin protein has been shown to induce cachexia (Zimmers *et al.* 2002). Functional myostatin blockade in *mdx* mice, a model of Duchenne Muscular Dystrophy, results in an increase in muscle mass and more importantly, muscle force production (Bogdanovich *et al.* 2002). Therefore, it is well established that myostatin plays a critical role during the induction of cachectic conditions; however the mechanism behind this process is not known.

Thus *in vitro* and *in vivo* models of myostatin-induced cachexia have been utilised to identify the mechanism by which myostatin induces this cachexia. It is proposed that myostatin acts independently of NF-κB to induce skeletal muscle atrophy by inhibiting muscle protein synthesis via the down-regulation of Pax3 and the subsequent loss of MyoD. In addition, it appears that myostatin induces atrophy by activating the expression of components of the ubiquitin-proteasome pathway, such as Atrogin-1, through regulation of the Forkhead Box O transcription factor FoxO1.

5.2 Materials and Methods

5.2.1 *Cell cultures*

For *in vitro* studies of myostatin-induced muscle wasting, C2C12 myoblasts (American Type Culture Collection; ATCC, Manassas, VA) were used (Yaffe and Saxel 1977). Cells were cultured in Dulbecco's Modified Eagle Medium (DMEM; Invitrogen, Carlsbad, CA), buffered with 17 mM of $NaHCO_3$ (Sigma, St Louis, MO) and 5% gaseous CO_2. 2.93 nM of Phenol Red (Sigma) was used as a pH indicator and antibiotics 1 x 10^5 IU/L penicillin (Sigma) and 100 mg/L streptomycin (Sigma) were added. Foetal Bovine Serum (FBS, Invitrogen) was added to the DMEM for culturing cells under growth conditions. The recombinant Myostatin protein (Mstn) used in these *in vitro* experiments was generated and purified in our laboratory (Sharma *et al.* 1999).

5.2.2 *In vitro atrophy model*

To assess the ability of myostatin to induce cachexia *in vitro*, C2C12 cells were grown as above, on Thermanox coverslips (Nalge Nunc International, Rochester, NY). The C2C12 cells were differentiated for 72 hr in Differentiation Medium (DMEM + 2% Horse Serum; HS) followed by a further 24 hr in Differentiation Medium with 0, 3 or 10 μg/mL Mstn. The coverslips were then stained with Gill's haematoxylin and eosin. Dimensions of myotubes were analysed microscopically using the Windows Version 4.0.1 SPOT Basic software program (Diagnostic Instruments Inc). Fifty images of non-overlapping areas of each of three coverslips were taken under 200 x magnification. The maximal width of all myotubes within each image (n = 150) was measured.

5.2.3 Establishment and testing of an in vivo model of myostatin-induced cachexia

The AgResearch Ruakura Animal Ethics Committee approved the animal manipulations described in this study. Athymic nude mice were used for the generation of the *in vivo* model of myostatin-induced cachexia. Animals were maintained in rooms set at a constant temperature (20-22°C) with a 12:12 hr day/night cycle. They were provided with sterile water and near-sterile food *ad libitum*. All animals were handled in accordance with the guidelines set out in both the AgResearch Small Animal Containment Facility and AgResearch Small Animal Colony quarantine manuals.

The *in vivo* model of myostatin-induced skeletal muscle atrophy was developed based on that of Zimmers *et al* (Zimmers *et al.* 2002). These authors introduced high levels of circulatory Myostatin to nude mice via the injection of Myostatin-expressing Chinese Hamster Ovary (CHO) cells intramuscularly. These CHO cells express Myostatin under the control of a *metallothionein* promoter inducible by zinc. An aliquot of these Myostatin-expressing cells was kindly given to our laboratory by Dr S.J. Lee (Zimmers *et al.* 2002).

Control and Myostatin-expressing CHO cells were grown in DMEM/F12 + 10% FBS medium (Invitrogen). Cell cultures were trypsinised and resuspended in DMEM/F12 + 10% FBS, then centrifuged at 500 x g for 5 min. The cells were resuspended in 10 mL of Phosphate Buffered Saline (PBS) and re-centrifuged at 500 x g for 5 min. The supernatant was removed and the cells resuspended in PBS for injection into the mice.

Four week old male athymic nude mice were used for this experiment. Mice were anaesthetised with 1.2-1.6 mL of Ketamine/Rompun (National Veterinary Supplies Ltd) intra-peritoneally. Each mouse received an injection of 100 μL of cell suspension containing 5.0 x 10^6 cells in PBS. This injection was administered to a depth of 4 mm into the right *M. quadriceps femoris* muscle of each mouse. Tumours developed at the site of injection. Seven four-week old mice were injected with Myostatin-expressing CHO cells and six additional mice were given control CHO cells in PBS. All mice were given a sterile 25 mM $ZnSO_4$ solution in place of tap water to drink. The body mass of each mouse was monitored regularly. In the Zimmers *et al* paper, mice had lost body weight (~33%) by Day

16 of the experiment. Most of the mice in this *in vivo* trial had not lost body weight by Day 16, so the experiment was continued until each mouse was experiencing 15-20% of body mass loss. This occurred at approximately 30 days after cell administration.

5.2.4 *Transient co-transfections*

Transfections were performed on C2C12 cells to test the effect of Mstn on either the *pax3* promoter or the *myoD* promoter enhancer region. C2C12 myoblasts were seeded in 6 well plates at a density of 15,000 cells/cm^2. Following a 24 hr attachment period, the cells were transfected with 2 μg of each plasmid DNA using Lipofectamine 2000 (Invitrogen) reagent as per the manufacturer's guidelines (see Section 2.2.8.9). The myoblasts were then incubated overnight at 37^oC, in 5% CO_2. Proliferation medium (DMEM + 10% FBS) was then removed and replaced with Differentiation Medium with or without Mstn, for a further 24 hr. C2C12 cells were transfected with the *pax3* promoter and the β-galactosidase (β-gal) expression plasmid *pCH110* (GE Healthcare Bio-Sciences Corp. Piscataway, NJ), followed by treatment with 0, 4 or 8 μg/mL Mstn. The *pax3* promoter, a gift from Dr J.A. Epstein (Li *et al.* 1999), was sub-cloned into the pGL3b Luciferase vector. In addition, C2C12 cells were transfected with both the *myoD* core enhancer; gifted by Dr J.P. Capone (Hunter *et al.* 2001), and *pCH110* followed by treatment with 0 or 3 μg/mL Mstn. Following treatment the medium was removed and cells were washed twice with 5 mL PBS per plate and lysed in 300 μL of Reporter Lysis Buffer (Promega). Lysates were analysed for luciferase reporter gene activity (Promega) in a Turner Designs luminometer (Model TD-20/20). β-gal expression levels were also detected in each supernatant using the β-gal Enzyme Assay System (Promega) as per the manufacturer's guidelines (see Section 2.2.9). The luciferase values for each sample were normalised to the corresponding β-gal value as a measure of transfection efficiency.

5.2.5 Gene expression analysis of selected myogenic and proteolytic genes

C2C12 cells were seeded on 10 cm plates at a density of 25,000 cells/cm^2 in Proliferation Medium. After a 24 hr attachment period cultures were differentiated for 72 hr in Differentiation Medium followed by a further 48 hr in Differentiation Medium with or without 3 μg/mL of Mstn. RNA was isolated from both C2C12 cells and *M. quadriceps femoris* muscle from CHO injected mice using TRIZOL reagent (Invitrogen) as per the manufacturer's protocol (see Section 2.2.10). RNA was used for Northern analysis, and was also reverse-transcribed into cDNA for use in semi-quantitative RT-PCR (Q-RT-PCR) analysis of gene expression.

Northern analysis was performed as described by Sambrook *et al.* (Sambrook *et al.* 1989) (see Section 2.2.12). 15 μg of total RNA was separated by 1% formaldehyde agarose gel electrophoresis. RNA was transferred to Hybond N+ membrane (GE Healthcare Bio-Sciences) by capillary transfer using a 10 × SSC solution. The membrane was prehybridised in Church and Gilbert hybridisation buffer (0.5 M pH 7.2 Na_2HPO_4, 7% SDS and 1 mM EDTA) at 55°C for 1 hr, followed by hybridisation with ^{32}P-labeled DNA probe in fresh hybridisation buffer at 55°C, overnight. The membrane was rinsed twice with 5 × SSC + 0.5% SDS, and then washed successively with 2 × SSC + 0.5% SDS, and 1 × SSC + 0.5% SDS for 15 min each at 55°C.

In addition, the expression patterns of several genes were analysed by Q-RT-PCR. First-strand cDNA was synthesised in a 20 μL reverse transcriptase (RT) reaction from 5 μg of total RNA using a SuperScript II First-Strand Synthesis System (Invitrogen), according to the manufacturer's protocol (see Section 2.2.6.1). PCR was performed with *Taq* DNA polymerase (Roche Diagnostics Corporation, Indianapolis, IN) using 1 μL of the RT reaction at 94°C for 2 min, followed by 94°C for 20 s, a gene specific annealing temperature for 30 s (see Table 2.7), then 72°C for 2 min. This process was repeated for 35 cycles for the generation of cDNA probes, or for 14 cycles for *GAPDH* and 18 cycles for *myoD, pax3, E2$_{14k}$, atrogin-1, MuRF-1, NF-κB and FoxO1*. This was followed by a single 72°C extension step for 5 min. These PCR conditions were used for Q-RT-PCR expression analysis. The cDNA probes for Northern Blot analysis and Q-RT-PCR were made from 25 ng of RT-PCR product that was radioactively labelled with [α^{32}P]dCTP (GE Healthcare Bio-Sciences) and a Rediprime DNA labelling

system kit (GE Healthcare Bio-Sciences), according to the manufacturer's protocol (see Section 2.2.7).

The following murine specific primers were used for performing the Q-RT-PCR: *myoD* Fwd, 5'-GGA TCC TAA GAC GAC TCT CAC-3'; *myoD* Rev, 5'-GGA TCC AGT GCC TAC GGT GG-3'; *pax3* Fwd, 5'-GCA AGA TGG AGG AAA CAA GC-3'; *pax3* Rev, 5'-CGT TCT CAA GCA AGA GGT G-3'; $E2_{14k}$ Fwd, 5'-ATG TCG CCC CGG CCC GGA GGC TCA TG-3'; $E2_{14k}$ Rev, 5'-ATG AAT CAT TCC AGC TTT GTT CAA C-3'; *atrogin-1* Fwd, 5'-AAC ATG TGG GTG TAT CGG-3'; *atrogin-1* Rev, 5'-TCT TGA GGG GAA AGT GAG-3'; *MuRF-1* Fwd, 5'-GTT AAA CCA GAG GTT CGA G-3'; *MuRF-1* Rev, 5'-ATG GTT CGC AAC ATT TCG G-3'; *NF-κB* Fwd, 5'-ATG GAC GAT CTG TTT CCC CTC-3'; *NF-κB* Rev, 5'-TTA GGA GCT GAT CTG ACT C-3'; *GAPDH* Fwd, 5'-GTG GCA AAG TGG AGA TTG TTG GCC-3'; *GAPDH* Rev, 5'-GAT GAT GAC CCG TTT GGC TCC-3'; *FoxO1* Fwd, 5'-TTC AAG GAT AAG GGC GAC AG-3'; *FoxO1* Rev, 5'-ACT CGC AGG CCA CTT AGA AA-3'.

5.2.6 *NF-κB inhibitor cell line*

The IκBα super-repressor (IκBα SR) C2C12 cells were gifted by D.C. Guttridge (Guttridge *et al.* 1999). The IκBα SR expressing C2C12 cells were cultured in Differentiation Medium for 72 hr followed by a further 24 hr in Differentiation Medium with either 0 μg/mL or 10 μg/mL Mstn.

5.2.7 *Microarray analysis*

C2C12 cells were cultured in Differentiation Medium for 72 hr as outlined above followed by a further 24 hr in Differentiation Medium with or without 10 μg/mL Mstn. RNA was then isolated using TRIZOL (Invitrogen) according to manufacturer's guidelines (see Section 2.2.10). Contaminating DNA was removed by DNase1 (Invitrogen) treatment. The RNA was then column purified using the RNeasy Midi Kit (Qiagen) following the manufacturer's guidelines (see Section 2.2.11), ethanol precipitated overnight at -20°C and resuspended in RNase-free water. Microarray analysis was performed by MWG, Ebersberg,

Germany as per their standardised techniques, using the MWG mouse 30k array. Briefly, the Myostatin-untreated and -treated RNA samples were reverse transcribed and directly labelled with Cy3 or Cy5, respectively, or conversely Cy5/Cy3 as a control. Following co-hybridisation spots were scanned numerous times and signal intensities determined using Imagene software (BioDiscovery). The MWG proprietary software MAVI was then used for combining the data from multiple scans, normalisation and background correction. The ratio between signal intensity for both Cy3 to Cy5 and Cy5 to Cy3 was used to generate mean values for intensity of each gene, corresponding to fold up or down-regulation. Gene expression changes were deemed significant if expression was up-regulated or down-regulated by ≥ 1.5-fold.

5.2.8 *Protein isolation*

Cells were cultured for 72 hr in Differentiation Medium as outlined above followed by a further 24 hr in Differentiation Medium with 0, 4, 6 or 10 μg/mL Mstn. For quantitative FoxO1, phosphorylated FoxO1 (p-FoxO1) and phosphorylated AKT (p-AKT) immunoblot analyses, mouse C2C12 myotubes were cultured as described above. C2C12 cells were resuspended in 200 μL lysis buffer (50 mM Tris pH 7.6; 250 mM NaCl; 5 mM EDTA; 0.1% Nonidet P-40; Complete protease inhibitor [Roche]) and passed through a 26 gauge needle 10 times. Whole muscle lysates from *M. Biceps femoris* isolated from CHO-injected mice were resuspended in 500 μL of lysis buffer and homogenised. The cell and whole muscle extracts were then centrifuged to pellet cell debris. To isolate cytoplasmic and nuclear fractions, C2C12 cells were pelleted, washed in PBS and resuspended in ice cold Buffer A (10 mM HEPES pH 7.9, 1.5 mM $MgCl_2$, 10 mM KCl, 1 mM dithiothreitol (DTT) and Complete protease inhibitor cocktail tablets). The cells were passed through a 26 gauge needle 10 times on ice. The suspension was centrifuged at 20,000 x g for 15 s and the supernatant recovered as the cytoplasmic fraction. The pellets were resuspended in ice cold Buffer B (20 mM HEPES pH 7.9, 0.2 mM EDTA, 420 mM KCl, 1 mM DTT, and Complete protease inhibitor cocktail tablets), incubated 20 min on ice and passed through a 26 gauge needle 10 times on ice. The suspension was centrifuged at 20,000 x g for 15 s and the supernatant recovered as the nuclear fraction. Bradford Reagent

(Bio-Rad Laboratories, Hercules, CA) was used to estimate total protein content to ensure equal loadings.

5.2.9 *Western Blot analysis*

Total protein (15 μg) was separated by 4-12% SDS-PAGE (Invitrogen) and transferred to nitrocellulose membrane by electroblotting. The membranes were blocked in 0.3% BSA, 1% PEG (polyethylene glycol 4,000; Sigma), 1% PVP (polyvinylpyrrolidone 10,000; Sigma) for 1 hr at room temperature, then incubated with specific primary antibodies overnight at 4°C. Alternatively, the membranes were blocked overnight at 4ºC using a solution of TBST/5% milk, then incubated with specific primary antibodies for 3 hr at room temperature. The following primary antibodies were used for immunoblotting; 1:5,000 dilution of purified rabbit polyclonal anti-$E2_{14k}$ antibody (A-605; Boston Biochem, Cambridge, MA); 1:5,000 dilution of rabbit anti-atrogin-1 antibody, kindly given to our laboratory by Dr Cam Patterson (Li *et al.* 2004); 1:10,000 dilution of purified mouse monoclonal anti-Ubiquitin antibody (sc-8017; Santa Cruz Biotechnology Inc, Santa Cruz, CA); 1:1,000 dilution of purified rabbit polyclonal anti-NF-κB (p65) antibody (sc-372; Santa Cruz Biotechnology Inc.); 1:5,000 dilution of purified rabbit polyclonal anti-SP1 antibody (sc-59; Santa Cruz Biotechnology Inc.); 1:1,000 dilution of purified rabbit polyclonal anti-FKHR (FoxO1) antibody (sc-11350; Santa Cruz Biotechnology Inc.); 1:3,000 dilution of purified rabbit polyclonal anti-p-FKHR (p-FoxO1; Ser256) antibody (sc-22158-R; Santa Cruz Biotechnology Inc.); 1:1,000 dilution of purified rabbit polyclonal anti-p-AKT (Ser473) antibody (sc-7985; Santa Cruz Biotechnology Inc.) or 1:10,000 dilution of purified mouse monoclonal α-Tubulin antibody (T-9026; Sigma). The membranes were washed (5 x 5 min) with TBST and further incubated with anti-rabbit IgG Horseradish Peroxidase (HRP) conjugate, 1:5,000 dilution (P0448; Dako, Glostrup, Denmark) or anti-mouse IgG HRP conjugate, 1:5,000 dilution (P0447; Dako) secondary antibodies for 1 hr at room temperature. The membranes were washed as above, and HRP activity was detected using Western Lightning Chemiluminescence Reagent Plus (NEL104; PerkinElmer Life And Analytical Sciences, Inc., Wellesley, MA).

5.2.10 *FoxO1 siRNA analysis*

C2C12 cells were transfected at ~70% confluence with 1 nM of each specific siRNA. The siRNA transfections were performed with HiPerFect Transfection Reagent (Qiagen) as per the manufacturer's protocol (see Section 2.2.8.10). The specific siRNA's were generated and obtained from Qiagen: Non-silencing control siRNA, rUUC UCC GAA CGU GUC ACG UdT dT; Mouse FoxO1 siRNA, r(CGU UUG UUA GUG UGU GUU A)dTdT.

5.2.11 *Statistics*

The Student's-T test was also used for the comparison of Myostatin-treated samples with control samples, for factors such as muscle weights. For the transfection experiments, the mean luciferase values were calculated per well and the three means averaged, and analysis of variance (ANOVA) performed. ANOVA was also used to analyse the data for the myotube size. There were three slides of cells per treatment, with fifty images each slide. The mean number of myotubes in each slide was calculated, and the mean of the means calculated. A P value <0.05 was deemed significant for all experiments.

5.3 Results

5.3.1 *In vitro and in vivo models of myostatin-induced cachexia*

To study the mechanism behind myostatin-induced muscle wasting, both *in vitro* and *in vivo* models of myostatin-induced cachexia were generated. In this study C2C12 cells were differentiated for 72 hr followed by a further 24 hr in Differentiation Medium with or without Myostatin. The addition of recombinant Myostatin protein to the differentiated myotube cultures induced prominent atrophic changes (Figure 5.1A). In fact, treatment with increasing levels of recombinant Myostatin protein resulted in a concomitant decrease in myotube diameter. Specifically, the median myotube diameter was reduced by 57% with maximal Myostatin protein treatment (10 μg/mL) (Figure 5.1B).

Next, an *in vivo* model of myostatin-induced cachexia was developed based on the report by Zimmers *et al* (Zimmers *et al.* 2002). As such, mice were injected intramuscularly with Myostatin over-expressing CHO cells. After a treatment period of 30 days the body mass of mice injected with Myostatin over-expressing CHO cells was 18% lower when compared to mice injected with control CHO cells (data not shown).

5.3.2 *Myostatin and myogenic gene expression*

Since Myostatin treatment resulted in atrophic changes both *in vitro* and *in vivo*, the myogenic gene expression patterns, in response to the Myostatin treatment, were monitored in both models. MyoD is a Myogenic Regulatory Factor, and as such is a key regulator of muscle synthesis and regeneration (Megeney *et al.* 1996; Black *et al.* 1998; Guttridge *et al.* 2000). Myostatin has been previously shown to inhibit both MyoD expression and activity (Langley *et al.* 2002; Amthor *et al.* 2004). Thus *myoD* expression was monitored to elucidate a possible role for MyoD in myostatin-induced cachexia. Indeed, *myoD* was found to be dramatically down-regulated following Myostatin treatment *in vitro* (Figure 5.2A) furthermore, *myoD* expression was down-regulated by ~84% *in vivo* (Figure

5.2B). This evidence suggests that Myostatin acts via a down-regulation of *myoD* to prevent muscle synthesis and regeneration.

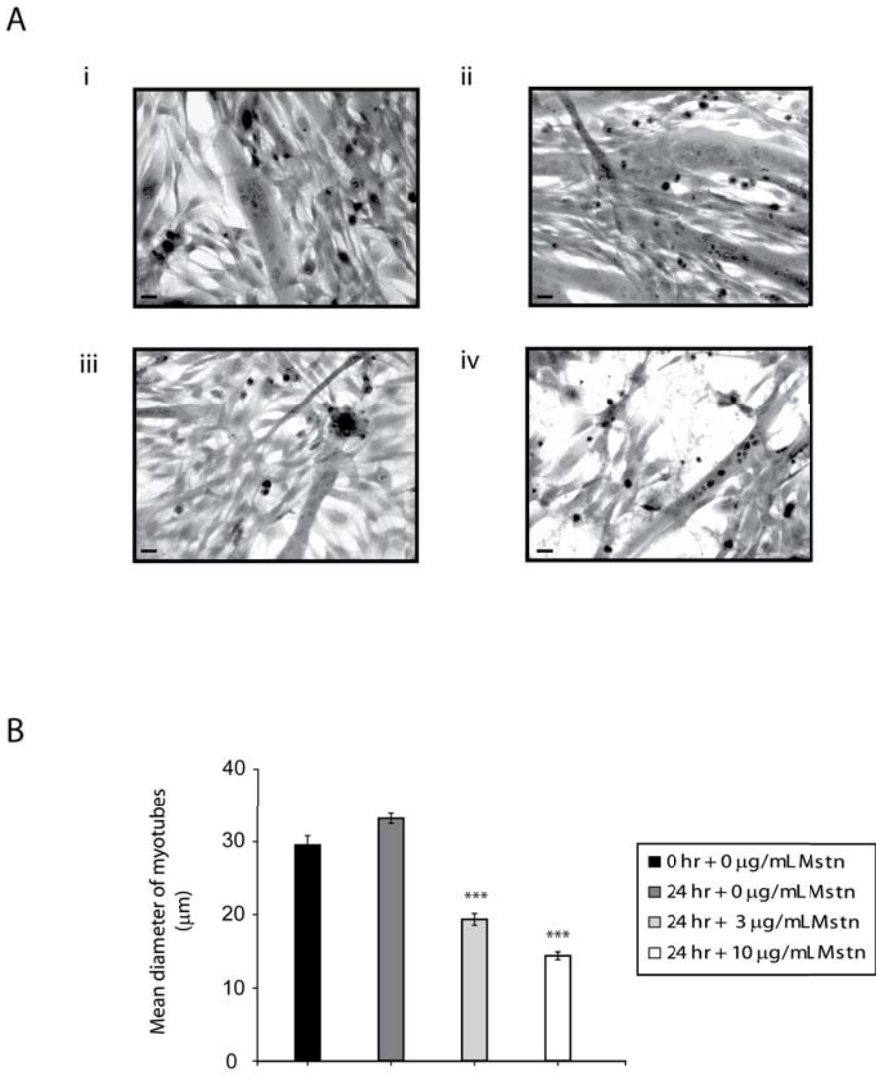

Figure 5.1 *Myostatin decreases the size of myotubes in vitro*

C2C12 myotubes were stained with Gill's haematoxylin and eosin and the physiology of the cells analysed. A) C2C12 cells were seeded on coverslips in wells with Proliferation Medium at a density of 25,000 cells/cm^2 for 24 hr and then differentiated for 72 hr (0 hr + 0 μg/mL Mstn) without Mstn (i). Other cells were differentiated for a further 24 hr with 0 μg/mL (24 hr + 0 μg/mL Mstn) (ii), 3 μg/mL (24 hr + 3 μg/mL Mstn) (iii) or 10 μg/mL (24 hr + 10 μg/mL Mstn) (iv) of Mstn. Scale bar represents 25 μm. B) The maximal diameter of each stained myotube was measured. Bars represent the average median width of three independent experiments. Statistical differences determined by ANOVA are indicated; P< 0.001 (***) compared to both untreated 0 hr (0 hr + 0 μg/mL Mstn) and 24 hr (24 hr + 0 μg/mL Mstn) controls.

Figure 5.2 *Myogenic gene expression is altered during myostatin-induced cachexia in vitro and in vivo*

A) The myogenic gene expression differences for C2C12 cells treated with Mstn were measured by Northern Blot analyses. Cells were seeded at a density of 25,000 cells/cm^2. Following a 24 hr attachment period, cells were switched to Differentiation Medium for 72 hr. The cells were then treated for an additional 48 hr in Differentiation Medium with either 0 μg/mL (-) or 3 μg/mL (+) Mstn. The *in vitro* Northern Blots demonstrate the effect of Mstn on *myoD* and *pax3* expression, with the 28S and 18S RNA bands demonstrating equal loading of RNA. B) The myogenic gene expression differences for nude mice injected intra-muscularly with either control CHO cells (-) or Myostatin-expressing CHO cells (+) were measured by Q-RT-PCR. Q-RT-PCR was performed to analyse the expression of *myoD* and *pax3*. *GAPDH* expression was analysed as a measure of RNA amounts used in Q-RT-PCR. All Northern and Southern Blots pictured represent three independent experiments. C) *In vitro* analysis of the effect of Myostatin on *pax3* promoter activity. The *pax3* promoter and β-galactosidase (β-gal) expression plasmids were transfected into C2C12 myoblasts using Lipofectamine 2000 reagent. The cells were grown for a further 24 hr in Differentiation Medium, after which luciferase and β-gal activities were measured. Results reflect relative *pax3* promoter-luciferase activity with increasing Mstn concentrations of 4 μg/mL (4.0) and 8 μg/mL (8.0) as compared to the untreated control (0). Values were normalised to β-gal and the bars indicate means ± standard error of three independent experiments. Statistical significance was analysed using ANOVA, where $P < 0.001$ (***) compared to untreated control (0). D) *In vitro* analysis of the effect of Mstn on the *myoD* core enhancer (promoter) activity. The *myoD* promoter and β-galactosidase (β-gal) expression plasmids were transfected into C2C12 myoblasts. The cells were grown for a further 24 hr in Differentiation Medium after which luciferase and β-gal activities were measured. Results reflect relative *myoD* promoter luciferase activity following treatment with 3 μg/mL (3.0) Mstn as compared to the untreated control (0). Values were normalised to β-gal and the bars indicate mean ± standard error of three independent experiments. Statistical significance was analysed for the normalised luciferase values using ANOVA, where $P < 0.01$ (**) compared to untreated control (0).

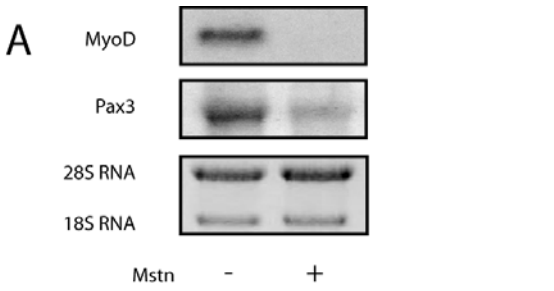
A
MyoD
Pax3
28S RNA
18S RNA
Mstn - +

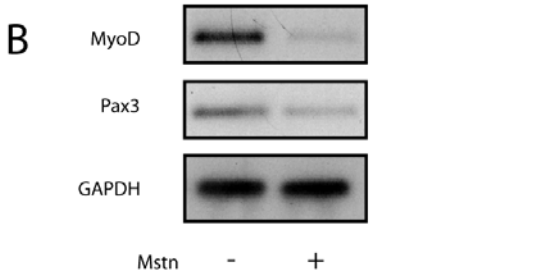
B
MyoD
Pax3
GAPDH
Mstn - +

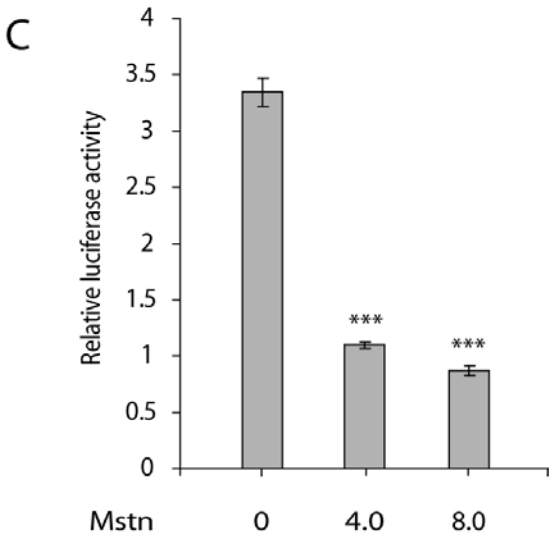
C
Relative luciferase activity
4
3.5
3
2.5
2
1.5
1
0.5
0
***
***
Mstn 0 4.0 8.0

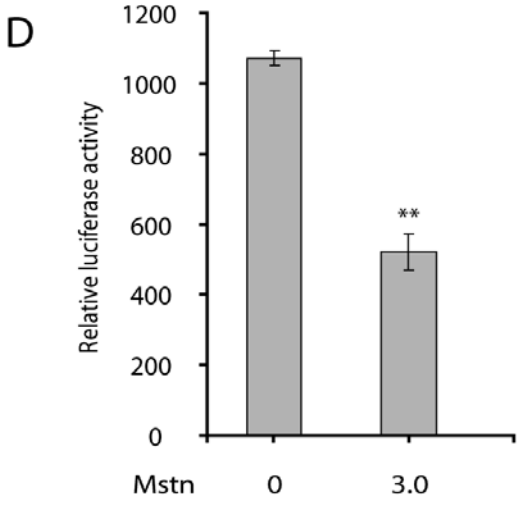
D
Relative luciferase activity
1200
1000
800
600
400
200
0
**
Mstn 0 3.0

In addition, the expression of *pax3* was measured to further clarify how myostatin might signal the down-regulation of *myoD* during cachexia. Myostatin has been shown to decrease the expression of *pax3* and *myoD* in embryonic chick limb buds (Amthor *et al.* 2004). In addition, it is well established that *pax3* acts upstream to activate *myoD* expression (Epstein *et al.* 1995; Maroto *et al.* 1997; Tajbakhsh *et al.* 1997). Based on this data, it was anticipated that myostatin may act via a Pax3 dependent pathway to down-regulate *myoD* during muscle atrophy. As expected, *pax3* gene expression was down-regulated by ~52% *in vitro* and ~30% *in vivo* following Myostatin treatment (Figure 5.2A and Figure 5.2B). To demonstrate Myostatin regulation of *pax3,* C2C12 myoblasts were transiently transfected with a *pax3* promoter-luciferase reporter construct. Subsequent reporter analysis confirmed Myostatin inhibition of *pax3* activity, as treatment with 8 μg/mL Myostatin resulted in a ~75% decrease in *pax3* promoter activity (Figure 5.2C). Furthermore, C2C12 myoblasts were transiently transfected with a *myoD* promoter/enhancer reporter construct in the presence or absence of recombinant Myostatin protein. As shown in Figure 5.2D, treatment with 3 μg/mL Myostatin resulted in a ~52% reduction in *myoD* reporter activity. These data indicate that myostatin indeed inhibits the activity of both *pax3* and *myoD* in differentiated C2C12 myotubes.

5.3.3 *Myostatin and proteolytic gene expression*

One of the major systems believed to be pivotal in inducing the skeletal muscle atrophy associated with many forms of disease is the ubiquitin-proteasome pathway. Therefore the effect of myostatin on the induction of the ubiquitin-proteasome pathway was assessed. Proteins degraded by the ubiquitin-proteasome pathway are first covalently bound to ubiquitin, a process that is regulated by an enzyme cascade consisting of ubiquitin-activating enzymes (E1), ubiquitin-conjugating enzymes (E2), and ubiquitin ligases (E3) (Hasselgren *et al.* 2002). The resulting ubiquitinated proteins are then degraded by the 26S proteasome complex in an ATP-dependent process (Lecker *et al.* 1999). Thus the expression levels of several candidate proteins including the ubiquitin-conjugating enzymes $E2_{14k}$ and $E2_{20k}$, and the ubiquitin-ligases MuRF-1 and Atrogin-1, were monitored by Northern and Southern Blot analysis. As shown in Figure 5.3A,

C2C12 myotubes treated with Myostatin exhibited a ~90% increase in $E2_{14k}$ mRNA levels; however no significant change in $E2_{14k}$ expression was detected *in vivo* (Figure 5.3B). In addition, no change was observed in the expression of $E2_{20k}$ mRNA in response to Myostatin treatment *in vitro* (Data not shown). The expression levels of E3 enzymes in response to Myostatin treatment were subsequently evaluated. A ~60% increase in *atrogin-1* expression during myostatin-induced myotube atrophy was observed (Figure 5.3A) and a dramatic ~150% increase in *atrogin-1* expression during myostatin-induced cachexia *in vivo* (Figure 5.3B). In contrast, *MuRF-1* levels did not increase in response to Myostatin treatment *in vitro* (Figure 5.3A) however, a ~58% increase in *MuRF-1* expression was observed following *in vivo* treatment (Figure 5.3B). The protein expression of both $E2_{14k}$ and Atrogin-1 were also measured by Western Blot analysis. As shown in Figure 5.3C, myostatin up-regulates $E2_{14k}$ expression by 55%, furthermore, Myostatin treatment resulted in a dramatic up-regulation of Atrogin-1 expression (Figure 5.3C). To assess the effect of myostatin on the level of ubiquitinated proteins a Western Blot using an anti-ubiquitin-specific antibody was performed and as shown in Figure 5.3D, Myostatin treatment resulted in a 60% increase in the level of ubiquitin-conjugated proteins. This increased ubiquitin-conjugation is particularly prevalent in proteins ~70 kDa or smaller. These observations confirm that Myostatin up-regulates several genes involved with ubiquitination of muscle proteins and indeed Myostatin treatment enhances the level of ubiquitin-conjugated proteins.

Figure 5.3 *Proteolytic gene expression is altered during myostatin-induced cachexia in vitro and in vivo*

A) The proteolytic gene expression differences for C2C12 cells treated with Mstn were measured by Northern Blot analyses. Cells were seeded at a density of 25,000 cells/cm^2. Following a 24 hr attachment period cells were switched to Differentiation Medium for 72 hr. The cells were treated for an additional 48 hr of differentiation with either 0 μg/mL (-) or 3 μg/mL (+) of Mstn. The *in vitro* Northern Blots demonstrate the effect of Mstn on *$E2_{14k}$, atrogin-1* and *MuRF-1,* all members of the ubiquitin-proteasome pathway, with the 28S and 18S RNA bands demonstrating equal loading of RNA. B) The proteolytic gene expression differences for immune-deficient mice injected intra-muscularly with either control CHO cells (-) or Myostatin-expressing CHO cells (+) were measured by Q-RT-PCR. The *in vivo* Southern Blots demonstrate the effect of Mstn on *$E2_{14k}$, atrogin-1* and *MuRF-1*, with *GAPDH* expression was analysed as a measure of RNA amounts used in Q-RT-PCR. All Northern and Southern Blots pictured represent three independent experiments. C) Western Blot to demonstrate the effect of Mstn on the protein levels of the proteolytic genes $E2_{14k}$ and Atrogin-1. Cells were seeded at a density of 25,000 cells/cm^2 and after a 24 hr attachment period cells were switched to Differentiation Medium for 72 hr. To study $E2_{14k}$ the cells were treated for 1 hr with either 0 μg/mL (-) or 1 μg/mL (+) of Mstn, and to study Atrogin-1 the cells were treated for an additional 24 hr in Differentiation Medium with either 0 μg/mL (-) or 10 μg/mL (+) of Mstn. Tubulin levels were measured to ensure equal loadings. The graph represents relative densitometry analysis of each $E2_{14k}$ band normalised to Tubulin. D) Western Blot analysis of the effect of Mstn on protein ubiquitination. Cells were seeded at a density of 25,000 cells/cm^2 and after a 24 hr attachment period cells were switched to Differentiation Medium for 72 hr. The cells were treated for 3 hr with either 0 μg/mL (-) or 3 μg/mL (+) of Mstn. Tubulin levels were measured to ensure equal loadings. The graph represents relative densitometry analysis of each band normalised to Tubulin.

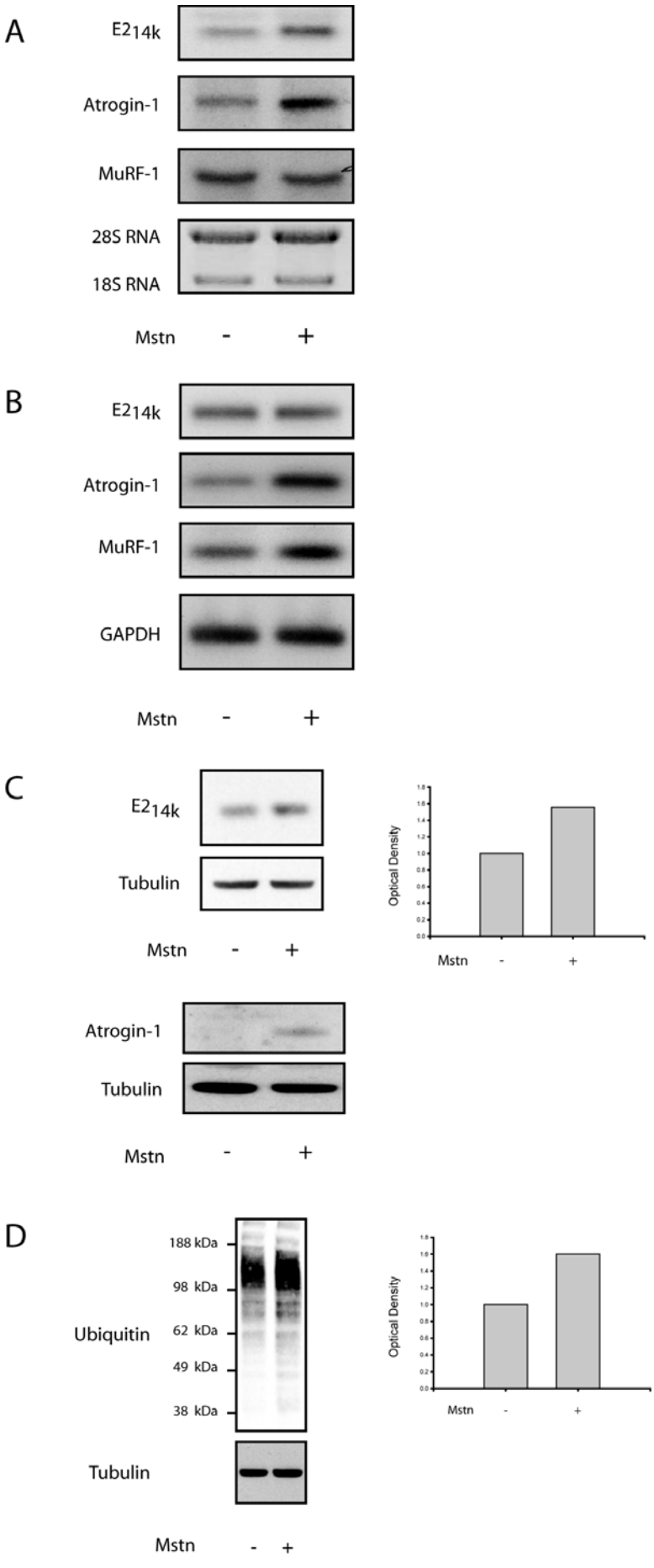
A
E2 14k
Atrogin-1
MuRF-1
28S RNA
18S RNA
Mstn - +
B
E2 14k
Atrogin-1
MuRF-1
GAPDH
Mstn - +
C
E2 14k
Tubulin
Mstn - +
Optical Density
Mstn - +
Atrogin-1
Tubulin
Mstn - +
D
188 kDa
98 kDa
62 kDa
49 kDa
38 kDa
Ubiquitin
Tubulin
Mstn - +
Optical Density
Mstn - +

5.3.4 Myostatin signals independently of NF-κB to regulate cachexia

NF-κB is activated by TNF-α, a cytokine that is believed to be an inducer of cachexia (Guttridge *et al.* 2000). In fact, the down-regulation of *myoD* during cachexia has been shown to occur via a mechanism involving TNF-α, IFN-γ and NF-κB (Guttridge *et al.* 2000). Therefore, it is conceivable that myostatin acts via NF-κB to cause a down-regulation of *myoD* expression during cachexia. However, despite previous evidence linking NF-κB with atrophic conditions, *NF-κB (p65)* expression was not altered in both *in vitro* and *in vivo* models of myostatin-induced cachexia (Figure 5.4A and Figure 5.4B). In addition, there was no change in the nuclear localisation of p65 following Myostatin treatment (Figure 5.4C). To further confirm that myostatin signalling to induce cachexia is independent of NF-κB, the ability of myostatin to up-regulate Atrogin-1 was assessed in a stable C2C12 cell line expressing the IκBα SR protein. The IκBα SR protein acts as a potent and specific inhibitor of NF-κB activity (Guttridge *et al.* 1999). As shown in Figure 4D, myostatin is still able to increase the expression of Atrogin-1 by 110% in the absence of NF-κB activity. Thus myostatin may signal independently of NF-κB to mediate the induction of cachexia.

Figure 5.4 *Myostatin signals independently of NF-κB p65 to regulate cachexia*

A) The expression of p65 *in vitro* with Mstn treatment. Cells were seeded at a density of 25,000 cells/cm^2 and after a 24 hr attachment period cells were switched to Differentiation Medium for 72 hr. The cells were treated for 48 hr with either 0 μg/mL (-) or 10 μg/mL (+) of Mstn. Tubulin levels were measured to ensure equal loadings. B) The *p65* gene expression differences for nude mice injected intra-muscularly with either control CHO cells (-) or Myostatin-expressing CHO cells (+) were measured by Q-RT-PCR. *GAPDH* expression was analysed as a measure of RNA amounts used in Q-RT-PCR. All Northern and Southern Blots pictured represent three independent experiments. C) Western Blot demonstrating the effect of Mstn treatment on the nuclear localisation of p65. Cells were seeded at a density of 25,000 cells/cm^2 and after a 24 hr attachment period cells were switched to Differentiation Medium for 72 hr. The cells were treated for an additional 24 hr with either 0 μg/mL (-) or 5 μg/mL (+) of Mstn. Ponceau S staining was shown as a measure of equal loading and SP1 protein expression shows nuclear enrichment of the protein samples. D) Analysis of *atrogin-1* gene expression in C2C12 cells which express the IκBα SR protein. The IκBα SR cells were differentiated for 72 hr followed by a further 24 hr with either 0 μg/mL (-) or 10 μg/mL (+) of Mstn. The Northern Blot shows the effect of Mstn on *atrogin-1* expression in the IκBα SR cell line, with 28S and 18S RNA bands shown as a measure of RNA loading. The graph represents relative densitometry analysis of each band normalised to 28S and 18S RNA. All Northern Blots pictured represent three independent experiments.

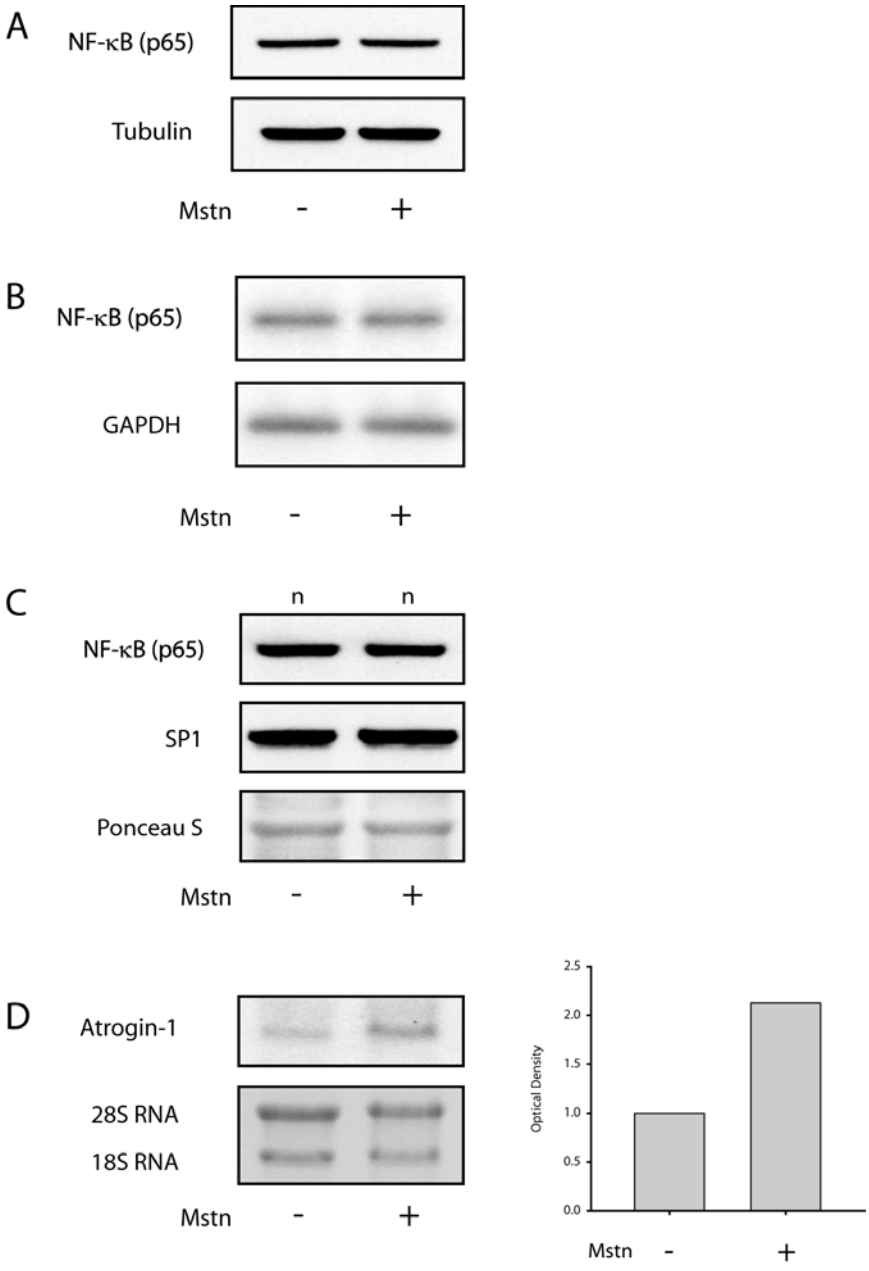
A
NF-κB (p65)
Tubulin
Mstn - +
B
NF-κB (p65)
GAPDH
Mstn - +
C
n n
NF-κB (p65)
SP1
Ponceau S
Mstn - +
D
Atrogin-1
28S RNA
18S RNA
Mstn - +
Optical Density
2.5
2.0
1.5
1.0
0.5
0.0
Mstn - +

5.3.5 Microarray analysis of myostatin-induced cachexia

In addition to the candidate gene approach outlined above, global gene expression changes were analysed during a model of myostatin-induced cachexia via microarray technology. Microarray analysis was performed using an *in vitro* model of myostatin-induced muscle atrophy. As identified by microarray analysis several myofibrillar structural proteins including Myosin Heavy Chain, Troponin C, Tropomyosin 3 (gamma) and Titin-cap were significantly down-regulated during myostatin-induced cachexia (Table 5.1). In agreement with additional *in vitro* and *in vivo* data presented in this Chapter, microarray analysis has identified several members of the ubiquitin-proteasome pathway significantly up-regulated by myostatin (Table 5.1). Recent publications have demonstrated that the ubiquitin E3 ligases Atrogin-1 and MuRF-1 are significantly up-regulated in many forms of muscle atrophy (Bodine *et al.* 2001; Gomes *et al.* 2001). Consistent with this published data, myostatin-mediated myotube atrophy also induces the E3 ligase Atrogin-1 (Table 5.1).

Function	Sequence Name	Accession No.	Fold change	
Protein degradation	Atrogin-1 (fbxo32)	NM_026346	1.7	⇧
	Ubiquitin c (ubc)	NM_019639	1.5	⇧
	Ubiquitin-specific protease 2 (USP2)	NM_016808	2.3	⇧
	Ubiquitin-conjugating enzyme (mhr6br	AF299059	1.5	⇧
	Ring finger protein 31 (Rnf31)	NM_194346	2.5	⇧
Myofibrillar proteins	Myosin heavy chain 2A (myh2)	NM_144961	2.7	⇩
	Troponin c (tcns)	NM_009394	2.2	⇩
	Tropomyosin 3 (Gamma) (tprn3)	NM_022314	1.7	⇩
	Titin-cap (tcap)	NM_011540	2	⇩

Table 5.1 *Microarray identification of genes altered in a model of myostatin-induced cachexia*

C2C12 cells were grown in Differentiation Medium for 72 hr followed by a further 24 hr in Differentiation Medium without or with 10 μg/mL Mstn. Genes are separated into structural or proteolytic function and were at least 1.5 fold up-regulated (⇧) or down-regulated (⇩).

In addition, several other genes critically involved during different stages of the ubiquitin-proteasome pathway are up-regulated during myostatin-induced myotube atrophy. These include the polyubiquitin gene c (UBC), ubiquitin-specific protease 2, ubiquitin-conjugating enzyme (mhr6bn) and Ring finger protein 31 (Rnf31), a gene sharing characteristics with many E3 ligases (Table 5.1). This indicates that myostatin induces atrophy through the up-regulation of specific components of the ubiquitin-proteasome pathway, concomitant with a significant down-regulation of several myofibrillar proteins.

5.3.6 *Myostatin signals atrophy through a FoxO1-dependent pathway*

Microarray analysis of myostatin treated myotube cultures identified an ~85% increase in the expression of *foxO1* (data not shown). FoxO transcription factors have been shown to induce skeletal muscle wasting via the regulation of atrophy-related genes, including the ubiquitin ligase Atrogin-1 (Sandri *et al.* 2004; Stitt *et al.* 2004). In addition, hypertrophy-inducing factors such as IGF-1 function by down-regulating the activity of FoxO1 through a PI3-K/AKT dependent pathway (Stitt *et al.* 2004). Since lack of *myostatin* induces hypertrophy, and high levels of it induce muscle wasting, it was hypothesised that myostatin may induce atrophy by reversing canonical hypertrophy signalling pathways, including the IGF/PI3-K/AKT pathway. Hence, to further elucidate the role of FoxO1 signalling in myostatin-induced cachexia, the levels and the phosphorylation status of FoxO1 were monitored following myostatin treatment. Initial Q-RT-PCR analysis of *foxO1* demonstrated a ~100% increase in *foxO1* expression with Myostatin treatment (Figure 5.5A). Subsequent Western Blot analysis demonstrated that FoxO1 protein expression is directly up-regulated upon addition of recombinant Myostatin protein to C2C12 myotubes (Figure 5.5B). A ~650% increase in FoxO1 expression was also detected in *M. Biceps femoris* excised from Myostatin CHO injected mice as compared to controls (Figure 5.5C). In addition, it appears that Myostatin treatment reduces the levels of phosphorylated FoxO1 in a dose-dependent manner, thus resulting in an accumulation of active FoxO1 (Figure 5.5D).

Figure 5.5 *Myostatin-induced cachexia occurs via a FoxO-dependent pathway*

A) Q-RT-PCR demonstrating the effect of Mstn on *foxO1* mRNA expression. C2C12 cells were grown in Differentiation Medium for 72 hr followed by a further 24 hr in Differentiation Medium without (-) or with 10 μg/mL (+) Mstn. RNA was subsequently extracted, reverse transcribed and subjected to PCR specific for *foxO1* and *GAPDH*. The Southern Blot was hybridised with probes specific for murine *foxO1* and *GAPDH*. *FoxO1* expression was normalised to total *GAPDH* levels. B) Western Blot demonstrating the effect of Mstn on FoxO1 expression. C2C12 cells were grown in Differentiation Medium for 72 hr followed by a further 24 hr in Differentiation Medium without (0) or with 4 μg/mL (4.0) or 6 μg/mL (6.0) Mstn. Tubulin levels were measured to ensure equal loadings. The graph represents relative densitometry analysis of each band normalised to Tubulin. C) Western Blot analysis of FoxO1 gene expression differences between immune-deficient mice injected intra-muscularly with either control CHO cells (-) or Myostatin-expressing CHO cells (+). Tubulin levels were measured to ensure equal loadings. The graph represents relative densitometry analysis of each band normalised to Tubulin. D) Western Blot demonstrating the effect of Mstn on the levels of phosphorylated FoxO1 (p-FoxO1 Ser 256). C2C12 cells were grown in Differentiation Medium for 72 hr followed by a further 24 hr in Differentiation Medium without (0) or with 4 μg/mL (4.0), 6 μg/mL (6.0) or 10 μg/mL (10.0) Mstn. Tubulin levels were measured to ensure equal loadings. The graph represents relative densitometry analysis of each band normalised to Tubulin. E) Western Blot showing the effect of Mstn on FoxO1 nuclear localisation. C2C12 cells were grown in Differentiation Medium for 72 hr followed by a further 24 hr in Differentiation Medium without (0) or with 10 μg/mL (10.0) Mstn. C2C12 samples were enriched for cytoplasmic (c) or nuclear (n) content with FoxO1 expression in both fractions analysed. Ponceau S staining was shown as a measure of equal loading and SP1 was used as a control to verify the purity of nuclear enrichment. The graph represents relative densitometry analysis of each band. F) Western Blot demonstrating the effect of Mstn on the levels of phosphorylated AKT (p-AKT Ser 473). C2C12 cells were grown in Differentiation Medium for 72 hr followed by a further 24 hr in Differentiation Medium without (0) or with 4 μg/mL (4.0) or 6 μg/mL (6.0) Mstn. Tubulin levels were analysed to ensure equal loadings. The graph represents relative densitometry analysis of each band normalised to Tubulin. All Western and Southern Blots pictured represent three independent experiments.

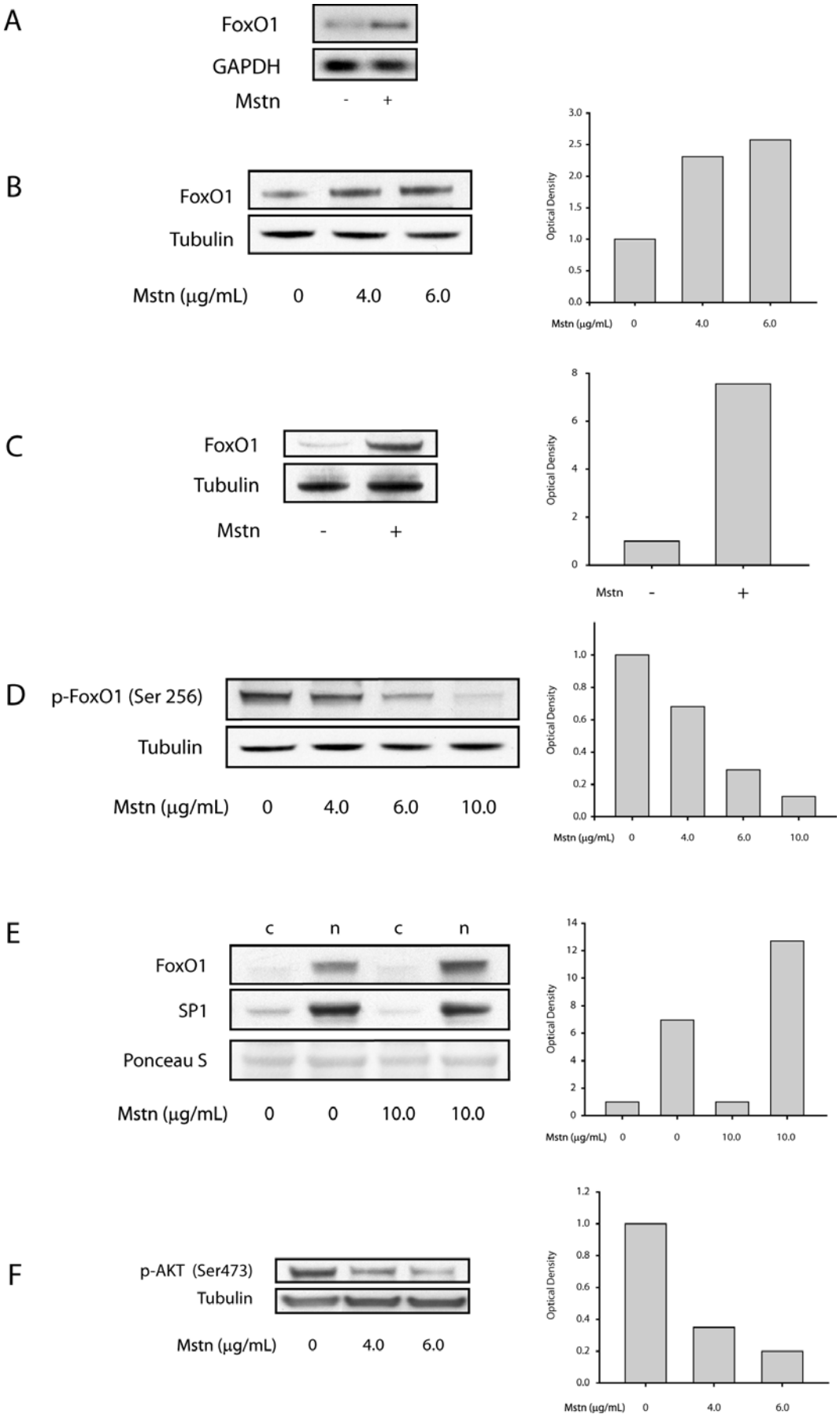
A
FoxO1
GAPDH
Mstn - +
B
FoxO1
Tubulin
Mstn (μg/mL) 0 4.0 6.0
Optical Density
Mstn (μg/mL) 0 4.0 6.0
C
FoxO1
Tubulin
Mstn - +
Optical Density
Mstn - +
D
p-FoxO1 (Ser 256)
Tubulin
Mstn (μg/mL) 0 4.0 6.0 10.0
Optical Density
Mstn (μg/mL) 0 4.0 6.0 10.0
E
c n c n
FoxO1
SP1
Ponceau S
Mstn (μg/mL) 0 0 10.0 10.0
Optical Density
Mstn (μg/mL) 0 0 10.0 10.0
F
p-AKT (Ser473)
Tubulin
Mstn (μg/mL) 0 4.0 6.0
Optical Density
Mstn (μg/mL) 0 4.0 6.0

Dephosphorylated, and thus active, FoxO1 readily translocates to the nucleus. Therefore, nuclear accumulation of FoxO1 was analysed following Myostatin treatment. As shown in Figure 5.5E, Myostatin treatment resulted in an 83% increase in nuclear FoxO1 expression when compared to untreated controls (Figure 5.5E). To determine if the myostatin-mediated reduction in phosphorylated FoxO1 was in some manner due to an interference with the PI3-K/AKT pathway, the levels of phosphorylated AKT were measured, and as shown in Figure 5.5F, Myostatin treatment resulted in diminished levels of phosphorylated AKT in a dose-dependent manner. Therefore myostatin appears to induce cachexia by antagonising IGF-1 hypertrophy signalling through targeting and inactivating AKT, leading to activated FoxO1 and increased Atrogin-1 expression.

5.3.7 *Myostatin signals through FoxO1 to regulate Atrogin-1 expression*

To confirm that myostatin signals through both FoxO1 and Atrogin-1 during the induction of cachexia, the ability of myostatin to regulate *atrogin-1* expression in the presence of siRNA specific for FoxO1 was analysed. As shown in Figure 5.6A, Myostatin is able to induce *atrogin-1* expression by ~250% in the presence of non-silencing siRNA. However, induction of *atrogin-1* by Myostatin is impaired in the presence of FoxO1 specific siRNA, when compared to non-silencing controls (Figure 5.6A). The expression of FoxO1 was also analysed to measure the efficiency of siRNA silencing. As shown in Figure 5.6B, the levels of FoxO1 were reduced by ~70% in the presence of the FoxO1-specific siRNA. Thus myostatin may signal through FoxO1 to regulate Atrogin-1 expression and the induction of cachexia.

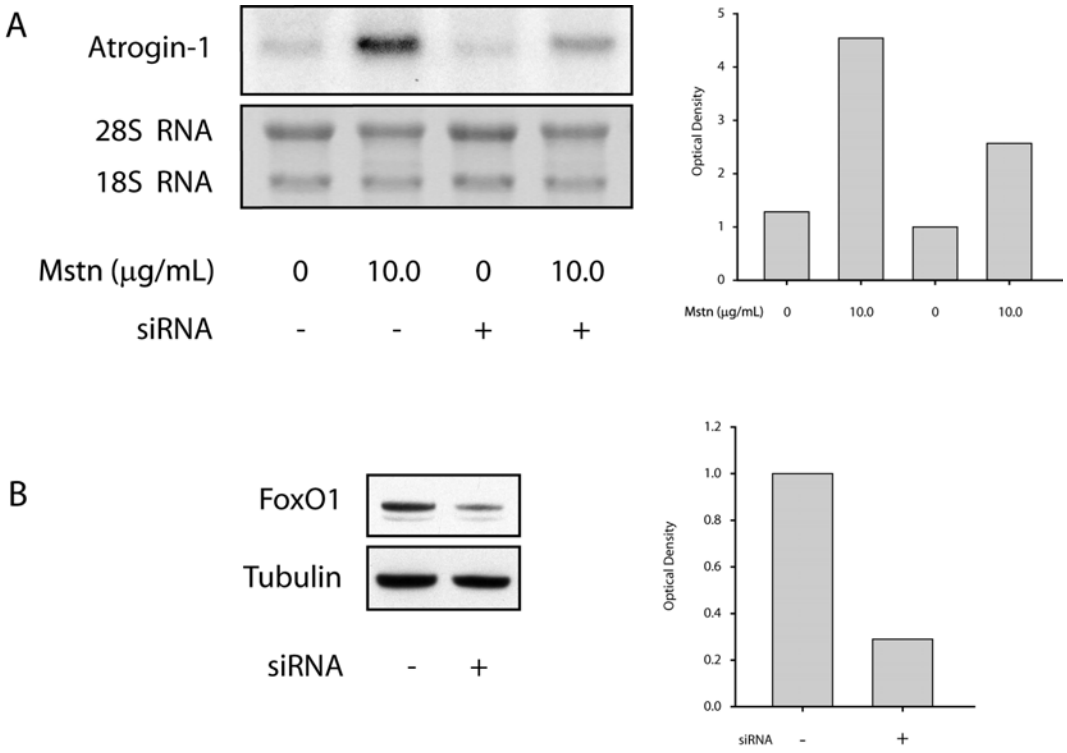

Figure 5.6 *Myostatin regulation of Atrogin-1 is dependent on FoxO1*

C2C12 cells were grown in Differentiation Medium for 72 hr followed by a further 24 hr in Differentiation Medium without (0) or with 10 µg/mL (10.0) Mstn. A) Northern Blot showing the effect of Mstn on *atrogin-1* expression in the presence of non-silencing control siRNA (-) or FoxO1-specific siRNA (+). The level of RNA loading was determined by 28S and 18S RNA bands. The graph represents relative densitometry analysis of each band normalised to 28S and 18S RNA. B) Western Blot analysing the expression of FoxO1 in the absence (-) or presence (+) of a FoxO1-specific siRNA. Tubulin levels were measured to ensure equal loadings. The graph represents relative densitometry analysis of each band normalised to Tubulin. Both Western and Northern Blots pictured represent three independent experiments.

5.4 Discussion

The role of myostatin as a negative regulator of muscle growth is now well established. Indeed, myostatin has been implicated in atrophic conditions such as AIDS (Gonzalez-Cadavid *et al.* 1998) and disuse atrophy (Carlson *et al.* 1999; Lalani *et al.* 2000; Wehling *et al.* 2000). Furthermore, systemic administration of Myostatin protein has been shown to induce skeletal muscle atrophy (Zimmers *et al.* 2002). Although it is reported that myostatin plays a role in muscle atrophy little is known about the mechanism behind this process. Therefore, in this Chapter the molecular mechanism behind myostatin-induced cachexia is defined.

Both *in vitro* and *in vivo* models were used to delineate the mechanism behind myostatin-induced cachexia. Differentiated C2C12 myotubes when treated with Myostatin, showed signs of atrophy (Figure 5.1A and 5.1B). Specifically, Myostatin treatment resulted in a dramatic dose-dependent reduction in C2C12 myotube diameter (Figure 5.1B), indicating that treatment of C2C12 myotubes with Myostatin protein could be used to establish an *in vitro* model to delineate the molecular mechanism(s) behind myostatin-induced cachexia. In addition to the *in vitro* model, an *in vivo* model of myostatin-induced cachexia was generated based upon the previously published protocol by Zimmers *et al*. In this report Zimmers *et al* demonstrated that CHO cells which over-express Myostatin were very effective in inducing cachexia, as a dramatic body weight loss of ~33% was observed with only 16 days of treatment (Zimmers *et al.* 2002). However in this Chapter an 18% drop in mean body mass after 30 days of treatment was observed. The reduced atrophic response presented in this Chapter compared to that of Zimmers *et al.* could be due to lowered Myostatin secretion as a result of a higher passage number for the CHO cells used in this study. Consistent with this theory, the tumours excised from mice injected with Myostatin-CHO cells were consistently smaller (data not shown) than those reported by Zimmers *et al.* (Zimmers *et al.* 2002). However, due to the observed reduction in mean body mass this approach was deemed suitable to investigate myostatin-induced cachexia *in vivo*.

Molecular analysis clearly indicates that Myostatin down-regulates *myoD* expression in both *in vitro* and *in vivo* models of cachexia (Figure 5.2A and 5.2B). In addition, promoter analysis confirmed that Myostatin inhibits the *myoD*

promoter (Figure 5.2D). Thus, myostatin functions to prevent muscle growth and regeneration through the regulation of *myoD* expression, ultimately resulting in a loss of muscle mass. Previous results indicate that MyoD is a direct down-stream target of the transcription factor NF-κB which is activated during cachexia by TNF-α (Guttridge *et al.* 2000). NF-κB is a potent inhibitor of MyoD expression, therefore it was hypothesised that myostatin may signal through NF-κB to regulate *myoD* expression. However, the results presented here clearly indicate that Myostatin treatment did not alter the expression or cellular localisation of NF-κB (p65) (Figure 5.4A, Figure 5.4B and Figure 5.4C). This data is in agreement with previously published results showing that Myostatin signalling does not activate NF-κB in C2C12 cells (Bakkar *et al.* 2005). Thus myostatin appears to function independently of NF-κB to regulate cachectic events. One gene of particular importance with respect to myogenesis is Pax3. Interestingly, Pax3 lies genetically upstream of MyoD (Tajbakhsh *et al.* 1997) and ectopic expression of Pax3 has been shown to activate MyoD (Maroto *et al.* 1997). Furthermore, an *in vivo* gain of function mutation in *pax3*, through the insertion of a Pax3-FKHR fusion sequence, also results in activation of *myoD* (Relaix *et al.* 2003). Current gene expression (Figure 5.2A and Figure 5.2B) and promoter analysis (Figure 5.2C) indicates that myostatin inhibits *pax3* expression. Together these data suggest that myostatin may regulate *myoD* expression through a preceding inhibition of *pax3*, thus contributing towards the observed cachectic phenotype following Myostatin treatment. Myostatin-induced loss of MyoD has serious repercussions on skeletal muscle tissue, as without MyoD the transcription of several muscle specific genes is inhibited, leading to reduced myogenesis (Bergstrom *et al.* 2002; Bean *et al.* 2005). During atrophy, an attempt is made to repair the loss of muscle fibres by activating satellite cells which in turn migrate to the site of injury and either replace lost muscle cells, or self-renew to refurnish the quiescent satellite cell pool (Hawke and Garry 2001). Myostatin has previously been shown to inhibit the activation and self-renewal of satellite cells (McCroskery *et al.* 2003). MyoD is also essential for the activation of satellite cells (Megeney *et al.* 1996), therefore the down-regulation of *myoD* that is evident in myostatin-induced cachexia may also result in an inhibition of satellite cell activation. This would further prevent the regeneration of skeletal muscle, thus

contributing greatly to the maintenance of muscle wasting due to increased myostatin expression.

One of the salient features of cachexia is the increased degradation of muscle proteins; this is due to activation of the ubiquitin-proteasome pathway and other proteolytic systems by various cachexia-inducing factors. Although myostatin has been previously shown to induce cachexia *in vivo* (Zimmers *et al.* 2002), there is no prior documentation demonstrating the ability of myostatin to regulate genes involved with proteolytic degradation. Both candidate gene expression analysis (Figure 5.3) and microarray analysis (Table 5.1) presented in this Chapter indicate that proteolytic genes are indeed significantly up-regulated following Myostatin treatment, including the recently characterised E3 ligase Atrogin-1. In addition Myostatin treatment results in an increase in the levels of ubiquitin-conjugated proteins. This result is consistent with previous publications highlighting the role of the ubiquitin-proteasome pathway in muscle atrophy. Indeed, increased Atrogin-1 expression is detected following starvation and dexamethasone treatment of C2C12 myotubes (Sandri *et al.* 2004). Furthermore, Atrogin-1 levels are elevated in rats experiencing muscle wasting induced by diabetes, uraemia, tumour growth and fasting (Lecker *et al.* 2004). In contrast, MuRF-1, an E3 ligase that has also been associated with many forms of muscle wasting, was only marginally up-regulated during myostatin-induced cachexia *in vivo* (Figure 5.3B). This selective gene regulation may form the underlying basis for myostatin-induced cachexia.

IκBα is a potent and specific inhibitor of NF-κB activity, which functions by binding to an inhibiting NF-κB nuclear import (Chen 2005). In the canonical NF-κB signalling pathway, IκB proteins are phosphorylated at amino-terminal serine residues (DiDonato *et al.* 1997; Regnier *et al.* 1997; Zandi *et al.* 1997). The resulting phosphorylated IκB proteins are targeted for polyubiquitination, with subsequent degradation by the proteasome (Chen *et al.* 1995), thus relieving NF-κB repression. As described above, stable cell lines expressing a mutated IκBα protein, whereby the serine residues have been replaced with alanines, were utilised in this Chapter (Guttridge *et al.* 1999). The resulting IκBα protein is no longer phosphorylated or targeted for degradation, thus proving to be a very potent inhibitor of NF-κB activity. Therefore the ability of myostatin to regulate Atrogin-1 in these cells was analysed. As shown in Figure 5.4D Myostatin

treatment resulted in a ~110% increase in *atrogin-1* expression as determined by Northern Blot analysis. These data provide further evidence that myostatin signals independently of NF-κB to induce cachexia, as shown by the ability of Myostatin to induce *atrogin-1* expression in the absence of NF-κB activity. As stated, myostatin appears to induce cachectic conditions through an NF-κB independent pathway. Interestingly TNF-α has recently been shown to induce the expression of Atrogin-1 through a p38-dependent, NF-κB-independent pathway (Li *et al.* 2005). Indeed, myostatin has been shown to signal through the p38 MAPK pathway to mediate growth inhibition and up-regulation of the cyclin-dependent kinase inhibitor p21 (Philip *et al.* 2005). Thus it is feasible that myostatin may signal through the p38 MAPK pathway to induce factors associated with muscle degradation such as Atrogin-1.

FoxO transcription factors have recently been shown to induce skeletal muscle atrophy through the up-regulation of Atrogin-1 (Sandri *et al.* 2004). Therefore, myostatin may up-regulate genes involved in ubiquitin-mediated proteolysis through a FoxO1-dependent pathway. Consistent with this, myostatin signalling appears to up-regulate FoxO1 expression (Figure 5.5A, 5.5B, 5.5C) and reduce the amount of phosphorylated FoxO1 (Figure 5.5D). Furthermore, Myostatin treatment induces nuclear accumulation of FoxO1 thus leading to increased levels of active FoxO1 (Figure 5.5E). This is in contrast with factors that induce hypertrophy, such as IGF-1 which has been shown to signal through the PI3-K/AKT pathway to increase the levels of phosphorylated FoxO1, thus maintaining FoxO1 cytoplasmic localisation away from target genes (Stitt *et al.* 2004). Therefore, myostatin may function by targeting and inactivating AKT (Figure 5.5F), leading to active FoxO1 and increased Atrogin-1 expression. Furthermore, siRNA-mediated knockdown of FoxO1 impaired the ability of Myostatin to induce *atrogin-1* expression (Figure 5.6A); thus, providing further evidence for a FoxO1-dependent pathway during myostatin-induced cachexia. As seen in Figure 5.6A Myostatin was still able to increase the expression of *atrogin-1* in the presence of the FoxO1 siRNA when compared to non-silencing controls, albeit to a lesser degree. One possible explanation for this observation is that although a ~70% decrease in FoxO1 expression was observed with siRNA transfection (Figure 5.6B); FoxO1 was not completely silenced, thus allowing Myostatin to partially induce *atrogin-1* expression. Therefore myostatin appears to antagonise

the IGF-1/PI3-K/AKT hypertrophy signalling pathway during the induction of cachectic conditions.

Interestingly, microarray analysis suggests that several genes encoding specific structural proteins including Myosin Heavy Chain, Troponin C, Tropomyosin 3 and Titin-cap were down-regulated during myostatin-mediated cachexia (Table 5.1). The calcium-dependent Calpain system has previously been shown to degrade several myofibrillar proteins such as Troponin and Tropomyosin (Goll *et al.* 2003) therefore myostatin may regulate Calpain dependent degradation of primary muscle structure. However, no significant changes in Calpain expression were detected as a result of the microarray (data not shown). Calpain-mediated degradation is thought to occur early during muscle atrophy (Costelli *et al.* 2002; Jagoe *et al.* 2002), therefore any changes in Calpain expression as a result of Myostatin treatment may be undetectable using the current *in vitro* model of myostatin-mediated myotube atrophy. Alternatively myostatin may directly down-regulate the expression of the identified myofibrillar proteins thus directly affecting primary muscle structure.

Like other cachexia-inducing factors, myostatin appears to induce cachexia by blocking protein synthesis and activating protein degradation (Figure 5.7). However, it was discovered in this study that myostatin acts independently of the classical TNF-α and NF-κB pathway to inhibit *myoD* expression and signal cachexia (Figure 5.7). Functional blockade of Myostatin in *mdx* mice, a model of Duchenne Muscular Dystrophy, appears to ameliorate the muscle loss observed in this model (Bogdanovich *et al.* 2002). Therefore targeting myostatin or the mechanisms through which myostatin functions may provide new therapeutic strategies to combat the symptoms of cachexia.

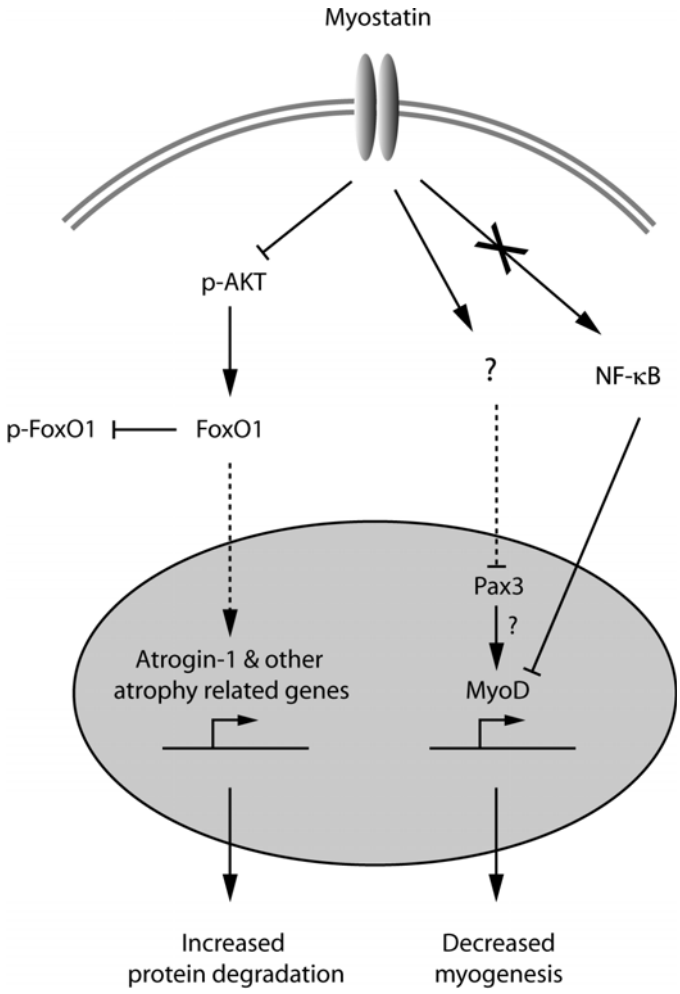

Figure 5.7 *Proposed mechanism behind myostatin-induced cachexia*

Unlike TNF-α, myostatin appears to induce cachexia independent of the NF-κB pathway. Increased levels of Myostatin blocks myogenesis by down-regulating *pax3* and *myoD* expression. In addition, myostatin appears to up-regulate the ubiquitin proteolysis system by hypo-phosphorylating FoxO1 through the inhibition of the PI3-K/AKT signalling pathway. Broken lines represent nuclear translocation. Arrows represent activation while blunt-ended lines represent inhibition.

5.5 Acknowledgements

Thanks to Dr Se-Jin Lee, Johns Hopkins University School of Medicine, Baltimore for gifting the Myostatin-expressing CHO cells used in this Chapter. Further thanks to Dr Denis C. Guttridge, Ohio State University, Ohio for gifting the IκBα SR cells used in this Chapter. Thanks also to Dr John P. Capone, McMaster University, Canada and Dr Jonathan A. Epstein, University of Pennsylvania, Philadelphia for gifting of constructs used in this Chapter. Thanks to Dr Cam Patterson, University of North Carolina, for gifting of Atrogin-1 antibody used in this Chapter. Thanks to Dr Chris McMahon, AgResearch, for advice on animal manipulations. Further thanks to the Foundation for Research Science and Technology (New Zealand) for financial support. Initial characterisation of the *in vitro* and *in vivo* Myostatin-mediated cachexia models was performed by Erin Plummer. Thanks to Mark Thomas for plating and maintaining the C2C12 myoblast cell line. Thanks also to Alex Hennebry for contributing to dissection of muscle tissues. Further thanks to Murray Ashby for injecting the Myostatin over-expressing CHO cells.

5.6 References

Amthor, H., G. Nicholas, I. McKinnell, C. F. Kemp, M. Sharma, R. Kambadur and K. Patel (2004). "Follistatin complexes Myostatin and antagonises Myostatin-mediated inhibition of myogenesis." Dev Biol **270**(1): 19-30.

Bakkar, N., H. Wackerhage and D. C. Guttridge (2005). "Myostatin and NF-κB Regulate Skeletal Myogenesis Through Distinct Signaling Pathways." Signal Transduction **5**(4): 202-210.

Bean, C., M. Salamon, A. Raffaello, S. Campanaro, A. Pallavicini and G. Lanfranchi (2005). "The Ankrd2, Cdkn1c and calcyclin genes are under the control of MyoD during myogenic differentiation." J Mol Biol **349**(2): 349-66.

Bergstrom, D. A., B. H. Penn, A. Strand, R. L. Perry, M. A. Rudnicki and S. J. Tapscott (2002). "Promoter-specific regulation of MyoD binding and signal transduction cooperate to pattern gene expression." Mol Cell **9**(3): 587-600.

Black, B. L., J. D. Molkentin and E. N. Olson (1998). "Multiple roles for the MyoD basic region in transmission of transcriptional activation signals and interaction with MEF2." Mol Cell Biol **18**(1): 69-77.

Bodine, S. C., E. Latres, S. Baumhueter, V. K. Lai, L. Nunez, B. A. Clarke, W. T. Poueymirou, F. J. Panaro, E. Na, K. Dharmarajan, Z. Q. Pan, D. M. Valenzuela, T. M. DeChiara, T. N. Stitt, G. D. Yancopoulos and D. J. Glass (2001). "Identification of ubiquitin ligases required for skeletal muscle atrophy." Science **294**(5547): 1704-8.

Bogdanovich, S., T. O. Krag, E. R. Barton, L. D. Morris, L. A. Whittemore, R. S. Ahima and T. S. Khurana (2002). "Functional improvement of dystrophic muscle by myostatin blockade." Nature **420**(6914): 418-21.

Carlson, C. J., F. W. Booth and S. E. Gordon (1999). "Skeletal muscle myostatin mRNA expression is fiber-type specific and increases during hindlimb unloading." Am J Physiol **277**(2 Pt 2): R601-6.

Chen, Z., J. Hagler, V. J. Palombella, F. Melandri, D. Scherer, D. Ballard and T. Maniatis (1995). "Signal-induced site-specific phosphorylation targets I

kappa B alpha to the ubiquitin-proteasome pathway." Genes Dev **9**(13): 1586-97.

Chen, Z. J. (2005). "Ubiquitin signalling in the NF-kappaB pathway." Nat Cell Biol **7**(8): 758-65.

Cornelison, D. D., B. B. Olwin, M. A. Rudnicki and B. J. Wold (2000). "MyoD(-/-) satellite cells in single-fiber culture are differentiation defective and MRF4 deficient." Dev Biol **224**(2): 122-37.

Costelli, P., M. Bossola, M. Muscaritoli, G. Grieco, G. Bonelli, R. Bellantone, G. B. Doglietto, F. M. Baccino and F. R. Fanelli (2002). "Anticytokine treatment prevents the increase in the activity of ATP-ubiquitin- and Ca(2+)-dependent proteolytic systems in the muscle of tumour-bearing rats." Cytokine **19**(1): 1-5.

Costelli, P., M. Muscaritoli, M. Bossola, R. Moore-Carrasco, S. Crepaldi, G. Grieco, R. Autelli, G. Bonelli, F. Pacelli, F. J. Lopez-Soriano, J. M. Argiles, G. B. Doglietto, F. M. Baccino and F. Rossi Fanelli (2005). "Skeletal muscle wasting in tumor-bearing rats is associated with MyoD down-regulation." Int J Oncol **26**(6): 1663-8.

DiDonato, J. A., M. Hayakawa, D. M. Rothwarf, E. Zandi and M. Karin (1997). "A cytokine-responsive IkappaB kinase that activates the transcription factor NF-kappaB." Nature **388**(6642): 548-54.

Epstein, J. A., P. Lam, L. Jepeal, R. L. Maas and D. N. Shapiro (1995). "Pax3 inhibits myogenic differentiation of cultured myoblast cells." J Biol Chem **270**(20): 11719-22.

Goll, D. E., V. F. Thompson, H. Li, W. Wei and J. Cong (2003). "The calpain system." Physiol Rev **83**(3): 731-801.

Gomes, M. D., S. H. Lecker, R. T. Jagoe, A. Navon and A. L. Goldberg (2001). "Atrogin-1, a muscle-specific F-box protein highly expressed during muscle atrophy." Proc Natl Acad Sci U S A **98**(25): 14440-5.

Gonzalez-Cadavid, N. F., W. E. Taylor, K. Yarasheski, I. Sinha-Hikim, K. Ma, S. Ezzat, R. Shen, R. Lalani, S. Asa, M. Mamita, G. Nair, S. Arver and S. Bhasin (1998). "Organization of the human myostatin gene and expression in healthy men and HIV-infected men with muscle wasting." Proc Natl Acad Sci U S A **95**(25): 14938-43.

Guttridge, D. C., C. Albanese, J. Y. Reuther, R. G. Pestell and A. S. Baldwin, Jr. (1999). "NF-kappaB controls cell growth and differentiation through transcriptional regulation of cyclin D1." Mol Cell Biol **19**(8): 5785-99.

Guttridge, D. C., M. W. Mayo, L. V. Madrid, C. Y. Wang and A. S. Baldwin, Jr. (2000). "NF-kappaB-induced loss of MyoD messenger RNA: possible role in muscle decay and cachexia." Science **289**(5488): 2363-6.

Hasselgren, P. O., C. Wray and J. Mammen (2002). "Molecular regulation of muscle cachexia: it may be more than the proteasome." Biochem Biophys Res Commun **290**(1): 1-10.

Hawke, T. J. and D. J. Garry (2001). "Myogenic satellite cells: physiology to molecular biology." J Appl Physiol **91**(2): 534-51.

Hunter, J. G., M. F. van Delft, R. A. Rachubinski and J. P. Capone (2001). "Peroxisome Proliferator-activated Receptor gamma Ligands Differentially Modulate Muscle Cell Differentiation and MyoD Gene Expression via Peroxisome Proliferator-activated Receptor gamma - dependent and - independent Pathways." J Biol Chem **276**(41): 38297-306.

Jagoe, R. T., C. P. Redfern, R. G. Roberts, G. J. Gibson and T. H. Goodship (2002). "Skeletal muscle mRNA levels for cathepsin B, but not components of the ubiquitin-proteasome pathway, are increased in patients with lung cancer referred for thoracotomy." Clin Sci (Lond) **102**(3): 353-61.

Kambadur, R., M. Sharma, T. P. Smith and J. J. Bass (1997). "Mutations in myostatin (GDF8) in double-muscled Belgian Blue and Piedmontese cattle." Genome Res **7**(9): 910-6.

Karayiannakis, A. J., K. N. Syrigos, A. Polychronidis, M. Pitiakoudis, A. Bounovas and K. Simopoulos (2001). "Serum levels of tumor necrosis factor-alpha and nutritional status in pancreatic cancer patients." Anticancer Res **21**(2B): 1355-8.

Lalani, R., S. Bhasin, F. Byhower, R. Tarnuzzer, M. Grant, R. Shen, S. Asa, S. Ezzat and N. F. Gonzalez-Cadavid (2000). "Myostatin and insulin-like growth factor-I and -II expression in the muscle of rats exposed to the microgravity environment of the NeuroLab space shuttle flight." J Endocrinol **167**(3): 417-28.

Langley, B., M. Thomas, A. Bishop, M. Sharma, S. Gilmour and R. Kambadur (2002). "Myostatin Inhibits Myoblast Differentiation by Down-regulating MyoD Expression." J Biol Chem **277**(51): 49831-40.

Langley, B., M. Thomas, C. McFarlane, S. Gilmour, M. Sharma and R. Kambadur (2004). "Myostatin inhibits rhabdomyosarcoma cell proliferation through an Rb-independent pathway." Oncogene **23**(2): 524-34.

Lecker, S. H., R. T. Jagoe, A. Gilbert, M. Gomes, V. Baracos, J. Bailey, S. R. Price, W. E. Mitch and A. L. Goldberg (2004). "Multiple types of skeletal muscle atrophy involve a common program of changes in gene expression." Faseb J **18**(1): 39-51.

Lecker, S. H., V. Solomon, S. R. Price, Y. T. Kwon, W. E. Mitch and A. L. Goldberg (1999). "Ubiquitin conjugation by the N-end rule pathway and mRNAs for its components increase in muscles of diabetic rats." J Clin Invest **104**(10): 1411-20.

Li, H. H., V. Kedar, C. Zhang, H. McDonough, R. Arya, D. Z. Wang and C. Patterson (2004). "Atrogin-1/muscle atrophy F-box inhibits calcineurin-dependent cardiac hypertrophy by participating in an SCF ubiquitin ligase complex." J Clin Invest **114**(8): 1058-71.

Li, J., K. C. Liu, F. Jin, M. M. Lu and J. A. Epstein (1999). "Transgenic rescue of congenital heart disease and spina bifida in Splotch mice." Development **126**(11): 2495-503.

Li, Y. P., Y. Chen, J. John, J. Moylan, B. Jin, D. L. Mann and M. B. Reid (2005). "TNF-alpha acts via p38 MAPK to stimulate expression of the ubiquitin ligase atrogin1/MAFbx in skeletal muscle." Faseb J **19**(3): 362-70.

Li, Y. P. and M. B. Reid (2000). "NF-kappaB mediates the protein loss induced by TNF-alpha in differentiated skeletal muscle myotubes." Am J Physiol Regul Integr Comp Physiol **279**(4): R1165-70.

Li, Y. P., R. J. Schwartz, I. D. Waddell, B. R. Holloway and M. B. Reid (1998). "Skeletal muscle myocytes undergo protein loss and reactive oxygen-mediated NF-kappaB activation in response to tumor necrosis factor alpha." Faseb J **12**(10): 871-80.

Ma, K., C. Mallidis, S. Bhasin, V. Mahabadi, J. Artaza, N. Gonzalez-Cadavid, J. Arias and B. Salehian (2003). "Glucocorticoid-induced skeletal muscle

atrophy is associated with upregulation of myostatin gene expression." Am J Physiol Endocrinol Metab **285**(2): E363-71.

Maroto, M., R. Reshef, A. E. Munsterberg, S. Koester, M. Goulding and A. B. Lassar (1997). "Ectopic Pax-3 activates MyoD and Myf-5 expression in embryonic mesoderm and neural tissue." Cell **89**(1): 139-48.

McCroskery, S., M. Thomas, L. Maxwell, M. Sharma and R. Kambadur (2003). "Myostatin negatively regulates satellite cell activation and self-renewal." J Cell Biol **162**(6): 1135-47.

McCroskery, S., M. Thomas, L. Platt, A. Hennebry, T. Nishimura, L. McLeay, M. Sharma and R. Kambadur (2005). "Improved muscle healing through enhanced regeneration and reduced fibrosis in myostatin-null mice." J Cell Sci **118**(Pt 15): 3531-41.

McPherron, A. C., A. M. Lawler and S. J. Lee (1997). "Regulation of skeletal muscle mass in mice by a new TGF-beta superfamily member." Nature **387**(6628): 83-90.

Megeney, L. A., B. Kablar, K. Garrett, J. E. Anderson and M. A. Rudnicki (1996). "MyoD is required for myogenic stem cell function in adult skeletal muscle." Genes Dev **10**(10): 1173-83.

Moldawer, L. L. and E. M. Copeland, 3rd (1997). "Proinflammatory cytokines, nutritional support, and the cachexia syndrome: interactions and therapeutic options." Cancer **79**(9): 1828-39.

Montarras, D., C. Lindon, C. Pinset and P. Domeyne (2000). "Cultured myf5 null and myoD null muscle precursor cells display distinct growth defects." Biol Cell **92**(8-9): 565-72.

Nelson, K. A. (2000). "The cancer anorexia-cachexia syndrome." Semin Oncol **27**(1): 64-8.

Philip, B., Z. Lu and Y. Gao (2005). "Regulation of GDF-8 signaling by the p38 MAPK." Cell Signal **17**(3): 365-75.

Reardon, K. A., J. Davis, R. M. Kapsa, P. Choong and E. Byrne (2001). "Myostatin, insulin-like growth factor-1, and leukemia inhibitory factor mRNAs are upregulated in chronic human disuse muscle atrophy." Muscle Nerve **24**(7): 893-9.

Regnier, C. H., H. Y. Song, X. Gao, D. V. Goeddel, Z. Cao and M. Rothe (1997). "Identification and characterization of an IkappaB kinase." Cell **90**(2): 373-83.

Relaix, F., M. Polimeni, D. Rocancourt, C. Ponzetto, B. W. Schafer and M. Buckingham (2003). "The transcriptional activator PAX3-FKHR rescues the defects of Pax3 mutant mice but induces a myogenic gain-of-function phenotype with ligand-independent activation of Met signaling in vivo." Genes Dev **17**(23): 2950-65.

Sambrook, J., E. F. Fritsch and T. Maniatis (1989). Molecular cloning: A labatory manual, 2nd ed. N.Y., Cold Spring Harbour Laboratory Press.

Sandri, M., C. Sandri, A. Gilbert, C. Skurk, E. Calabria, A. Picard, K. Walsh, S. Schiaffino, S. H. Lecker and A. L. Goldberg (2004). "Foxo transcription factors induce the atrophy-related ubiquitin ligase atrogin-1 and cause skeletal muscle atrophy." Cell **117**(3): 399-412.

Schuelke, M., K. R. Wagner, L. E. Stolz, C. Hubner, T. Riebel, W. Komen, T. Braun, J. F. Tobin and S. J. Lee (2004). "Myostatin mutation associated with gross muscle hypertrophy in a child." N Engl J Med **350**(26): 2682-8.

Schulte, J. N. and K. E. Yarasheski (2001). "Effects of resistance training on the rate of muscle protein synthesis in frail elderly people." Int J Sport Nutr Exerc Metab **11 Suppl**: S111-8.

Sharma, M., R. Kambadur, K. G. Matthews, W. G. Somers, G. P. Devlin, J. V. Conaglen, P. J. Fowke and J. J. Bass (1999). "Myostatin, a transforming growth factor-beta superfamily member, is expressed in heart muscle and is upregulated in cardiomyocytes after infarct." J Cell Physiol **180**(1): 1-9.

Stitt, T. N., D. Drujan, B. A. Clarke, F. Panaro, Y. Timofeyva, W. O. Kline, M. Gonzalez, G. D. Yancopoulos and D. J. Glass (2004). "The IGF-1/PI3K/Akt pathway prevents expression of muscle atrophy-induced ubiquitin ligases by inhibiting FOXO transcription factors." Mol Cell **14**(3): 395-403.

Stovroff, M. C., D. L. Fraker, W. D. Travis and J. A. Norton (1989). "Altered macrophage activity and tumor necrosis factor: tumor necrosis and host cachexia." J Surg Res **46**(5): 462-9.

Tajbakhsh, S., D. Rocancourt, G. Cossu and M. Buckingham (1997). "Redefining the genetic hierarchies controlling skeletal myogenesis: Pax- 3 and Myf-5 act upstream of MyoD." Cell **89**(1): 127-38.

Thomas, M., B. Langley, C. Berry, M. Sharma, S. Kirk, J. Bass and R. Kambadur (2000). "Myostatin, a negative regulator of muscle growth, functions by inhibiting myoblast proliferation." J Biol Chem **275**(51): 40235-43.

Tisdale, M. J. (2002). "Cachexia in cancer patients." Nat Rev Cancer **2**(11): 862-71.

Tisdale, M. J. (2003). "The 'cancer cachectic factor'." Support Care Cancer **11**(2): 73-8.

Torelli, G. F., M. M. Meguid, L. L. Moldawer, C. K. Edwards, 3rd, H. J. Kim, J. L. Carter, A. Laviano and F. Rossi Fanelli (1999). "Use of recombinant human soluble TNF receptor in anorectic tumor-bearing rats." Am J Physiol **277**(3 Pt 2): R850-5.

Wehling, M., B. Cai and J. G. Tidball (2000). "Modulation of myostatin expression during modified muscle use." Faseb J **14**(1): 103-10.

Yaffe, D. and O. Saxel (1977). "Serial passaging and differentiation of myogenic cells isolated from dystrophic mouse muscle." Nature **270**(5639): 725-7.

Yarasheski, K. E., S. Bhasin, I. Sinha-Hikim, J. Pak-Loduca and N. F. Gonzalez-Cadavid (2002). "Serum myostatin-immunoreactive protein is increased in 60-92 year old women and men with muscle wasting." J Nutr Health Aging **6**(5): 343-8.

Zachwieja, J., S. Smith, I. Sinha-Hikim, N. Gonzalez-Cadavid and S. Bhasin (1999). "Plasma myostatin-immunoreactive protein is increased after prolonged bed rest with low-dose T3 administration." J Gravit Physiol **6**(2): 11-5.

Zandi, E., D. M. Rothwarf, M. Delhase, M. Hayakawa and M. Karin (1997). "The IkappaB kinase complex (IKK) contains two kinase subunits, IKKalpha and IKKbeta, necessary for IkappaB phosphorylation and NF-kappaB activation." Cell **91**(2): 243-52.

Zimmers, T. A., M. V. Davies, L. G. Koniaris, P. Haynes, A. F. Esquela, K. N. Tomkinson, A. C. McPherron, N. M. Wolfman and S. J. Lee (2002). "Induction of cachexia in mice by systemically administered myostatin." Science **296**(5572): 1486-8.

Chapter 6 Global gene expression analysis during myostatin-mediated cachexia

6.1 Introduction

The results presented in Chapter 5 outline the candidate gene approach used to identify the molecular mechanism behind myostatin-induced cachexia. To support the candidate approach, global gene expression changes were analysed in an *in vitro* model of myostatin-mediated cachexia. The widely used C2C12 myoblast cell line provides a convenient means to analyse gene expression patterns in response to a plethora of stimuli. Therefore, the C2C12 myotube model system was used to study myostatin-induced gene expression changes. In this Chapter results of the microarray analysis are described. In addition, the novel CXXC zinc finger motif-containing gene, CXXC5, was identified as one of the molecules that mediate myostatin signalling during muscle wasting.

The CXXC (Cys-X-X-Cys) zinc finger domain has eight conserved cysteine residues that bind to zinc. The CXXC domain is found in proteins that methylate cytosine and in proteins that bind to the methyl cytosine (Lee *et al.* 2001; Jorgensen *et al.* 2004; Allen *et al.* 2006). Methylation is used by mammals to prevent transcriptional initiation and to ensure the silencing of some genes (Wolffe *et al.* 1999); therefore genes that contain the CXXC domain appear to function as transcriptional regulators. CXXC5, initially characterised in 2004 (Katoh and Katoh 2004b), belongs to a family of CXXC motif-containing proteins consisting of eleven members: CXXC1, CXXC2 (FBXL10), CXXC3 (MBD1), CXXC4 (IDAX), CXXC5, CXXC6, CXXC7 (MLL), CXXC8 (FBXL11), CXXC9 (DNMT1) CXXC10 and CXXC11 (FBXL19) (Katoh and Katoh 2004a; Katoh and Katoh 2004b). CXXC5, a homolog of CXXC4, shares 45% homology with CXXC4. CXXC4, also known as Idax (inhibition of Dvl and Axin complex), has been shown to inhibit Wnt signalling through direct binding to the protein Dishevelled (Hino *et al.* 2001). Like Idax, CXXC5 has been linked with regulation of the Wnt signalling pathway (Kim *et al.* 2005); however, to date little

is known about the function of CXXC5. One recent paper gives a role for CXXC5 as a positive regulator of the NF-κB signalling cascade (Matsuda *et al.* 2003). Interestingly, NF-κB signalling has been found to have a role in the induction of muscle wasting (Li and Reid 2000; Cai *et al.* 2004). Furthermore, CXXC5 has been identified as a downstream target of both the TGF-β and BMP signalling cascades, and in fact is up-regulated in response to treatment of C2C12 cells with both BMP-2 and TGF-β1 (de Jong *et al.* 2002).

6.2 Materials and Methods

6.2.1 *Cell cultures*

For *in vitro* studies of myostatin-induced muscle wasting, C2C12 myoblasts (American Type Culture Collection; ATCC, Manassas, VA) were used (Yaffe and Saxel 1977). Cells were cultured in Dulbecco's Modified Eagle Medium (DMEM; Invitrogen, Carlsbad, CA), buffered with 17 mM of $NaHCO_3$ (Sigma, St Louis, MO) and 5% gaseous CO_2. 2.93 nM of Phenol Red (Sigma) was used as a pH indicator and antibiotics 1 x 10^5 IU/L penicillin (Sigma) and 100 mg/L streptomycin (Sigma) were added. Foetal Bovine Serum (FBS, Invitrogen) was added to the DMEM at 10% of the total volume for culturing cells under growth conditions. The recombinant Myostatin protein (Mstn) used in these *in vitro* experiments was generated and purified in our laboratory (Sharma *et al.* 1999). To assess the ability of myostatin to induce cachexia *in vitro*, C2C12 cells were grown as above, on Thermanox coverslips (Nalge Nunc International, Rochester, NY). The C2C12 cells were differentiated for 72 hr in Differentiation Medium (DMEM + 2% Horse Serum; HS) followed by a further 24 hr in Differentiation Medium with or without 10 μg/mL Mstn.

6.2.2 *Stable transfection and generation of clonal cell lines*

CXXC5 over-expressing C2C12 cells were generated by stable transfection of a pcDNA3-CXXC5 construct, which encodes full-length murine CXXC5 driven by a CMV promoter and includes both neomycin and ampicillin resistance cassettes. The pcDNA3-CXXC5 construct was generated by Bridgette Wilson, Functional Muscle Genomics, AgResearch, Hamilton, New Zealand (Wilson 2006). These stable cell lines were generated by transfection with 12.5 μg of pcDNA3-CXXC5 or pcDNA3 in 0.8 mL DMEM (no serum) mixed with 40 μL of Lipofectamine 2000 (Invitrogen) in 0.8 mL DMEM (no serum). After 20 min at room temperature the transfection mixture was added to the appropriate plates and incubated for 24 hr at 37˚C. Cells were then subjected to neomycin treatment at a concentration of 0.6 mg/mL and selected based on their ability to grow in the

presence of neomycin. After 21 days, neomycin-resistant cells were taken for further analysis or frozen in liquid nitrogen for later use. Clonal cell lines were generated by plating CXXC5 transfected cells at a clonal density of 25 cells/cm^2; individual neomycin-resistant colonies were isolated and further expanded to allow for analysis of CXXC5 expression. Three CXXC5 over-expressing clonal cell lines were selected for further study (CXXC5 clones 1, 2 and 3).

6.2.3 *Microarray analysis*

C2C12 cells were cultured in Differentiation Medium for 72 hr as outlined above followed by a further 24 hr in Differentiation Medium with or without 10 μg/mL Mstn. RNA was then isolated using TRIZOL reagent (Invitrogen) according to manufacturer's guidelines (see Section 2.2.10). Contaminating DNA was removed by DNase1 (Invitrogen) treatment. The RNA was then column purified using the RNeasy Midi Kit (Qiagen) following the manufacturer's guidelines (see Section 2.2.11), ethanol precipitated overnight at -20°C and resuspended in RNase-free water. Microarray analysis was performed by MWG, Ebersberg, Germany as per their standardised techniques, using the MWG mouse 30k array. Briefly, the Myostatin-untreated and -treated RNA samples were reverse transcribed and directly labelled with Cy3 or Cy5, respectively, or conversely Cy5/Cy3 as a control. Following co-hybridisation spots were scanned numerous times and signal intensities determined using Imagene software (BioDiscovery). The MWG proprietary software MAVI was then used for combining the data from multiple scans, normalisation and background correction. The ratio between signal intensity for both Cy3 to Cy5 and Cy5 to Cy3 were used to generate mean values for intensity of each gene, corresponding to fold up- or down-regulation. Gene expression changes were deemed significant if expression was up-regulated or down-regulated by ≥ 1.5-fold.

6.2.4 *Western Blot analysis*

Total protein was isolated as per the described method (see Section 2.2.13). Total protein (15 μg) was separated by 4-12% SDS-PAGE (Invitrogen) and transferred

to nitrocellulose membrane by electroblotting. The membranes were blocked in 0.3% BSA, 1% PEG (polyethylene glycol 4,000; Sigma), 1% PVP (polyvinylpyrrolidone 10,000; Sigma) for 1 hr at room temperature, then incubated with specific primary antibodies overnight at 4°C. Alternatively, the membranes were blocked overnight at 4ºC using a solution of TBST/5% milk, then incubated with specific primary antibodies for 3 hr at room temperature. The following primary antibodies were used for immunoblotting; 1:10,000 dilution of purified mouse monoclonal anti-ubiquitin antibody (sc-8017; Santa Cruz Biotechnology Inc., Santa Cruz, CA); 1:1,000 dilution of purified rabbit polyclonal anti-FKHR (FoxO1) antibody (sc-11350; Santa Cruz Biotechnology Inc.); 1:3,000 dilution of purified rabbit polyclonal anti-p-FKHR (p-FoxO1; Ser256) antibody (sc-22158-R; Santa Cruz Biotechnology Inc.); 1:400 dilution of rabbit polyclonal anti-MyoD antibody (sc-304; Santa Cruz Biotechnology Inc.); 1:400 dilution of purified rabbit polyclonal anti-myogenin antibody (sc-576; Santa Cruz Biotechnology Inc.); 1:400 dilution of purified mouse monoclonal anti-p21 antibody (556430; BD Pharmingen, San Diego, CA) or 1:10,000 dilution of purified mouse monoclonal anti-GAPDH antibody (RDI-TRK5G4-6C5, Research Diagnostics, Concord, MA). The membranes were washed (5 x 5 min) with TBST and further incubated with anti-rabbit IgG Horseradish Peroxidase (HRP) conjugate, 1:5,000 dilution (P0448; Dako, Glostrup, Denmark), or anti-mouse IgG HRP conjugate, 1:5,000 dilution (P0447; Dako) secondary antibodies for 1 hr at room temperature. The membranes were washed as above, and HRP activity was detected using Western Lightning Chemiluminescence Reagent Plus (NEL104; PerkinElmer Life And Analytical Sciences, Inc., Wellesley, MA).

6.2.5 *Cloning of atrogin-1 and FoxO1 upstream promoter elements*

The promoter fragments were PCR amplified using purified DNA from Bacterial Artificial Chromosome (BAC) clones, which contained regions of chromosome specific to murine *atrogin-1* (RP23-48C24, BACPAC resources) and murine *FoxO1* (RP24-337A16, BACPAC resources). Following PCR amplification, promoter regions were cloned into the pGEM-T easy vector, briefly, PCR purified PCR products were ligated into the pGEM-T easy vector, transformed into the DH5-α *E.coli* strain (Invitrogen) followed by DNA prurification using the

QIAprep Spin miniprep kit (27104; QIAGEN Inc. Valencia, CA). Positive transformants were selected and subjected to double restriction digestion using KpnI/BglII and KpnI/NheI for *atrogin-1* and *FoxO1* respectively. The now purified promoter regions were further subcloned into the pGL3b luciferase vector (Promega Corporation, Madison, WI). Clones positive for *atrogin-1* and *FoxO1* promoter regions were sequenced and subjected to restriction mapping using HindIII to confirm correct cloning of the promoter insert. One positive transformant for *atrogin-1* and *FoxO1* was selected and subjected to plasmid DNA isolation and purification using the QIAGEN Maxiprep plasmid DNA kit (12163; QIAGEN Inc.). The purified plasmids were subsequently transfected (see Section 6.2.6), and promoter-luciferase activity measured (see Section 2.2.9). PCR was performed with 1 μL of the purified BAC clone DNA at 98°C for 30 s, 60°C for 30 s, and 72°C for 4 min 30 s for 30 cycles using *ThermalAce* DNA polymerase (Invitrogen). This was followed by a single 72°C extension step for 10 min. The following murine-specific primers were used to PCR amplify the promoter fragments. *atrogin-1* promoter Fwd, 5'-GGG GTA CCC TTC TCC AGG CCA GTA GGT G-3'; *atrogin-1* promoter Rev, 5'-GGA AGA TCT TGG TAC AGA GCG CGG ACG CG-3'; *FoxO1* promoter Fwd, 5'-GGT ACC AGT GCC CAT GAA GTT TGG AG-3'; *FoxO1* promoter Rev, 5'-GCT AGC CCC ACC AGC AGA GAA GTA CC-3'.

6.2.6 *Transient co-transfections*

Transfections were performed on stably transfected CXXC5 clones to test the effect of CXXC5 on either the *atrogin-1* promoter or the *FoxO1* promoter enhancer region. Clones were seeded in 6 well plates at a density of 15,000 cells/cm^2. Following a 24 hr attachment period, the cells were transfected with 2 μg of each plasmid DNA using Lipofectamine 2000 (Invitrogen) reagent as per the manufacturer's guidelines (see Section 2.2.8.9). The myoblasts were then incubated overnight at 37^{o}C in 5% CO_2. Proliferation Medium (DMEM + 10% FBS) was then removed and replaced with Differentiation Medium for a further 72 hr for *FoxO1* transfections and 48 hr and 72 hr for *atrogin-1* transfections. Clones were transfected with either *atrogin-1* or *FoxO1* promoter constructs in conjunction with the β-galactosidase (β-gal) expression plasmid *pCH110* (GE

Healthcare Bio-Sciences Corp. Piscataway, NJ). Following treatment the medium was removed and cells were washed twice with 5 mL PBS per well and lysed in 300 µL of Reporter Lysis Buffer (Promega). Lysates were analysed for luciferase reporter gene activity (Promega) in a Turner Designs luminometer (Model TD-20/20). β-gal expression levels were also detected in each supernatant using the β-gal Enzyme Assay System (Promega) as per the manufacturer's guidelines (Promega) (see Section 2.2.9). The luciferase values for each sample were normalised to the corresponding β-gal value as a measure of transfection efficiency.

6.2.7 *Gene expression analysis by semi-quantitative RT-PCR*

RNA was isolated from C2C12 cells using TRIZOL reagent (Invitrogen) as per the manufacturer's protocol (See Section 2.2.10). RNA was reverse-transcribed into cDNA for use in semi-quantitative RT-PCR (Q-RT-PCR) analysis of gene expression. First-strand cDNA was synthesised in a 20 µL reverse transcriptase (RT) reaction from 5 µg of total RNA using a SuperScript II First-Strand Synthesis System (Invitrogen), according to the manufacturer's protocol (See Section 2.2.6.1). PCR was performed with *Taq* DNA polymerase (Roche Diagnostics Corporation, Indianapolis, IN) using 1 µL of the RT reaction at 94°C for 2 min, followed by 94°C for 20 s, a gene-specific annealing temperature for 30 s (see Table 2.7), then 72°C for 2 min. This process was repeated for 30 cycles for a*trogin-1, MuRF-1,* $E2_{14k}$, and $E2_{20k}$, 27 cycles for *RC2* and 20 cycles for *GAPDH*. This was followed by a single 72°C extension step for 5 min. These PCR conditions were used for Q-RT-PCR expression analysis

The following murine specific primers were used for performing the Q-RT-PCR: *CXXC5* Fwd, 5'-AAG CTT ATG TCG AGC CTC GGC GGT-3'; *CXXC5* Rev, 5'-GGA TCC TCA CTG AAA CCA CCG GAA-3'; $E2_{14k}$ Fwd, 5'-ATG TCG CCC CGG CCC GGA GGC TCA TG-3'; $E2_{14k}$ Rev, 5'-ATG AAT CAT TCC AGC TTT GTT CAA C-3'; *atrogin-1* Fwd, 5'-AAC ATG TGG GTG TAT CGG-3'; a*trogin-1* Rev, 5'-TCT TGA GGG GAA AGT GAG-3'; *MuRF-1* Fwd, 5'-GTT AAA CCA GAG GTT CGA G-3'; *MuRF-1* Rev, 5'-ATG GTT CGC AAC ATT TCG G-3'; $E2_{20k}$ Fwd, 5'- GGC GAC ACC ATG TCA TC -3'; $E2_{20k}$ Rev, 5'- ATG TCC TGG GCC TCA TC -3'; *RC2* Fwd, 5'- TCC AAA CCT GCC CAT

CTG CTA ACT -3'; *RC2* Rev, 5'- AGG CTG TGC TTT TCT CTG TGG TCT -3'; *GAPDH* Fwd, 5'-GTG GCA AAG TGG AGA TTG TTG GCC-3'; *GAPDH* Rev, 5'-GAT GAT GAC CCG TTT GGC TCC-3'.

6.2.8 *Proliferation assay*

Myoblast proliferation was assessed as described previously (Thomas *et al.* 2000). Briefly, C2C12 cultures were seeded on 96 well plates (Nalge Nunc) at a density of 1,000 cells per well in Proliferation Medium. After an overnight attachment period, cells were supplemented with fresh Proliferation Medium (DMEM 10% FBS). Cultures were subsequently fixed at 24 hr intervals. Cells were fixed in 100 μL of 10% formal saline (0.17% saline, 10% formaldehyde). Following the incubation periods, proliferation was assessed using the methylene blue photometric end-point assay, as previously described (Oliver *et al.* 1989). Briefly, the fixative was removed, 100 μL of stain (1% methylene blue, 0.01 M Borate buffer, pH 8.5) was added to each well and the cells were incubated for 30 min at room temperature. The stain solution was removed and the cells washed four times with 200 μL Borate buffer, followed by the addition of 200 μL 0.1 N HCl:70% ethanol, (1:1). The absorbance of the cells was read on a microplate reader (model 3550; Bio-Rad), at 655 nm. In this assay absorbance at 655 nm is directly proportional to final cell number. Samples were run in replicates of eight with the results representing two independent experiments.

6.2.9 *DNA fragmentation assay*

Genomic DNA isolation and fragmentation assay were based on the protocol from (Jiang *et al.* 2005). Following removal of the medium, cells were washed twice with PBS then lysed by addition of 200 μL of apoptosis lysis buffer [10 mM Tris-HCL (pH 8.0), 10 mM EDTA, 0.5% Triton X-100 and 0.1 mg/mL RNase A] with cells collected by scraping. Following 1 hr incubation at 37°C the lysates were treated with Proteinase K (0.2 mg/mL) at 54°C for 30 min. Genomic DNA was isolated by one separation with phenol/chloroform followed by two additional choloroform steps. Genomic DNA was precipitated with 100% ethanol and

sodium acetate for 1 hr at -20°C, washed with 70% ethanol and resuspended in 100 μL of 10 mM Tris-HCL, 1 mM EDTA (TE) buffer. Aliquots of genomic DNA from control and CXXC5 over-expressing clones were subjected to DNA electrophoresis on a 1.0% agarose gel and visualised with ethidium bromide using the Gel Doc imaging system (Bio-Rad Laboratories, Hercules, CA).

6.2.10 *Detection of Tubulin by immunocytochemistry*

Myotube cultures grown on Permanox chamber slides (Nalge Nunc) were fixed with 70% ethanol:formaldehyde:glacial acetic acid (20:2:1) for 30 s, then rinsed three times with PBS. Cells were permeabilised with 0.1% triton X-100 in PBS for 10 min at room temperature then washed with PBS. Cells were then blocked in 5% NGS in 0.35% Carrageenen λ (Sigma) in PBS for 1 hr at room temperature; the same solution was used for subsequent antibody and fluorophore dilutions. Cells were incubated with mouse monoclonal anti-α-Tubulin antibody (T-9026; Sigma) overnight at 4˚C. The next day, slides were washed 3 times for 5 min in TBST before secondary incubation with biotinylated sheep anti-mouse IgG (RPN1001; GE Healthcare Bio-Sciences) at 1:300 for 1 hr at room temperature. Following another 3 washes in TBST, fluorescent complex Alexa Fluor 488 (S11223; Invitrogen) was added at 1:400 and incubated for 1 hr at room temperature. After a further 3 washes in TBST, slides were incubated with DAPI (1:1000 in PBS, Invitrogen) for 5 min at room temperature, rinsed with PBS, and mounted using fluorescent mounting medium (Dako, Glostrup, Denmark). Cells were visualised using an Olympus BX50 microscope (Olympus Optical Co, Germany) with a SPOT RT camera (Diagnostic Instruments Inc, Sterling Heights, MI) and the Windows Version 4.0.1 SPOT Basic software program (Diagnostic Instruments Inc).

6.2.11 *Cell staining*

To assess CXXC5 clone myotube formation during differentiation, cultures were grown on Thermanox coverslips (Nalge Nunc) in Differentiation Medium (DMEM + 2% HS), fixed with 20:2:1 and stained with Gill's haematoxylin

followed by 1% eosin (see Section 2.2.17). Cells were then photographed as above with myotube number counted.

6.2.12 *Statistics*

For CXXC5 over-expressing clone and control myotube assessment, average myotube number (±SEM) over 3 coverslips per timepoint was calculated. Total myotubes were counted in 5 random images per coverslip. For the transfection experiments, the mean luciferase values were calculated per well and the three means averaged over three independent experiments. To determine the significance level of differences between two groups, comparisons were made using Student's-T test. Statistical analysis was performed in Excel. A P value of <0.05 was deemed significant for all experiments.

6.3 Results

6.3.1 Microarray identification of myostatin downstream target genes

Microarray analysis was performed to compare the *in vitro* gene expression changes which occur in a model of myostatin-induced muscle wasting. Alterations in gene expression were quantified for 30,000 mouse genes in response to treatment with Myostatin. Table 6.1 summarises the global gene changes that were identified by microarray, with genes separated on the basis of function. The number given in the fold-change column represents the difference in gene expression when comparing cells treated with Myostatin to untreated controls (Table 6.1). For the purpose of substantiating the candidate gene approach, microarray-identified changes in mRNA levels of genes involved in protein degradation and myofibrillar structure were integrated into the communicated paper described in Chapter 5 (see Section 5.3.5 and Table 5.1).

The mRNA expression of genes involved in several cellular processes was altered in response to treatment with Myostatin. Treatment with recombinant Myostatin protein enhanced the expression of the extracellular matrix protein collagen. In particular, mRNA levels for *type-III* and *type-VI collagen* and *type-III* and *type*-IX *procollagen* were up-regulated following Myostatin treatment (Table 6.1).

The mRNA levels of two fundamental genes involved in energy production were altered following addition of Myostatin. The expression of the gene encoding *lactate dehydrogenease a* (*LDH-A*), an enzyme responsible for converting lactate to pyruvate during glycolysis (Lehninger *et al.* 1993), was down-regulated following Myostatin treatment. Conversely, the gene encoding *glutamine synthetase* (*glns*) was significantly up-regulated following addition of Myostatin (Table 6.1). Glutamine synthetase is an enzyme that catalyses the conversion of glutamate and ammonia into glutamine (Lehninger *et al.* 1993).

Several additional genes of interest were differentially regulated in response to increased levels of Myostatin. In particular, gene expression of the metal-binding metallothionein proteins 1 and 2 (*mt1 and mt2*) was down-regulated following treatment with Myostatin; while the mRNA expression of *stress-induced protein 18* (*sip18*) was up-regulated in response to increased Myostatin (Table 6.1).

Furthermore, genes encoding the proteolytic enzymes matrix metalloproteinase-2 and -23 (mmp-2 and mmp-23) were up-regulated following Myostatin treatment, while in contrast, expression of *tissue inhibitor of matrix metalloproteinase-1* (*timp-1*) was down-regulated (Table 6.1). The gene *lipin-1* which encodes for Lipin protein was also significantly induced following addition of Myostatin. In addition, genes encoding the transcription factors, myocyte enhancer factor 2b (mef2b), forkhead box O 1 (FoxO1), and the CXXC finger 5 (CXXC5) zinc finger protein were all up-regulated in response to myostatin treatment (Table 6.1). The mRNA expression of the gene encoding CXXC5 was dramatically up-regulated, demonstrating an almost 9.5-fold induction in response to Myostatin treatment (Table 6.1). As shown in Figure 6.1, Q-RT-PCR analysis has subsequently confirmed Myostatin up-regulation of *CXXC5*, albeit to a lesser degree than that seen in the microarray data. Despite the variation, the putative zinc finger transcription factor CXXC5 has potential as a myostatin downstream target gene and therefore was selected to be studied further.

Function	Sequence Name	Accession No.	Fold change	
Extracellular matrix	collagen, type VI, alpha 2 chain	Z18272	2.2	⇧
	collagen, type III, alpha 1; (col3a1)	X52046	3.6	⇧
	procollagen, type IX, alpha 1	X57984	3.2	⇧
	procollagen, type III, alpha 1	AK019448	2.2	⇧
Metabolism	glutamine synthetase (glns)	NM_008131	2.3	⇧
	lactate dehydrogenase 1, a chain (ldh1)	NM_010699	2.2	⇩
Transcription factors	myocyte enhancer factor 2b (mef2b)	NM_008578	2.1	⇧
	forkhead box O1a (foxO1)	NM_019739	1.9	⇧
	CXXC5	NM_133687	9.5	⇧
Miscellaneous	Metallothionein 1 (mt1)	NM_013602	3.1	⇩
	Metallothionein 2 (mt2)	AK002567	3.9	⇩
	Stress-induced protein 18 (sip18)	AY034611	2.8	⇧
	Matrix metalloproteinase 2 (mmp2)	NM_008610	1.7	⇧
	Matrix metalloproteinase 23 (mmp23)	NM_011985	1.9	⇧
	Tissue inhibitor of matrix metalloproteinase 1 (timp1)	NM_011593	2.1	⇩
	Lipin-1	NM_015763	3.0	⇧

Table 6.1 *Microarray identification of genes altered in a model of myostatin-induced cachexia*

C2C12 cells were grown in Differentiation Medium for 72 hr followed by a further 24 hr in Differentiation Medium without or with 10 μg/mL Mstn. Genes are separated into structural or proteolytic function and were at least 1.5 fold up-regulated (⇧) or down-regulated (⇩).

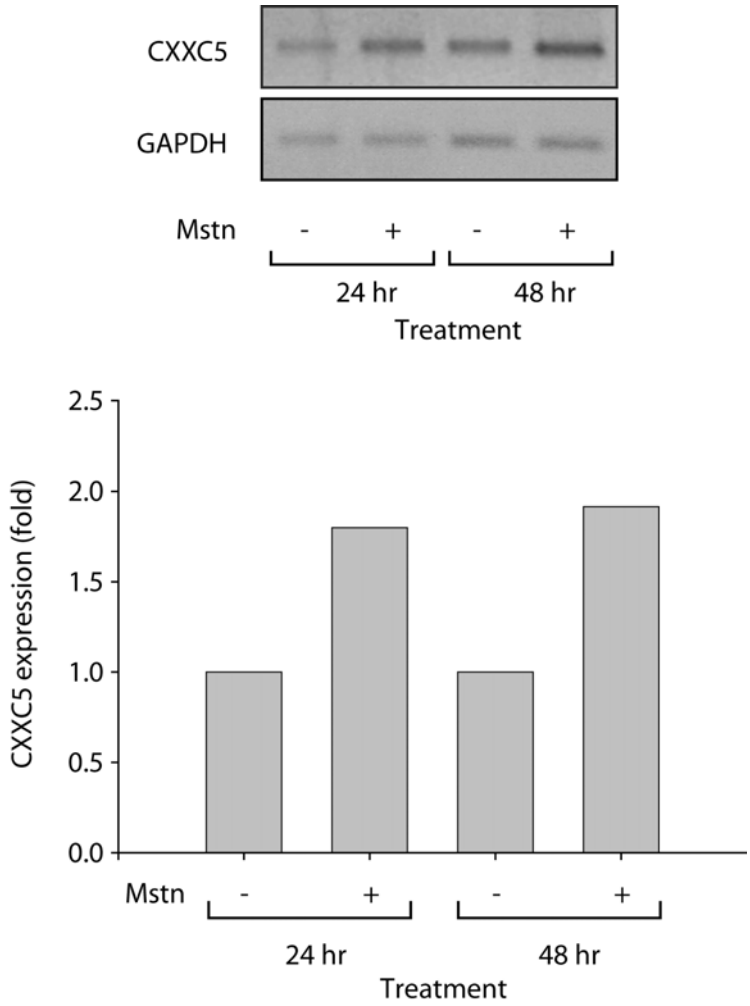

Figure 6.1 *Myostatin up-regulates the expression of CXXC5*

Semi-quantitative RT-PCR analysis of CXXC5 expression following treatment of C2C12 cells with recombinant Myostatin protein (Mstn). C2C12 cells were grown in Differentiation Medium for 72 hr followed by a further 24 hr or 48 hr in Differentiation Medium without (-) or with 10 μg/mL (+) Mstn. GAPDH levels were measured to ensure equal loadings. The graph represents fold change in CXXC5 expression normalised to GAPDH levels.

6.3.2 Stable over-expression of CXXC5 in the C2C12 myoblast cell line

To further characterise the function of CXXC5 a set of CXXC5 over-expressing stable clonal cell lines were generated. Briefly, the murine CXXC5 coding sequence was cloned into the pcDNA3 expression vector (Invitrogen) (see Section 6.2.2). The pcDNA3 expression vector contains a neomycin cassette, which allows for antibiotic-mediated selection of C2C12 cells which have stably integrated the CXXC5/pcDNA3 construct. Following transfection, the CMV promoter contained within pcDNA3 constitutively drives the expression of the gene of interest, in this case CXXC5. C2C12 cells were subjected to several rounds of antibiotic selection followed by quantification of CXXC5 expression. Q-RT-PCR identified that clones 1, 2, and 3 significantly up-regulated the mRNA expression of *CXXC5*, and thus were utilised to aid in the identification of putative functions for CXXC5 in skeletal muscle (Figure 6.2A).

A proliferation assay was performed to compare the proliferative potential of the CXXC5 clones compared to the control C2C12 cell line. As shown in Figure 6.2B, the growth rate of the CXXC5 clones (CXXC5 clone 1 and CXXC5 clone 3) was reduced to a statistically significant level when compared to that of control (C2C12) through the periods of 48 hr, 72 hr and 96 hr proliferation (Figure 6.2B). However, the difference between CXXC5 clones and control was not dramatic.

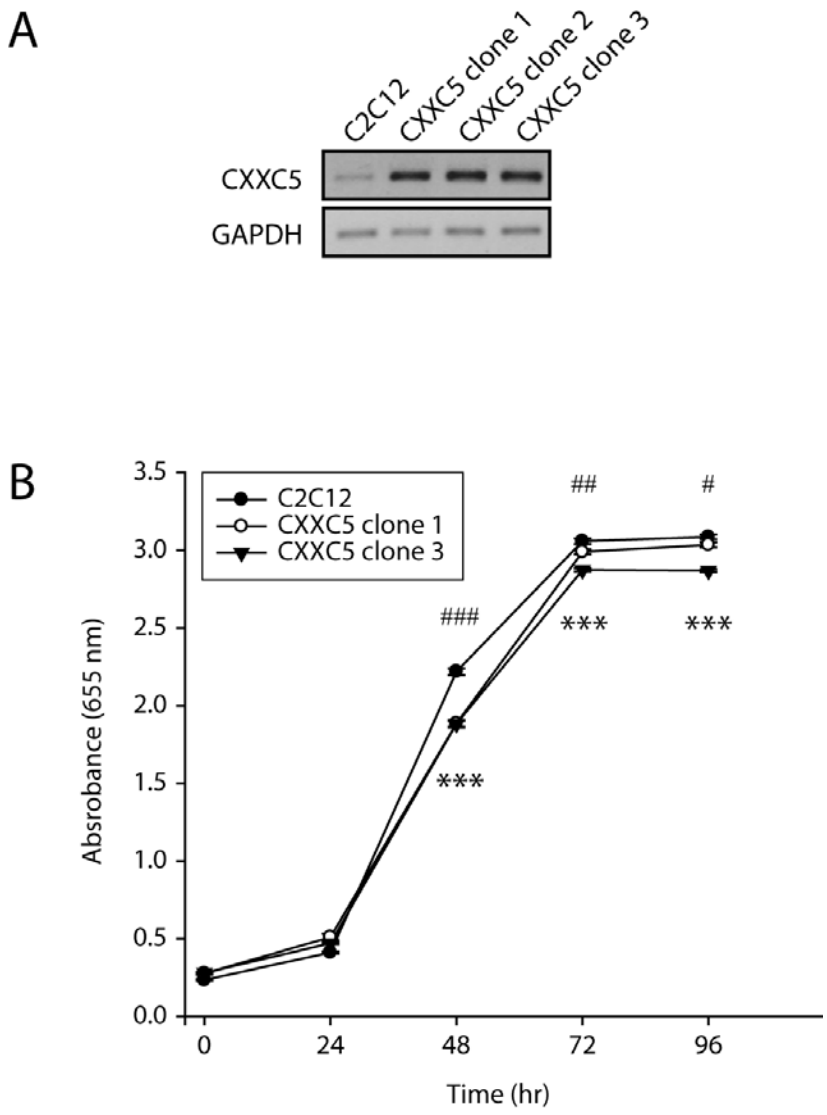

Figure 6.2 *CXXC5 alters C2C12 myoblast proliferation*

A) Q-RT-PCR showing mRNA expression of *CXXC5* during actively growing conditions in CXXC5 over-expressing (CXXC5 clone 1, CXXC5 clone 2 and CXXC5 clone 3) lysates compared to control (C2C12) lysates. *GAPDH* expression was analysed to ensure equal loading of samples. B) Methylene blue assay showing proliferation of control (C2C12) cells compared to CXXC5 over-expressing clones (CXXC5 clone 1 and clone 3) over a 96 hr period. Statistical differences determined by Student's-T test are indicated, P< 0.001 (***) for clone 3 compared to C2C12 and P< 0.001 (###), P< 0.01 (##), P< 0.05 (#) for clone 1 compared to C2C12.

Upon serum withdrawal, C2C12 myotubes rapidly exit the cell cycle, fuse and form multinucleated myotubes. The differentiation capacity of the CXXC5 clones was thus examined and compared to that of the control C2C12 cell line. Myotube populations were stained with Gill's haematoxylin and eosin and total myotube number was counted. As shown in Figure 6.3A and 6.3B, a dramatic reduction in myotube formation during the progression of myogenic differentiation was observed in the CXXC5 clones when compared with the control (C2C12). Indeed, the CXXC5 clones exhibited a dramatic 10-100-fold reduction in myotube number at 48 hr differentiation (Figure 6.3B). CXXC5 clone 1 had a ~10-fold reduction in myotube number at 72 hr and a ~8-fold reduction in myotube number at 96 hr differentiation as compared to C2C12 control. In addition, CXXC5 clone 3 had a ~2.6-fold reduction in myotube number at 72 hr and a ~3-fold reduction in myotube number at 96 hr differentiation as compared to C2C12 control (Figure 6.3B). The CXXC5 clones also demonstrated several morphological characteristics distinctive from control cells. As can be seen in Figure 6.3A, very few myotubes were observed at 48 hr differentiation; however, by 72 hr, large myotubes began to appear in CXXC5 clones 1 and 3, although, compared to the densely populated control cell line the CXXC5 clone myotube cultures were relatively sparse (Figure 6.3A). By 96 hr differentiation the typical elongated myotube morphology was radically altered in the CXXC5 clones, whereby characteristic myotubes were progressively replaced with circular "myosac-like" formations, which appeared to be primarily comprised of large numbers of nuclei (Figure 6.3A). Therefore, in addition to a delay in myogenic differentiation, over-expression of CXXC5 appears to alter the typical myotube phenotype associated with the C2C12 myogenic cell line.

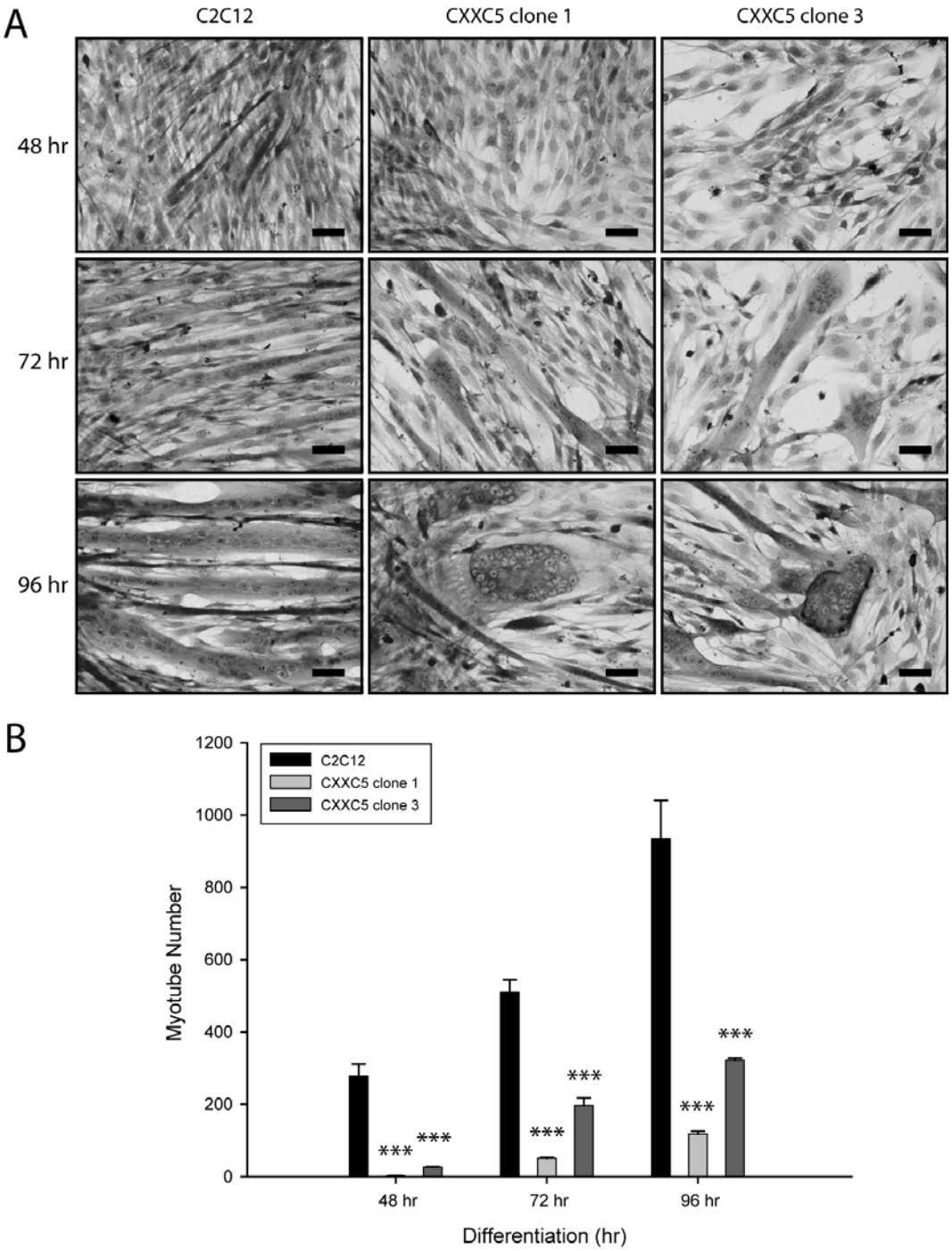

Figure 6.3 *CXXC5 alters myotube formation and physiology in C2C12 myoblasts*

A) Representative images of differentiating cells for CXXC5 over-expressing clones (CXXC5 clone 1 and 3) compared to control (C2C12) cells at 48 hr, 72 hr and 96 hr differentiation; cells were stained with Gill's haematoxylin and eosin. Scale bar represents 5 μm. B) The graph shows the average myotube number ±SEM over 3 coverslips per timepoint for CXXC5 over-expressing clones (CXXC5 clone 1 and 3) and control (C2C12) cells; total myotubes were counted in 5 random images per coverslip. Statistical differences determined by Student's-T test are indicated, $P<0.001$ (***) compared to C2C12.

6.3.3 Time-lapse microscopy of CXXC5 over-expressing clones during differentiation

To further characterise the "myosac" phenomenon, time-lapse microscopy was employed. CXXC5 clones were differentiated for 72 hr prior to time-lapse microscopy. During microscopy, cells were maintained under optimal conditions (37°C/5% CO_2), with images collected every minute over a 24 hr period spanning 72 hr-96 hr differentiation. Figure 6.4, Figure 6.5 and Figure 6.6 display still images of representative timepoints from C2C12 control, CXXC5 clone 1 and CXXC5 clone 3 respectively. As shown in Figure 6.4, the size of the indicated myotube appeared to increase with time, a phenomenon consistent with the progression of myogenic differentiation. Furthermore, no observed myosac formation was detected in the control cell line cultures (Figure 6.4). In contrast however, over-expression of CXXC5 resulted in a dramatic change in myotube morphology with what appeared to be gradual myotube collapse (Figure 6.5 and Figure 6.6). Interestingly, the myotube nuclei appeared to coalesce at one end of the myotube, followed by the eventual collapse of the remaining cytoplasm to that same general area. The resulting myotube disintegration resulted in the formation of the myosac-like phenotype characterised in Section 6.3.2 (Figure 6.5 and Figure 6.6). The 1441 time-lapse images taken at 1 min intervals were combined into movies and are included on the DVD attached to the back cover of this thesis (Appendix 2).

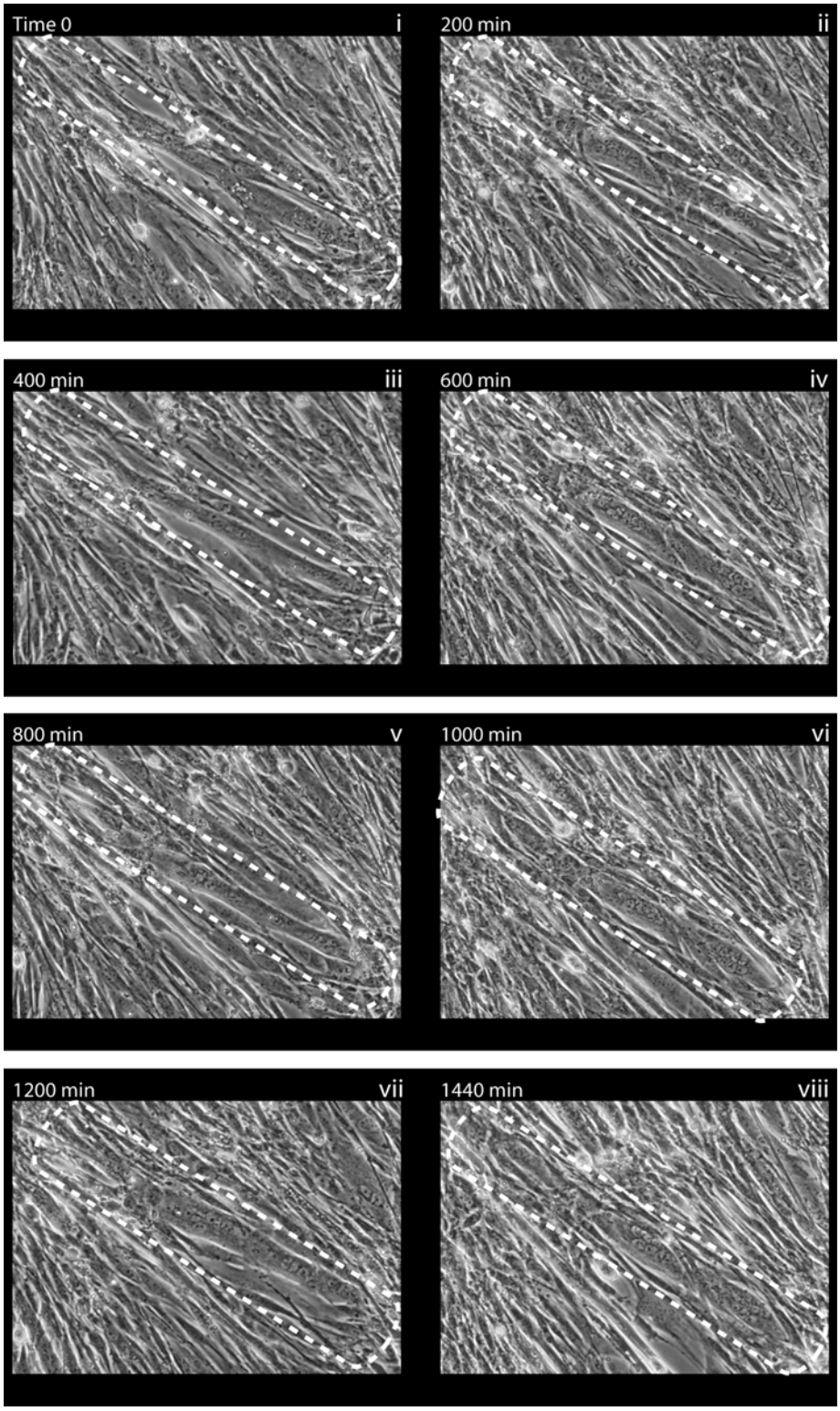

Figure 6.4 *Time-lapse microscopy of normal myotube growth in control C2C12 cells*

Time-lapse phase contrast microscopy covering a 24 hr period of differentiation between 72 hr and 96 hr in the control C2C12 cell line. Box i-viii show representative timepoints through the course of the time-lapse experiment with the corresponding minutes (min) indicated in the top left of each box. Dotted lines indicate the myotube of interest.

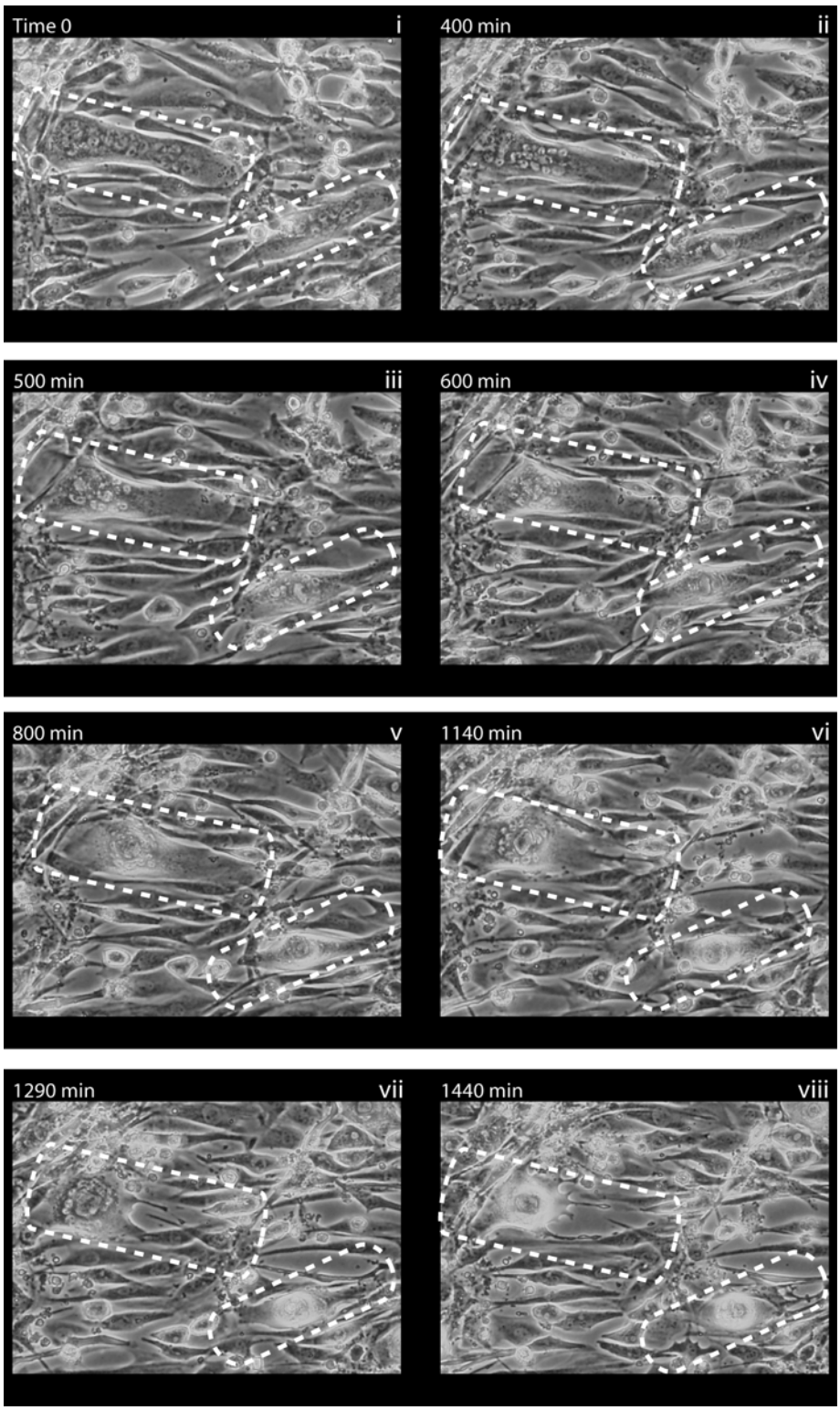

Figure 6.5 *Time-lapse microscopy of myosac formation in CXXC5 clone 1*

Time-lapse phase contrast microscopy covering a 24 hr period of differentiation between 72 hr and 96 hr in CXXC5 Clone 1. Box i-viii show representative timepoints through the course of the time-lapse experiment with the corresponding minutes (min) indicated in the top left of each box. Dotted lines indicate the myotube of interest.

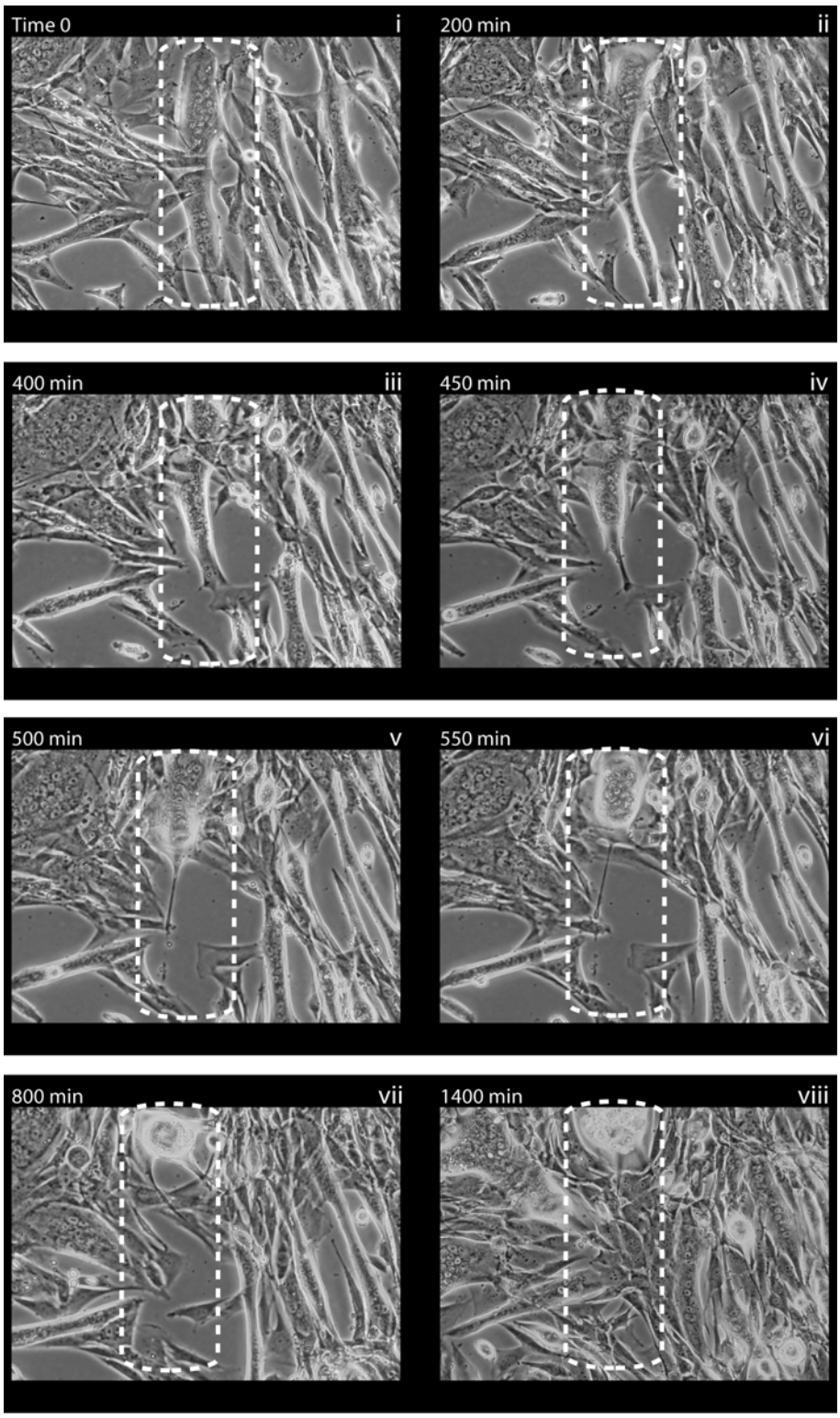

Figure 6.6 *Time-lapse microscopy of myosac formation in CXXC5 clone 3*

Time-lapse phase contrast microscopy covering a 24 hr period of differentiation between 72 hr and 96 hr in CXXC5 Clone 3. Box i-viii show representative timepoints through the course of the time-lapse experiment with the corresponding minutes (min) indicated in the top left of each box. Dotted lines indicate the myotube of interest.

6.3.4 Gene expression analysis of CXXC5 over-expressing clones

Gene expression analysis was undertaken to gain further insights into the effect of CXXC5 on C2C12 myoblast growth and differentiation. The Myogenic Regulatory Factors (MRFs), MyoD and myogenin play a critical role in the ability of myogenic cells to exit the cell cycle and adopt a differentiated phenotype. Furthermore, the cyclin-dependent kinase inhibitor (CKI) p21 is a target of MyoD, and in fact plays a critical role in MyoD-mediated myoblast cell cycle exit and commitment to differentiation (Guo *et al.* 1995; Halevy *et al.* 1995; Megeney and Rudnicki 1995). Therefore the expression patterns of these critical genes were analysed in the stable CXXC5 over-expressing clones during the progression of myogenic differentiation. MyoD expression was up-regulated in all cell lines following the induction of differentiation (Figure 6.7 and Figure 6.8). As expected the expression pattern of p21 closely followed that of MyoD and was up-regulated following the switch to differentiation, with peak p21 expression detected at 48 hr differentiation (Figure 6.7 and Figure 6.8). In addition, myogenin peak expression was detected at 48 hr differentiation in both the CXXC5 clones and C2C12 control, however, the peak expression of myogenin, and for that matter MyoD and p21, appeared to be higher in the CXXC5 clones as compared to the control (C2C12) cell line (Figure 6.7 and Figure 6.8). Thus as shown in Figure 6.7 and Figure 6.8, although peak gene expression was elevated in the CXXC5 over-expressing clones, the general pattern of MRF expression was similar to that observed in the control (C2C12) cells through the process of myogenic differentiation (Figure 6.7 and Figure 6.8).

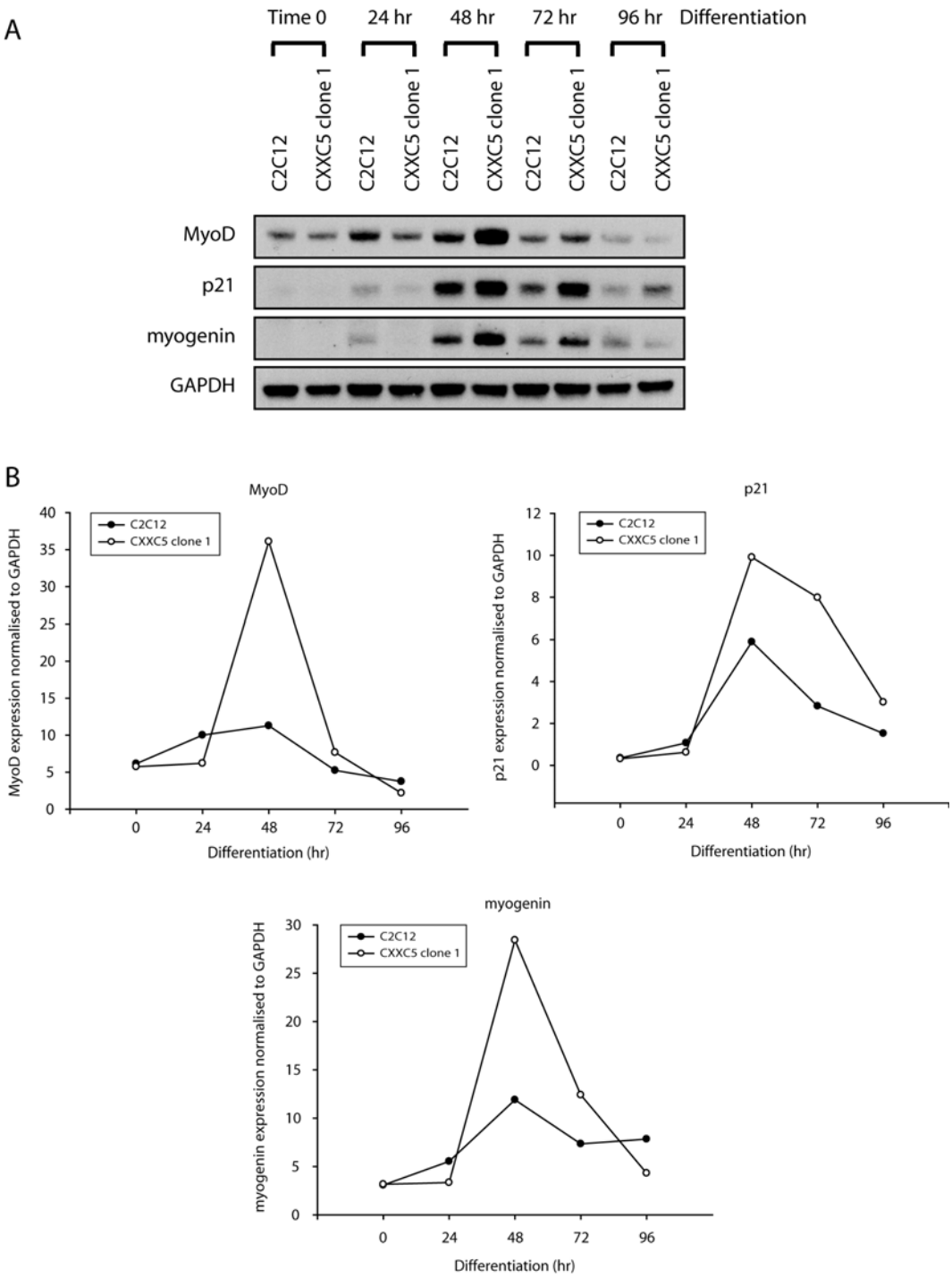

Figure 6.7 *Over-expression of CXXC5 alters myogenic gene expression during differentiation*

A) Western Blots showing protein expression of MyoD, p21 and myogenin at Time 0 and after 24, 48, 72 and 96 hr of differentiation in CXXC5 over-expressing (CXXC5 clone 1) lysates compared to control (C2C12) lysates. GAPDH expression was analysed to ensure equal loading of samples. B) Densitometry analysis of protein expression for Western Blots (MyoD, p21, myogenin), normalised to GAPDH expression, for CXXC5 over-expressing clones (CXXC5 clone 1) compared to control (C2C12) cells.

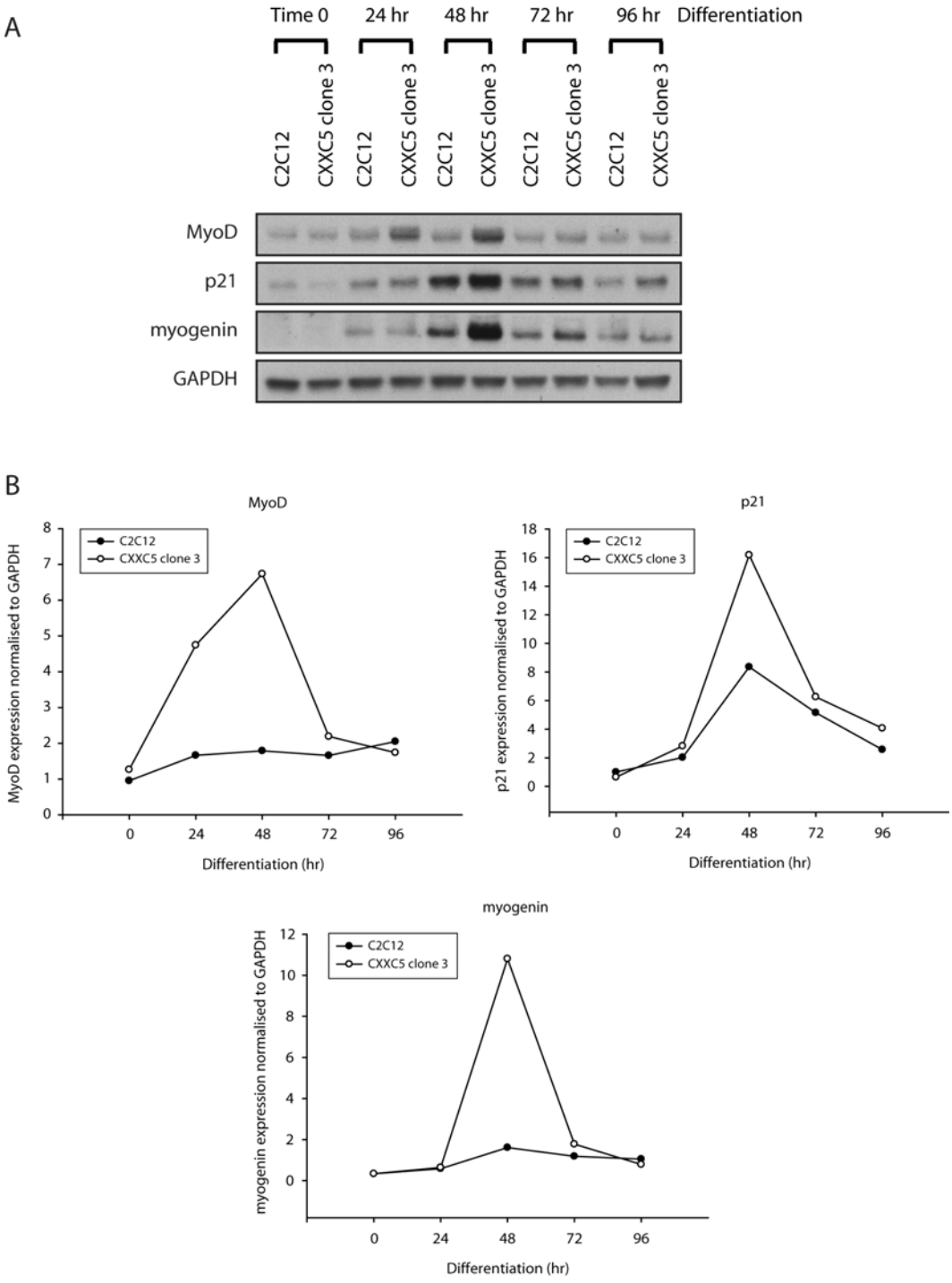

Figure 6.8 *Over-expression of CXXC5 alters myogenic gene expression during differentiation*

A) Western Blots showing protein expression of MyoD, p21 and myogenin at Time 0 and after 24, 48, 72 and 96 hr of differentiation in CXXC5 over-expressing (CXXC5 clone 3) lysates compared to control (C2C12) lysates. GAPDH expression was analysed to ensure equal loading of samples. B) Densitometry analysis of protein expression for Western Blots (MyoD, p21, myogenin), normalised to GAPDH expression, for CXXC5 over-expressing clones (CXXC5 clone 3) compared to control (C2C12) cells.

As outlined in Chapter 5, myostatin is capable of promoting muscle wasting through regulation of the ubiquitin-proteasome pathway; thus gene expression patterns in the CXXC5 over-expressing clonal cell lines were analysed, to determine if CXXC5 is capable of regulating components of the ubiquitin-proteasome pathway. Semi-quantitative RT-PCR (Q-RT-PCR) was used to measure the expression of several genes involved with ubiquitin-mediated degradation. As shown in Figure 6.9, Q-RT-PCR analysis of the CXXC5 clones demonstrated an up-regulation in the expression of the ubiquitin E3 ligase *atrogin-1*, however, no significant change was observed in the E3 ligase *MuRF-1* in response to increased expression of CXXC5 (Figure 6.9). Furthermore, expression levels of the ubiquitin-conjugating enzymes $E2_{14k}$ and $E2_{20k}$ as well as the proteasome sub-unit *RC2* were also significantly up-regulated in the CXXC5 over-expressing clones as compared with the control (C2C12) cell line (Figure 6.9). To further confirm CXXC5 regulation of *atrogin-1* an *atrogin-1* promoter-luciferase construct was generated. Specific primers were synthesised based on the published sequences from Sandri *et al* 2004 (Sandri *et al.* 2004). The resulting 3.5 Kb PCR product (Figure 6.10Ai) was purified and ligated into the pGEM-T easy cloning vector. The pGEM-T easy construct was transformed into the DH5α strain of *E.coli*. Following plasmid DNA purification the 3.5 kb promoter fragment was mobilised through Kpn1 and BglII restriction enzyme digestion, purified, and subcloned into the pGL3b luciferase vector. Restriction digestion using HindIII was performed to confirm the presence of the *atrogin-1* promoter in the pGL3b vector (Figure 6.10Aii). The *atrogin-1* promoter-luciferase construct was subsequently transfected into the CXXC5 over-expressing clones. As shown in Figure 6.10B, Over-expression of CXXC5 resulted in a significant increase in *atrogin-1*-dependent luciferase activity (Figure 6.10B). Specifically, *atrogin-1* promoter activity was up-regulated by ~2.5 and ~3.7 fold in CXXC5 clone 1 and 3 respectively at both 48 hr and 72 hr differentiation. Moreover, a dramatic ~40 fold up-regulation in *atrogin-1* promoter activity was observed following transfection into CXXC5 clone 2 at both 48 hr and 72 hr differentiation timepoints (Figure 6.10B). Thus CXXC5 appears to induce the expression of several components of the ubiquitin-proteasome pathway and therefore may contribute to ubiquitin-mediated muscle proteolysis. In support, over-expression of CXXC5 results in an increase in the levels of ubiquitin-conjugated proteins as determined

by Western Blot analysis (Figure 6.11). Moreover, the increase in ubiquitinated proteins was particularly prevalent during later differentiation timepoints (Figure 6.11). Conjugation of ubiquitin to proteins is a critical step in ubiquitin-mediated proteolysis; in fact ubiquitin-conjugation targets proteins for degradation through the proteasome. Therefore increased ubiquitin-conjugation is indicative of enhanced ubiquitin-proteasome pathway activity and thus increased protein degradation.

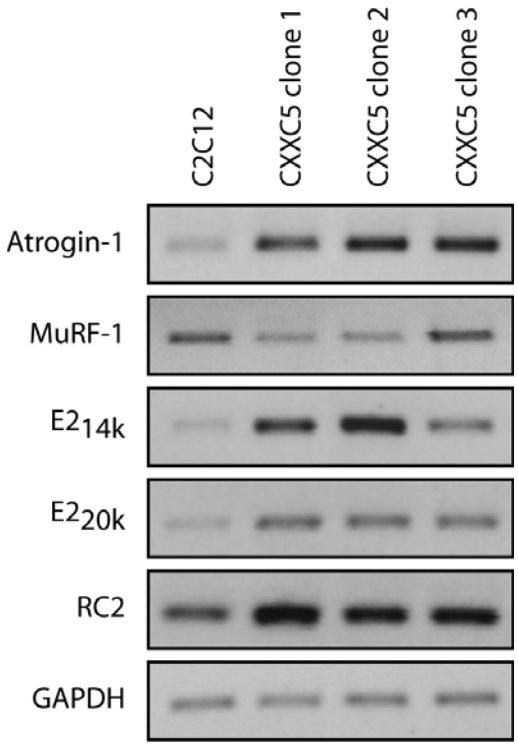

Figure 6.9 *Over-expression of CXXC5 up-regulates the expression of atrophy-related genes*

Q-RT-PCR showing the expression of *atrogin-1*, *MuRF-1, $E2_{14k}$*, *$E2_{20k}$* and *RC2* during proliferating conditions in CXXC5 over-expressing (CXXC5 clone 1, clone 2 and clone 3) lysates compared to control (C2C12) lysates. GAPDH expression was analysed to ensure equal loading of samples.

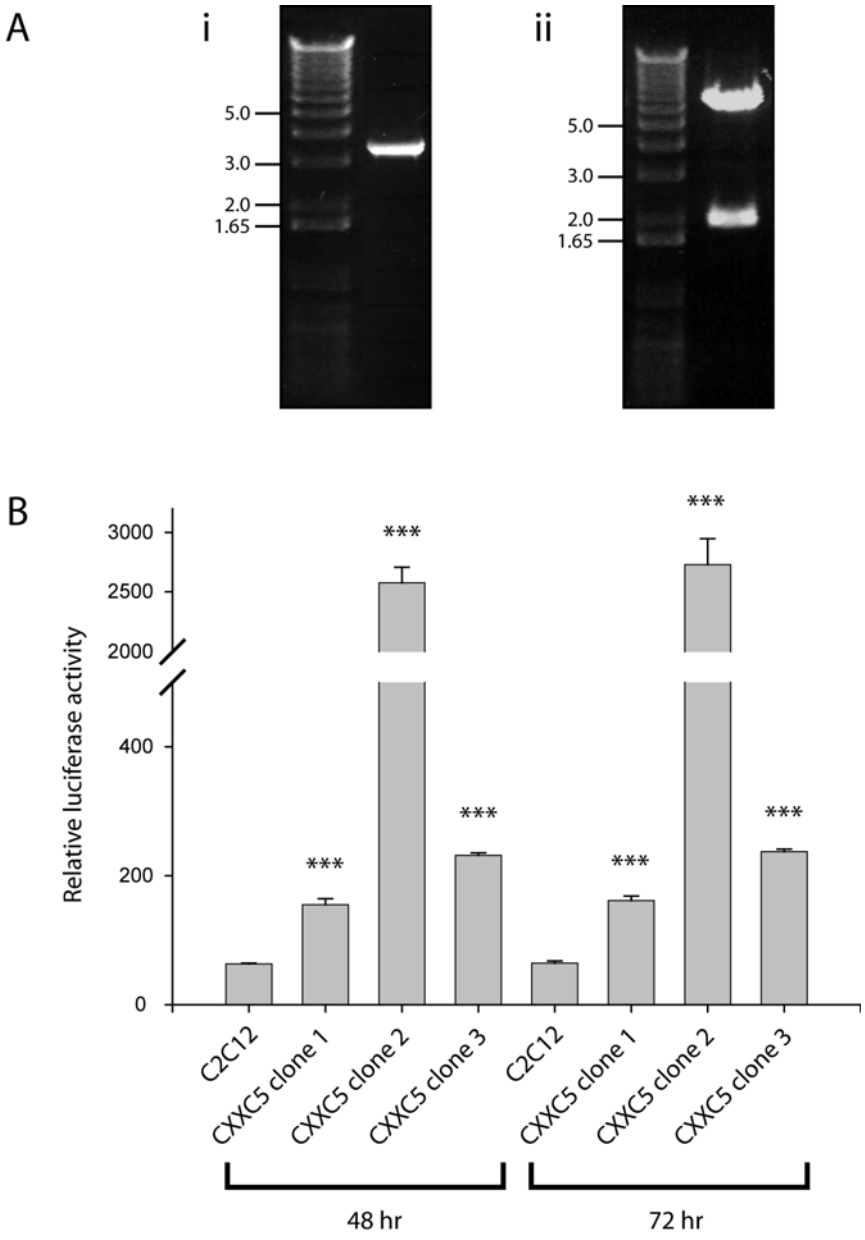

Figure 6.10 *Over-expression of CXXC5 up-regulates atrogin-1 promoter activity*

Ai) Agarose gel visualisation of the ~3.5 kb *atrogin-1* promoter PCR product. Aii) Agarose gel visualisation of the ~7 kb and ~2 kb products from the pGL3b/*atrogin-1* promoter HindIII restriction digest. A 1kb plus DNA ladder (Invitrogen) was run with each sample with representative band sizes indicated. B) Graph demonstrating the activity of the *atrogin-1* promoter in the CXXC5 over-expressing clones (CXXC5 clone 1, clone 2 and clone 3) compared to control (C2C12) cells. Relative luciferase activity is represented as values normalised to β-gal activity. Statistical differences determined by Student's-T test are indicated, $P<0.001$ (***) compared to C2C12.

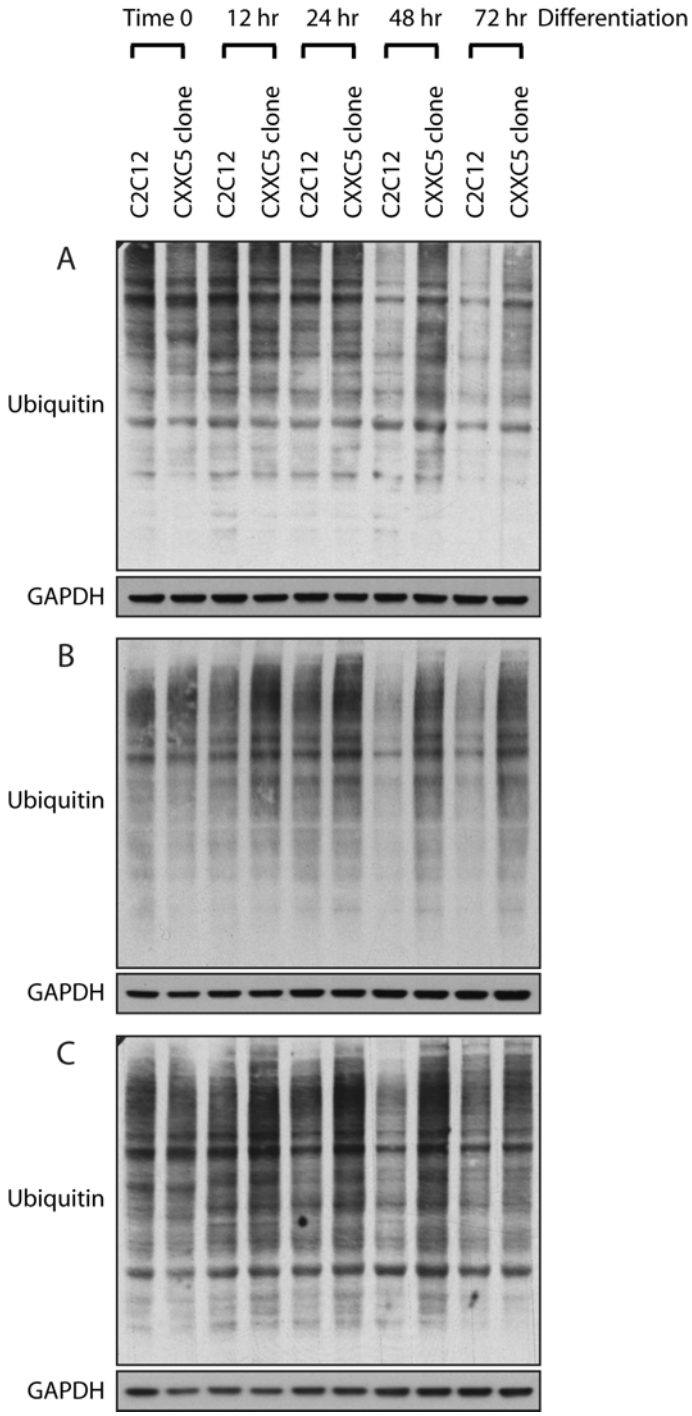

Figure 6.11 *CXXC5 over-expression increases the levels of ubiquitin-conjugated proteins.*

Western Blots showing the level of ubiquitin-conjugated proteins at Time 0 and after 12, 24, 48 and 72 hr of differentiation in CXXC5 over-expressing (CXXC5 clone) lysates compared to control (C2C12) lysates. The level of ubiquitin-conjugated proteins was assessed in CXXC5 clone 1 (A), CXXC5 clone 2 (B) and CXXC5 clone 3 (C). GAPDH expression was analysed to ensure equal loading of samples.

As previously described, myostatin induces muscle wasting through antagonising IGF-1 signalling, allowing for up-regulation of FoxO1 expression and activity, thereby increasing the expression of the Ubiquitin E3 Ligase Atrogin-1 (see Chapter 5). Therefore, the ability of CXXC5 to regulate FoxO1 was assessed. Initially a FoxO1 promoter-luciferase construct was generated. Specific primers were synthesised based on the upstream sequence of the murine FoxO1 gene. The resulting 4 kb PCR product (Figure 6.12Ai) was purified and ligated into the pGEM-T easy cloning vector. The pGEM-T easy construct was transformed into the DH5α strain of E.coli. Following plasmid DNA purification the 4 kb promoter fragment was mobilised through Kpn1 and Nhe1 restriction enzyme digestion, purified, and subcloned into the pGL3b luciferase vector. Restriction digestion using HindIII was performed to confirm the presence of the FoxO1 promoter in the pGL3b vector (Figure 6.12Aii). The FoxO1 promoter-luciferase construct was subsequently transfected into the stable CXXC5 over-expressing cell lines, with luciferase activity analysed as a measure of FoxO1 promoter activity (Figure 6.12B). As shown in Figure 6.12B, Over-expression of CXXC5 resulted in a significant increase in FoxO1-dependent luciferase activity; indicating that CXXC5 is capable of regulating transcriptional activity of the FoxO1 gene. Furthermore, the protein levels of FoxO1 were measured in the CXXC5 over-expressing clones. The expression of FoxO1 was markedly increased in the three CXXC5 over-expressing clones when compared to C2C12 control, as measured by Western Blot analysis (Figure 6.13A, Figure 6.13B, Figure 6.13C and Figure 6.13D). In addition, the CXXC5-stimulated increase in FoxO1 expression was more apparent at later timepoints during the progression of myogenic differentiation (Figure 6.13A, Figure 6.13B, Figure 6.13C and Figure 6.13D). To become active FoxO1 must first be de-phosphorylated (Sandri et al. 2004), therefore the levels of phosphorylated FoxO1 (p-FoxO1) were measured in the CXXC5 over-expressing clones. As shown in Figure 6.13D, the level of p-FoxO1, expressed as a proportion of total FoxO1, was reduced in the CXXC5 over-expressing cell lines compared with control. Specifically, reduced levels of p-FoxO1 were evident in all three CXXC5 over-expressing clones from 48 hr differentiation onwards (Figure 6.13D). Therefore, increased expression of CXXC5 appears to up-regulate the expression of FoxO1 as well as promote the accumulation of active FoxO1.

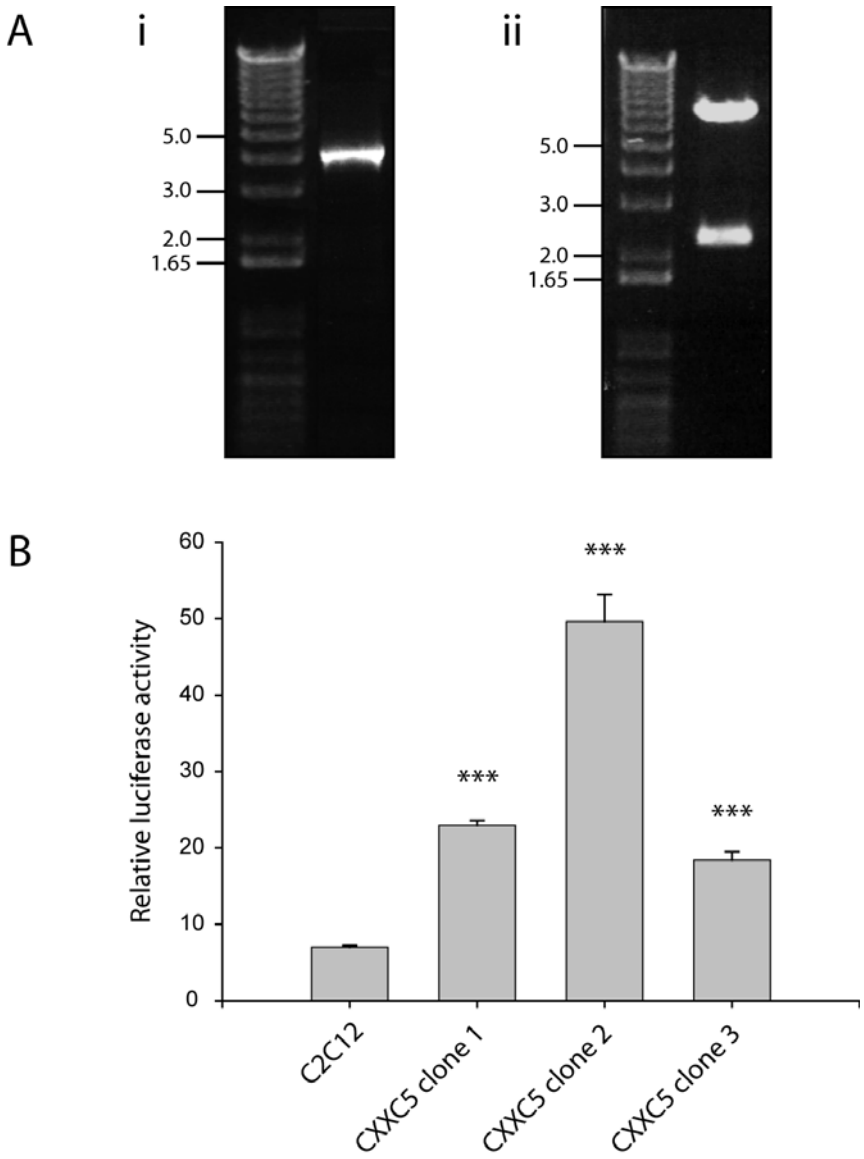

Figure 6.12 *Over-expression of CXXC5 up-regulates FoxO1 promoter activity.*

Ai) Agarose gel visualisation of the ~4 kb *FoxO1* promoter PCR product. Aii) Agarose gel visualisation of the ~7 kb and ~2.4 kb products from the pGL3b/*FoxO1* promoter HindIII restriction digest. A 1kb plus DNA ladder (Invitrogen) was run with each sample with representative band sizes indicated. B) Graph demonstrating the activity of the *FoxO1* promoter in the CXXC5 over-expressing clones (CXXC5 clone 1, clone 2 and clone 3) compared to control (C2C12) cells. Relative luciferase activity is represented as values normalised to β-gal activity. Statistical differences determined by Student's-T test are indicated, $P<0.001$ (***), compared to C2C12.

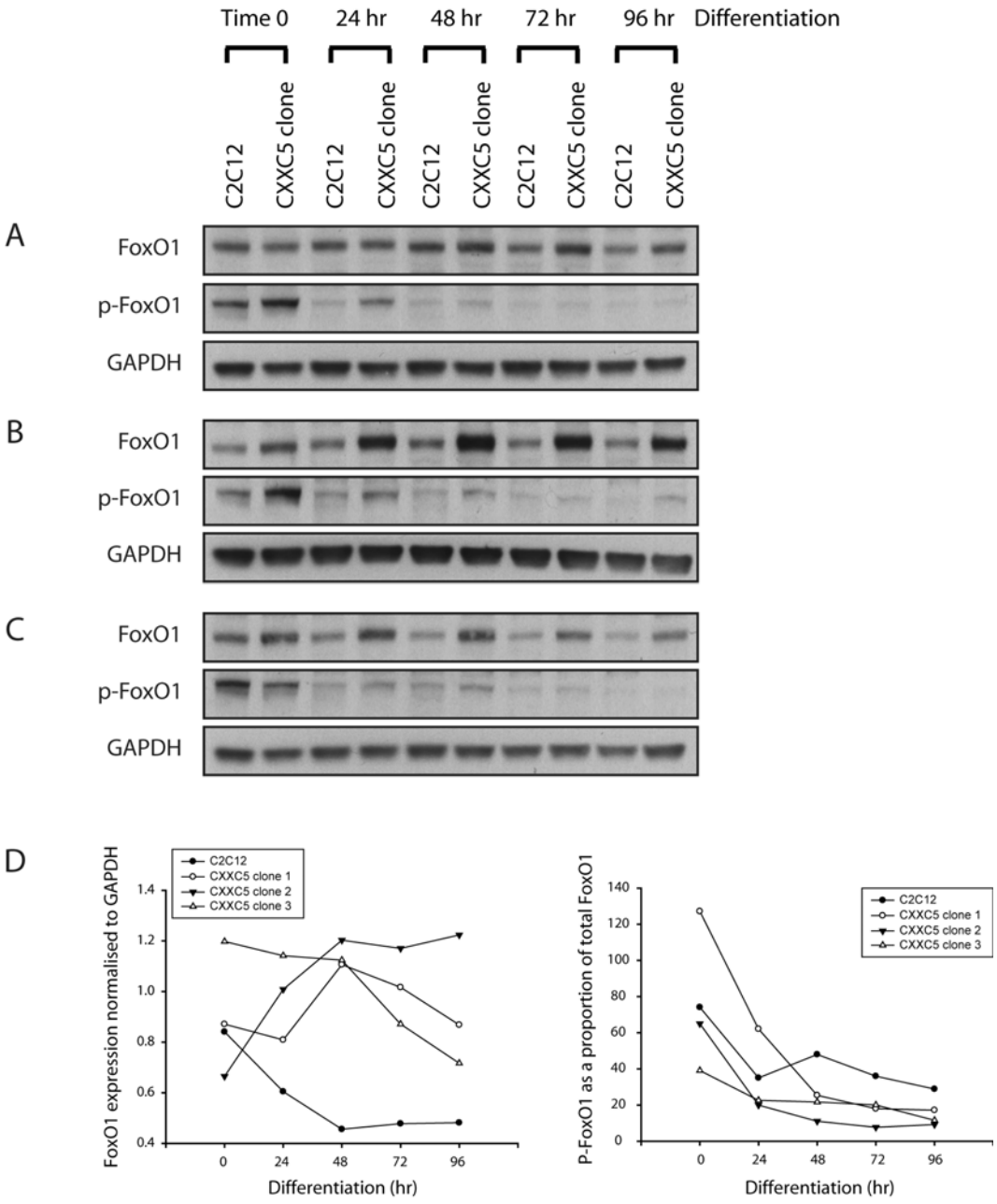

Figure 6.13 *CXXC5 regulates the Forkhead box O transcription factor FoxO1.*

A), B), C) Western Blots showing the expression of FoxO1 and p-FoxO1 at Time 0 and after 12, 24, 48 and 72 hr of differentiation in CXXC5 over-expressing (CXXC5 clone) lysates compared to control (C2C12) lysates. The expression of FoxO1 and p-FoxO1 was assessed in CXXC5 clone 1 (A), CXXC5 clone 2 (B) and CXXC5 clone 3 (C). GAPDH expression was analysed to ensure equal loading of samples. D) Densitometry analysis of protein expression for Western Blots (FoxO1 and p-FoxO1), normalised to GAPDH expression, for CXXC5 over-expressing clones (CXXC5 clone 1, clone 2 and clone 3) compared to control (C2C12) cells. The level of p-FoxO1 is expressed as a proportion of total FoxO1.

6.3.5 Over-expression of CXXC5 does not promote aberrant apoptosis in the C2C12 cell line

The level of cell apoptosis was assessed in the CXXC5 over-expressing clones compared with control (C2C12) cells. The extent of DNA fragmentation, or DNA laddering, is used as a measure of apoptosis. Thus, genomic DNA was extracted from proliferating CXXC5 clones and control (C2C12) cells, subjected to gel electrophoresis and visualised using ethidium bromide. As shown in Figure 6.14, control (C2C12) cells and the CXXC5 over-expressing clones had similar low levels of DNA fragmentation, thus CXXC5 may not induce aberrant apoptosis in the C2C12 cell line.

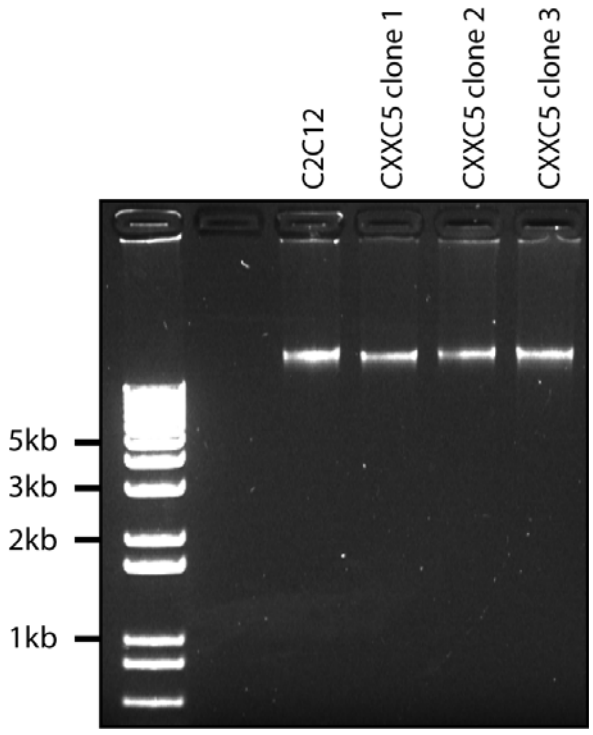

Figure 6.14 *CXXC5 over-expression does not alter the level of apoptosis.*

DNA fragmentation assay showing the levels of apoptosis in the CXXC5 over-expressing clones (CXXC5 clone 1, clone 2 and clone 3) and control (C2C12) cells. Genomic DNA was isolated and subjected to electrophoresis. 1 kb plus ladder (Invitrogen) is shown with representative marker sizes indicated.

6.3.6 Over-expression of CXXC5 alters microtubule structure

Myotube "myosac" formation is a phenomenon that has been previously reported. Indeed, treatment of myotube cultures with several inhibitors of microtubule polymerisation, including the drugs colchicine, colcemid and nocodazole, result in myotube disassembly and the formation of multinucleated myosacs (Bischoff 1968; Saitoh *et al.* 1988). Microtubules are filamentous cytoskeletal structures which are involved in maintaining cell shape and strength, controlling cell movement and the formation of the spindle apparatus during cell division (Martini 2001). Therefore, over-expression of CXXC5 may alter microtubule structure during differentiation, to promote the formation of the distinctive myosac phenotype (see Figure 6.3A). Microtubules are composed of repeating units of dimerised Tubulin molecules, thus to study microtubule morphology alpha-Tubulin localisation was assessed in the CXXC5 over-expressing clones by immunofluorescence. As shown in Figure 6.15A, control (C2C12) myotubes differentiated for 72 hr and stained with alpha-Tubulin show a typical microtubule phenotype, with parallel bundles of microtubules running along the length of the myotube structure. In addition, CXXC5 clone 1 and CXXC5 clone 3 demonstrate a similar microtubule pattern to that seen in controls, although the presence of myosac-like myotubes was becoming more apparent at this stage of differentiation (Figure 6.15B and Figure 6.15C). By 96 hr differentiation the typical microtubule morphology is dramatically altered in CXXC5 clone 1 and CXXC5 clone 3 (Figure 6.16B and Figure 6.16C), as compared with the control (C2C12) cell line (Figure 6.16A). Microtubules appear to be severely degraded, with only minimal microtubule content remaining, following over-expression of CXXC5. The residual microtubules are localised in an irregular pattern surrounding the resulting myosac that encloses the myotube nuclei (Figure 6.16B and Figure 6.16C).

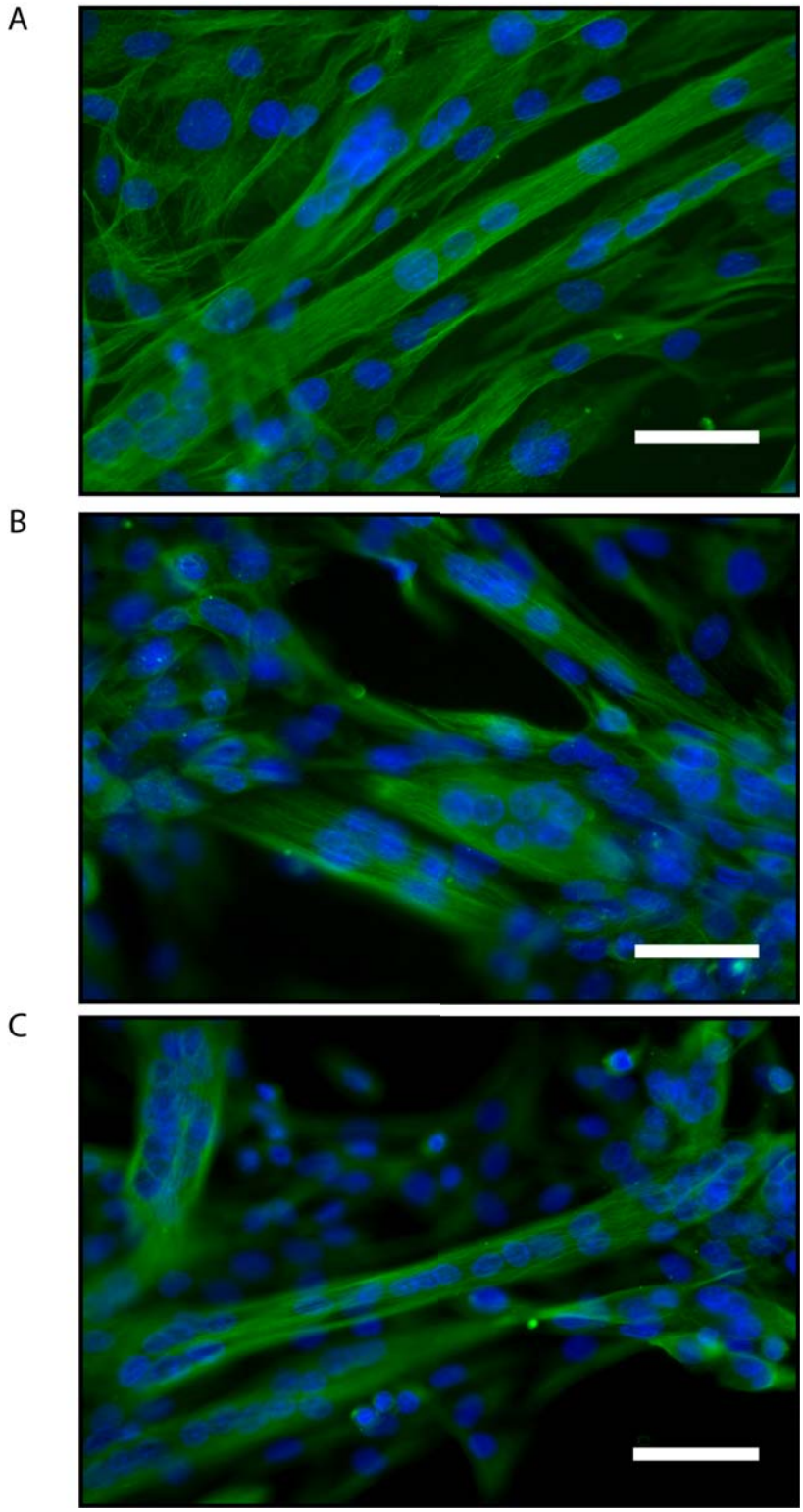

Figure 6.15 *Over-expression of CXXC5 alters microtubule structure at 72 hr differentiation*

Tubulin immunocytochemistry (green) for control (C2C12) cells (A), CXXC5 over-expressing clone 1 (B) and CXXC5 over-expressing clone 3 (C) after 72 hr differentiation. Corresponding nuclei are stained with DAPI (blue). Scale bar represents 5 μm.

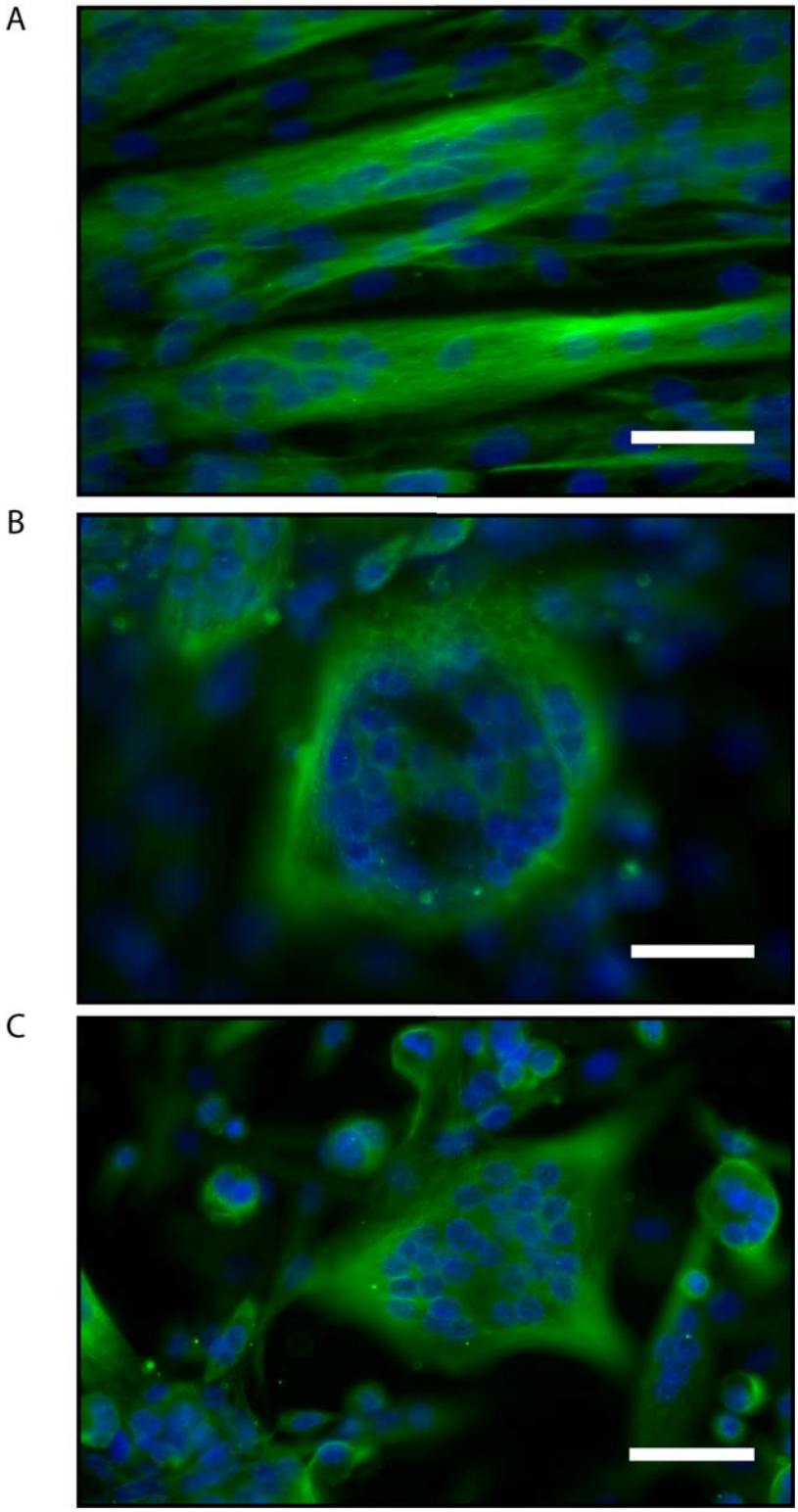

Figure 6.16 *Over-expression of CXXC5 disrupts microtubule structure at 96 hr differentiation*

Tubulin immunocytochemistry (green) for control (C2C12) cells (A), CXXC5 over-expressing clone 1 (B) and CXXC5 over-expressing clone 3 (C) after 96 hr differentiation. Corresponding nuclei are stained with DAPI (blue). Scale bar represents 5 µm.

6.4 Discussion

Myostatin is a potent inhibitor of skeletal muscle growth; furthermore, over-expression of Myostatin has been shown to induce skeletal muscle degradation, resulting in symptoms common with a severe form of muscle wasting, cachexia (Zimmers *et al.* 2002). As outlined in Chapter 5 of this thesis, myostatin-mediated cachexia was shown to induce the up-regulation of components of the ubiquitin-proteasome pathway as well as enhance ubiquitin-conjugation of cellular proteins. This Chapter describes research undertaken to extend on the observations outlined in Chapter 5, and thus describes the global gene changes that occur in a model of myostatin-mediated cachexia via microarray. Furthermore, this Chapter provides an initial characterisation of a novel myostatin downstream target gene during skeletal muscle wasting.

As previously discussed (see Chapter 5), microarray analysis has identified that myostatin-induced myotube atrophy was associated with an up-regulation in the expression of genes encoding several components of the ubiquitin-proteasome pathway; with concomitant down-regulation of genes encoding for critical myofibrillar proteins. These data highlighted a possible mode of action for myostatin in the regulation of skeletal muscle catabolism. In addition, microarray analysis has identified several further genes regulated by myostatin during the induction of skeletal muscle wasting. Importantly, increased levels of Myostatin resulted in the enhanced expression of genes encoding collagen and procollagen isoforms. Recently it has been demonstrated that in *myostatin*-null mice skeletal muscle regeneration is enhanced, while scar tissue formation and collagen deposition are dramatically reduced in response to notexin-stimulated muscle injury (McCroskery *et al.* 2005). Therefore, elevated levels of Myostatin may promote collagen formation during muscle wasting. In support, unpublished results from our laboratory demonstrate that myostatin acts as a chemo-attractant for fibroblast cells, which are responsible for the production and deposition of collagen (Asakura *et al.* 2004).

Myostatin-mediated myotube atrophy also resulted in the inhibition of the gene encoding lactate dehydrogenease A (LDH-A). Conversely, increased mRNA

expression of *glutamine synthetase* (*glns*) was observed following Myostatin treatment (Table 6.1). Interestingly, similar changes in the mRNA expression of *LDH-A* and *glns* are observed in several models of muscle wasting (Lecker *et al.* 2004). Lactate dehydrogenase-A catalyses the formation of pyruvate from lactate (Lehninger *et al.* 1993). Therefore, inhibition of *LDH-A* may reduce the available pool of pyruvate for subsequent conversion into glucose or oxidation to acetyl-CoA for energy production. In skeletal muscle, glutamine is formed from glutamate and ammonia through the action of glutamine synthetase (Lehninger *et al.* 1993). During skeletal muscle wasting conditions including cachexia and sepsis, glutamine is exported from muscle and taken up by organs such as the liver (Karinch *et al.* 2001; Argiles *et al.* 2006). Glutamine influx to the liver appears to assist in Acute-Phase Protein (APP) synthesis and gluconeogenesis (Argiles *et al.* 2006).

Metallothionein-1 and *-2* were down-regulated during myostatin-mediated myotube atrophy (Table 6.1). Metallothionein proteins are induced in response to conditions such as oxidative stress, and can function to protect cells from the effects of Reactive Oxygen Species (ROS) (Nath and Norby 2000). ROS have been associated with increased skeletal muscle protein degradation; indeed, ROS-mediated modification targets muscle proteins for rapid removal during burn-injury associated muscle proteolysis (Fagan *et al.* 1999). Therefore Myostatin treatment may result in enhanced susceptibility to oxidative stress and increased ROS-mediated protein modification. Interestingly, the stress-induced protein *SIP18*, was up-regulated during myostatin-induced muscle wasting. As the name suggests, SIP18 is induced in response to various conditions of stress, including UV exposure, heat shock and oxidative stress (Tomasini *et al.* 2001). Over-expression of SIP18 has been shown to promote cellular apoptosis *in vitro* (Tomasini *et al.* 2001); therefore myostatin-mediated myotube atrophy may also be associated with an increase in the level of apoptosis.

Matrix metalloproteinases-2 and -23 (*MMP-2 and MMP-23*) were also up-regulated during myostatin-mediated myotube atrophy, while the expression of *Tissue Inhibitor of Matrix Metalloproteinase-1* (*TIMP-1*) was dramatically down-regulated following treatment with Myostatin (Table 6.1). MMPs are zinc-dependent proteolytic enzymes which are responsible for degrading several components of the extracellular matrix (ECM) (Carmeli *et al.* 2004).

Furthermore, MMPs have been shown to play a role in skeletal muscle remodelling in response to muscle wasting. Certainly, increased MMP activity is detected in skeletal muscle tissue following prolonged periods of hindlimb unloading, as a result of congestive heart failure, and in response to nerve crush induced muscle denervation (Reznick *et al.* 2003; Demestre *et al.* 2005; Schiotz Thorud *et al.* 2005). Therefore myostatin-mediated up-regulation of *MMP* expression may promote degradation of the extracellular matrix, thus supporting the formation of the myostatin atrophic phenotype as previously described (Figure 5.1).

The expression of *Lipin-1* was shown to be up-regulated during myostatin-mediated myotube atrophy (Table 6.1). Indeed, *Lipin-1* has been previously shown to be up-regulated in muscle atrophy associated with diabetes, starvation, uraemia and tumour growth (Lecker *et al.* 2004). *Lipin-1* is required for the induction of adipocyte differentiation (Phan *et al.* 2005). Furthermore, muscle specific over-expression of *Lipin-1* results in increased adipose tissue content coupled with insulin resistance and obesity (Phan and Reue 2005) Interestingly, over-expression of myostatin has previously been shown to result in adipocyte conversion, while lack of *myostatin* results in decreased adipose tissue formation (McPherron and Lee 2002; Artaza *et al.* 2005; Feldman *et al.* 2006). In addition, Mcpherron and Lee demonstrated that crossing *myostatin*-null mice with the Agouti Lethal Yellow mouse model of obesity and diabetes, reduced the levels of fed glucose and insulin to normal (McPherron and Lee 2002). Therefore myostatin-mediated up-regulation of *Lipin-1* may induce adipocyte formation resulting in alterations in glucose homeostasis.

These data outlined in this Chapter identify the putative zinc finger binding transcription factor, CXXC5, as a novel downstream target of myostatin during the progression of myotube atrophy. CXXC5, like Idax (CXXC4), has previously been linked with inhibition of Wnt signalling (Kim *et al.* 2005). In addition, CXXC5 was identified as a positive regulator of the NF-κB signalling cascade, through a large-scale screening process (Matsuda *et al.* 2003). However, little is known about the function of CXXC5, therefore this research endeavoured to characterise the role of CXXC5 in skeletal muscle. Initial studies were performed using the well characterised C2C12 mouse myoblast cell line through the generation of a set of clonally selected cell lines over-expressing CXXC5. One of

the defining features of the CXXC5 over-expressing clones was the observed gradual myotube collapse and subsequent development of the myosac phenotype (Figure 6.3A, Figure 6.5 and Figure 6.6). The myosac phenotype has been previously described and is associated with disintegration of cytoplasmic microtubule structure (Bischoff 1968; Saitoh *et al.* 1988). Consistent with this previous data, between 72 hr and 96 hr differentiation the Tubulin microtubule structure is dramatically altered in the CXXC5 clones, whereby the typical parallel microtubule structure is degraded resulting in generalised myotube collapse and myosac formation (Figure 6.15 and Figure 6.16). Thus over-expression of MM1 may induce microtubule de-polymerisation, resulting in reduced myotube structural integrity and subsequent myotube collapse. Indeed one of the critical functions of microtubules is to provide strength and rigidity to cells (Martini 2001).

The mode of action of CXXC5 in regulating microtubule structure remains undefined, however, CXXC5, as a putative transcription factor, could signal to downstream effectors which may then regulate microtubule structure. Indeed, several factors have been shown to result in microtubule destabilisation and depolymerisation. The AAA ATPases, katanin and spastin, appear to destabilise microtubule structure by severing microtubules (Quarmby 2000; Evans *et al.* 2005). Furthermore, the kinesins XKCM1 and MCAK also result in microtubule depolymerisation (Walczak *et al.* 1996; Helenius *et al.* 2006). In addition, over-expression of a novel Tubulin-destabilising protein, termed E-like protein (El), results in microtubule depolymerisation and targeted degradation of Tubulin through the ubiquitin-proteasome pathway (Bartolini *et al.* 2005). Therefore the ubiquitin-proteasome pathway may play a role in CXXC5-mediated microtubule disruption. In fact, over-expression of CXXC5 resulted in the up-regulation of components of the ubiquitin-proteasome pathway. The well-characterised E3 ligase *atrogin-1*, the ubiquitin-conjugating enzymes $E2_{14k}$ and $E2_{20k}$ and the proteasome sub-unit *RC2* were all up-regulated in response to over-expression of CXXC5 (Figure 6.9). Furthermore, a dramatic increase in the levels of ubiquitinated proteins was observed following over-expression of CXXC5 (Figure 6.11). Therefore, CXXC5 over-expression may induce skeletal muscle proteolysis and microtubule depolymerisation through mediation of the ATP-dependent ubiquitin-proteasome pathway.

Over-expression of CXXC5 appeared to affect the normal progression of myogenesis in the C2C12 myoblast cell line. Over-expression of CXXC5 reduced the growth rate of the C2C12 cell lines, without inducing cellular apoptosis (Figure 6.2B and Figure 6.14). While the reduction in growth rate was statistically significant, the differences between CXXC5 clones and C2C12 control were not dramatic and thus may not be physiologically significant (Figure 6.2B). Microtubules play an important role in cell division and form the spindle apparatus during mitosis (Martini 2001), thus it is interesting to surmise that CXXC5-mediated microtubule depolymerisation may result in disruption of normal cell cycle progression. In support, treatment of cells with a low dose of the microtubule-stabilising chemical taxol results in mitotic delay (Ikui *et al.* 2005). However, taxol-mediated cell cycle delay, unlike CXXC5, eventually induces cellular apoptosis (Ikui *et al.* 2005). Over-expression of CXXC5 resulted in a significant reduction in myotube number as compared to the control C2C12 cell line at all timepoints analysed (Figure 6.3B). However, expression of the myogenic genes MyoD and myogenin as well as the cell cycle regulator p21, appeared to follow a similar expression pattern to that observed in the control C2C12 cell line (Figure 6.7 and Figure 6.8). Therefore, it is unlikely that the dramatic reduction in myotube number observed in the CXXC5 over-expressing clones was due to insufficiencies in the expression of key regulators of myogenic differentiation; in fact, a characteristic feature of the CXXC5 clones was the up-regulation of MyoD, myogenin and p21, to levels greater than those observed in the control C2C12 cell line during differentiation (Figure 6.7 and Figure 6.8). The enhanced up-regulation of MyoD and myogenin may be a compensatory mechanism, to counteract the CXXC5-mediated myotube wasting and protein degradation during differentiation. During denervation-induced muscle atrophy, the levels of MyoD and myogenin are rapidly up-regulated (Hyatt *et al.* 2003; Raffaello *et al.* 2006). This mechanism may involve activation of the C2C12 quiescent reserve cell pool, which are cells analogous to quiescent satellite cells, and are able to activate, proliferate and differentiate to form new myotubes (Kitzmann *et al.* 1998; Yoshida *et al.* 1998). Indeed, MyoD expression is detected during myoblast growth and initiates differentiation, whereas myogenin is expressed during early stages of myotube formation to execute the differentiation program (Guo *et al.* 1995; Halevy *et al.* 1995; Megeney and

Rudnicki 1995). Further support for this proposed mechanism is the sparse nature of the differentiated CXXC5 clone cultures (Figure 6.3A), presumably due to an enhanced contribution of the reserve cell pool to myogenesis.

Due to the dramatic effect of CXXC5 on C2C12 myotube morphology and gene expression, CXXC5 has tentatively been renamed to "Menos músculo 1" (MM1), simply meaning "less muscle". As outlined in Chapter 5, myostatin appears to regulate protein degradation through a decrease in the activity of AKT, resulting in enhanced FoxO1 activity and subsequent up-regulation of components of the ubiquitin-proteasome pathway. Results in this Chapter indicate that MM1 may play a role in myostatin-mediated myotube atrophy. In support, over-expression of MM1 results in enhanced FoxO1 expression as well as increased FoxO1 activation (Figure 6.12 and Figure 6.13). Therefore myostatin may signal through MM1 to regulate FoxO1 expression and activity, resulting in an increase in the expression of Atrogin-1 and enhanced ubiquitin-mediated proteolysis. An adapted model for the tentative involvement of MM1 in myostatin-mediated muscle wasting is shown in Figure 6.17. However, it is noteworthy to mention that treatment of C2C12 myotubes with recombinant Myostatin protein does not induce the formation of the myosac phenotype (see Figure 5.1). Therefore, it is plausible that Myostatin treatment failed to up-regulate MM1 expression to levels comparable to those detected in the over-expressing clones; or more importantly, MM1 may trigger responses independent of myostatin stimulation to promote protein degradation and myotube collapse (Figure 6.17). Nevertheless, MM1 over-expression has yielded some exciting results and warrants further investigation.

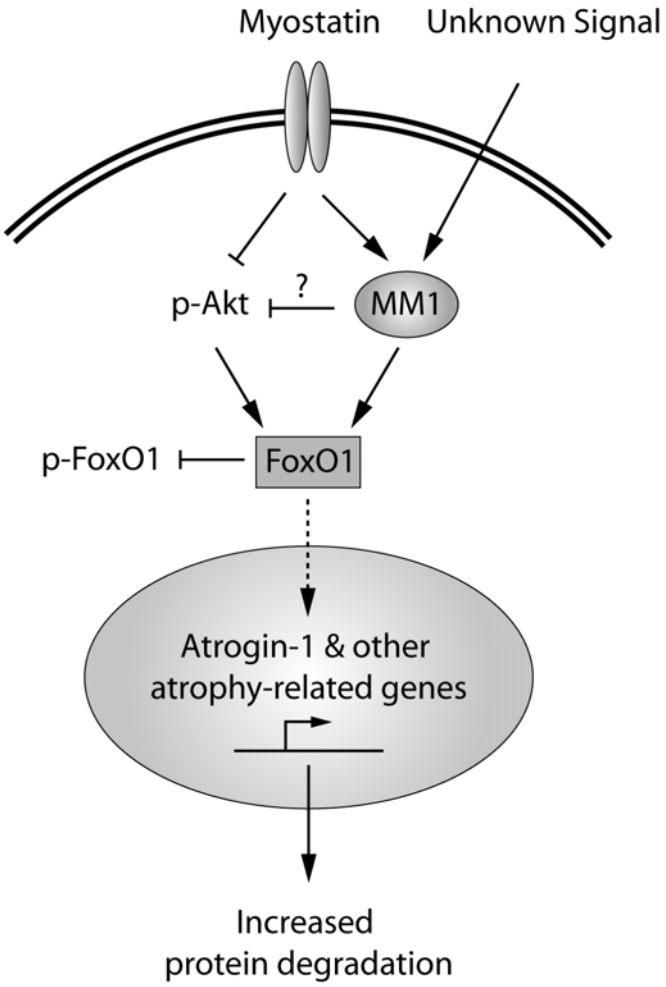

Figure 6.17 *Proposed model of MM1 (CXXC5) function during muscle wasting*

Myostatin appears to up-regulate the ubiquitin-proteolysis system by hypo-phosphorylating FoxO1 through the inhibition of the PI3-K/AKT signalling pathway. Results presented in this Chapter identify a role for MM1 in enhancing FoxO1 activity and promoting the expression of downstream target atrophy-related genes. MM1 may therefore be a downstream mediator of myostatin-induced skeletal muscle wasting. In addition to myostatin, currently undetermined signals may also promote MM1 expression and subsequent protein degradation. Broken lines represent nuclear translocation. Arrows represent activation while blunt-ended lines represent inhibition.

6.5 References

Allen, M. D., C. G. Grummitt, C. Hilcenko, S. Y. Min, L. M. Tonkin, C. M. Johnson, S. M. Freund, M. Bycroft and A. J. Warren (2006). "Solution structure of the nonmethyl-CpG-binding CXXC domain of the leukaemia-associated MLL histone methyltransferase." Embo J **25**(19): 4503-12.

Argiles, J. M., S. Busquets, A. Felipe and F. J. Lopez-Soriano (2006). "Muscle wasting in cancer and ageing: cachexia versus sarcopenia." Adv Gerontol **18**: 39-54.

Artaza, J. N., S. Bhasin, T. R. Magee, S. Reisz-Porszasz, R. Shen, N. P. Groome, M. F. Meerasahib and N. F. Gonzalez-Cadavid (2005). "Myostatin inhibits myogenesis and promotes adipogenesis in C3H 10T(1/2) mesenchymal multipotent cells." Endocrinology **146**(8): 3547-57.

Asakura, T., Y. Ishii, K. Chibana and T. Fukuda (2004). "Leukotriene D4 stimulates collagen production from myofibroblasts transformed by TGF-beta." J Allergy Clin Immunol **114**(2): 310-5.

Bartolini, F., G. Tian, M. Piehl, L. Cassimeris, S. A. Lewis and N. J. Cowan (2005). "Identification of a novel tubulin-destabilizing protein related to the chaperone cofactor E." J Cell Sci **118**(Pt 6): 1197-207.

Bischoff, R., Holtzer, H. (1968). "The effect of mitotic inhibitors on myogenesis in vitro." The Journal of Cell Biology **36**: 111-127.

Cai, D., J. D. Frantz, N. E. Tawa, Jr., P. A. Melendez, B. C. Oh, H. G. Lidov, P. O. Hasselgren, W. R. Frontera, J. Lee, D. J. Glass and S. E. Shoelson (2004). "IKKbeta/NF-kappaB Activation Causes Severe Muscle Wasting in Mice." Cell **119**(2): 285-98.

Carmeli, E., M. Moas, A. Z. Reznick and R. Coleman (2004). "Matrix metalloproteinases and skeletal muscle: a brief review." Muscle Nerve **29**(2): 191-7.

de Jong, D. S., E. J. van Zoelen, S. Bauerschmidt, W. Olijve and W. T. Steegenga (2002). "Microarray analysis of bone morphogenetic protein, transforming growth factor beta, and activin early response genes during osteoblastic cell differentiation." J Bone Miner Res **17**(12): 2119-29.

Demestre, M., G. Parkin-Smith, A. Petzold and A. H. Pullen (2005). "The pro and the active form of matrix metalloproteinase-9 is increased in serum of patients with amyotrophic lateral sclerosis." J Neuroimmunol **159**(1-2): 146-54.

Evans, K. J., E. R. Gomes, S. M. Reisenweber, G. G. Gundersen and B. P. Lauring (2005). "Linking axonal degeneration to microtubule remodeling by Spastin-mediated microtubule severing." J Cell Biol **168**(4): 599-606.

Fagan, J. M., M. Ganguly, H. Stockman, L. H. Ferland and M. Toner (1999). "Posttranslational modifications of cardiac and skeletal muscle proteins by reactive oxygen species after burn injury in the rat." Ann Surg **229**(1): 106-14.

Feldman, B. J., R. S. Streeper, R. V. Farese, Jr. and K. R. Yamamoto (2006). "Myostatin modulates adipogenesis to generate adipocytes with favorable metabolic effects." Proc Natl Acad Sci U S A **103**(42): 15675-80.

Guo, K., J. Wang, V. Andres, R. C. Smith and K. Walsh (1995). "MyoD-induced expression of p21 inhibits cyclin-dependent kinase activity upon myocyte terminal differentiation." Mol Cell Biol **15**(7): 3823-9.

Halevy, O., B. G. Novitch, D. B. Spicer, S. X. Skapek, J. Rhee, G. J. Hannon, D. Beach and A. B. Lassar (1995). "Correlation of terminal cell cycle arrest of skeletal muscle with induction of p21 by MyoD." Science **267**(5200): 1018-21.

Helenius, J., G. Brouhard, Y. Kalaidzidis, S. Diez and J. Howard (2006). "The depolymerizing kinesin MCAK uses lattice diffusion to rapidly target microtubule ends." Nature **441**(7089): 115-9.

Hino, S., S. Kishida, T. Michiue, A. Fukui, I. Sakamoto, S. Takada, M. Asashima and A. Kikuchi (2001). "Inhibition of the Wnt signaling pathway by Idax, a novel Dvl-binding protein." Mol Cell Biol **21**(1): 330-42.

Hyatt, J. P., R. R. Roy, K. M. Baldwin and V. R. Edgerton (2003). "Nerve activity-independent regulation of skeletal muscle atrophy: role of MyoD and myogenin in satellite cells and myonuclei." Am J Physiol Cell Physiol **285**(5): C1161-73.

Ikui, A. E., C. P. Yang, T. Matsumoto and S. B. Horwitz (2005). "Low concentrations of taxol cause mitotic delay followed by premature

dissociation of p55CDC from Mad2 and BubR1 and abrogation of the spindle checkpoint, leading to aneuploidy." Cell Cycle **4**(10): 1385-8.

Jiang, B., W. Xiao, Y. Shi, M. Liu and X. Xiao (2005). "Role of Smac/DIABLO in hydrogen peroxide-induced apoptosis in C2C12 myogenic cells." Free Radic Biol Med **39**(5): 658-67.

Jorgensen, H. F., I. Ben-Porath and A. P. Bird (2004). "Mbd1 is recruited to both methylated and nonmethylated CpGs via distinct DNA binding domains." Mol Cell Biol **24**(8): 3387-95.

Karinch, A. M., M. Pan, C. M. Lin, R. Strange and W. W. Souba (2001). "Glutamine metabolism in sepsis and infection." J Nutr **131**(9 Suppl): 2535S-8S; discussion 2550S-1S.

Katoh, M. and M. Katoh (2004a). "Identification and characterization of FBXL19 gene in silico." Int J Mol Med **14**(6): 1109-14.

Katoh, M. and M. Katoh (2004b). "Identification and characterization of human CXXC10 gene in silico." Int J Oncol **25**(4): 1193-9.

Kim, M., H.-S. Kim and S. Lee (2005). Characterization of Novel Target Gene of WT1. NIH Research Festival, Natcher Conference Center, National Institutes of Health, Bathesda, MA, USA.

Kitzmann, M., G. Carnac, M. Vandromme, M. Primig, N. J. Lamb and A. Fernandez (1998). "The muscle regulatory factors MyoD and myf-5 undergo distinct cell cycle-specific expression in muscle cells." J Cell Biol **142**(6): 1447-59.

Lecker, S. H., R. T. Jagoe, A. Gilbert, M. Gomes, V. Baracos, J. Bailey, S. R. Price, W. E. Mitch and A. L. Goldberg (2004). "Multiple types of skeletal muscle atrophy involve a common program of changes in gene expression." Faseb J **18**(1): 39-51.

Lee, J. H., K. S. Voo and D. G. Skalnik (2001). "Identification and characterization of the DNA binding domain of CpG-binding protein." J Biol Chem **276**(48): 44669-76.

Lehninger, A. L., D. L. Nelson and M. M. Cox (1993). Principles of Biochemistry. New York, Worth Publishers.

Li, Y. P. and M. B. Reid (2000). "NF-kappaB mediates the protein loss induced by TNF-alpha in differentiated skeletal muscle myotubes." Am J Physiol Regul Integr Comp Physiol **279**(4): R1165-70.

Martini, F. H. (2001). Fundamentals of Anatomy and Physiology. New Jersey, Prentice Hall International Inc.

Matsuda, A., Y. Suzuki, G. Honda, S. Muramatsu, O. Matsuzaki, Y. Nagano, T. Doi, K. Shimotohno, T. Harada, E. Nishida, H. Hayashi and S. Sugano (2003). "Large-scale identification and characterization of human genes that activate NF-kappaB and MAPK signaling pathways." Oncogene **22**(21): 3307-18.

McCroskery, S., M. Thomas, L. Platt, A. Hennebry, T. Nishimura, L. McLeay, M. Sharma and R. Kambadur (2005). "Improved muscle healing through enhanced regeneration and reduced fibrosis in myostatin-null mice." J Cell Sci **118**(Pt 15): 3531-41.

McPherron, A. C. and S. J. Lee (2002). "Suppression of body fat accumulation in myostatin-deficient mice." J Clin Invest **109**(5): 595-601.

Megeney, L. A. and M. A. Rudnicki (1995). "Determination versus differentiation and the MyoD family of transcription factors." Biochem Cell Biol **73**(9-10): 723-32.

Nath, K. A. and S. M. Norby (2000). "Reactive oxygen species and acute renal failure." Am J Med **109**(8): 665-78.

Oliver, M. H., N. K. Harrison, J. E. Bishop, P. J. Cole and G. J. Laurent (1989). "A rapid and convenient assay for counting cells cultured in microwell plates: application for assessment of growth factors." J Cell Sci **92**(Pt 3): 513-8.

Phan, J., M. Peterfy and K. Reue (2005). "Biphasic expression of lipin suggests dual roles in adipocyte development." Drug News Perspect **18**(1): 5-11.

Phan, J. and K. Reue (2005). "Lipin, a lipodystrophy and obesity gene." Cell Metab **1**(1): 73-83.

Quarmby, L. (2000). "Cellular Samurai: katanin and the severing of microtubules." J Cell Sci **113 (Pt 16)**: 2821-7.

Raffaello, A., P. Laveder, C. Romualdi, C. Bean, L. Toniolo, E. Germinario, A. Megighian, D. Danieli-Betto, C. Reggiani and G. Lanfranchi (2006). "Denervation in murine fast-twitch muscle: short-term physiological changes and temporal expression profiling." Physiol Genomics **25**(1): 60-74.

Reznick, A. Z., O. Menashe, M. Bar-Shai, R. Coleman and E. Carmeli (2003). "Expression of matrix metalloproteinases, inhibitor, and acid phosphatase in muscles of immobilized hindlimbs of rats." Muscle Nerve **27**(1): 51-9.

Saitoh, O., T. Arai and T. Obinata (1988). "Distribution of microtubules and other cytoskeletal filaments during myotube elongation as revealed by fluorescence microscopy." Cell Tissue Res **252**(2): 263-73.

Sandri, M., C. Sandri, A. Gilbert, C. Skurk, E. Calabria, A. Picard, K. Walsh, S. Schiaffino, S. H. Lecker and A. L. Goldberg (2004). "Foxo transcription factors induce the atrophy-related ubiquitin ligase atrogin-1 and cause skeletal muscle atrophy." Cell **117**(3): 399-412.

Schiotz Thorud, H. M., A. Stranda, J. A. Birkeland, P. K. Lunde, I. Sjaastad, S. O. Kolset, O. M. Sejersted and P. O. Iversen (2005). "Enhanced matrix metalloproteinase activity in skeletal muscles of rats with congestive heart failure." Am J Physiol Regul Integr Comp Physiol **289**(2): R389-R394.

Sharma, M., R. Kambadur, K. G. Matthews, W. G. Somers, G. P. Devlin, J. V. Conaglen, P. J. Fowke and J. J. Bass (1999). "Myostatin, a transforming growth factor-beta superfamily member, is expressed in heart muscle and is upregulated in cardiomyocytes after infarct." J Cell Physiol **180**(1): 1-9.

Thomas, M., B. Langley, C. Berry, M. Sharma, S. Kirk, J. Bass and R. Kambadur (2000). "Myostatin, a negative regulator of muscle growth, functions by inhibiting myoblast proliferation." J Biol Chem **275**(51): 40235-43.

Tomasini, R., A. A. Samir, M. I. Vaccaro, M. J. Pebusque, J. C. Dagorn, J. L. Iovanna and N. J. Dusetti (2001). "Molecular and functional characterization of the stress-induced protein (SIP) gene and its two transcripts generated by alternative splicing. SIP induced by stress and promotes cell death." J Biol Chem **276**(47): 44185-92.

Walczak, C. E., T. J. Mitchison and A. Desai (1996). "XKCM1: a Xenopus kinesin-related protein that regulates microtubule dynamics during mitotic spindle assembly." Cell **84**(1): 37-47.

Wilson, B. (2006). Cloning and Characterisation of a Novel Muscle Wasting Gene: *menos musculo-1* (*mm1*). Department of Biological Sciences. Hamilton, University of Waikato**:** 147.

Wolffe, A. P., P. L. Jones and P. A. Wade (1999). "DNA demethylation." Proc Natl Acad Sci U S A **96**(11): 5894-6.

Yaffe, D. and O. Saxel (1977). "Serial passaging and differentiation of myogenic cells isolated from dystrophic mouse muscle." Nature **270**(5639): 725-7.

Yoshida, N., S. Yoshida, K. Koishi, K. Masuda and Y. Nabeshima (1998). "Cell heterogeneity upon myogenic differentiation: down-regulation of MyoD and Myf-5 generates 'reserve cells'." J Cell Sci **111**(Pt 6)): 769-79.

Zimmers, T. A., M. V. Davies, L. G. Koniaris, P. Haynes, A. F. Esquela, K. N. Tomkinson, A. C. McPherron, N. M. Wolfman and S. J. Lee (2002). "Induction of cachexia in mice by systemically administered myostatin." Science **296**(5572): 1486-8.

Chapter 7 Final discussion

The majority of research undertaken in the Functional Muscle Genomics Laboratory, AgResearch, Hamilton, New Zealand has been focussed on understanding myostatin function during the progression of embryonic and foetal myogenesis. However, recent publications from our laboratory and others have highlighted a role for myostatin in the regulation of post-natal myogenesis. Specifically, in *myostatin*-null mice there is increased satellite cell activation and self-renewal as well as enhanced skeletal muscle regeneration in response to injury (McCroskery *et al.* 2003; McCroskery *et al.* 2005). Conversely, increased levels of myostatin are associated with numerous skeletal muscle wasting conditions (Gonzalez-Cadavid *et al.* 1998; Reardon *et al.* 2001; Schulte and Yarasheski 2001; Ma *et al.* 2003) and exogenous over-expression of Myostatin has been shown to promote the progression of the cachexia syndrome (Zimmers *et al.* 2002). While evidence suggests a role for myostatin in skeletal muscle wasting, little is known about the mechanism of action for myostatin in this process of muscle degeneration. Thus the overall aim of this thesis is to further clarify the role of myostatin in post-natal skeletal muscle growth and repair and delineate mechanisms through which myostatin acts to regulate skeletal muscle wasting.

The major site of synthesis for myostatin is skeletal muscle, with expression of myostatin detected in satellite cell, myoblast and myotube populations. The presence of myostatin in satellite cells may form the basis of an autocrine signalling mechanism, through which myostatin negatively regulates the activation of satellite cells. However, the paracrine and/or endocrine mode of action for myostatin cannot be ruled out, given that subcutaneous injection of Myostatin results in muscle wasting. Thus further work needs to be performed to clarify this mechanism.

Like other members of the TGF-β superfamily, myostatin is synthesised, proteolytically processed and secreted into circulation as a latent complex to elicit biological responses (Lee and McPherron 2001). Thus myostatin acts as a circulatory factor in an endocrine or perhaps paracrine manner to regulate

downstream targets. The rate-limiting step in the activation of myostatin appears to be the proteolytic processing or cleaving of the full length Myostatin peptide into LAP and mature Myostatin portions. Myostatin processing was thus examined, and interestingly the level of Myostatin processing appears to be developmentally regulated, with reduced processing observed during foetal stages of growth. In addition, I have characterised a mechanism through which myostatin negatively auto-regulates its own processing through targeted down-regulation of the proprotein convertase furin. This level of regulation may provide a mechanism through which myostatin is effectively removed, thus allowing for successive rounds of primary and secondary myogenesis to occur during foetal growth. Future work will be performed creating dominant-negative *furin* cell lines; wherein myostatin expression and processing will be assessed, thus allowing us to confirm the requirement of furin in the regulation of myostatin activity. In addition, techniques designed to target and inactivate furin may be useful as possible therapies to counteract myostatin-induced skeletal muscle atrophy. However myostatin is not the only target of furin, in fact, furin is responsible for processing other members of the TGF-β superfamily including TGF-β1 and BMP-4 (Cui *et al.* 1998; Dubois *et al.* 2001). Furthermore, *furin*-null mice are lethal around embryonic day 10.5 (Zhou *et al.* 1999), therefore total inactivation of *furin* as a means to disrupt myostatin function is not a viable approach. Perhaps an approach to impart furin inhibitors in a muscle specific manner, during post-natal muscle repair, may become a viable option for inactivating myostatin.

Skeletal muscle stem cells, or satellite cells, form a distinct population of myogenic precursor cells responsible for post-natal skeletal muscle growth and repair (Seale and Rudnicki 2000). Myostatin has been implicated in the regulation of satellite cell activation, proliferation and self-renewal. Indeed, McCroskery *et al.* demonstrated that in the absence of *myostatin*, satellite cell number is significantly increased; moreover it was shown that satellite cells isolated from *myostatin*-null mice are more active and have an enhanced rate of proliferation (McCroskery *et al.* 2003). The significantly increased satellite cell number in *myostatin*-null mice may arise through enhanced satellite cell self-renewal, increased specification of somitic precursor cells or enhanced contribution of non-muscle derived cells to the satellite cell pool. Firstly, satellite

cell self-renewal may provide a means through which satellite cell number is enhanced in *myostatin*-null mice. In this thesis I have addressed the role of myostatin in satellite cell self-renewal. Specifically, I have identified a mechanism behind myostatin-mediated inhibition of satellite cell self-renewal, whereby myostatin regulates the pool of self-renewed satellite cells through inhibition of Pax7. A mechanism involving regulation of Pax7 is consistent with current evidence supporting a role for Pax7 in satellite cell self-renewal (Olguin and Olwin 2004; Zammit *et al.* 2004). However, further work will be performed to characterise the signalling mechanism behind myostatin regulation of Pax7 during satellite cell self-renewal. Candidate pathways that will be studied are the Smad signalling pathway, which is the typical signalling pathway of TGF-β superfamily members. Furthermore, the p38 MAPK signalling pathway, which has been shown to play a role in myostatin-mediated inhibition of cell proliferation will be studied (Philip *et al.* 2005). In addition the notch signalling cascade will be analysed, indeed the notch signalling cascade has previously been identified as playing a role in satellite cell fate determination and self-renewal (Conboy and Rando 2002). Future studies will also be performed based on the elegant experiments of Collins *et al.* (Collins *et al.* 2005), specifically transgenic mice will be generated by crossing *myostatin*-null (*mstn*$^{-/-}$) mice with *Myf5*$^{nLacZ/+}$ mice, wherein β-gal activity represents Myf5 expression in both satellite cell nuclei and newly formed muscle fibres. Single muscle fibres will be isolated from the *mstn*$^{-/-}$/ *Myf5*$^{nLacZ/+}$ mice and injected into injured immune-deficient nude mice, with the resulting β-gal^{+} (blue) cells identified and quantified. Satellite cell self-renewal will be assessed through quantification of the β-gal^{+}/Pax7^{+} cells that progressively associate with the satellite cell niche beneath the basal lamina. The effect of myostatin on satellite cell self-renewal will be analysed through quantification of β-gal^{+}/Pax7^{+} satellite cells in mice injected with *mstn*$^{-/-}$/ *Myf5*$^{nLacZ/+}$ fibres compared with mice injected with *Myf5*$^{nLacZ/+}$ fibres.

The widely accepted theory is that satellite cells are derived from myogenic precursor cells in the somite. Indeed, recently identified populations of Pax7^{+}/Pax3^{+} cells present in the somite have been shown to give rise to adult skeletal muscle satellite cells (Kassar-Duchossoy *et al.* 2005; Relaix *et al.* 2005; Schienda *et al.* 2006). Therefore, these populations of Pax7^{+}/Pax3^{+} cells will be assessed by immunofluorescence and quantified to determine if the increased

satellite cell number detected in *myostatin*-null mice is due to enhanced specification of myogenic precursor cells during embryonic myogenesis.

Lastly, cells derived from other sources such as bone marrow may contribute to the increased satellite cell pool present in *myostatin*-null mice. To determine the contribution of non-muscle-derived cells, *myostatin*-null mice will be subjected to injury and injected with GFP-expressing bone marrow-derived cells from the $B6Tg^{GFP}$ transgenic mouse line. This experiment is based on the published paper of Dreyfus *et al.* (Dreyfus *et al.* 2004). The pool of GFP-labelled, Pax7-positive ($GFP^+/Pax7^+$) cells aligning to the satellite cell niche will be quantified to determine the contribution of non-muscle satellite cell sources to the enhanced satellite cell number observed in the *myostatin*-null transgenic mouse line. The populations of $GFP^+/Pax7^+$ cells will be analysed in both *myostatin*-null and wild-type mice injected with GFP-labelled, bone marrow-derived cells.

The role of myostatin as a growth factor which negatively regulates skeletal muscle growth is now well established. However, questions remain as to whether or not myostatin acts as a cachexia-inducing factor which functions in the regulation of skeletal muscle wasting. Enhanced myostatin expression is associated with many forms of skeletal muscle wasting including disuse atrophy, sarcopenia, AIDS and glucocorticoid-induced muscle wasting (Gonzalez-Cadavid *et al.* 1998; Reardon *et al.* 2001; Yarasheski *et al.* 2002; Ma *et al.* 2003). Moreover, exogenous addition of Myostatin has been shown to induce severe muscle wasting consistent with the phenotype observed during cachexia (Zimmers *et al.* 2002). Although research has been performed studying the role of myostatin in various other muscle wasting conditions, and despite the severity of cancer-related muscle loss, evidence for the role of myostatin in cancer-cachexia is currently lacking. Therefore future studies will be performed, whereby the levels of circulating and thus potentially active myostatin will be assessed in human patients suffering from various forms of cancers. This data would highlight whether or not myostatin expression correlates with cancer-related muscle loss. In addition, *myostatin*-null mice will be tested for resistance to cancer-associated cachexia through injection of colon-26 adenocarcinoma and Lewis lung carcinoma cells. These model systems of tumour associated muscle wasting will be used to assess the efficacy of *myostatin* disruption in reducing the severity of cancer-associated cachexia. As outlined in this thesis, myostatin

appears to induce skeletal muscle degradation though regulation of the ubiquitin-proteasome pathway. In fact, *in vitro* and *in vivo* models of myostatin-induced cachexia have highlighted the ability of myostatin to antagonise IGF-1/PI3-K/AKT hypertrophy signalling, resulting in enhanced FoxO1 transcriptional activity and subsequent up-regulation of ubiquitin-related genes including the widely studied E3 ligase Atrogin-1. However, further work needs to be performed to confirm myostatin regulation of ubiquitin-proteasome mediated protein degradation. Thus *atrogin-1*-null (*atrogin-1*$^{-/-}$) transgenic mice will be obtained (Bodine *et al.* 2001) and tested for resistance to myostatin-mediated muscle wasting through injection of Myostatin-expressing CHO cells (see Section 5.2.3). Furthermore, primary myoblast cultures will be isolated from *atrogin-1*$^{-/-}$ mice and treated with recombinant Myostatin protein. These experiments will allow us to test whether Atrogin-1 is mandatorily required for the progression of myostatin-mediated muscle wasting. Interestingly, myostatin has recently been shown to be a downstream target of FoxO1 (Allen and Unterman 2006). In particular, over-expression of FoxO1 was shown to up-regulate the mRNA expression of *myostatin* as well as enhance *myostatin* promoter activity (Allen and Unterman 2006). It is thus interesting to surmise that FoxO1-mediated up-regulation of myostatin may enhance the process of skeletal muscle wasting. Alternatively, myostatin has been shown to negatively auto-regulate its expression through the action of Smad7. Therefore FoxO1 up-regulation of myostatin may be a mechanism through which myostatin negatively auto-regulates its own expression during muscle wasting, however, further work will need to be performed to ascertain the validity of this mechanism. The recent study by Allen and Unterman employed *in vitro* techniques to identify myostatin as a downstream target of FoxO1 (Allen and Unterman 2006). To expand on this research I will undertake a set of experiments characterising this mechanism *in vivo*, by obtaining FoxO1 over-expressing transgenic mice (Kamei *et al.* 2004). Furthermore, FoxO1 over-expressing mice will be crossed with *myostatin*-null mice. The resulting double mutant will be tested for resistance to skeletal muscle wasting enabling clarification of the role of FoxO1-mediated up-regulation of myostatin during muscle wasting conditions.

The evidence to date associates increased myostatin expression with many forms skeletal muscle atrophy. Furthermore, the candidate gene approach utilised in this

thesis has highlighted a possible mechanism through which myostatin signals muscle atrophy, however, more comprehensive approaches should be undertaken to enhance our understanding of myostatin as a cachexia-inducing factor. To that end I employed a microarray approach to analyse the global gene expression changes that occurred in a model of myostatin-mediated cachexia. Microarray analysis identified that expression of the gene *CXXC5* (*MM1*) was significantly up-regulated during myostatin-mediated myotube atrophy. MM1 was subsequently characterised as a muscle wasting-inducing gene through a series of *in vitro* experiments. Specifically, MM1 was shown to up-regulate components of the ubiquitin-proteasome pathway. Moreover, MM1 over-expression resulted in the progressive collapse of the myotube population during differentiation, resulting in the formation of multinucleated myosacs. However, the data presented in this thesis focuses on characterising the function of MM1 *in vitro*, thus future work will be performed to clarify the role of this gene during muscle wasting *in vivo*. As such, muscle-specific *MM1* over-expressing transgenic mice are currently being generated. In addition, muscle specific *MM1* knockout transgenic mice will be generated. The *MM1* knockout mice ($MM1^{-/-}$) will prove useful in analysing the role of MM1 in myostatin-mediated muscle wasting. Indeed treatment of $MM1^{-/-}$ mice with Myostatin-expressing CHO cells will allow us to confirm the link between myostatin, MM1, Atrogin-1 and subsequent protein degradation.

In conclusion, I believe that myostatin is a cachexia-inducing factor which is capable of signalling through established systems to regulate ubiquitin-mediated protein degradation. With this in mind, methods should be employed to target and potentially inactivate myostatin, especially in patients suffering from muscle wasting diseases. If successful, these gene-based therapies may ameliorate the severe symptoms associated with devastating diseases such as cancer and AIDS, and may improve the quality and longevity of life in these patients.

7.1 References

Allen, D. L. and T. G. Unterman (2006). "Regulation of Myostatin Expression and Myoblast Differentiation by FoxO and SMAD Transcription Factors." Am J Physiol Cell Physiol.

Bodine, S. C., E. Latres, S. Baumhueter, V. K. Lai, L. Nunez, B. A. Clarke, W. T. Poueymirou, F. J. Panaro, E. Na, K. Dharmarajan, Z. Q. Pan, D. M. Valenzuela, T. M. DeChiara, T. N. Stitt, G. D. Yancopoulos and D. J. Glass (2001). "Identification of ubiquitin ligases required for skeletal muscle atrophy." Science **294**(5547): 1704-8.

Collins, C. A., I. Olsen, P. S. Zammit, L. Heslop, A. Petrie, T. A. Partridge and J. E. Morgan (2005). "Stem cell function, self-renewal, and behavioral heterogeneity of cells from the adult muscle satellite cell niche." Cell **122**(2): 289-301.

Conboy, I. M. and T. A. Rando (2002). "The regulation of notch signaling controls satellite cell activation and cell fate determination in postnatal myogenesis." Dev Cell **3**(3): 397-409.

Cui, Y., F. Jean, G. Thomas and J. L. Christian (1998). "BMP-4 is proteolytically activated by furin and/or PC6 during vertebrate embryonic development." Embo J **17**(16): 4735-43.

Dreyfus, P. A., F. Chretien, B. Chazaud, Y. Kirova, P. Caramelle, L. Garcia, G. Butler-Browne and R. K. Gherardi (2004). "Adult bone marrow-derived stem cells in muscle connective tissue and satellite cell niches." Am J Pathol **164**(3): 773-9.

Dubois, C. M., F. Blanchette, M. H. Laprise, R. Leduc, F. Grondin and N. G. Seidah (2001). "Evidence that furin is an authentic transforming growth factor-beta1- converting enzyme." Am J Pathol **158**(1): 305-16.

Gonzalez-Cadavid, N. F., W. E. Taylor, K. Yarasheski, I. Sinha-Hikim, K. Ma, S. Ezzat, R. Shen, R. Lalani, S. Asa, M. Mamita, G. Nair, S. Arver and S. Bhasin (1998). "Organization of the human myostatin gene and expression in healthy men and HIV-infected men with muscle wasting." Proc Natl Acad Sci U S A **95**(25): 14938-43.

Kamei, Y., S. Miura, M. Suzuki, Y. Kai, J. Mizukami, T. Taniguchi, K. Mochida, T. Hata, J. Matsuda, H. Aburatani, I. Nishino and O. Ezaki (2004). "Skeletal muscle FOXO1 (FKHR) transgenic mice have less skeletal muscle mass, down-regulated Type I (slow twitch/red muscle) fiber genes, and impaired glycemic control." J Biol Chem **279**(39): 41114-23.

Kassar-Duchossoy, L., E. Giacone, B. Gayraud-Morel, A. Jory, D. Gomes and S. Tajbakhsh (2005). "Pax3/Pax7 mark a novel population of primitive myogenic cells during development." Genes Dev **19**(12): 1426-31.

Lee, S. J. and A. C. McPherron (2001). "Regulation of myostatin activity and muscle growth." Proc Natl Acad Sci U S A **98**(16): 9306-11.

Ma, K., C. Mallidis, S. Bhasin, V. Mahabadi, J. Artaza, N. Gonzalez-Cadavid, J. Arias and B. Salehian (2003). "Glucocorticoid-induced skeletal muscle atrophy is associated with upregulation of myostatin gene expression." Am J Physiol Endocrinol Metab **285**(2): E363-71.

McCroskery, S., M. Thomas, L. Maxwell, M. Sharma and R. Kambadur (2003). "Myostatin negatively regulates satellite cell activation and self-renewal." J Cell Biol **162**(6): 1135-47.

McCroskery, S., M. Thomas, L. Platt, A. Hennebry, T. Nishimura, L. McLeay, M. Sharma and R. Kambadur (2005). "Improved muscle healing through enhanced regeneration and reduced fibrosis in myostatin-null mice." J Cell Sci **118**(Pt 15): 3531-41.

Olguin, H. C. and B. B. Olwin (2004). "Pax-7 up-regulation inhibits myogenesis and cell cycle progression in satellite cells: a potential mechanism for self-renewal." Dev Biol **275**(2): 375-88.

Philip, B., Z. Lu and Y. Gao (2005). "Regulation of GDF-8 signaling by the p38 MAPK." Cell Signal **17**(3): 365-75.

Reardon, K. A., J. Davis, R. M. Kapsa, P. Choong and E. Byrne (2001). "Myostatin, insulin-like growth factor-1, and leukemia inhibitory factor mRNAs are upregulated in chronic human disuse muscle atrophy." Muscle Nerve **24**(7): 893-9.

Relaix, F., D. Rocancourt, A. Mansouri and M. Buckingham (2005). "A Pax3/Pax7-dependent population of skeletal muscle progenitor cells." Nature **435**(7044): 948-53.

Schienda, J., K. A. Engleka, S. Jun, M. S. Hansen, J. A. Epstein, C. J. Tabin, L. M. Kunkel and G. Kardon (2006). "Somitic origin of limb muscle satellite and side population cells." Proc Natl Acad Sci U S A **103**(4): 945-50.

Schulte, J. N. and K. E. Yarasheski (2001). "Effects of resistance training on the rate of muscle protein synthesis in frail elderly people." Int J Sport Nutr Exerc Metab **11 Suppl**: S111-8.

Seale, P. and M. A. Rudnicki (2000). "A new look at the origin, function, and "stem-cell" status of muscle satellite cells." Dev Biol **218**(2): 115-24.

Yarasheski, K. E., S. Bhasin, I. Sinha-Hikim, J. Pak-Loduca and N. F. Gonzalez-Cadavid (2002). "Serum myostatin-immunoreactive protein is increased in 60-92 year old women and men with muscle wasting." J Nutr Health Aging **6**(5): 343-8.

Zammit, P. S., J. P. Golding, Y. Nagata, V. Hudon, T. A. Partridge and J. R. Beauchamp (2004). "Muscle satellite cells adopt divergent fates: a mechanism for self-renewal?" J Cell Biol **166**(3): 347-57.

Zhou, A., G. Webb, X. Zhu and D. F. Steiner (1999). "Proteolytic processing in the secretory pathway." J Biol Chem **274**(30): 20745-8.

Zimmers, T. A., M. V. Davies, L. G. Koniaris, P. Haynes, A. F. Esquela, K. N. Tomkinson, A. C. McPherron, N. M. Wolfman and S. J. Lee (2002). "Induction of cachexia in mice by systemically administered myostatin." Science **296**(5572): 1486-8.